Copyright Warning & Restrictions

The copyright law of the United States (Title 17, United States Code) governs the making of photocopies or other reproductions of copyrighted material.

Under certain conditions specified in the law, libraries and archives are authorized to furnish a photocopy or other reproduction. One of these specified conditions is that the photocopy or reproduction is not to be "used for any purpose other than private study, scholarship, or research." If a, user makes a request for, or later uses, a photocopy or reproduction for purposes in excess of "fair use" that user may be liable for copyright infringement,

This institution reserves the right to refuse to accept a copying order if, in its judgment, fulfillment of the order would involve violation of copyright law.

Please Note: The author retains the copyright while the New Jersey Institute of Technology reserves the right to distribute this thesis or dissertation

Printing note: If you do not wish to print this page, then select "Pages from: first page # to: last page #" on the print dialog screen

Order Number 9409125

Pyrolysis and oxidation of chloromethanes: Experiment and modeling

Ho, Wenpin, Ph.D.

New Jersey Institute of Technology, 1993

U·M·I
300 N. Zeeb Rd.
Ann Arbor, MI 48106

PYROLYSIS AND OXIDATION OF CHLOROMETHANES EXPERIMENT AND MODELING

by
Wenpin Ho

A Dissertation
Submitted to the Faculty of
New Jersey Institute of Technology
in Partial Fulfillment of the Requirements for the Degree of
Doctor of Philosophy

Department of Chemical Engineering,
Chemistry, and Environmental Science

October 1993

APPROVAL PAGE

PYROLYSIS AND OXIDATION OF CHLOROMETHANES EXPERIMENT AND MODELING

Wenpin Ho

Dr. Joseph W. Bozzelli, Dissertation Advisor — date
Distinguished Professor of Chemistry, NJIT

Dr. Barbara B. Kebbekus, Committee Member — date
Professor of Chemitry and Associate Chairperson of the Department of Chemical Engineering, Chemistry and Environmental Science, NJIT

Dr. Henry Shaw, Committee Member — date
Professor of Chemical Engineering, NJIT

Dr. Robert B. Barat, Committee Member — date
Assistant Professor of Chemical Engineering, NJIT

Dr. Edward R. Ritter, Committee Member — date
Assistant Professor of Chemical Engineering, Villanova University

ABSTRACT

Pyrolysis and Oxidation of Chloromethanes
Experiment and Modeling

by
Wenpin Ho

An experimental study on pyrolysis and oxidation of CH_2Cl_2 and CH_3Cl in oxygen/hydrogen or oxygen/methane mixtures and argon bath gas was carried out at 1 atmosphere pressure in tubular flow reactors. Degradation of CH_2Cl_2, or CH_3Cl, along with the formation and destruction of intermediate and final products was analyzed systematically over 873 to 1273°K, with average residence times of 0.2 to 2.0 seconds.

Thermochemical parameters: enthalpy, entropy, and heat capacities for many chloro-oxy-carbon products and intermediates are calculated using the techniques of group additivity and the THERM computer code. Kinetic analysis on the reactions of hydroxy radical with vinyl chloride are performed using thermochemical analysis and a statistical chemical activation formalism based on the Quantum Kassel Theory for the addition reactions. The two abstraction paths have been also analyzed by using Evans-Polanyi relation for activation energy and Transition State Theory for pre-exponentials. Good agreement with the experimental data in the literature was obtained.

A nonlinear group additivity formalism to estimate the normal boiling points has been developed because boiling points are important to calculate critical properties needed for flame modeling. The model is straightforward and applies to compounds with a wide range of molecular weight, varied functional groups, and complex structures. We further utilize the proposed model for normal boiling points and adapt Joback's method into Benson type groups to calculate critical properties (Tc, Pc, Vc). Transport coefficients such as Lennard Jones Parameters (collision diameter and well depth), polarizability, and rotational relaxation collision numbers can also be estimated.

The same group information (input data) needed for thermo properties estimation is then used to estimate transport properties required in flame modeling.

A detailed kinetic reaction mechanism based upon fundamental thermochemical and kinetic principles, Transition State Theory and evaluated literature rate constant data is developed. The mechanism is used to model results obtained from our experiments, in addition to results from other studies, on the thermal reactions of CH_2Cl_2 and/or CH_3Cl. Comparison of the model to experimental data of other researchers for a wide range of conditions (tubular flow reactor, flat flame, perfect stirred reactor) showed good agreement in most cases.

Sensitivity analysis determined important reactions in the mechanism to several "target" products including reactions effective in inhibiting CO conversion to CO_2. The results indicate that the reaction OH + HCl ---> H_2O + Cl is a major cause of OH loss. This decrease in OH effectively stops CO burnout. In addition, the reaction H + HCl --> H_2 + Cl is also important when H_2 concentrations are very low. Sensitivity analysis also indicates that the reaction OH + OH <---> H_2O + O, which usually forms H_2O during hydrocarbon incineration, reacts in the reverse direction when HCl is present at concentrations comparable to CO, due to the large extent of OH depletion. The addition of moderate levels of high temperature steam are predicted to help CO conversion by shifting the above equilibria to more OH.

Knowledge and application of the reaction mechanisms to emulation of incineration operation allows calculation of modifications to incinerator design and/or feed to minimize pollutant formation. We predict that adding high temperature steam to the incinerators will improve Cl conversion to HCl by shifting the equilibrium of the OH + OH = H_2O + O reaction to the left. The viability of computer modeling is illustrated as a diagnostic for understanding and for improvement or optimization in combustion processes with assumed ideal mixing.

BIOGRAPHICAL SKETCH

Author: Wenpin Ho

Degree: Doctor of Philosophy in Chemical Engineering

Date: October 1993

Undergraduate and Graduate Education:

- Doctor of Philosophy in Chemical Engineering,
  New Jersey Institute of Technology, NJ, 1993
- Master of Science in Environmental Science,
  New Jersey Institute of Technology, NJ, 1989
- Bachelor of Science in Chemical Engineering,
  Chinese Culture University, Taiwan, R.O.C., 1984

Major: Chemical Engineering

Presentations and Publications :

Ho, W. and Bozzelli, J.W. "Reaction of OH Radical with C_2H_3Cl - Reaction Pathway Analysis", Chemical and Physical Processes in Combustion, p 665-669, 1993.

Ho, W. and Bozzelli, J.W. "Validation of A Mechanism for Use in Modeling CH_2Cl_2 and/or CH_3Cl Combustion and Pyrolysis", Twenty-Fourth International Symposium on Combustion, The Combustion Institute, Pittsburgh, PA, p743-748, 1992.

Ho, W., Yu, Q.R., and Bozzelli, J.W. "Kinetic Study on Pyrolysis and Oxidation of CH_3Cl in $Ar/H_2/O_2$ Mixtures", Combustion Science and Technology, vol.85, p23-63, 1992.

Ho, W., Barat, R.B., and Bozzelli, J.W. "Thermal Reaction of CH_2Cl_2 in O_2/H_2 Mixtures: Implications for Chlorine Inhibition of CO Conversion to CO_2", Combustion and Flame, vol.88, p265-295,1992

Ho, W., Yu, Q.R., and Bozzelli, J.W. "Kinetic Study on Pyrolysis and Oxidation of $CH_3Cl/CH_4/O_2$ Mixtures", Chemical and Physical Processes in Combustion, 1991.

Ho, W., Barat, R.B., and Bozzelli, J.W. "Mechanism of Acceleration and Inhibition in Hydrocarbon Combustion by Chlorocarbons or HCl", Organohalogen Compounds, vol.3, p87-90, 1990

Ho, W. and Bozzelli, J.W. "Thermal Decomposition of Dichloromethane in Hydrogen/Oxygen/Argon Mixtures and in Pure Oxygen", Chemical and Physical Processes in Combustion, vol. 27, no.1, p4, 1989

This thesis is dedicated to
Shu-hsia and Samantha

ACKNOWLEDGMENT

The author wishes to express his sincere gratitude to his advisor, Professor Joseph W. Bozzelli, for his precious guidance, expert assistance and patience throughout this research. I acknowledge the helpful corrections and productive comments by Dr. Barbara B. Kebbekus, Dr. Henry Shaw, Dr. Robert B. Barat, and Dr. Edward R. Ritter.

Special thanks to Dr. Edward R. Ritter for providing useful computer programs: THERM, CHEMACT, DISSOC, RADICAL, TRANSCAL, and INCIN. It is my pleasure to thank my colleagues at Kinetics Research Laboratory of the New Jersey Institute of Technology: Dr. Yangsoo Won, Dr. Greg Wu, and Dr. Edward R. Ritter who shared with me their experience. My appreciation for the friendship and assistance that I have received from current and past students in the laboratory can not be overstated, nor can it be fully expressed in this space.

Finally, I would like to thank my parents and my wife for their endless love and support. Without their encouragement, I would not have been able to accomplish my goal.

TABLE OF CONTENTS

Chapter **Page**

Chapter **Page**

Chapter **Page**

LIST OF TABLES

Table **Page**

LIST OF FIGURES

Figure **Page**

Figure **Page**

Figure **Page**

Figure **Page**

CHAPTER 1

INTRODUCTION

Chlorinated Hydrocarbons (CHC) have been used on a large scale by industry either as raw materials for production or as solvents; with both cases often leading to the production of large amounts of chlorinated organic wastes. Since the Toxic Substance Control Act (TSCA) was enacted in 1976, the disposal of chlorocarbons as industrial wastes has became more and more difficult and costly. One popular disposal method that has been used is landfill, but this method is not a permanent solution because of potential contamination of ground waters by leakage from the toxic waste site. In the USA where many storage sites that were deemed to be safe by waste producers now require remedistion at great cost, with the originators of the wastes having to pick up the bill. Newer processes including biological degradation, incineration and fixation in cement kilns are gaining market acceptance[1], because they destroy the toxic species, even though they are expensive.

Incineration seems to be a more effective way of handling the disposal of many wastes, such as combustible solids, semi-solids, sludge and concentrated liquid wastes. It reduces, if not eliminates, potential environmental risks and converts wastes into recoverable energy. When one compares incineration with other disposal options, advantages often become evident, especially as more wastes become regulated and added prohibitions and increasingly burdensome costs are placed on land disposal.

Although the incineration of hazardous wastes presents a viable and effective disposal methodology, the use of this technology has been severely hindered by environmental concerns regarding the effluents from such systems. Two important issues are the capability of incinerators to effect the high level of destruction that is desired and the possibility that other hazardous chemicals may be formed and thus impact the environment.

Hazardous waste incineration involving chlorine compounds deserves attention because the behavior of chlorine is unique among the halogenated compounds. Organic chlorine compounds serve as a source of chlorine atoms, which readily abstract H atoms from other organic hydrocarbons accelerating hydrocarbon production and soot formation. HCl is a desirable product because it removes the Cl and can be easily neutralized, but it can also inhibit combustion through reactions like OH + HCl --> H_2O + Cl, which depletes OH needed for CO burnout.

The incineration of chlorocarbons is generally performed in an oxygen rich environment that contains excess O_2 and N_2, in addition to the carbon and chlorine from the halocarbon, with relatively small amounts of available hydrogen from the limiting fuel operation[2]. One desired and thermodynamically favorable product from a chlorocarbon conversion process is HCl, providing there exists sufficient H_2 to achieve stoichiometric formation. The O-H bond in water is, however, stronger than the H-Cl bond and oxygen rich conditions favor H_2O and therefore limit hydrogen availability for HCl. Oxygen and Cl are, therefore, both competing for the available fuel hydrogen and this is one reason that chlorocarbons serve as flame inhibitors. The C-Cl bond is the next strongest compared with other possible chlorinated products such as Cl-Cl, N-Cl, or O-Cl bonds. Consequently, C-Cl may persist in a oxygen rich or hydrogen limited atmosphere[2]. This is one reason why emission of toxic chlorine-containing organic products persists through an oxygen-rich incineration, as carbon species are one of the more stable sinks for the chlorine. One possible method to obtain quantitative formation of HCl, as one of the desired and thermodynamically favorable products, from chlorocarbons, might be a straightforward thermal conversion of these compounds under a more reductive atmosphere of hydrogen. Here the carbon would be converted to a hydrocarbon such as ethane or ethylene.

The presence of chlorocarbons has long been known to slow or inhibit the oxidation rate of hydrocarbons through studies of flame velocity, temperature, and flame

stability. Westbrook[2] has modeled the inhibition of hydrocarbon oxidation in laminar flames by halogenated compounds. He suggested that the halogenated species serve to catalyze the recombination of H atoms into relatively nonreactive H_2 molecules, reducing the available radical pool, specifically H atoms, and thereby lowering the overall rate of chain branching. Senkan et. al.[3,4] have developed mechanisms for CH_3Cl, C_2H_3Cl, and HCl-doped CO oxidation flame systems. These later studies reached similar conclusions, suggesting that the reaction of H + HCl --> H_2 + Cl is responsible for the inhibition of CO conversion to CO_2 in the oxidations.

Alternately, Benson and Weissman[5] and Senkan et. al.[3] have reported that use of CH_3Cl in CH_4 or in CH_4 plus 2-3% O_2 respectively accelerated CH_4 conversion to higher hydrocarbons. They concluded that this might lead to effective methods for converting CH_4 to useful higher molecular weight hydrocarbons without either soot or excessive oxidation occurring[3].

Both acceleration and inhibition effects are apparent in hydrocarbon reaction systems with a chlorinated hydrocarbon present. Therefore, there is a significant need to develop quantitative insights into the mechanism of chlorocarbon pyrolysis and oxidation in order to better understand and ultimately to optimize these reaction processes, for use in conversion of chlorocarbons by incineration, or for use in CH_4 upgrading or other industrial processes.

In this study, a global rate constant and a detailed kinetic mechanism for the high temperature pyrolysis in H_2 and of combustion of dichloromethane (CH_2Cl_2) and methyl chloride (CH_3Cl) under fuel rich conditions are presented. I develop and use detailed chemical kinetic mechanisms for the high temperature combustion of chlorocarbons. The mechanisms are developed from fundamental thermochemical principles and used to model results obtained from our tubular flow experimental results. I also compare calculations using our model with data of other researchers, providing a wide range of experimental conditions to validate our mechanism. The data presented will be for 1 atm

reaction systems, but approximately 1/3 of the reactions in the mechanism are analyzed by using Quantum Kassel method of Dean[6,7] so the mechanism can be easily modified for use in other pressure regimes and still incorporate fall-off and pressure dependence.

Reactions of dichloromethane (DCM, CH_2Cl_2) with hydrogen but, without the presence of oxygen, have been studied throughly and systematically in these laboratories at NJIT.

Tsao[8] studied the thermal decomposition of DCM with hydrogen over the temperature range of 973 - 1173K, in a 1 atm total pressure tubular flow apparatus. Activation energies of the global bulk and wall reactions on hydrogen reaction with DCM were 50.0 Kcal/mol, 57.8 Kcal/mole, with Arrhenius A factors of 2.84E+10 and 2.65E+10 $sec.^{-1}$ respectively reported. The major products of reaction of DCM in the temperature range 973 to 1073 K were methane and methyl chloride. The minor products were ethylene, acetylene and HCl. Trace amounts of ethane, chloroethylene, 1,2--dichloroethylene, trichloroethylene, benzene were also observed. No chlorocarbons were found over 1223K and one second residence time where the only products were methane, hydrogen

chloride, acetylene, ethane and benzene.

Huang[9] studied the kinetics of the reaction of atomic hydrogen with DCM in a flow system at a pressure of 2.1 to 2.7 mm Hg and room temperature. The major products observed were hydrogen chloride and methane. The extent of conversion of DCM increases first to a maximum and then decreases with increasing concentration of DCM. Through the modeling of the reaction scheme and comparision with experimental data, the rate constant of the initial steps were determined as follows :

$H + CH_2Cl_2$ ----> $HCl + CH_2Cl$ (k_1)

$H + CH_2Cl_2$ ----> $H_2 + CHCl_2$ (k_2)

where

k_1 = 3.63 E+9 cm^3/mole/sec , 298 K

k_2 = 2.08E+7 cm^3/mole/sec , 298 K

Won[10] investigated the decomposition of dichloromethane/1,1,1--trichloroethane mixtures in a hydrogen bath gas. These experiments were carried out at one atmosphere total pressure in a tubular flow reactor. In his study, he demonstrated that selective formation of HCl can result from thermal reaction of chlorocarbon mixture and showed that synergistic effects of 1,1,1--trichloroethane decomposition accelerate the rate of DCM decomposition. There is significant interaction of the decay products from 1,1,1--trichloromethane with the parent dichloromethane.

Earlier kinetic studies on methyl chloride pyrolysis were reported in 1959 by Shilov and Sabirova[11]. Measurements were made at initial CH_3Cl pressures of 10.1-34.3 torr, temperatures of 1062K-1147K, and at contact times of 0.4- 5.0 seconds. They found HCl, CH_4, and C_2H_2 in the ratios of 3:1:0.6. These yields were reported to be consistent with the following proposed mechanism:

$CH_3Cl = CH_3 + Cl$

$CH_3 + CH_3Cl = CH_4 + CH_2Cl$

$Cl + CH_3Cl = CH_2Cl + HCl$

$2CH_2Cl = CH_2ClCH_2Cl$

$CH_2ClCH_2Cl = C_2H_3Cl + HCl$

$C_2H_3Cl = C_2H_2 + HCl$

They also reported that the measured apparent first-order rate constants increased with increasing pressure.

Slater's theory was used by Holbrook[12] to calculate the rate constant for the decomposition of CH_3Cl in the fall-off region. The value obtained was 5-6 orders of magnitude lower than the reported experimental values above. Frost and Laurent[13] obtained a better fit to this value using RRKM theory, where rotations were considered inactive, and activation energy was taken from the experimental data. With harmonic energy levels the calculated rate constant was 32 times smaller than experimental value,

and with a correction for an-harmonicity the calculated rate constant was only 20 times smaller. These modeling calculation may have indicated that the rate constants was not correctly fit experimental data.

In 1980, Kondo, Saito, Murakami[14] pyrolyzed CH_3Cl in a shock tube at temperatures between 1680K and 2430K, at total pressures of 1-5 atm, using reactant mixtures of 0.2%-0.5% methyl chloride in argon. CH_3 concentrations were measured via the CH_3 absorption band at 216 nm. From the initial rate of CH_3 formation the elementary rate constant for breaking the C-Cl bond was obtained. The reaction was in the fall-off region even at the highest pressures. For these high temperature shock tube data, the mechanism was considered to include the following likely reactions:

$CH_3Cl + M = CH_3 + Cl + M$ (1)

$CH_3Cl + Cl = CH_2Cl + HCl$ (2)

$CH_3Cl + CH_3 = CH_2Cl + CH_4$ (3)

$CH_3Cl + CH_2Cl = CH_3 + CH_2Cl_2$ (4)

$C_2H_6 + M = 2CH_3 + M$ (5)

$Cl_2 + M = 2Cl + M$ (6)

$2CH_2Cl = C_2H_4Cl_2$ (7)

$C_2H_4Cl_2 = C_2H_3Cl + HCl$ (8)

$C_2H_3Cl + M = C_2H_2 + HCl + M$ (9)

$CH_2Cl + CH_3 = C_2H_5Cl$ (10)

$C_2H_5Cl = C_2H_4 + HCl$ (11)

$C_2H_4 + M = C_2H_2 + H_2 + M$ (12)

Computer simulation of the CH_3 profiles without reaction (4), and with k_7 and k_{10} equal to k_5 fitted the experimental data at high temperatures exactly and were higher by a factor of 2 at low temperatures. Low- and high-pressure rate constants (ko [Ar] and $k\infty$) were obtained from the experimental data by applying a refined RRKM theory which involved a weak collision effect: logko/[Ar] = 12.56- 59/θ L/mole/sec log $k\infty$ = 13.86-91.0/θ sec-1.

The low-pressure rate constant is in agreement with the value derived by Holbrook[12] from the data reported in reference 11.

Data on the pyrolysis of CH_3Cl at a high degree of conversion were reported by LeMoan[15]. The reaction was run at 993K for 30 hours in a batch reactor yielded conversions larger than 95%. The gas phase contained HCl, CH_4, and small quantities of H2, benzene, and toluene. Low transient concentrations of CH_2Cl_2, C_2H_6, and C_2H_5Cl were detected at the beginning of the pyrolysis. In the liquid phase, benzene (72%), toluene (11%), xylene (1%), and monochlorobenzene (12%) were identified. There were two distinct solid phases: carbon in the reactor and naphthalene and soot at the exit from the reactor. The reaction mechanism, despite the large number of products identified, was considered to be schematically simple. It was proposed that, initially, CH_3Cl would decompose into HCl and $^1CH_2$, which would dimerize into C_2H_4 or decompose into CH + H or C + H_2. The combination of two CH radicals would form acetylene. Acetylene would combine, then cyclize to form benzene, from which the identified higher molecular weight compounds would be formed. The hydrogenation of CH_2 radicals would lead to methane. As we shall see later, this mechanism is not plausible.

CH_3Cl decomposition was also studied by Weissman and Benson[5] using a flow system to generate product distributions at temperatures of 1260 and 1310K and over the pressure range of 180 - 370 torr. They measured CH_4, C_2H_2, C_2H_4, and HCl as the major products with lower quantities of aromatic hydrocarbons and soot using Gas Chromatography and Mass Spectrometry techniques.

In 1988, Senkan et al.[16] constructed a CH_3Cl combustion mechanism by combining a mechanism describing CH_4 combustion together with a sub-mechanism describing the chlorine inhibition of CO oxidation. This mechanism was used to calculate the stable species concentration profiles in atmospheric pressure sooting (fuel rich) $CH_3Cl/CH_4/O_2/Ar$ premixed flat flames. Their studies concluded that CH_3Cl promotes not only the decay of CH_4 to CO_2 and H_2O but also soot formation by

simultaneously increasing the rates of C_2H_3 and C_2H_2 formation. However a number of their rate constants were from estimation techniques and their mechanism extended only up to C_2-species. The C_1 reaction mechanism involving unimolecular decomposition, abstraction, and oxidation is reasonably well understood in describing CH_4 combustion at present. The C_2 chemistry, however, is in need of improvement, specifically the reactions of chlorinated C_2 radicals. Thermal decomposition, oxidation by O and O_2, recombination and addition of CH_3 and C_2 radicals are five competitive reactions. These are all important because Cl abstracts H rapidly (high Arrhenius A factor and low energy of activation), which produces the active hydrocarbons and a H radical pool early in the reaction. These hydrocarbon radicals combine to form more C_2 radicals due to the presence of Cl atoms. The C_2 chemistry is therefore more important here even though the species at molecular weights above 2 carbons account for under 15% of the carbon in the $CH_3Cl/CH_4/O_2$ system.

Miller et al.[17] studied the high temperature product distributions from reaction of CH_4 and CH_3Cl under pyrolysis, preignition oxidation and flame conditions. For pyrolysis and preignition studies, 3% fuel/zero O_2 or stoichiometric O_2/10% N_2/Ar were heated behind reflected shocks to temperatures between 1200 - 2600K at a density of 2.5 $\pm$ 0.25 x 10^{-5} mole/cm^3. Flame studies were conducted at atmospheric pressure for CH_4/air and CH_3Cl/CH_4/air mixtures with equivalence ratios of 1.15 and 1.35 respectively. They reported that CH_3Cl is more easily decomposed than CH_4 in either pyrolysis or preignition oxidation. In the flame environment, the CH_4 and CH_3Cl disappear at approximately the same rate. They also reported that the presence of chlorine decreases the measured ethane concentration and promotes the formation of acetylene which may explain the propensity for soot formation from chlorinated hydrocarbons.

Roesler et al.[18] studied moist CO oxidation chemistry inhibited by HCl experimentally and numerically with dilute mixtures of CO (~1%), H_2O (~0.5%), O_2 and HCl reacting in N_2 at a temperature near 1000K. The effect of increasing the Cl/H ratio

was investigated by increasing HCl concentrations from 0 to 200 ppm while the effect of excess O_2 was studied by varying the fuel oxidizer equivalence ratio from 1.0 to 0.33. The results showed that small quantities of HCl inhibit CO oxidation and that increasing O_2 concentrations to stoichiometric mixtures further decreases the oxidation rate, a counter intuitive result. They used sensitivity and reaction flux analysis to determine the rate-controlling inhibition steps/pathways created by HCl. They found the principal chain terminating step at 1000K to be the reaction $Cl + HO_2 \text{---> } HCl + O_2$.

Experimental and numerical studies of the thermal destruction of CH_3Cl in the post-flame zone of a turbulent combustor under fuel lean conditions (equivalence ratio 0.3 - 0.6) were conducted by Koshland et al.[19] Their results showed that there is an optimal concentration level (ca. 100 ppm) where CH_3Cl is most effectively destroyed in the post-flame region, with higher or lower levels more difficult to destroy. They proposed that the injection of fuels into the post-flame region (under fuel lean conditions) can increase the destruction efficiency or reduce the peak temperature needed for adequate destruction of CH_3Cl and its by-products by increasing the radical concentrations and the rate of subsequent destruction reactions.

A recent study on the pyrolysis and oxidation of CH_3Cl was also conducted by Huang and Pfefferle[20] using a tubular flow reactor at 863.4 torr and a temperature range from 1100 to 1350K. They modified two models published by Senkan and by Miller primarily increasing the rate for the initial CH_3Cl pyrolysis and by adding two routes for reaction of oxygen with CH_2Cl to formaldehyde and chloroformaldehyde. They concluded that the CH_3Cl decomposition was faster than previously reported.

Although some investigations of the reaction of H_2/O_2 with chloromethanes have been implemented, detailed kinetic models of these reactions are necessary to explain the experimentally observed behavior. It is hoped that, taken together, these steps will adequately describe the experimental observations.

CHAPTER 2

EXPERIMENTAL METHOD

2.1 Experimental Apparatus

A diagram of the experimental apparatus is shown in Figure 2.1. The high temperature tubular flow reactors, operated isothermally and at atmospheric pressure in this study. The tubular flow reactor was made of quartz and maintained at a constant temperature by a three-zone oven, with each zone controlled separately.

Argon, carrier gas, was passed through one set of series saturation bubblers in parallel to pick up the Dichloromethane which was kept at 0°C using an ice bath. A second line of argon (after the bubblers) was brought in as make-up to meet the exact ratio of flow needed. Oxygen and hydrogen were then brought into the flow stream as required. Before entering the reactor, the mixtures were preheated to limit cooling at the reactor entrance and help ease the reactor heating requirement. Each quartz reactor tube was housed within a three--zone Lindberg electric tube furnace.

The reactor effluent was monitored by an on-line Gas Chromatograph (GC) equipped with a Flame Ionization Detector (FID) and either a Thermal Conductivity Detector (TCD) or a methanation catalyst converter (for CO and CO_2) & FID. The lines between the reactor exit and the GC were heated to 80°C to limit condensation. When the reactor inlet switch valves were properly selected, the vapor mixture would be transferred directly from the bubbler to the GC sampling inlet via a reactor by-pass line. This was necessary to determine the GC peak area which corresponded to the initial input concentration (and ratio) of the mixtures. The reactor effluent gas passed through a heated 85°C transfer line to the GC gas sample valve and exhaust.

In this experiment, three different diameter reactors were studied. They were 4.0, 10.5, and 16 mm ID and allowed us to vary reactor surface to volume (S/V) ratio. Use of these S/V ratios allowed us to decouple apparent wall and bulk phase decomposition rates

using a plug flow assumption and pseudo first order reaction system. The pseudo first order reaction was first validated for each reactor via straight line graphs on a ln C/Co versus time plot where C is concentration of parent chlorocarbon.

Outlet gases from the reactor were passed to the GC through Pyrex tubing, packed with glass wool to trap carbon particles and prevent contamination of the GC sampling valve. The bulk of the effluent was passed through a sodium bicarbonate ($NaHCO_3$) flask for neutralization before release to the atmosphere via a fume hood.

2.2 Temperature Control and Measurement

This study was carried out with nearly isothermal reaction conditions (± 5°C) at the desired temperature using a three zone furnace. Each zone was equipped with independent solid state temperature controllers (Omega Engineering, Inc.). These controllers operated a solenoid for switching of a controlled voltage (time proportional switching) to the respective heater.

The circuitry for the temperature controller operated solenoids and Variac control of the switched voltage (via relays) was designed at NJIT. It is described here for completeness.

1. Both the relays and Omega temperature controllers were operated via 110 volt AC; i.e. the coil in the relays was run at 110 VAC.
2. The voltage applied to the relay contacts; i.e. voltage that is applied to the heater coils, was controlled with a Variac of proper current rating.
3. The resistance heater voltage was typically 50% of the rated capacity of the heater and thus insured long life of the heater elements.
4. A schematic of voltage and thermocouple inputs to temperature controller is shown in Fig 2.2.

The actual temperature profile of the tubular reactor was obtained using a K type thermocouple which could be moved coaxially within reactor from one end to the other. The temperature measurement was performed with a steady flow rate of argon gas through the reactor to emulate actual reaction conditions. Temperature profiles obtained as shown in Figure 2.3 were isothermal to within ± 5°C for 41.9 cm of reactor length.

2.3 Quantitative Analysis of Reaction Products

A Perkin Elmer 900 gas chromatograph with FID/TCD or FID/catalyst converter FID was used on-line to quantitatively determine the concentration of the reaction products. The lines between the reactor exit and the GC were heated to 85°C to limit condensation. The GC column for the FID is a 1.5 m long by 1/8" O.D. stainless steel tube packed with 1 % Alltech AT-1000 on Graphpac GB and the column for the TCD is a 1.8 m long by 1/8" O.D. stainless steel tube packed with GCA-013 SPHEROCARB 100/120 mesh.

The GC inlet sampling used a ten port sample valve (Valco Instrument Co.) with two 1.0 ml volume loops maintained at 175°C and 1 atm pressure (allowed dual sample injections onto each GC column). When the sample valve was in the load position, Helium, carrier gas, passed directly to GC column and reactor effluent gas filled these two sample loops. Turning the valve to the inject position, Helium would go into the sample loops and then flush the sample into the two different columns and detectors.

Integration of the peaks on each chromatogram was performed with a dual channel Spectraphysics 4270 integrator using an attenuation of 1 and chart speed of 0.25 cm/min. Representative chromatograms are shown in Figure 2.4, 2.5 and Table 2.1 with retention times and peak identification.

Table 2.1 Average Retention Time of Products

Compounds	Average Retention Time (min.)
CH_4	1.55
C_2H_2	1.95
C_2H_4	2.20
CH_3Cl	3.65
$C_3H_6 + C_3H_8$	5.45
C_2H_3Cl	6.40
CH_2Cl_2	8.80
C_4H_{10}	10.40
CH_2CCl_2	11.15
CHClCHCl	12.45
$CHCl_3$	15.10
$CHClCCl_2$	16.70
$CH_2ClCHCl_2$	17.60
H_2	0.9 (TCD)
O_2	1.9 (TCD)
CO	3.1 (TCD)
CH_4	6.3 (TCD)
CO_2	9.8 (TCD)

Calibration of the flame ionization detector to obtain appropriate molar response factors was done by injecting a known quantity of the relevant compound such as CH_4, C_2H_6, CH_2Cl_2, C_2H_3Cl etc., into the injection port then measuring the corresponding response area. The relative response factor has been determined for compounds shown in Table 2.2. The response factors for C_1 compounds are all similar which is consistent with the converter that FID's are carbon counters and that we had sufficient H_2 flow to convert the Cl's to HCl as well as hydrogen to H_2O, and the response factor of C_2 compounds are nearly twice the response of C_1 compounds. These results agree with the general principle of flame ionization detector which is well known as a carbon counter[21]. Thus, the effect of chlorine on the relative response factor can be neglected for this flame ionization detector and the relative response factors can be considered to correspond the number of carbon in the molecule. Based on the experimentally verified relative response

factors, the specific component peak area from each set of samples was converted to the equivalent number of moles of each compound.

A series of eight residence times at each reaction temperature were run for a given inlet concentration set by systematic variation in the total flow rate, while maintaining a constant reactant ratio. Every third run was repeated to ensure reproducibility of results.

Table 2.2 Relative Response Factor in FID and TCD

Compounds	Relative Response Factor (RRF)
Methane CH_4	1.07
Acethylene C_2H_2	1.60
Ethylene C_2H_4	2.00
Ethane C_2H_6	1.96
Propene C_3H_6	3.47
Propane C_3H_8	3.42
Dichloromethane CH_2Cl_2	1.00
Butane C_4H_{10}	4.31
1,1 Dichloroethylene CH_2CCl_2	2.10
1,1,1 Trichloroethane CH_3CCl_3	1.85
Chloroform $CHCl_3$	0.98
Tetrachloromethane CCl_4	1.18
1,1,2 Trichloroethane $CH_2ClCHCl_2$	2.10
Hydrogen H_2	0.02 (TCD)
Oxygen O_2	1.71 (TCD)
Carbon monoxide CO	2.25 (TCD)
Carbon dioxide CO_2	1.82 (TCD)

2.4 Hydrochloric Acid Analysis

Quantitative analysis of HCl product was performed for reactions in each reactor and residence time. The samples for HCl analysis were collected independently from the GC sampling as illustrated as Figure 4.1. In this analysis, the effluent was bubbled through a two stage bubbler before being exhausted to the fume hood. Each stage contained 20 ml of 0.01 M NaOH and two drops of phenolphthalein indicator. The gas passed through

these two stage bubblers until the first stage solution reached its end point. The time required for this to occur was recorded. At this point, the bubbling was stopped and the two solutions were combined. The effluent HCl concentration was calculated based upon titration of the combined solution with standardized 0.01 M HCl to the phenolphthalein end point. Several titrations were performed using buffered solution (pH 4.7) to discern if CO_2 was affecting the quantitative measurement of HCl. No significant effect was observed due to the relatively low levels of CO_2.

2.5 Qualitative Identification of Reaction Products

Positive identifications of all reactor effluent species were made by GC/Mass Spectrometry applied to batch samples drawn from the reactor exit into previously evacuated 25 ml stainless steel or Pyrex glass sample cylinders. A Finnigan 4000 series GC/MS, with a 50m×0.22mm I.D. methyl silicone stationary phase column was used. Gas samples were inlet by cryofocussing (at 78 K) on a 12 cm length of the capillary column.

CHAPTER 3

ESTIMATION OF THERMOCHEMICAL DATA

Thermochemical data are required to determine the energy balance in chemical reactions and in determining the Gibbs free energy of a reaction as a function of temperature. It also provides a convenient way to determine reverse reaction rate constants from the calculated equilibrium constant of the reaction and the known forward rate. In this study, a detailed elementary reaction mechanism has been developed based upon literature data, general trends, fundamental thermodynamic principles and Transition-State-Theory[22]. An accurate thermodynamic database for all radical and molecular species in the mechanism is extremely important. In addition, the thermochemical parameters including enthalpy of formation, entropy and heat capacities for many chloro-oxy-carbon products and intermediates have not been previously measured or calculated and they are required for input to detailed modeling codes.

The thermochemical database including enthalpy of formation (H_f), entropy (S_f), and heat capacities (Cp) is based upon our evaluation of the best currently available thermochemical data. Appendix A shows a summary of the species involved and thermochemical quantities employed. When experimental thermochemical data were not available, the values were estimated using the techniques of group additivity and the THERM[23,24] computer code.

The use of group additivity methods and THERM is described in detail in references 23, 24, and THERM user manual. Thermodynamic data can often be calculated easier and faster using THERM than if one searched through the literature.

When required properties for various Benson type groups[22] were not available, estimates were made based on reasonable modifications of the properties of groups from similar compounds or from properties of a series of species with the concerned chemical functional group. Items considered were structure, number of chlorines, effect of Cl atom

on intramolecular bond strength and Cl - Cl repulsion. After estimating the data, the estimated data were compared to recently published experimental data where available. If the experimental measured data were not available, the estimated data were judged reasonable if similar results were obtained by two different estimation methods such as shown in the following example.

Two different methods are used and their results compared to estimate the H_f^{298} for CH_2ClOH. Group additivity was then used to back calculate the C/Cl/H2/O group.

Method 1. CH_2ClOH ---> $CH_2Cl + OH$

$\Delta H_{rxn} = -H_f(CH_2ClOH) + H_f(CH_2Cl) + H_f(OH) = BE$

$= -H_f(CH_2ClOH) + 29.1 + 9.45 = -H_f(CH_2ClOH) + 38.6$

H_f^{298} of 29.1 Kcal/mole for CH_2Cl, 9.45 Kcal/mole for OH. The existence of Cl affects a Resonant Stabilization Energy (RSE) as illustrated below:

BE of CH_3 - H and BE of CH_2Cl - H, that is, 105.1 - 100.8 = 4.3 Kcal/mole

CH_4 ---> $CH_3 + H$ ΔH_{rxn} = 105.1 Kcal/mole (BE of CH_3 - H)

CH_3Cl ---> $CH_2Cl + H$ ΔH_{rxn} = 100.8 Kcal/mole. (BE of CH_2Cl - H)

The RSE due to Cl is 105.1 - 100.8 = 4.3 Kcal/mole. Hence BE of CH_2Cl - OH is 92.7 - 4.3 = 88.4 Kcal/mole, where 92.7 is the CH_3 - OH bond.

Therefore

$H_f(CH_2ClOH) = 38.6 - 88.4 = -49.8$ Kcal/mole

Method 2. CH_2ClOH ---> $CH_2OH + Cl$

$\Delta H_{rxn} = -H_f(CH_2ClOH) + H_f(CH_2OH) + H_f(Cl) = BE$

$= -H_f(CH_2ClOH) - 2.16 + 28.9 = -H_f(CH_2ClOH) + 26.74$

Start with the bond energy of CH_3 - Cl, which is 83.61 Kcal/mole. Here the presence of OH effects a Resonant Stabilization Energy (RSE) as shown:

BE of CH_3 - H and BE of CH_2OH - H, that is, 105.1 - 98 = 7.1 Kcal/mole for the RSE due ti OH.

CH_4 ---> CH_3 + H ΔH_{rxn} = 105.1 Kcal/mole

CH_3OH ---> CH_2OH + H ΔH_{rxn} = 98 Kcal/mole

Hence 83.61 - 7.1 = 76.51 Kcal/mole is the BE for CH_2Cl - OH. Therefore

$H_f(CH_2ClOH)$ = 26.74 - 76.51 = -49.77 Kcal/mole

The enthalpy of formation for CH_2ClOH is -49.8 Kcal/mole. We can now use this H_f^{298} for calculation of the C/Cl/H2/O group

Species	H_f
C/Cl/H2/O	?
O/C/H	-37.9
CH_2ClOH	-49.8

C/Cl/H2/O = -49.8 - (-37.9) = -11.9

We can further calculate corresponding groups using the same estimation method. The calculated results are listed in Table 3.1

Table 3.1 New groups for C/Cl/H/O

Groups	H_f
C/Cl/H2/O	-11.9
C/C/Cl/H/O	-14.6
C/Cl2/H/O	-15.1
C/C/Cl2/O	-18.37

The above groups were input into the THERM computer code to calculate H_f for CH_2ClOOH and $CHCl_2OOH$. Results were compared with the estimation method results. As shown in Table 3.2, the estimation results are in good agreement with the THERM[20] group additivity.

Estimations of entropy and heat capacity are made based on reasonable modifications of the values of similar groups. In this example, the contribution of S of (C/C/Cl/H/O) can be estimated from the S of (C/C2/Cl/H) because the carbon atom is similar to oxygen atom in mass. This assumption must be varified and compensate the

difference between C and O. We can look at the difference between S(C/C2/H2) group versus S(C/C/H2/O) group and S(C/C/H3) group versus S(C/H3/O) group.

Table 3.2 Validation of estimation method

Reaction	BE	H_f	THERM
CH_2ClOOH ---> $C.H_2OOH + Cl$	72.51	-32.59	-32.7
CH_2ClOOH ---> $CH_2Cl. + OOH$	64.90	-32.30	
CH_2ClOOH ---> $CH_2ClO. + OH$	104.0	-32.68	
$CHCl_2OOH$ ---> $C.HClOOH + Cl$	69.70	-36.30	-35.90
$CHCl_2OOH$ ---> $CHCl_2 + OOH$	62.90	-35.90	
$CHCl_2OOH$ ---> $CHCl_2O. + OH$	44.28	-35.88	

From THERM group database,

S(C/C2/H2) - S(C/C/H2/O) = 9.42 - 9.8 = -0.38

S(C/C/H3) - S(C/H3/O) = 30.41 -30.41 = 0.0

Set the adjustment in S^{298} as -0.38 for substitution of O for C. Then:

S (C/C2/Cl/H) - S (C/C/Cl/H/O) = S (C/C2/H2) - S (C/C/H2/O) = -0.38

S (C/C/Cl/H/O) = S (C/C2/Cl/H) + 0.38 = 17.6 + 0.38 = 17.98

Based upon the above calculation, we can further estimate S(C/Cl/H2/O) group.

S (C/C2/Cl/H) - S (C/C/Cl/H2) = S (C/C/Cl/H/O) - S (C/Cl/H2/O)

S (C/Cl/H2/O) = S (C/C/Cl/H/O) - S (C/C2/Cl/H) + S (C/C/Cl/H2)

= 0.38 + 37.8 = 38.18

The estimation technique for heat capacity is similar to the above calculations for S. The final calculation results are listed in Table 3.3.

Table 3.3 New groups for S^{298} and Cp

Groups	S^{298}	Cp_{300}	Cp_{400}	Cp_{500}	Cp_{600}	Cp_{800}	Cp_{1000}
C/Cl/H2/O	38.18	8.39	10.60	12.35	13.48	15.35	16.69
C/C/Cl/H/O	17.98	8.49	9.80	9.95	11.28	13.94	14.59
C/Cl2/H/O	44.08	11.59	13.90	15.45	16.58	17.94	18.69
C/C/Cl2/O	22.78	11.69	14.78	16.00	16.56	17.00	17.01

CHAPTER 4

ESTIMATION OF KINETIC PARAMETERS

4.1 Background

Benson postulated that in a dilute gas there are only two type of elementary kinetic processes. The first is unimolecular process wherein an energetically activated chemical species reacts, when it is isolated from other gas phase species by internal rearrangement of atoms, breaking a bond, or molecular elimination. The second process is bimolecular and requires the collision of two chemical species to form a collision complex. The resulting collision complex is an energized adduct which follows a subsequent unimolecular chemical process.

There are extensive rate constant data for hydrocarbon (HC) oxidation processes and methods have been developed for making estimations. Allara and Shaw[25] carried out a systematic kinetic study on the thermal degradation of n-alkane molecules. Unfortunately, most of those measurements are at low temperature; therefore, the results must be extrapolated and a certain degree of error is introduced here.

Baulch et al.[26] have published an extensive review of the kinetic data for the reaction of inorganic chlorinated species with themselves and with other atoms and diatoms likely to be found in a combustion system. There exists a considerable base of older data on the reactions of chlorine with organic systems due to the industrial importance of the chlorination of hydrocarbons.

Atkinson et al.[27] update and extend the previous critical evaluations of the kinetics and photochemistry of air pollutant chemical reactions on a routine basis. The NIST Chemical Kinetics Database[28] provides a tool for rapidly examining the literature for the chemical kinetics community. The program will find data on a particular reaction, all of the reactions of a species, or subsets of all of the reactions.

4.2 Unimolecular Dissociation

4.2.1 Simple fission

Based on Transition-State-Theory (TST), the rate constant for simple fission can be expressed in thermodynamic terms, since it is more useful to work with the rate constant in this form than with partition functions. Consider the unimolecular reaction

$CH_2Cl_2 \leftrightarrow CH_2Cl_2^{\#} \dashrightarrow CH_2Cl + Cl$

The first order rate constant for decomposition of CH_2Cl_2 is given by

$k = (k_BT/h)K_{eq}^{\#}$

where $K_{eq}^{\#}$ is the equilibrium constant for formation of the $[CH_2Cl_2]^{\#}$ complex.

($^{\#}$ denotes a Transition-State-Theory complex)

If the equilibrium constant is expressed in terms of the molar Gibbs free energy using the van't Hoff relation $\Delta G^{\#} = -RT \ln K_{eq}^{\#}$

the rate constant can be written as

$k = (k_BT/h)\exp(-\Delta G^{\#}/RT)$

where k_B, h, R are the Boltzman, Planck's and gas constant respectively.

$\Delta G^{\#}$ may be expressed in terms of enthalpy (ΔH) and entropy (ΔS) changes by

$\Delta G^{\#} = \Delta H^{\#} - T\Delta S^{\#}$

In thermodynamic language

$k = (k_BT/h)\exp(\Delta S^{\#}/R)\exp(-\Delta H^{\#}/RT)$

This equation is similar to the Arrhenius equation

$k = A\exp(-E_a/RT)$

and the thermodynamic parameters can be related to the Arrhenius parameters. We can use thermodynamics and equilibrium theory to estimate the Arrhenius activation energy in terms of the thermodynamic properties of the transition state:

$d(\ln k) / dT = E_a/RT^2$

From $k = (k_BT/h)K_{eq}^{\#}$ and differentiating with respect to T gives

$d(\ln k)/dT = 1/T + d(\ln K_{eq}^{\#})/dT$

Since $K_{eq}^{\#}$ is a equilibrium constant, its variation with temperature is given by the Gibbs-Helmholtz equation

$d(\ln K_{eq}^{\#})/dT = \Delta E/RT^2$

Comparing with Arrhenius activation energy, we can obtain

$E_a = RT + \Delta E$

Since $H = E + PV$, for a constant-pressure process and there is no change in the number of molecules in going from the reactants to the transition state (ΔV is zero); therefore, in this case

$E_a = \Delta H^{\#} + RT$

Insertion of this equation into

$k = (k_B T/h)\exp(\Delta S^{\#}/R)\exp(-\Delta H^{\#}/RT)$

leads to

$k = (ek_B T/h)\exp(\Delta S^{\#}/R)\exp(-E_a/RT)$

Hence

$A = (ek_B T/h)\exp(\Delta S^{\#}/R)$

where T is the temperature at which the experiments have been carried out.

Usually, $\Delta S^{\#}$ is unknown, therefore A factors are estimated from literature values or by using generic reaction series. In this case, a comparison of the reaction to a similar reaction system, where the rate parameters are known is made. As listed in Table 4.1, 4.2, and 4.3, the generic reaction series shows a consistent trend based on heat of reaction. We can also estimate $\Delta S^{\#}$ from statistical mechanics and an assume Transition-State structure geometry. In pratice we do not use the Transition-State thermodynamic $Ea^{\#}$ or $H^{\#}$ but often use conventional thermodynamic properties which are known.

Table 4.1 C-H Rupture in Hydrocarbon Molecules

Reactions	log A	E_a	ΔH
CH_4 ---> CH_3 + H	15.4	105.0	104.8
C_2H_6 ---> C_2H_5 + H	15.3	100.7	100.7
C_3H_8 ---> C_3H_7 + H	15.4	100.7	100.7
C_4H_{10} ---> C_4H_9 + H	15.4	100.7	100.7

(Ref: Dean, A.M., J. Phys. Chem., 89, 4600, 1985)

Simple unimolecular (elimination) rate constants are determined by two methods similar to beta scission reactions. The unimolecular Quantum Kassel formalism was used. Here, the reverse reaction (combination) parameters for the high pressure case are determined. Then the corresponding high pressure unimolecular beta scission rate constants using microscopic reversibility <MR> are calculated.

$\Delta G = - RT \ln K_{eq} = \Delta H - T\Delta S$ for the reaction

$\Delta H/RT - \Delta S/R = (E_f - E_r)/RT - \ln(A_f / A_r)$

where f and r denote forward and reverse reaction.

Transforming the above equation to a standard state expressed in concentration units:

$(\Delta H_c + \Delta nRT)/RT - (\Delta S_c + \Delta nR\ln(R'T))/R = (E_f - E_r)/RT - \ln(A_f / A_r)$

where Δn is the mole change in the reaction.

$(E_f - E_r) = \Delta H_c$

$\ln(A_f / A_r) = \Delta S_c/R + \Delta n \ln(eR'T)$

The high pressure unimolecular elimination parameters are then input to the Quantum Kassel formalism to calculate the apparent rate constants at the appropriate pressure. The second method is simple use of the reverse rate constants from the Quantum Kassel combination reaction calculations.

Table 4.2 C-C Rupture in Hydrocarbon Molecules

Reactions	log A	E_a	ΔH
C_2H_6 ---> CH_3 + CH_3	16.9	89.4	89.8
C_3H_8 ---> C_2H_5 + CH_3	16.9	84.4	85.5
C_4H_{10} ---> C_3H_7 + CH_3	17.0	84.7	85.9
C_4H_{10} ---> C_2H_5 + C_2H_5	16.9	80.2	81.9
C=CC ---> C=C. + CH_3	16.9	99.5	100.3

(Ref: Dean, A.M., J. Phys. Chem., 89, 4600, 1985)

Table 4.3 C-H Rupture in Hydrocarbon Radicals

Reactions	log A	E_a	ΔH
C_2H_5 ---> C=C + H	13.2	40.9	38.7
CCC. ---> CC=C + H	12.8	38.5	36.0
CCCC. ---> CCC=C + H	12.7	38.3	36.1
C=CC. ---> CC=C=C + H	13.1	61.3	58.9
CC.C ---> CC=C + H	12.8	39.6	38.8
CCC.C ---> CCC=C + H	12.7	39.6	39.1
CCC.C ---> CC=CC + H	12.2	39.6	36.4

(Ref: Dean, A.M., J. Phys. Chem., 89, 4600, 1985)

4.2.2 Complex fission (molecular elimination)

The second kind of unimolecular reaction is the formation of a cyclic transition state and the elimination of a molecule. For example, we may consider the elimination of HCl from chlorinated hydrocarbons (CHCs); for example,

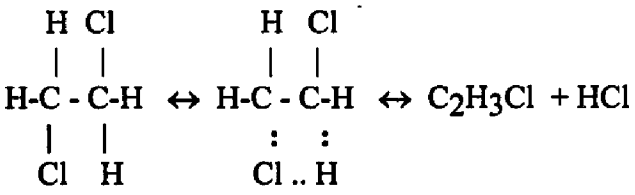

These seem to involve four atoms in a ring transition state and are refered to as four-center reaction. Cases are also found of three-center reactions:

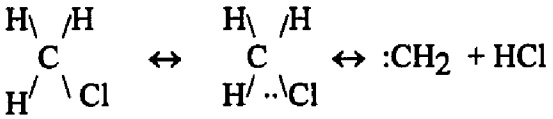

Benson[22] declared that the overall rate constants for these kinds of reactions are dependent on the relative rate of ring closure and biradical fission and are not completely understood. We may estimate Arrhenius A factor from Transition-State-Theory [22](TST)

$A = (ek_BT/h)\exp(\Delta S^{\#}/R)*g$

where g is degeneracy; for example, CH_2ClCH_2Cl ---> $C_2H_3Cl + HCl$

each of 2 Cl's can react with 2 H's, so g = 2 *2 = 4. $\Delta S^{\#}$ is about -4.3 cal/mole/K for loss each rotor (C-C bond).

Activation energy E_a can be estimated as

$E_a = \Delta H$ + Energy Barrier

Bozzelli[29] proposed that the energy barrier is about 35 - 45 Kcal/mole. Zabel[30] indicated that for

C_2H_3Cl ---> $C_2H_2 + HCl$

The energy barrier is 45 Kcal/mole. Here, we break two single bonds add to double bond to form a triple bond, with no rotor loss because of the double bond.

In this study, we calculated a barrier for CH_3Cl three-center reaction to ^{1}:CH_2 + HCl of 3.75 Kcal/mole. The E_a is from analysis of reaction of ^{1}:CH_2 which is widely shown to insert into hydrocarbons with an E_a of 0.0 and on insertion of ^{1}:CCl_2 into HCl, which we have experimentally measured to be 15 Kcal/mole. One possible reason for this apparent activation energy is that the electrons from the Cl atom may reduce the ability of the un-occopied orbital on the singlet methylene to combine with bonding electrons in the molecule.

An Evans-Polanyi[22] relationship between Ea and ΔH for HCl elimination reaction can be made. A plot of Ea versus ΔH for HCl elimination reaction is shown in Fig. 4.1. A best fit relationship of Ea = 1/2 (ΔH + 100) is obtained for the ΔH = 0 - 100 Kcal/mole range.

4.2.3 Beta Scission Reactions

These reactions utilize the Quantum Kassel formalism and are treated in one of two ways. In the first method, a Quantum Kassel formalism is used. The reverse reaction (addition) parameters for the high pressure case are determined. The corresponding high pressure unimolecular beta scission rate constants using microscopic reversibility <MR> are then calculated. The high pressure unimolecular elimination parameters are then input to the Quantum Kassel formalism to determine the high pressure limit and to calculate the apparent rate constants at the appropriate pressure. The second method is simple use of the reverse rate constants from the QRRK calculations.

4.3 Bimolecular reactions

4.3.1 Abstraction reaction

There are two types of abstraction reactions: first is atom + stable molecule

A + RH ---> AH + R.

second is radical + stable molecule

R. + R'H ---> RH + R'.

Abstraction reaction rate constants are not pressure dependent and therefore do not incorporate any Quantum Kassel Analysis. The rate constants are taken from evaluated literature[28,31] wherever possible. When estimation is required for an abstraction rate constant, a generic reaction is used as a model and adjusted for steric effects as best we can. An example of the generic type of Arrhenius A factor analysis is Cl atom abstracting an H from 1,1, dichloroethylene, where experiments can not determine whether the measured values are for the abstraction or the addition reaction. Use the abstraction by Cl of H from 1,1,1 Trichlorethane where both the mass and the reaction degeneracy are similar. The Ea is calculated separately.

Typical A factors range for abstraction reactions range from 1.0E11 to 1.0E14. Bozzelli[29] summarized A factors for different atoms and radicals as lised in Table 4.4.

Table 4.4 Kinetic Parameters for Varies Types of Reactions

Type of Reaction	A	Ea
simple fission	1.0E15 - 5.0E17	ΔH - RT
disproportionation	3.0E11 - 2.0E12	0.0
beta scission	3.0E12 - 3.0E13	ΔH + 2 - 6
intermolecular rearrangement	1.0E13 - 1.0E14	ΔH + RS + Eabs
abstraction for H atom		
H + RH	1.0E14	literature
OH + RH	3.0E13	or
O + RH	3.0E13	Evans-Polanyi
Cl + RH	1.0E13	
CH3 + RH	1.0E12	
C2H5 + RH	1.0E11	
addition to olefin		
H	1.0E13	2.0
CH3	2.0E11	7.5
C2H5	5.0E10	7.5
recombination	1.0E12 - 1.0E14	0.0

Evans-Polanyi analysis is used on the reaction in the exothermic direction to estimate the energy of activation for the rate constant. An Evans-Polanyi plot, Ea versus ΔH of reaction, is shown in figure 4.2 for Cl atom abstraction reactions of H atoms from chlorinated hydrocarbons. One may easily see from the shallow slope that there is only a very small Ea for these reactions and it does not change much for changes in ΔH of the reaction. Clearly, the abstraction reaction in an endo-thermic reaction must incorporate the del H of the reaction or it, the reaction rate constant, will violate thermodynamics and unfortunately there are a number of examples of rate constants in the literature where the estimated Ea is less than the endothermicity.

Bozzelli[29] summarized a general rule for the activation energy for H atom abstraction by organic radicals and/or H atom from organic molecules. In exothermic reactions, Bozzelli proposed that Ea can be approximated as

$Ea = 12.5 \pm 1 - 0.35\Delta H_{rxn}$ (Kcal/mole)

with the stipulation that Ea can not be less than zero.

Bozzelli further predicts that Cl atom abstractions procede with low Ea's for exothermic reactions (1.5 Kcal/mole or lower) and Ea ≈ ΔH_{rxn} for endothermic reactions. For organic radicals abstracting F or Br atoms, Benson[22] estimates Ea's are 16 and 6 Kcal/mole respectively. Evans-Polanyi plot is a set of a plot of Ea versus ΔH from similar reactions. After completing the plot, the best slope is determined and put into form of general equation for determination of Ea knowing only ΔH. Figs 4.2-4.5 show some Evans-Polanyi plots developed in this study. A good relationship between Ea and ΔH is obtained and serves as useful tool to estimate kinetic parameters of abstraction reaction when literature values are not available.

4.3.2 Addition Reactions

Addition reactions are treated with the Quantum Kassel formalism described above. The reactions involve addition of an atom or radical to an unsaturated species and typically form an energized adduct with ca 20 to 50 Kcal/mole of energy above the ground state. This is sometimes sufficient to allow the adduct to react with other reaction products (lower energy) before stabilization occurs. An example would be H atom addition to vinyl chloride, an olefin, forming one of two chloro-ethyl radicals with ca 40 Kcal/mole energy above the ground state. In the case of H atom addition to the carbon containing the Cl atom, the chloro-ethyl adduct formed C.H2CH2Cl could rapidly eliminate (beta scission) to form the lower energy products Cl atom plus ethylene. An example of the Quantum Kassel analysis for this reaction is fully described in Bozzelli and Barat[32].

It is important to note that reactions to other channels as well as isomerization, in addition to stabilization and reverse reaction are included in this calculation.

4.3.3 Combination and Insertion Reactions

These reactions involve the combination of two radical species, or an atom and a radical. The energy of the adduct formed before stabilization is equal to the bond energy of the new bond(s) formed and typically on the order of 80 to 120 Kcal/mole. This is usually sufficient for an adduct, with this initial energy above it's ground state energy, to react to lower energy products before stabilization occurs. The high pressure limit rate constant for combination is obtained from the literature or estimated from known generic combinations. The Quantum Kassel chemical activation formalism[6,7] is then used to determine the high pressure limit and to calculate the apparent rate constants at the appropriate pressure to all the recognized available channels.

Again, reaction to other channels as well as isomerization, in addition to stabilization and reverse reaction are included in this calculation. This is an important aspect of reaction analysis for both these combination as well as insertion and addition reactions that other modelers do not incorporate.

This leads to a more correct treatment of fall-off and pressure dependence for these non-elementary reaction systems. Rate constants for the model are obtained which incorporate these pressure effects and dependency therefore make the model more fundamentally correct.

CHAPTER 5

REACTION OF OH RADICAL WITH C_2H_3Cl REACTION PATHWAY ANALYSIS

5.1 Background

The gas phase reactions of OH radical are important in combustion and incineration of chlorinated hydrocarbons (CHCs) as well as atmospheric chemistry. In combustion environments, OH is often the active radical present in the highest concentrations, where it serves to initiate breakdown of hydrocarbons (HCs). It is also very important in CO burnout producing CO_2, plus energy, and H atoms. Here if temperature is high, the H atoms may react with O_2 in the critically important chain branching step H + O_2 ---> OH + O. In atmospheric chemistry, OH is probably the most important active species. It abstracts hydrogen atom from saturated hydrocarbons forming HC radicals, which then react with O_2 and NO, sequentially forming intermediates that contribute to photo chemical smog. OH radical also adds to unsaturated hydrocarbons and oxy hydrocarbons forming radicals which then further react with O_2 and NO. Previous studies on OH radical reactions with unsaturated hydrocarbons such as vinyl chloride as well as this analysis show that the addition reaction is predominate at low temperature, while abstraction of H atom becomes important at high temperatures.

Howard[33] has determined the rate constant for reaction of OH with vinyl chloride and other halogenated ethylenes at 296 K at low pressure, 0.7 - 7.0 torr, using a discharge flow reactor with Laser Magnetic Resonance (LMR) detection of OH. The rate constant for reaction with vinyl chloride was observed to be pressure dependent (in the fall-off regime), increasing from ca. 1.2E12 cm^3 $mole^{-1}$ s^{-1} at 0.7 torr to ca. 3.01E12 cm^3 $mole^{-1}$ s^{-1} at 7.0 torr, where it still was not at the high pressure limit.

Perry et al.[34] measured absolute rate constants for reactions of OH radical with vinyl chloride, vinyl fluoride, and vinyl bromide by using a flash photolysis-resonance fluorescence technique between 299 - 426 K at a total pressure of 50 torr (C_2H_3Cl and C_2H_3Br) or 100 torr (C_2H_3F). They combined their kinetic data on these halogenated ethylenes with the room temperature high pressure rate constant for the reaction of OH with ethylene to obtain the following relative OH radical rate constants: C_2H_3F, 0.71; C_2H_3Cl, 0.84; C_2H_3Br, 0.87; C_2H_4, 1.00. The above rate constants appear to show a trend with electronegativity of the halogen substituent - the more electronegative the substituent, the lower the rate constant.

Recently Liu et al.[35] studied the gas phase reaction of OH radical with vinyl chloride at atmosphere pressure (760 torr argon) over the temperature range 313 - 1173 K by pulse radiolysis. The temperature dependence of the rate constants showed behavior similar to that of ethylene in that the predominant reaction changed from an addition reaction below 588 K to hydrogen atom abstraction reaction above 723 K. They also observed a negative temperature dependence and proposed the Arrhenius expression rate constant (high pressure limit) for the addition reaction as: 1.29E12 exp(700/RT) $cm^3mole^{-1}s^{-1}$. The nonlinear form Arrhenius rate constant for the H atom abstraction reaction was $8.43E6*T^2$ exp(-2400/RT) or in linear Arrhenius form 1.79E13 exp (-4020/RT) cm^3 $mole^{-1}$ s^{-1}.

The low temperature (addition) reactions are, however, complex and non elementary. An adduct is being formed, which can undergo stabilization via collisions, or before stabilization it may undergo unimolecular reaction to products, or reverse reaction - dissociation back to reactants. OH Addition to this unsaturated chloro-olefin can, in addition, occur at the two different carbon atoms. The addition Arrhenius A factors or activation energies may also change with either the increasing size or electronegativity of the halogen atoms. The total addition rate constants for OH radical with C_2H_3Cl and 1,2 dichloro ethylenes are, in an added complexity, shown to decrease with increasing

temperature[34].

There are two distinct carbon atom sites where addition of OH may occur and two different types of H atoms where abstraction can occur. It would be helpful in both combustion and atmospheric chemical analysis and kinetic modeling, to know the rate constants and specific reaction pathways for reaction of OH in each of the above four cases. In this work, the addition and abstraction reactions to the two carbon atom sites in vinyl chloride. The addition reactions are analyzed by multi-frequency Quantum Kassel (QK) analysis, with the QK results compared to predictions from RRKM analysis for the specific case of unimolecular dissociation of the $CH_2OHC.HCl$ adduct. The abstraction reactions are analyzed using the Transition-State-Theory (TST) of Benson[22]. Rate constants for the two different abstraction paths and for addition reactions to specific products versus pressure are given. Thermodynamic parameters of the intermediate radicals and products are also listed.

5.2 Quantum Kassel Calculations for Addition Reaction

Energized Complex/QK Theory as described by Dean[6,7] and Bozzelli et al.[36] was used to model OH radical addition reactions to C_2H_3Cl. Further details on specifics of the chemical activation calculation are presented in reference 36. Pre-exponential A factors and activation energies (Ea) for the bimolecular addition reaction at the high pressure limit are obtained from evaluation of experimental data in the literature, combined with thermochemical analysis. Isomerization reactions are analyzed via Transition-State-Theory (TST) and the thermochemical kinetic methods of Benson[22].

A and Ea for the dissociation reactions come from analysis of thermodynamic heats of formation and entropies for the species involved and by analogy to similar (generic) reactions. Specific kinetic parameters for dissociation to reactants and products are obtained from application of microscopic reversibility, where the reverse-addition or combination reaction rate constant is obtained from experimental data in the

literature.

5.3 Thermodynamic Properties

The thermodynamic properties including enthalpy of formation, entropy, and heat capacities were obtained from the literature when available. Thermodynamic properties for many chloro-oxy-carbon species have not, however, been previously measured or calculated. These have been calculated here using the techniques of group additivity[4] and the "THERM" computer code[23,24]. Bond dissociation energies (BE) from the literature[37] and bond dissociation (BD) groups developed by Lay et.al.[38] to calculated the respective radicals are included. These thermodynamic properties involved in the OH radical with vinyl chloride reaction system are listed in Table 5.1.

The potential energy diagram and input parameters for the chemical activation calculations, both α - and ß - addition (to the CD/Cl/H and CD/H2 carbons respectively), are shown in Fig.5.1, 5.2 and Table 5.2, 5.3. respectively. The parameters in Table 5.2, 5.3 are referenced to the ground (stabilized) state of the complex because this is the formalism used in QK Theory.

Table 5.1 Thermodynamic Property Data

Species	Hf	S	Cp300	400	500	600	800	1000
OH	9.49	43.88	7.16	7.08	7.05	7.05	7.15	7.33
C2H3Cl	5.0	63.10	12.78	15.58	17.88	19.77	22.56	24.44
CH2O	-26.40	52.26	8.45	9.46	10.49	11.49	13.34	14.86
CH2Cl	29.10	59.60	9.22	10.18	11.14	12.13	14.10	15.83
CHClO	-39.30	61.80	11.12	12.46	13.55	14.42	15.70	16.58
CH2OHC.HCl	-14.60	78.32	18.15	21.22	23.74	25.86	29.23	31.71
CH2O.CH2Cl	-7.74	73.60	16.19	19.89	23.00	25.58	29.54	32.34
CHClOHC.H2	-9.63	77.81	18.20	20.95	22.55	25.21	29.97	32.17
CHClO.CH3	-6.21	73.53	17.14	20.14	21.97	24.91	30.24	32.90
CH2CHOH	-29.51	64.71	13.60	25.89	18.14	20.23	23.74	26.33
CH3CHO	-39.18	63.13	13.22	15.71	18.22	20.47	24.22	26.97

. represents radical site

5.4 Addition Reactions

5.4.1 α - Addition

The rate constant (high pressure limit) for addition at the α- site k1 (k definded in Table 5.2), is assigned as follows: A_1 is 0.5 that for 1,2 dichloroethylene + OH because the probability of OH addition to the CD/Cl/H carbon is half of what that of 1,2 dichloroethylene. E_1 = -0.14 assigned same as 1,2 dichloroethylene + OH. The reverse reaction k_{-1} can be calculated from thermodynamics and microscopic reversibility:

$\Delta G = - RT \ln K_{eq} = \Delta H - T\Delta S$ for the reaction

$\Delta H/RT - \Delta S/R = (E_f - E_r)/RT - \ln(A_f / A_r)$

where f and r denote forward and reverse reaction.

Transforms above equation to standard states expressed in concentration units.

$(\Delta H_c + \Delta nRT)/RT - (\Delta S_c + \Delta nR\ln(R'T))/R = (E_f - E_r)/RT - \ln(A_f / A_r)$

where Δn is the mole change in the reaction.

$(E_f - E_r) = \Delta H_c$

$\ln(A_f / A_r) = \Delta S_c/R + \Delta n \ln(eR'T)$

where E, A, R', T are the activation energy, Arrhenius pre-exponential factor, gas constant (82.06 cm^3atm/mole/K) and mean temperature respectively.

The isomerization reaction k_3 (see Table 5.2) is obtained from unimolecular TST. Including the loss of two rotors, ΔS can be estimated as -8.5. Then

$A_3 = (ek_BT/h) \exp(\Delta S/R) = 6.06E+11$ at T = 298K

where k_B, h, R are the Boltzman, Planck's and gas constant respectively; e = 2.718.

Activation energy of this isomerization E_3 can be calculated from:

E_3 = ring strain + E_{abs} + ΔH_{rxn} = 39.42 Kcal/mole

where the ring strain for four member ring is 26 Kcal/mole, abstraction energy of H atom by a primary carbon, E_{abs}, is 10 Kcal/mole, and ΔH_{rxn} of isomerization is 3.42 Kcal/mole.

Dissociations to products k_2, k_4, k_5 (see Table 5.2) are obtained from application

of thermodynamics and microscopic reversibility to the reverse addition reactions. The rate constants, both forward and reverse used the references to the combination rates are listed in Table 5.2. The high pressure limit input parameters of α- addition reaction for the chemical activation calculation are listed in Table 5.2.

The α- addition reaction forms the CHClOHC.H2# energized adduct. Further unimolecular reaction (isomerization) of this adduct is endothermic and relative small fractions of the adduct will isomerize and further react at higher temperature due to the tight transition state. The obvious presence of the low energy channel for the α- addition adduct is Cl atom elimination.

$OH + C_2H_3Cl \rightarrow [CHClOHC.H_2]^{\#} \rightarrow Cl + CH2CHOH$

This makes vinyl alcohol as the dominate product for all conditions (temperature and pressure) of this adduct formation path.

Table 5.2. Input parameters for the QK Calculation C2H3Cl + OH α- addition

Reaction	A	Ea[a]
k1 C2H3Cl + OH ---> CHClOHCH2.	6.05E+11	-0.14
k-1 CHClOHCH2. ---> C2H3Cl + OH	2.16E+13	23.96
k2 CHClOHCH2. ---> Cl + CH2CHOH	2.15E+13	9.52
k3 CHClOHCH2. ---> CHClO.CH3	6.06E+11	39.42
K-3 CHClO.CH3 ---> CHClOHCH2.	5.52E+12	36.00
K4 CHClO.CH3 ---> CHClO + CH3	2.74E+14	10.02
K5 CHClO.CH3 ---> Cl + CH3CHO	4.25E+14	1.06

[a]units are cm^3 mole sec and Kcal/mole <v> = 1086.89 cm^{-1} (from CPFIT[7])

k1 A_1 factor taken as 0.5 that for CHClCHCl + OH (A= 1.21E+12, Ea=-0.14)
(ref. Abbatt et.al., J.Phys.Chem. 95,2382,1991)
k-1 thermodynamics and microscopic reversibility <mr>
k2 A_2 from A_{-2} = 8.0E+12, E_{-2}=0.5 from Cl + C2H4 (Kerr,J.A. and Moss, 1981)
k3 A_3 = (ekT/h)exp(S/R) x degeneracy (S=-8.5)
E_3 = ring strain + Eabs + H= 26 + 10 + 3.42 = 39.42
k-3 thermodynamics and microscopic reversibility <mr>
k4 A_4 from A_{-4} = 3.16E+11, E_{-4} = 8.0 from 0.5 for CH3 + C2H4 (Kerr and Moss, 1981)
k5 A_5 from A_{-5} = 1.78E+13, E_5 = 1.06 (Kerr and Moss, 1981)

<v> = 1136.93 cm^{-1} (from CPFIT[24]); Lennard-Jones parameters: σ = 4.55 Å, ε/k = 576.7 K

5.4.2 β- addition

The rate constant for addition at the β- site, k'_1 (see Table 5.3), is assigned as 0.4 (0.5× 0.78 = 0.38 ≈ 0.4) that for ethylene + OH where the probability of OH adding to CD/H2 carbon is half that of C_2H_4 and 0.78 accounts for reduced volume fraction[39]. The reverse reaction k'_{-1} is calculated from thermodynamics and the microscopic reversibility method described previously.

The unimolecular isomerization reaction k'_2 (see Table 5.3) is analyzed by TST where ΔS = -8.5 (includes loss of two rotors) and E_2 = ring strain + E_{abs} + ΔH_{rxn} = 26 + 10 + 6.9 = 42.9 Kcal/mole. Dissociation reaction k'_3 to products (CH_2O + CH_2Cl) is obtained from the reverse combination and microscopic reversibility. The high pressure limit input parameters and literature references are listed in Table 5.3.

The ß- addition reaction forms the $CH_2OHCHCl^{\#}$ energized adduct. Further unimolecular reaction (isomerization) of this adduct is, however, endothermic when ring strain + Ea of H abstraction + ΔH_{rxn} are considered. A relatively small fraction of the adduct will isomerize and further react at higher temperatures due to high barrier energies (above the enthalpy change) and the tight transition state. The adduct is, therefore, either stabilized or it dissociates back to the initial reactants (C_2H_3Cl + OH), as this is the lowest energy dissociation channel.

Geometric mean frequencies were obtained from heat capacity estimates[24], and Lennard-Jones parameters were obtained from tabulations[40] and a calculation method based on molar volumes and compressibility[41].

Table 5.3 Input parameters for the QK Calculation C2H3Cl + OH ß - addition

Reaction	A	Ea[a]
k1 C2H3Cl + OH ---> CH2OHCHCl.	2.17E+12	-0.14
k-1 CH2OHCHCl. ---> C2H3Cl + OH	6.03E+13	28.96
k2 CH2OHCHCl. ---> CH2O.CH2Cl	6.06E+11	42.9
K-2 CH2O.CH2Cl ---> CH2OHCHCl	7.17E+12	36.0
K3 CH2O.CH2Cl ---> CH2O + CH2Cl	1.18E+14	17.1

[a]units are cm^3 mole sec and Kcal/mole

k1 A_1 factor taken as 0.4 that for C2H4 + OH(A=5.42E+12), (Tsang,W. and Hampson,R.F., J.Phys.Chem.Ref.Data,15,1087, 1986). Ea same as CHClCHCl + OH.
k-1 thermodynamics and microscopic reversibility <mr>
k2 A_2 = (ekT/h)exp(S/R) x degeneracy (S=-8.5),
E_2 = ring strain + Eabs + H= 26 + 10 + 6.9 = 42.9
k-2 thermodynamics and microscopic reversibility <mr>
k3 A3 from A_{-3} = 1.6E+11, E_{-3} = 8.0 from C2H5 + C2H4 (Kerr,J.A. and Moss 1981)

<v> = 1136.93 cm^{-1} (from CPFIT[24])
Lennard-Jones parameters: σ = 4.55 Å, ε/k = 576.7 K

5.5 Transition-State-Theory Calculations for Abstraction Reaction

The calculation of pre-exponential A factors for the bimolecular abstraction reactions using Transition-State-Theory (TST) is described in detail by Cohen and coworkers.[42-45] They developed a procedure for obtaining activation entropies without the need for a fully characterized potential energy surface. The fundamental equation of TST is[44]:

$$k(T) = \kappa (RT/N_a h) * [Q(AB^{\#})/Q(A)Q(B)] \exp(-E/RT)$$

where κ is the transmission coefficient, R, N_a, and h are the ideal gas, Avogadro's, and Planck's constant respectively. Q's are the partition functions for the activated complex $AB^{\#}$ and reagents A and B. This equation can be expressed in practical thermochemical units as:

$$k(T) = 1.3E+13*T^2 \exp(\Delta S^{\#}/R) \exp(-E/RT)*g$$

where k in cc/mol/sec unit and g is degeneracy.

Transition-State-Theory, as described by Cohen et al.[44], will allow calculation only of the entropy of activation not the activation energy. A widely used method for predicting activation energy is offered by Evans and Polanyi[22]:

$E = a\Delta H + b$

where E is the experimental activation energy, ΔH is the enthalpy change of reaction, and a and b are constants. The enthalpy change of reaction is assumed to be proportional to the bond dissociation energy (BE, in Kcal/mole) for a homologous series of species :

$E/R = a' BE + b'$

where $E/R = -d(\ln k) / d(1/T)$ at 300K.

A modified Evans-Polanyi plot of OH abstraction of H atom from chlorinated hydrocarbons (CHCs) is illustrated in Fig. 5.3. The experimental E/R values are obtained from data in reference 44 and BEs are from Lay et.al.[38] The regression result shows that

$E/R = 149.3 (BE - 89.1)$

The bond dissociation energies evaluated for α- and β- abstraction (from the CD/Cl/H and CD/H2 carbons respectively) are 107 and 110 Kcal/mole (1.5 and 3.5 Kcal/mole resonance stablilization energy respectively); thus we calculate activation energies from the above correlation (Fig 5.3.) are 5.31 and 6.2 Kcal respectively.

The calculation for entropy of activation, $\Delta S^{\#}$, requires knowledge of the activated complex (its bond lengths and angles, vibrational frequencies, internal rotor parameters, electronic degeneracy, and symmetry properties) along with similar parameters of the reactants (C_2H_3Cl and OH).

Consider abstraction of H by reaction of OH with C2H3Cl:

C2H3Cl + OH ---> (C2H2Cl)...H...OH ---> C2H2Cl. + H2O

$\Delta S^{\#} = S^{\#} - S_{C2H3Cl} - S_{OH}$

where $S^{\#}$ = entropy of TST complex ($^{\#}$ denote as TST complex).

Begin with C2H3Cl as a model compound and then make corrections to the various degrees of freedom to obtain $\Delta S^{\#}$ as indicated below:

$S^{\#} = S_{C2H3Cl} + \Delta S_{trans} + \Delta S_{vib} + \Delta S_{rot} + \Delta S_{ir} + \Delta S_e + \Delta S_n + \Delta S_\sigma$

where the ΔS terms represent the corrections required in adjusting the properties (translation, vibration, rotation, internal rotation, electronic, optical isomer, symmetry) of the model compound to those of the activated complex.

Define C...H as a one electron-bond in the TST structure and assume that the C...H, H...O and O-H bond lengths and C...H...O and H...O-H bond angles are 1.7Å, 1.5Å, 0.9Å, 180°, and 105° respectively. From this data, we can calculate the product of moments of inertia of the complex $I^{\#3}$ then

$\Delta S_{rot} = 0.5R \ln (I^{\#3}/I^3)$

$= 0.5R \ln [(14.29x744.13x757.83)/(15.15x133.64x148.79)] = 3.27$ cal/mole/K

ΔS_{trans} is given by $1.5R \ln (M^{\#}/M) = 0.72$ cal/mole/K where M is molecular weight of species. The electronic degeneracy of the activated complex is 2 so that

$\Delta S_e = R \ln(2) = 1.38$ cal/mole/K.

The external symmetry is assumed to be the same as the model compound, but one optical isomer exists in the TST, so

$\Delta S_n = R \ln(n^{\#}/n) = R \ln(2) = 1.38$ cal/mole/K.

The calculation results are listed in Table 5.4.

The contribution of the vibrational frequencies ΔS_{vib} and internal rotations ΔS_{ir} to entropies and heat capacities of the activated complex can be calculated by using the "RADICALC" computer code developed by Bozzelli and Ritter[38]. The frequency changes are obtained from tables in Benson[22] and Cohen[44]. Corrections to the entropy due to changes in the barrier to rotation are interpolated from tables developed by Pitzer and coworkers[46]. Cohen and Benson[44] analyzed the reactions of OH with haloalkanes and proposed that the entropy of free rotation about the C...H bond is 4.5 cal/mol/K and H...O bond is 4.3 for halomethanes. They report values of 4.7 and 4.6 cal/mol/K for C...H and H...O bonds respectively in haloethanes. The average value of halomethanes and haloethanes for the C...H bond is used:

($\Delta S_{C...H}$ = [4.5+4.7]/2 = 4.6)

and the H...O bond

($\Delta S_{H...O}$ = [4.3+4.6]/2 = 4.45).

Unlike the haloethanes, there is no internal rotation about the C=C bond.

Hence

$\Delta S_{ir} = \Delta S_{C...H} + \Delta S_{H...O}$ = (4.5+4.7)/2 + (4.3+4.6)/2 = 9.05 cal/mol/K at 300K.

The entropy of activation, $\Delta S^{\#}$, is obtained from the sum of the ΔS terms minus entropy of OH radical as shown in Table 5.3.

$\Delta S^{\#} = \Sigma \Delta S - S_{OH}$

Values of ΔS for specific translation, vibration, rotation, internal rotation, electronic, and optical isomer are listed in Table 5.4. The activation energy and an entropy of activation for both abstraction channels are:

k_a = 1.40E+07*T^2exp(-5310/RT)

k_b = 2.54E+07*T^2exp(-6200/RT)

$k_b / k_a = (A_b / A_a) \exp(E_a/RT - E_b/RT)$

$= 1.81 \exp(-488/T)$

where k_a, k_b are the rate constants for α- and β-abstraction channels respectively.

Table 5.4 Calculated Contribution to $\Delta S^{\#}$ for OH + C2H3Cl Abstraction Reaction

Types	ΔS_{trans}	ΔS_{vib}	ΔS_{rot}	ΔS_{ir}	ΔS_e	ΔS_n	$\Sigma \Delta S$	$\Delta S^{\#}$
CD/Cl/H	0.72	0.8	3.27	9.05	1.38	1.38	16.58	-27.3
CD/H2	0.72	0.6	3.27	9.05	1.38	1.38	16.38	-27.5

A second method to estimate the Arrhenius A factors for specific H atom sites is to modify the observed experimental value for represents all H atoms into a sum where each term represents specific H atom sites. Cohen[42] had indicated that a reasonable approximation for abstraction of a specific H atom from a molecule is that: "The probability of OH colliding with H is proportional to a total cross section divided by

number of available H atoms"

In this case, we are dealing with the cross section observed for vinyl chloride, so the pre-exponential A factors for α- and β-abstraction are proportional to number of H atom.

$A_\beta / A_\alpha = 2$

It is interesting to compare this rate constant ratio for relative number of H atom estimation with that of the TST method. The ratio of the pre-exponential A factors for α- and β-abstraction from this emperical counting method is only slightly higher than the TST method (2.0 versus 1.8).

5.6 Results and Discussion

Howard[33] has predicted that elimination of Cl and formation of vinyl alcohol dominates for the α- addition. Perry et al.[34] estimated that the rate constant of this channel is about 6.0E+11 $cm^3mol^{-1}s^{-1}$ at room temperature which is about 15% of the total rate constant. The present calculation shows that the α- addition to the CD/Cl/H carbon appears to be a similar fraction of that for β- addition to the CD/H2 carbon, 10 - 20%, in agreement with the estimation of Perry et al.[34] This β- channel behaves much differently than α- addition due to the lower energy (exothermic) reaction channel available to the α-adduct - unimolecular elimination of Cl, forming vinyl alcohol + Cl. This product slate dominates for the α- addition for all pressures with stabilization important at higher pressure (7600 torr).

Fig. 5.4 presents a plot of rate constants for the various channels of α-addition at 760 torr. The apparent rate parameters to the specific product channels are listed in Table 5.5. The vinyl alcohol + Cl channel dominates the reaction in the temperature range 300 - 1200K. As temperature increases, other product channels (excluding stabilization) start to become more important; but are still 5 orders of magnitude below the major product channel: vinyl alcohol + Cl. The stabilization rate constant is 1% of that for the vinyl

alcohol + Cl channel at 300K and decreases with increasing temperature.

A plot of rate constants for β-addition product channels is shown in Fig. 5.5. The stabilization channel dominate the reaction by more than 4 orders of magnitude in the temperature range 300 - 1200K. The apparent rate parameters to the specific product channels are listed in Table 5.5.

Fig 5.6 shows the rate constants versus pressure at 300 K for all addition reaction channels. The β-addition channel dominates the reaction at high pressure and through the fall off regime as suggested by previous researchers[33,34,35]. The vinyl alcohol + Cl from α-addition becomes dominate when pressure is decreased below than 1 torr.

Table 5.5 Apparent Rate Constants for OH + C2H3Cl at 760 torr
$k = A*T^{n}*\exp(-E_a/RT)$, units in cc mole-sec, Ea in Kcal/mole

Reaction	A	n	Ea	remark
OH+C2H3Cl --->H2O+CH2CCl	1.40E+07	2.0	5.31	α-abstraction
OH+C2H3Cl--->H2O+CHClCH.	2.54E+07	2.0	6.2	β-abstraction
OH+C2H3Cl--->CHClOHCH2.	2.83E+18	-3.191	0.938	α-addition
OH+C2H3Cl--->Cl+CH2CHOH	7.49E+11	-0.029	-0.108	
OH+C2H3Cl--->CHClO.CH3	2.51E-11	4.028	8.874	
OH+C2H3Cl--->CHClO+CH3	5.34E-19	7.901	6.441	
OH+C2H3Cl--->Cl+CH3CHO	1.94E-11	5.893	8.488	
OH+C2H3Cl--->CH2OHCHCl.	1.33E+32	-6.638	5.718	β-addition
OH+C2H3Cl--->CH2O.CH2Cl	9.45E+18	-3.828	15.804	
OH+C2H3Cl--->CH2O+CH2Cl	8.91E+10	-0.177	14.37	

Fig. 5.7 illustrates a plot of calculated and observed rate constant over the temperature range 300 - 1200 K at 760 torr. At low temperature, the ß-addition channel dominates the reaction, as reported by Liu et.al.[35] At high temperature, however, the reverse reaction - dissociation of the adduct to vinyl chloride + OH (experimentally observed as reduced reaction rate) dominates over addition. A small, near constant (15%) fraction of the reactions proceed via α-addition to products C_2H_3OH + Cl. The Quantum Kassel calculation does not include abstraction which is calculated separately by the TST

method described previously. The apparent rate constants of the two abstraction channels calculated by Transition-State-Theory are also shown in Fig. 5.7. One can see that total abstraction reaction (ka + kb) becomes important above 850 K, while Liu et.al.[35] report that it dominates above 723 K. The total rate constant - addition and abstraction - is slightly over predicted when compared to experimental data in the temperature range 600 to 1000K at 760 torr. Here the absolute rate constant difference is within a factor of 2 for the worst case (600 to 1000K), but it is still reasonable compared to the literature.

Fig. 5.8 shows a comparison of the calculated results for important addition and abstraction channels with the experimental data of other researchers. At room temperature, the rate constants for the addition reaction channels only vary over a wide pressure range. Howard[18] extrapolated his experimental data (0.7 to 7 torr) for the reaction of OH radicals with C_2H_3Cl using a curved Lindemann plot and estimated a value for $k \approx 4.20E+12$ cm^3 $mole^{-1}$ s^{-1} in the high pressure limit (ca. 100 torr) while Perry et.al.[19] proposed that their work at 50 torr were at the high pressure limit and estimated a value of $k \approx 3.97E+12$ cm^3 $mole^{-1}$ s^{-1}. The current model is in good agreement with both research groups, as shown in Fig 5.8. but predicts the high pressure limit to be more near 760 torr with only 5% increase between 100 and 760 torr as illustrated in Fig. 5.8.

It is interesting to compare the QK calculation[6,7,36] to RRKM[47] theory. The reverse reaction of β- addition (k'_{-1}), a unimolecular dissociation, will be used for this comparison.

$CH_2OHC.HCl$ ---> $C_2H_3Cl + OH$

because the β- addition channel dominates the reaction at low temperature. The Quantum Kassel calculation shows that this unimolecular dissociation (k'_{-1}) dominates over stablization at 1 atm and high temperature which is experimentally observed as reduced reaction rate. The input parameters for the RRKM calculation are listed in Table 5.6 which is run with the UNIMOLE code of Gilbert[47].

Table 5.6 Input parameters for RRKM calculation

	Reactant molecule	Transition State
critical energy at 298K	28.9 (Kcal/mole)	
external symmetry number	1	1
collision diameter (Å)	4.55	
well depth (K)	576.7	
overall rotation (cm^{-1})	0.19	0.15
moments of inertia (amu A^2)	88.737	112.4
dimensions of adiabatic rotation	3	3
frequencies and degeneracies	3400, 3000(3),1300, 700,1150(3), 400(2), 1400(2),1050(3), 1200,730	3400,3000(3), 1650, 700, 1050(4), 420(2), 1400, 500, 600,

Fig. 5.9 shows a plot of rate constant versus 1/T at 760 torr for the two different calculations. The unimolecular dissociation rate constant increases with increasing temperature for 16 orders of magnitude in the temperature range 300 to 1000K. One can see that calculation results from two techniques are in good agreement.

Fig. 5.10 illustrates a plot of the two calculated rate constants versus pressure at 300K and 1000K. At atmospheric condition (300K), the unimolecular reaction reaches its high pressure limit at 760 torr as predicted by QK and RRKM calculations. Both calculation techniques give the same high pressure limit rate constant, 1.90E-8 $sec.^{-1}$ The difference of only 2% is purly coincidental, as no changes were made in the vibration frequencies or moment of inertia from the intial calculation. The difference between two technique for low pressure limit rate constant is due to the complete omission of the Beta Collision (Bc), the weak collision assumption in the RRKM calculation, while Bc is fully included in the QK and is calculated via the method of Troe[48]. Here the low pressure values are offset in pressure by the Bc factor between the two calculations, as they should be. The Bc (at 1200K and 760 torr, Bc = 0.13) was not used in the RRKM calculation but to compare the results in this manner. The offset in the two calculations resulting from Bc will effectively increase the pressure in the QK result over the RRKM result by the Bc

factor at the low pressure limit. This offset will decrease as pressure is increased to a point at the high pressure limit where the offset will be zero. In combustion environment, both the QK and the RRKM calculations show that dissociation reaction is still in the fall-off regime.

5.7 Summary

The addition reactions of vinyl chloride with hydroxy radical have been analyzed using thermochemical analysis and a statistical chemical activation formalism based on the Quantum Kassel Theory. Rate constant and reaction paths are predicted versus temperature and pressure and compared to experimental data where possible. Good agreement was obtained with the experimental data in the literature. The two abstraction paths have been analyzed by using an Evans-Polanyi relation for the activation energy of abstraction and Transition-State-Theory. The calculations serve as useful estimates for rate constants and reaction paths in applications of combustion and atmospheric modeling (pressure and temperature), where experimentally data are not available. Rate constants over a wide pressure and temperature range for OH addition and OH abstraction of H atom from the two distinct sites on vinyl chloride molecule are evaluated and recommended. The important addition reaction and rate constants at 760 torr pressure are:

$OH + C_2H_3Cl \rightarrow CH_2OHCHCl$, $k = 1.33E32*T^{-6.64}\exp(-5718/RT)$ $cm^3/mole/sec$

$OH + C_2H_3Cl \rightarrow Cl + CH_2CHOH$, $k = 7.49E11*T^{-0.03}\exp(108/RT)$ $cm^3/mole/sec$

Abstraction reactions are not dependent on pressure. The recommended rate constants for each of the channels are:

$OH + C_2H_3Cl \rightarrow CH_2CCl + H_2O$, $k = 1.40E7*T^2\exp(-5310/RT)$ $cm^3/mole/sec$

$OH + C_2H_3Cl \rightarrow CHClCH + H_2O$, $k = 2.54E7*T^2\exp(-6200/RT)$ $cm^3/mole/sec$

Extension of these analysis technique should allow reasonable estimation of the expected product distributions for a variety of addition reactions of hydroxy radicals to other halogenated ethylenes.

CHAPTER 6

THERMAL REACTIONS OF CH_2Cl_2 IN O_2/H_2 MIXTURES : IMPLICATIONS FOR CHLORINE INHIBITION OF CO CONVERSION TO CO_2

6.1 Background

Reasonable methods for effective destruction of chlorinated hydrocarbons include: (a) conversion to HCl and CO_2 by oxidation (e.g. incineration), and (b) conversion to HCl and hydrocarbons by pyrolysis in a hydrogen or methane rich atmosphere[49]. The presence of these chlorocarbons has long been known to slow the oxidation rate of hydrocarbons through studies of flame velocity, temperature, and flame stability. Westbrook[2] has modeled the inhibition of hydrocarbon oxidation in laminar flames by halogenated compounds. He suggested that the halogenated species serve to catalyze the recombination of H atoms into relatively nonreactive H_2 molecules, reducing the available radical pool, specifically H atoms, and thereby lowering the overall rate of chain branching. Senkan et. al.[3,4] have developed mechanisms for CH_3Cl, C_2H_3Cl, and HCl-doped CO oxidation flame systems. These later studies reached similar conclusions, suggesting that the reaction of H + HCl --> H_2 + Cl is responsible for the inhibition of CO conversion to CO_2 in the oxidations.

Alternately, Benson and Weissman[5] and Senkan et. al.[3] have reported that use of CH_3Cl in CH_4 or in CH_4 plus 2-3% O_2 respectively accelerated CH_4 conversion to higher hydrocarbons. They concluded that this might lead to effective methods for converting CH_4 to useful higher molecular weight hydrocarbons without either soot or excessive oxidation occurring[3]. Both acceleration and inhibition effects are apparent in hydrocarbon reaction systems with a chlorinated hydrocarbon present. Therefore, there is a significant need to develop quantitative insights into the mechanism of chlorocarbon

pyrolysis and oxidation in order to better understand and ultimately to optimize these reaction processes, especially for the conversion of chlorocarbons by incineration.

Tsao[8] studied the thermal decomposition of DCM with hydrogen over the temperature range of 973 - 1173K, in a 1 atm total pressure tubular flow apparatus. Activation energies of the global bulk and wall reactions on hydrogen reaction with DCM were 50.0 Kcal/mol, 57.8 Kcal/mole, with Arrhenius A factors of 2.84E+10 and 2.65E+10 $sec.^{-1}$ respectively reported. The major products of reaction of DCM in the temperature range 973 to 1073 K were methane and methyl chloride. The minor products were ethylene, acetylene and HCl. Trace amounts of ethane, chloroethylene, 1,2--dichloroethylene, trichloroethylene, benzene were also observed. No chlorocarbons were found over 1223K and one second residence time where the only products were methane, hydrogen chloride, acetylene, ethane and benzene.

Huang[9] studied the kinetics of the reaction of atomic hydrogen with DCM in a flow system at a pressure of 2.1 to 2.7 mm Hg and room temperature. The major products observed were hydrogen chloride and methane. The extent of conversion of DCM increases first to a maximum and then decreases with increasing concentration of DCM. Through the modeling of the reaction scheme and comparision with experimental data, the rate constant of the initial steps were determined as follows :

$H + CH_2Cl_2$ ----> $HCl + CH_2Cl$ (k_1)

$H + CH_2Cl_2$ ----> $H_2 + CHCl_2$ (k_2)

where

k_1 = 3.63 E+9 cm^3/mole/sec , 298 K

k_2 = 2.08E+7 cm^3/mole/sec , 298 K

Won[10] investigated the decomposition of dichloromethane/1,1,1--trichloroethane mixtures in a hydrogen bath gas. These experiments were carried out at one atmosphere total pressure in a tubular flow reactor. In his study, he demonstrated that selective formation of HCl can result from thermal reaction of chlorocarbon mixture and showed

that synergistic effects of 1,1,1--trichloroethane decomposition accelerate the rate of DCM decomposition. There is significant interaction of the decay products from 1,1,1--trichloromethane with the parent dichloromethane.

In this chapter, an experimental study on CH_2Cl_2 reactions in H_2/O_2 atmospheres and a detailed chemical kinetic mechanism developed from fundamental thermochemical principles are presented. The model is based on reactant and product profiles and shows good agreement with a wide range of experimental data. Sensitivity analysis on the mechanism provides insights into the effects of chlorocarbons in pyrolysis and oxidation environments. One such insight is that a major cause of the chlorocarbon induced inhibition of CO conversion to CO_2 is loss of OH radical through the reaction:

$OH + HCl \rightarrow H_2O + Cl.$

6.2 Experimental Result

The thermal decomposition of CH_2Cl_2 in H_2/O_2 mixtures in an Ar bath gas was studied at 1 atmosphere total pressure in tubular flow reactors of different surface to volume (S/V) ratios. Data at different S/V ratios were used to decouple the apparent wall and bulk phase decomposition rates. The reaction systems were analyzed systematically over a temperature range from 883 to 1093°K, with average residence times ranging from 0.1 to 2.0 seconds. Three different size (0.4, 1.05, and 1.6 cm ID) flow reactors were used to study five different feeds, as listed in Table 6.1. Residence times and global kinetic parameters were determined using methods and analysis described by Chang and Bozzelli[50].

Table 6.1 Reactant Feed Ratios

Feed	Mole Percent CH_2Cl_2 : H_2 : O_2 : Ar				Equiv. Ratio	Cl/H Ratio
1.	1	1	1	97	1.5	0.5
2.	1	2	2	95	1.0	0.33
3.	1	3	1	95	2.5	0.25
4.	1	1	3	95	0.5	0.5
5.	1	1	98	0	0.015	0.5

Experimental results on the decomposition of CH_2Cl_2 are shown in Fig 6.1 and 6.2. The normalized concentration (C/C_0) is presented as a function of the average residence time for several temperatures and two widely varying initial reagent ratios in the 1.05 cm reactor; O_2:H_2:CH_2Cl_2:Ar = 1:1:1:97 and 98:1:1:0 respectively. It was found that complete decay (99%) of the CH_2Cl_2 at 1 second residence time occurs at 1093°K for all the reactant ratio sets. The continuity in the measured species levels plotted for a single residence time versus temperature provides an indication of the consistency in our experimental procedures. This is because our experiments were performed by varying flow times and feed conditions at a single oven temperature profile. The data at varied temperature, therefore, represents experiments performed over time periods of months.

The major products for CH_2Cl_2 decomposition at our conditions as shown in Fig 6.3 are CH_3Cl, CH_4, CO, CO_2, and HCl. The minor hydrocarbon products as shown in Fig 6.4, having concentrations below 5%, include C_2H_4, C_2H_2, 1,1 and 1,2 $C_2H_2Cl_2$, C_2HCl_3, and C_2H_3Cl. The sum of chlorocarbon products and CH_2Cl_2 reactant decreases with increasing temperature and residence time. The major products when CH_2Cl_2 conversion is above 90% are HCl and nonchlorinated species: CH_4, C_2H_2, C_2H_4, CO, and CO_2. Mass balance determinations for carbon and chlorine were within ±8% and ±7% respectively for all experiments.

The importance of O_2 in our system depends strongly on experimental conditions. As shown in Fig 6.5, oxygen has almost no effect on the decay of CH_2Cl_2 when conversion is below 50% (less than 1023°K, 1 sec. residence time) and/or the initial O_2 concentration is below about 5%. When conversion of CH_2Cl_2 is close to 1, almost all carbon is present as CO and CO_2. The CO concentration, as shown in Fig 6.6, is much higher than CO_2. At higher O_2 to H_2 ratios, more CO is converted to CO_2. At temperatures above 1033°K, O_2 plays a more significant role in conversion. The higher the ratio of O_2 to H_2, the lower the temperature needed to observe the formation of CO and CO_2.

An increase in the S/V ratio of the reactor was observed to accelerate the CH_2Cl_2 decomposition as shown in Fig 6.7. The relative magnitude of this effect, however, was small. For a 60% increase in S/V between the 1.05 and 1.6 cm ID flow tubes, there was only a 5% difference in conversion rate, with no effect on the relative distribution of principal products observed. Hence, while a surface effect exists, its magnitude is small relative to bulk (homogeneous) reaction. The relative change in decomposition of CH_2Cl_2 (acceleration in this case) is much larger for the 0.4 cm ID reactor. Analysis of our results on the several hundred kinetic runs lead us to strongly recommend a minimum reactor ID of 1.0 cm for data analysis on these chlorocarbon studies.

A first order plug flow model was utilized to analyze the overall (global) experimental data on CH_2Cl_2 loss. In addition, the homogeneous and wall rate constants were decoupled and separately evaluated. The Arrhenius rate expressions in Table 6.2 were found to fit the overall homogeneous reaction systems studied. The average contribution from wall reaction was less than 6% of the homogeneous reaction.

Table 6.2 Global Rate Constants (K_{exp}) for $CH_2Cl_2/O_2/H_2$ in Ar

$Ar:O_2:H_2:CH_2Cl_2$	K_{exp}
97 : 1 : 1 : 1	$3.76 \times 10^{14} \times \exp(-69982/RT)$
95 : 2 : 2 : 1	$5.00 \times 10^{12} \times \exp(-60405/RT)$
95 : 3 : 1 : 1	$2.25 \times 10^{15} \times \exp(-72645/RT)$
95 : 1 : 3 : 1	$4.25 \times 10^{13} \times \exp(-64969/RT)$

Clearly, these global rate constants are valid only for the specific reactant conditions. A detailed elementary reaction mechanism which explains the data at all reactant ratios is therefore preferred.

6.3 Kinetic Mechanism and Modeling

We have, therefore, developed a detailed elementary reaction mechanism (Appendix B) to model the CH_2Cl_2 pyrolysis/oxidation reaction systems. The principles of thermochemical kinetics have been applied. The inclusion of chlorine adds a fourth element to conventional hydrocarbon oxidation mechanisms and significantly increases overall complexity. In addition, the thermochemical parameters including enthalpy of formation, entropy, and heat capacities for many chloro-oxy-carbon products and intermediates have not been previously measured or calculated and they are required for input to detailed modeling codes. We have developed thermodynamics for a number of these compounds using the techniques of group additivity and the "THERM"[23] computer code.

The initiation steps of this reaction system involve unimolecular decomposition of CH_2Cl_2 or bimolecular reaction of H_2 or CH_2Cl_2 with O_2. The possible unimolecular reactions include:

CH_2Cl_2 ---> CHCl + HCl (6.1)

CH_2Cl_2 ---> CH_2Cl + Cl (6.2)

We base our estimate of the A factor for reaction (6.1) on Transition State Theory (1000°K). The Ea is from analysis of reactions of ^{1}:CH_2 which is widely shown to insert into hydrocarbons with an Ea of 0.0 and on insertion of ^{1}:CCl_2 into HCl, which we have experimentally measured[51] to be 15 kcal/mole, using ΔH_f^{298} (^{1}:CCl_2) of 39 Kcal/mole as recommended by NIST. An extrapolation to the insertion of ^{1}:CHCl into HCl yields a value of 7.5 kcal/mole. This trend is in agreement with OH radical addition reactions to chloro-olefins, Abbatt and Anderson[52]. Similar results were also determined by Blake et. al.[53] who show a 12 Kcal/mole Gibbs Free Energy barrier (suggested as mostly entropic in nature) for insertion of ^{1}:CCl_2 into ethylene. Setser[54] recommends an Ea of 8 Kcal/mol for insertion of ^{1}:CF_2 into HCl. One possible reason for this apparent activation energy is that the electrons from the Cl atom(s) may reduce the ability of the unoccupied orbital on the singlet methylene to combine with bonding electrons in the molecule undergoing insertion. In developing this mechanism, we have used the Hf^{298} of 39.0 Kcal/mol for ^{1}:CCl_2 as recommended by Lias et al.[55-57] There are a number of widely different values for this H_f^{298} ranging up to 52 Kcal/mol in a very recent publication[58]. The Ea's for rate constants involving ^{1}:CCl_2 are based on the 39.0 Kcal/mol value; where the reverse reaction rate constants calculated in the CHEMKIN[59] code from thermodynamics and micro-reversibility have been considered in all cases. Use of different thermo parameters in this mechanism will dramatically alter the reverse rate constants specific to this species. Rates calculated using Quantum Rice- Ramsperger-Kassel (QRRK)[6,7] analysis will be similiar if the input parameters are correctly scaled to account for the different H_f value. We are working on adjustments to the mechanism to account for this higher H_f^{298} for those researchers electing to use this value in their codes. We recommend the mechanism in this paper be used with thermo properties consistent with data in Appendix A and look forward to further studies clarifying the H_f of :CCl_2.

It is observed that step (6.2) dominates the dissociation by more than three orders of magnitude because of its lower Ea and high A factor.

Reactions with O_2 include :

$CH_2Cl_2 + O_2 <---> HO_2 + CHCl_2$ (6.3)

$H + HO_2 <---> H_2 + O_2$ (6.4)

We note that the relative rates of reaction of CH_2Cl_2 and H_2 with O_2 are a strong function of conversion. At close to initial conditions, these reactions contribute to initiation. At medium to high conversions, sensitivity analysis of the mechanism indicates that these reactions proceed in reverse.

The CH_2Cl radical formed in reaction (6.2) will abstract H atom from H_2 and form CH_3Cl:

$CH_2Cl + H_2 <---> CH_3Cl + H$ (6.5)

H atom is produced from steps (6.5) and (6.6)

$H + HCl <---> Cl + H_2$ (6.6)

The CH_2Cl radical also rapidly reacts with H atoms, which are present at significant concentrations in our system, forming a chemically activated adduct $[CH_3Cl]^{\#}$:

$CH_2Cl + H <---> [CH_3Cl]^{\#} ---> CH_3 + Cl$ (LEEC) (6.7)

$---> CH_3Cl$ (stabilization) (6.8)

where LEEC represents a Low Energy Exit Channel for the $CH_3 + Cl$ products relative to the $CH_2Cl + H$ reactants. The fraction of $[CH_3Cl]^{\#}$ which decomposes to reactants, lower energy products $CH_3 + Cl$, or to stabilized CH_3Cl is a function of energy distribution in the initially formed $[CH_3Cl]^{\#}$ adduct (temperature), stabilizing collisions (pressure), as well as unimolecular and stabilization rate constants.

We treat these non-elementary reactions systems such as (6.7),(6.8) with the bimolecular Quantum Rice-Ramsperger-Kassel (QRRK) theory[6,7] as modified by Ritter et. al.[60] The energy level diagram and input parameters for the chemical activation

calculations of the reaction of CH_2Cl + H are shown in Fig 6.8 and Appendix C. The QRRK analysis clearly indicates that at atmospheric pressure and the temperatures of interest, stabilization represents only about 1% of the reaction channel. Essentially all of the reaction proceeds to the Low Energy Exit Channel for the energized complex dissociation.

Sensitivity analysis tells us that the significant route to CH_3 radical in our reaction system is

$$CH_3Cl + H <---> CH_3 + HCl \qquad (6.9)$$

The formation of CH_4 as one of the major products results from reaction of CH_3 with the H_2 reagent.

$$H + CH_4 <---> CH_3 + H_2 \qquad (6.10)$$

Radicals such as CH_3, CH_2Cl, and $CHCl_2$ will combine to form energized complexes. At our temperatures (ca. 1000°K), these adducts rapidly react to lower energy products before stabilization. An example is the CH_2Cl + CH_2Cl system, whose energy level diagram and QRRK input parameters are shown in Fig 6.9 and listed Appendix III.

$$CH_2Cl + CH_2Cl <---> [CH_2ClCH_2Cl]^{\#} ---> Cl + CH_2ClCH_2. \qquad (6.11)$$

$$---> HCl + C_2H_3Cl \qquad (6.12)$$

$$---> CH_2ClCH_2Cl \qquad (6.13)$$

The CH_2ClCH_2 radical rapidly decomposes by beta scission to Cl + C_2H_4 because of the weak C-Cl bond, relative to the stronger C-C bond formed. The dominant reaction path in combination reactions of CH_2Cl + CH_2Cl is a function of both pressure and temperature. At one atmosphere pressure and low temperature, formation of the stable adduct (1,2 dichloroethane) dominates - ca 70%. This channel decreases with increasing temperature where reverse reaction (dissociation of the adduct to reactants - non reaction) is the other important channel here. At the temperatures of this study and 1 atm, reaction to Cl + ethyl radical and to HCl + ethylene are more important, with the Cl + chloroethyl radical path slightly favored over HCl elimination. Stabilization becomes less important as the

pressure is decreased. The Cl elimination from the energized adduct can dominate because: i, sufficient energy is available to it and ii, this channel has the higher Arrhenius A factor. The primary unimolecular reaction for the stabilized 1,2 dichloroethane is HCl elimination, because it is the lower energy channel.

The methyl and chloro-methyl radical combination pathways are significantly more important in the formation of C_2 hydrocarbons (HC) and chloro-hydrocarbons (CHC) in reaction systems with Cl present, than in HC oxidations alone. This is a result of atomic Cl being formed at early reaction times. The Cl reacts very rapidly with the reactant fuel molecules, which at early time are present at high levels. The important reaction paths at combustion temperature are abstraction of H by the Cl to form the corresponding HC radical and HCl. These abstraction reactions by Cl are fast, they have high Arrhenius A factors, usually greater than 1.0 E+13, with relatively low Ea's, typically just a few Kcal/mole, (if the reaction is endothermic the Ea is just a few kcal/mole over ΔH_{rxn}).

The result is a rapid, nearly - catalytic production of HC and ClC radicals early in the reaction, where there is recycle of a significant fraction of the HCl to Cl. This represents an acceleration of the fuel decay to the corresponding radicals. C_1 radical reactions with molecular oxygen are not as rapid as with C_2 and larger radicals. Conversion of the C_1 radicals into C_2's via combination is now very important. The oxidation and pyrolysis pathways of C_2 hydrocarbons are, therefore, also more important in this reaction system than in CH_4 oxidation when no Cl or HCl is present.

We note that our input parameters to the bimolecular QRRK[6,7] calculation on these chemical activation reaction systems (listed in Appendix C) are significantly different from those of Senkan and Karra[61] (over one order of magnitude in several cases). Our calculated results reflect these differences, which might result from use of different thermodynamic properties - enthalpies, entropies and heat capacities for the

relevant species. A listing of the thermodynamic properties of the stable chemical compounds and the radicals used in our mechanism is included in Appendix A.

Other important reactions involve the CH_3, CH_2Cl, and $CHCl_2$ radical reactions with O_2; for example,

addition Cl shift beta scission

$$CH_2Cl + O_2 <---> [CH_2ClOO.]^{\#} <---> [C.H_2OOCl]^{\#} ---> CH_2O+ClO \quad (20)$$

A potential energy level diagram and input parameters for the QRRK calculations, including reference, for the above reaction system are illustrated in Fig 6.10 and Appendix C. The energized complex can be stabilized, decompose back to initial reactants, or be further isomerized by Cl shift to $[C.H_2OOCl]^{\#}$. This second complex immediately dissociates to lower energy products CH_2O and ClO. Bimolecular QRRK calculations show that only a small fraction of the collisions of CH_2Cl radicals with O_2 form CH_2O and ClO. More than 95% of the energized complex formed decomposes back to initial reactants at temperatures of 873°K and 1073°K.

The kinetic reaction mechanism used in this study (Appendix II) includes 281 elementary reaction steps involving 61 stable compounds and free radical species. All addition and recombination reactions are analyzed by the CHEMACT[7,60] computer code based on bimolecular QRRK theory[6,7]. All unimolecular reactions including beta scission, simple dissociation, isomerization, and elimination are treated with unimolecular QRRK analysis. Further details on specific procedures followed in our bimolecular QRRK analysis has been discussed in chapter 4,5 and in the tables of input parameters in Appendix C.

Experimental data are compared with model predictions in Figs 6.11 to 6.13 for reagent decomposition and product distribution between 973 and 1073°K. The calculated mole fractions for CH_2Cl_2 are in very good agreement with those determined experimentally. For CO and CO_2, model predictions are also in reasonable accord with the experimental data. The model predicts the mole fraction levels of CH_4 and CH_3Cl

versus time and temperature reasonably well, but it slightly over-predicts CH_4 at higher temperature. The model predicts the low concentration (1-4%) chlorinated C_2 products reasonably well. It is worthwhile to point out that the scale is amplified (x25), and is not a log scale as used in many model comparisons.

CH_2Cl_2 decay along with intermediate and final product formation at 1053°K is plotted versus reaction time in Fig 6.14 to 6.16 as opposed to temperature in the figures above. Again one can see that the agreement between the model and experiment is very good.

It is valuable to compare both our experimental data for CH_2Cl_2 reactions as well as our model calculations with the data of other researchers. Fig 6.17 illustrates that our model predictions are in agreement with other experimental data on methylene chloride pyrolysis and oxidation (details in Table 6.3).

Table 6.3 Comparison with Other Researcher's Experimental Conditions

Temp Range °K	Reactant Conditions	Ref
973 - 1223	20% CH_2Cl_2 in H_2	8
748 - 1083	4% CH_2Cl_2 + 4% 1,1,1 $C_2H_3Cl_3$ in H_2	10
1023 - 1273	6.7% CH_2Cl_2 in (CH_4/Ar : 50/50)	62
1023 - 1273	1.2% CH_2Cl_2 + 1.2% C_2HCl_3 in (CH_4/Ar : 50/50)	62

absolute pressure = 1 atm (all cases)

The small deviation shown in Fig 6.17 between our model and the data of Won[10] at low temperatures is due to synergistic effects resulting from the decomposition of the co-reagent 1,1,1 $C_2H_3Cl_3$ to Cl + 1,1-$C_2H_3Cl_2$ radical. We note that less than 1% of the decomposition of the 1,1,1 $C_2H_3Cl_3$ parent follows this chain branching pathway. The major path is decomposition to HCl + 1,1 $C_2H_2Cl_2$. A separate model[63] for 1,1,1

$C_2H_3Cl_3$ verifies the importance of this step and other important reactions of 1,1,1 trichloroethane which we not included in this study.

Table 6.4. Sensitivity analysis relative to CO2 formation at 1053°K

	Residence Time (sec)			
Reaction	0.5	1.0	1.5	2.0
CH2Cl2=CH2Cl+Cl	1.12E00	1.23E00	1.67E00	2.64E-1
CH2Cl2+H=HCl+CH2Cl	-1.77E-1	-3.08E-2	2.12E-1	1.78E-1
CH2Cl2+Cl=HCl+CHCl2	-2.02E-1	-1.84E-1	-1.88E-1	-4.26E-2
CH2Cl2+OH=CHCl2+H2O	-1.78E-1	-1.45E-1	-8.05E-2	-2.28E-2
CH2Cl+CH2Cl=C2H3Cl+HCl	-1.39E-1	-1.66E-1	-2.96E-1	-5.54E-2
CH2Cl+CHCl2=CH2CCl2+HCl	-1.49E-1	-1.85E-2	-2.07E-1	-5.06E-2
CHCl2+CHCl2=C2HCl3+HCl	-1.25E-1	-1.44E-1	-1.29E-1	-3.38E-2
CH2Cl+CHCl2=CHClCHCl+HCl	-5.54E-1	-6.77E-1	-9.06E-1	-1.98E-1
CH2Cl+O2=CH2O+ClO	1.35E00	1.55E00	2.06E00	4.36E-1
CH2Cl+ClO=CHClO+HCl	-1.61E-1	-1.97E-1	2.21E-1	-3.14E-2
H+O2=O+OH	6.94E-1	9.38E-1	2.31E00	2.27E-1
H+H2O=H2+OH	-2.35E-1	-2.10E-1	-8.51E-2	-9.64E-2
OH+HCL=H2O+CL	-6.44E-2	-1.45E-1	-3.07E-1	-4.36E-1
H+HCl=H2+Cl	1.19E-1	1.40E-1	1.73E-1	3.61E-2
HOCl=Cl+OH	1.42E-1	2.65E-1	4.52E-1	6.32E-1
CO+ClO=CO2+Cl	1.50E-1	8.77E-2	2.04E-2	1.29E-2
CO+OH=CO2+H	5.18E-1	5.58E-1	5.32E-1	3.43E-1
CO+HO2=CO2+OH	3.05E-1	3.01E-1	2.78E-1	3.49E-1

The faster decay of CH_2Cl_2 in the data of Tsao[8], Fig 6.17, results from higher CH_2Cl_2 concentrations leading to more chain branching and not from the H_2 bath gas. The slower decay (higher temperature requirement) for CH_2Cl_2 in CH_4/Ar bath gas results from the slower reactions of Cl with CH_4 relative to H_2 and slower reactions of CH_3 relative to H atoms, where H_2 was present. Methane is, in addition, an intermediate product in CH_2Cl_2/H_2 pyrolysis and large CH_4 levels shift several of the CH_4 production channels toward the reverse.

The sensitivity computer code SENS[64] was utilized to determine the relative importance of the reactions in the mechanism to various products, and specifically to reactions effective in inhibiting CO conversion to CO_2. As shown in Table 6.4, the results indicate that the reaction OH + HCl ---> H_2O + Cl is a major OH sink, which depletes OH and effectively stops the CO conversion via CO + OH ---> CO_2 + H. The OH reaction with HCl is faster than OH + CO_2 and depletes the OH when chlorocarbons, which lead to HCl levels comparable to those of CO, are present. Reactions with HO_2 and ClO are now the primary mechanism for CO conversion to CO_2 e.g. via

CO + HO_2 ---> CO_2 + OH.

Westbrook[3] reports an important mechanism of chlorinated hydrocarbon inhibition as:

H + RCl = HCl + R

R + Cl2 = RCl + Cl

H + HCl = H2 + Cl

Cl + Cl + M = Cl2 + M

with the net result of these reactions being H + H = H_2. This "catalyzed" recombination of H atom reportedly results in a reduction in chain branching reactions such as

H + O_2 = O + OH.

We have used the sensitivity code and our mechanism to evaluate the importance of these abstraction reactions in our system and do not find high sensitivity. We have evaluated the literature data to select the most accurate rate constants for H atom abstraction of Cl from RCl and determined that these reactions have relatively high activation energies (E_a's). A best fit Evans-Polanyi relationship of $E_a = \Delta H/4 + 12.58$ is obtained for the H_{rxn} = -50 to -10 Kcal/mol range. For example:

H + CH_3Cl ---> HCl + CH_3 $\Delta H = -19.45$ Ea = 7.62

H + CH_2Cl_2 ---> HCl + CH_2Cl $\Delta H = -22.26$ Ea = 7.27

We find very little Cl_2 produced. Molecular chlorine has a relative weak bond, and its reactions with hydrocarbon radicals, H, OH, and O are all exothermic. The Cl_2 reactions, while rapid, are not indicated to be significant by the sensitivity analysis for our conditions, and OH + HCl is the most important inhibition reaction.

We have, in addition, used the sensitivity code with our mechanism to model more typical incineration conditions: CH_4 (4%) with 0.4% CH_2Cl_2, 16% O_2 in Ar, 1400°K. The results continue to show that the reaction of OH + HCl ---> H_2O + Cl dominates the inhibition, with H + HCl ---> H_2 + Cl also active, but less important as an inhibition mechanism. The Cl atoms produced, however, react rapidly with any H_2 or hydrocarbon present to produce HCl and a radical, thus continuing the chain. This accelerates the reaction under fuel rich or low conversion conditions. Under CO burnout conditions, however, HCl depletes OH and the Cl produced then competes for hydrogen with oxygen and oxy species where the thermodynamics for H abstraction are favorable. Our conclusions on the importance of OH + HCl to inhibition are in agreement with those of Barat et. al.[48] in Well Stirred Reactor studies of CH_3Cl inhibition in ethylene/O_2 flames. We also note that Roessler et. al.[49] report H + HCl = H_2 + Cl as the most important, but OH + HCl as the next most important inhibition reaction for CO oxidation in H_2/O_2 mixtures with HCl present.

The reaction of Cl + HO_2, part of which goes to HCl + O_2 (termination), now becomes an important part of the inhibition process. The lower degree of CO burnout decreases the system temperature, resulting in higher concentrations of HO_2.

The model indicates another interesting component relating to the effects of chlorocarbon inhibition. The addition of limited quantities of high temperature H_2O to the oxidation system, where Cl or oxygen atoms are present, shifts the reactions

OH + HCl <---> H_2O + Cl

OH + OH <---> H_2O + O

to the left. This increases the OH concentrations and improves CO conversion during the reaction of chlorocarbons in $CH_4/O_2/HCl$ atmospheres.

We also observe that chlorinated hydrocarbons initiate reactions in the fuel rich regions of chlorocarbon/hydrocarbon/O_2 mixtures faster than during the normal oxidation of hydrocarbons[65]. This results in pyrolysis or molecular weight growth reactions in the fuel rich zones and increased possibility of soot formation. The reason for the increased hydrocarbon reactions is again the presence of chlorine. Carbon-chlorine bonds are known to be weaker than carbon-hydrogen, carbon-carbon, or carbon-oxygen bonds. Therefore, the C-Cl bond can break at lower temperatures, resulting in chain branching. The Cl atoms generated will rapidly abstract H atom from the hydrocarbons due to low activation energies and relatively high Arrhenius A factors, thus propagating the chain.

6.4 Summary

A detailed kinetic reaction mechanism based upon fundamental thermochemical and kinetic principles, Transition State Theory, and evaluated literature rate constant data was developed. The mechanism was used to model results obtained from our experiments, in addition to results from other studies, on the thermal reactions of CH_2Cl_2. Reactions which demonstrated high sensitivity to CO burnout (inhibition) were evaluated. Here results indicate that the reaction OH + HCl ---> H_2O + Cl is a major cause of OH loss. This decrease in OH effectively stops CO burnout. The reaction H + HCl ---> H_2 + Cl is also important when H_2 concentrations are low. The lower temperatures resulting from decreased CO conversion caused the Cl + HO_2 reaction channel to HCl + O_2, termination, to become an important contributor to inhibition.

Sensitivity analysis indicates that the reaction OH + OH <---> H_2O + O, which usually forms H_2O during hydrocarbon incineration, reacts in the reverse direction when HCl is present at concentrations comparable to CO due to the large extent of OH depletion. The addition of moderate levels of high temperature steam is predicted to help

CO conversion by shifting the equilibrium to produce more OH for this and the OH + HCl <---> H_2O + Cl reaction.

CHAPTER 7

KINETIC STUDY ON PYROLYSIS AND OXIDATION OF CH_3Cl IN $Ar/H_2/O_2$ MIXTURES

7.1 Background

In recent years incineration has become a preferred method of destruction applicable to combustible organic wastes, with particular reference to the important family of hazardous wastes termed chlorinated hydrocarbons. The simplest subgroup within this family is the chlorinated methanes, which are widely used as industrial solvents. Reasonable methods for effective destruction of chlorinated hydrocarbons include: (a) conversion to H_2O, HCl, and CO_2 by oxidation (e.g. incineration), and (b) conversion to HCl and hydrocarbons by pyrolysis in a hydrogen or methane rich atmosphere[5].

There are no other studies on reactions of chloromethane in H_2/O_2 atmospheres to our knowledge. There are a number of studies on CH_3Cl oxidation or pyrolysis[3,5,20] in other atmospheres, including methane. These studies conclude that the CH_3Cl tends to initiate methane degradation faster, when present, and that the facile production of methyl radicals leads to relatively efficient formation of C_2 species, i.e. molecular weight growth.

Earlier kinetic studies on methyl chloride pyrolysis were reported in 1959 by Shilov and Sabirova[11]. Measurements were made at initial CH_3Cl pressures of 10.1-34.3 torr, temperatures of 1062K-1147K, and at contact times of 0.4- 5.0 seconds; They found HCl, CH_4, and C_2H_2 in the ratios of 3:1:0.6. They also reported that the measured apparent first-order rate constants increased with increasing pressure. This data has been re-analyzed by Holbrook[12] and Fost et al.[13] to test Slater and RRKM theories. The calculated rate constants were, however, 20 to 30 times smaller than those experimentally measured. Our present analysis indicates that the experiments incurred significant chain continuation reaction due to rapid atomic chlorine abstraction of hydrogen from hydrocarbons.

Data on the pyrolysis of CH_3Cl at a high degree of conversion were reported by LeMoan[15]. The reaction was run at 993K for 30 hours in a batch reactor yielded conversions larger than 95%. The gas phase contained HCl, CH_4, and small quantities of H2, benzene, and toluene. Low transient concentrations of CH_2Cl_2, C_2H_6, and C_2H_5Cl were detected at the beginning of the pyrolysis. In the liquid phase, benzene (72%), toluene (11%), xylene (1%), and monochlorobenzene (12%) were identified. There were two distinct solid phases: carbon in the reactor and naphthalene and soot at the exit from the reactor. The reaction mechanism, despite the large number of products identified, was considered to be schematically simple. It was proposed that, initially, CH_3Cl would decompose into HCl and $^1CH_2$, which would dimerize into C_2H_4 or decompose into CH + H or C + H_2. The combination of two CH radicals would form acetylene. Acetylene would combine, then cyclize to form benzene, from which the identified higher molecular weight compounds would be formed. The hydrogenation of CH_2 radicals would lead to methane. As we shall see later, this mechanism is not plausible.

CH_3Cl decomposition was also studied by Weissman and Benson[5] using a flow system to generate product distributions at temperatures of 1260 and 1310K and over the pressure range 180 - 370 torr. They measured CH_4, C_2H_2, C_2H_4, and HCl as the major products with lower quantities of aromatic hydrocarbons and soot using Gas Chromatography and Mass Spectrometry techniques.

Miller et al.[17] and Senkan et al.[16] have both examined flames from $CH_3Cl/CH_4/O_2$ mixtures. They presented kinetic modeling of the combustion of CH_3Cl in flames and suggested that the presence of chlorine decreases the concentration of ethane species and promotes soot formation by simultaneously increasing the rate of formation of C_2H_3 and C_2H_2, which enhances the rate of nucleation and surface growth processes.

Roesler et al.[18] studied moist CO oxidation chemistry inhibited by HCl experimentally and numerically with dilute mixtures of CO (~1%), H_2O (~0.5%), O_2 and

10.5.2 Fuel Lean Equivalence ratio 0.8 at in the PSR.

The major PICS calculated in this system, before addition of combustion modifiers, are Cl_2, Cl atom, HOCl, and Phosgene, and these range in mole fraction from 1.0×10^{-4} to 1.0×10^{-14}. Chloro-formaldehyde, trichloroethylene, and vinyl chloride concentrations are also calculated, but are at lower levels than the phosgene. Specifics are described below.

Figures 10.5 and 10.6 show the Cl atom mole fraction versus reaction time in the burnout and the low temperature cool-down regions respectively. Cl atom mole fraction at the PSR exit is at relatively high levels, probably super equilibrium. It decreases exponentially throughout the burnout and cool down zones.

The independent effects of adding 1% steam, hydrogen peroxide and formaldehyde at the beginning of the burnout zone are also illustrated in figure 10.5. Steam reduces the Cl mole fraction in the burnout region, i.e. it shifts the

$$Cl + H_2O <--> HCl + OH$$

equilibrium to the right, also increasing OH.

Formaldehyde addition at the 1% level increases Cl - creating a slightly higher temperature (initiates secondary combustion) and higher levels of the radical pool. Adding smaller amounts of CH_2O, (0.1 and 0.01 %) leaves the Cl level at that of the non-additive case. Cl in the cool down region, figure 10.6, shows similar trends but less difference in the Cl levels, for all additives.

The inlet of additives modifies the fuel equivalence ratio, as they are an added mass flow; the addition reduces the initial mole fraction of product species by 1 to 3 percent. The addition of 1 % formaldehyde for example increases the fuel equivalence ratio from 0.80 to 0.85.

Molecular chlorine levels in the cool down region are shown in Figure 10.7, where they are observed to increase from mole fraction of near 0.05 to 7.0 (xE-05) in 0.2

seconds for the non-additive case. Steam and H2O2 effect a reduction of ca 15 % and formaldehyde effects a reduction of ca 30 % in the effluent Cl2 levels.

HCl mole fractions throughout the reactor are shown in figure 10.8. HCl levels increase rapidly upon exit from the PSR and remain nearly constant throughout the cool-down region. Note that the abscissa scale in figure 10.8 is highly amplified and the differences in HCl through the cool-down region are all less than 2 %. All additives at the 1 % level show ca 1 % decreases in the HCl level, but this is the effect of increasing the total mole fraction while keeping the HCl nearly constant. The effluent HCl levels effectively remain unchanged for the different additives, in this fuel lean efficient combustion system.

Phosgene levels from the PSR through the higher temperature PFR are shown to decrease in the burnout region from mole fraction 1.0E-10 to 1.0E-14, figure 10.9. They increase, however, in the cool down region to ca. 1.2E13 as shown in figure 10.10. One percent CH_2O added in the burnout region effects a more rapid decay of phosgene in this zone, but results in a slightly higher steady state level. Injection of H_2O vapor results in the lowest mole fraction phosgene in the burnout region, while hydrogen peroxide effects the lowest overall level at the exit of the cool-down region.

10.5.3 Effects on CO/CO_2 Ratio

The CO/CO_2 ratio or level of CO emission is often used in the combustion community for determination of efficiency. We evaluate this ratio for both fuel rich and fuel lean conditions, and the conditions of 1 % water vapor, hydrogen peroxide, formaldehyde and oxygen added to the burnout region.

10.5.4 CO / CO_2 Fuel Rich Initial Conditions

Figures 10.11 and 10.12 correspond to the fuel rich system, which serves as a validation of the modeling. Clearly this fuel rich system, phi = 1.5, is oxygen starved, and anything

that serves to increase the oxidant will significantly benefit this inadequate combustion system. The CO/CO_2 ratio is used as an indicator of combustion efficiency for 10,000 ppm, 1.2%, CH_3Cl in the feed.

The Figures 10.11 and 10.12 show that addition of oxygen - 1 %, has the most dramatic effect, while hydrogen peroxide has a significant benefit, in agreement with the data of Cooper. It does not, however, equal the improvement of O_2, because one of the two oxygen atoms in each H_2O_2 is needed to form H_2O, the sink for H's from the peroxide. Steam has some benefit in CO/CO_2 ratio, at the expense of H_2 formation, while formaldehyde further inhibits the combustion system. While these improvements with added O_2 are expected, they are an important check on the model and suggest that the model is representative of the chemistry occurring. The quantitative predictions we are calculating might not be 100 % accurate, but the qualitative trends should exist, and a combustor operator could look for these trends in optimization.

10.5.5 CO / CO_2 Ratio Fuel Lean Initial Conditions - Equivalence ratio 0.8

The effect of steam addition, 0 to 0.4 mole fraction, on the CO / CO_2 effluent ratio, at two initial CH_3Cl to CH_4 ratios, 1:4 and 1:10, is illustrated in figure 10.13. The initial CO and CO/CO_2 ratio is observed to be higher in the CH3Cl/CH4 ratio 1:4 than for ratio 1:10.

$$1{:}4 = (CH_3Cl{:}CH_4{:}O_2 = 1.61{:}6.44{:}19.12)$$

$$1{:}10 = (CH_3Cl{:}CH_4{:}O_2 = 0.69{:}6.9{:}19.25)$$

A dramatic improvement - reduction in CO level and CO/CO_2 ratio, occurs as steam is added initially for the above CH_3Cl / CH_4 ratios. CO mole fractions first decrease by more than one half, then rise as the mole fraction H_2O added increases above 0.2. CO/CO_2 levels also decrease, then increase, but this ratio starts to increase faster than the CO.

The calculated effects from separate addition of steam, H_2O_2 and CH_2O, at the

1% level are illustrated in figures 10.14 and 10.15 for burnout and cool-down regions respectively. 1% formaldehyde increases the CO/CO_2 ratio in the burnout and at the start of the cooldown zone; but the 1% formaldehyde and the non-additive case are identical at the effluent point. This CO increase is primarily due to changes in the fuel equivalence ratio. 0.01 % CH_2O added has no effect. H_2O and H_2O_2 addition show a small benefit at this one percent level.

The fraction change, Xc reported as:

Xc = (Concentration - additive) / (Concentration - non additive) conditions

for the PICs: phosgene, OH radical, H_2, CO, Cl_2 and Cl atom, is illustrated in figure 10.16, for addition of: 1% steam, 1% H_2O_2 and 0.01% CH_2O at the 320 K effluent point. A value of 1 corresponds to no change.

10.5.6 Discussion

The temperature of the additives injected is relatively "cold", 400 K, compared to the near 2000 K temperature in the burnout zone. A decrease in temperature in the burnout region can result from injection of large quantities of additives and may reduce CO burnout. Super heated steam may be a better choice for an additive here.

Cl atoms add to CO in a stepwise process, in two steps, to form phosgene.

$Cl + CO <--> ClC.=O$

$Cl + ClC.=O <--> Cl_2C=O$

Two Cl atoms also combine to form chlorine gas.

$Cl + Cl + M = Cl_2 + M$

These appear to be the mechanism of phosgene and Cl_2 formation in the relatively low Cl to H ratio and ideal, well mixed, fuel lean combustion studies reported in this paper. Here the POHC is effectively completely destroyed at the end of the adiabatic burnout region, and the levels of chlorocarbon PIC's are not high enough to account for the phosgene formation.

The phosgene formation mechanism may be very different in non well mixed systems, in systems where there is higher chlorine loadings, or where the POHC or Chlorinated PICs are present in significant concentrations. This is most likely the case, for example, in the studies on phosgene formation reported by the Koshland or Sawyer research groups at Berkeley[19].

The fuel rich calculation results are an important check on the model and help support the model as representative of the chemistry occurring. We indicate that the quantitative predictions might not be 100 % accurate, but that the qualitative trends should be present.

10.6 Conclusions

We have illustrated several examples of the presently available analysis of combustion systems using a detailed mechanism and the assumption of complete mixing.

Under fuel rich conditions, addition of steam, hydrogen peroxide, and oxygen will improve CO/CO_2 ratio. Oxygen is the most effective here. Additions of formaldehyde or methane to the burnout region will produce more CO in a stepwise process which may increase CO/CO_2 ratio.

Under fuel lean conditions, formation of CO is low. Additions of steam and hydrogen peroxide to the burnout region slightly improve the CO/CO_2 ratio. Addition of CH_2O under fuel lean conditions may decrease other PICs while slightly increaseing formation of CO and $COCl_2$, unless an oxygen source is co-added. Formaldehyde addition at lower equivalence ratios should be more beneficial.

These results are specific to the conditions in this study and we note that that a fuel equivalence ration lower than 0.8 was calculated to yield lower pollutant levels and more efficient combustion.

APPENDIX A

THERMODYNAMIC PROPERTIES

SPECIES	HF(298)	S (298)	CP300	CP500	CP800	CP1000	CP1500	CP2000	Ref
AR	0.00	36.98	4.97	4.97	4.97	4.97	4.97	4.97	a
C(S)	0.00	21.83	2.06	3.50	4.74	5.15	5.65	5.89	a
Cl	28.90	39.50	5.20	5.40	5.35	5.30	5.24	3.40	b
H2	0.00	31.21	6.90	6.99	7.10	7.21	7.72	8.17	a
H	52.10	27.36	4.97	4.97	4.97	4.97	4.97	4.97	a
HCl	-22.07	44.64	6.96	6.99	7.29	7.56	8.10	8.40	c
Cl2	0.00	53.30	8.10	8.59	8.91	8.99	9.10	9.16	b
CH2	92.35	46.32	8.28	8.99	10.15	10.88	12.22	13.00	a
^{1}CH2	101.44	44.15	8.28	8.99	10.15	10.88	12.22	13.00	a
CH3	35.12	46.38	9.26	10.81	12.90	14.09	16.26	17.56	a
CH4	-17.90	44.48	8.51	11.10	15.00	17.20	20.61	22.61	a
C2H2	54.19	48.01	10.60	13.08	15.31	16.29	18.31	19.57	a
C2H3	70.40	56.20	10.89	13.87	17.16	18.73	21.34	23.20	e
C2H4	12.54	52.39	10.28	14.91	20.03	22.45	26.21	28.35	a
C2H5	28.36	57.90	12.26	17.13	22.85	25.74	30.54	33.31	e
C2H6	-20.24	54.85	12.58	18.68	25.80	29.33	34.91	38.37	a
CHCl	76.62	56.17	8.80	10.13	12.11	13.22	14.78	14.96	f
CH2Cl	29.10	59.60	9.32	11.14	14.10	15.83	18.31	18.93	h
CCl2	51.10	49.00	11.09	12.52	13.61	14.09	15.41	15.84	f
CHCl2	23.50	67.40	13.11	14.68	16.83	17.98	19.80	21.20	h
CH3Cl	-19.59	56.01	9.77	13.20	17.02	18.87	21.80	23.40	i
CH2Cl2	-22.80	64.59	12.26	15.88	19.36	20.81	22.90	24.00	c
CHCl3	-24.20	70.66	15.77	19.31	21.96	22.82	24.21	24.60	c
C2HCl	52.10	58.10	13.17	15.18	16.88	17.55	18.80	19.55	j
C2H3Cl	5.00	63.09	12.33	17.73	22.47	24.26	26.88	28.80	b
CH2CCl2	0.62	69.25	15.81	20.56	24.68	26.19	28.21	29.60	j
CHClCHCl	0.75	69.25	15.81	20.56	24.68	26.19	28.21	29.60	j
CHClCH	61.83	64.46	11.39	16.35	21.23	23.38	26.87	28.80	j
CH2CCl	60.40	64.46	11.39	16.35	21.23	23.38	26.87	28.80	j
CCl2CH	58.20	68.88	17.52	22.16	25.74	26.90	28.60	29.85	j
C2HCl3	-1.40	77.63	19.22	23.75	26.80	27.60	28.98	30.10	j
CH2ClCH2	21.18	68.50	14.01	20.09	25.88	28.98	33.44	34.21	j
CH3CHCl	17.68	67.31	14.10	19.79	25.42	27.99	32.50	34.70	h
CH3CCl2	11.50	73.60	17.28	22.86	28.09	30.18	33.09	35.01	j
CHCl2CH2	16.04	74.30	17.35	22.95	28.03	30.29	33.07	34.55	j
CH2ClCHCl	11.49	75.80	16.81	22.56	27.67	29.75	33.21	34.50	j
CH2ClCCl2	7.05	83.20	20.21	25.68	30.14	31.77	34.50	36.10	j
C2H2Cl3	8.50	83.10	20.21	25.68	30.14	31.77	34.50	36.10	j
C2H5Cl	-26.83	66.03	15.06	21.67	28.43	31.47	36.27	39.17	j
CH3CHCl2	-31.10	73.05	18.29	24.81	30.87	33.44	37.80	40.16	g
CH2ClCH2Cl	-30.60	74.16	18.99	24.74	30.32	33.06	38.79	40.77	g
CH3CCl3	-33.84	76.55	22.52	28.45	33.70	35.73	38.91	41.60	c

C2H2Cl4	-37.20	86.01	25.23	31.32	36.05	37.59	39.82	41.10	g
C2HCl4	5.80	87.90	23.50	28.76	32.52	33.68	35.70	36.30	j
CH2ClCHCl2	-34.70	81.50	21.01	27.67	33.26	35.36	38.91	41.10	c
O	59.55	38.47	5.23	5.08	5.01	5.01	4.98	4.98	a
O2	0.0	49.01	7.02	7.44	8.04	8.35	8.73	9.04	a
OH	9.49	43.88	7.16	7.05	7.15	7.33	7.87	8.27	a
H2O	-57.80	45.10	8.02	8.41	9.24	9.85	11.23	12.20	a
HO2	3.50	54.73	8.37	9.48	10.78	11.43	12.47	13.23	a
H2O2	-32.53	55.66	10.42	12.35	14.30	15.21	16.85	17.88	a
CO	-26.42	47.21	6.96	7.13	7.61	7.94	8.41	8.67	a
CHO	10.40	53.66	8.27	9.27	10.73	11.51	12.55	13.15	a
ClO	24.20	54.10	7.50	8.21	8.69	8.81	9.00	9.10	b
Cl2O	19.71	63.66	11.41	12.76	13.46	13.55	13.81	13.85	b
ClO2	25.00	61.50	9.99	11.72	12.97	13.32	13.80	13.86	b
CClO	-4.00	63.50	10.80	11.70	12.50	12.90	13.40	13.70	b
HOCl	-17.80	56.50	8.91	10.08	11.13	11.58	12.40	12.80	b
COCl2	-52.60	67.80	13.81	16.26	17.97	18.45	19.21	19.50	b
CHClO	-39.30	61.80	11.12	13.55	15.70	16.58	18.11	18.80	j
CO2	-94.05	51.07	8.90	10.65	12.30	12.97	13.93	14.45	a
CH2O	-26.00	52.26	8.45	10.49	13.34	14.86	16.95	18.14	a
CH3O	3.90	53.25	9.01	12.22	16.28	18.38	21.56	23.13	a
CH2OH	-2.60	59.61	9.72	12.58	15.99	17.60	19.80	21.00	a
CH2CO	-11.74	57.79	12.98	16.92	20.31	21.61	23.80	25.55	a
CH3OH	-48.06	57.28	10.48	14.34	19.00	21.35	24.96	27.25	b
HCCO	41.36	60.62	11.82	14.63	17.13	18.09	19.38		b
CH2ClO	2.16	63.27	11.22	15.05	18.65	20.33	22.40	23.70	j
CH2ClOO	3.50	73.11	15.84	17.98	22.92	24.57	27.10	28.40	j
CH2OOCl	10.00	78.60	17.50	22.10	27.10	28.80	31.70	33.30	j

Unit: Hf, Kcal/mol; S and Cp, cal/(mol °K)

References for Thermodynamic Properties

a. JANAF Thermochemical Tables, 3rd Edition, NSRDS-NBS 37 (1986)

b. Benson, S.W., Thermochemical Kinetics, John Wiley and Son, 1976

c. Stull,D.R., Westrum,R.F., and Sinke,G.C., The Chemical Thermodynamics of Organic Compounds, Robert E. Kreger Publishing Co., 1987

d. Orlov,Y.D., Lebedev,Y.A., and Korsunskii, B.L., Russ. J. Chem., 1424, 1985

e. Brouard, M., Lightfoot, P.D., and Pilling, M.J.; J. Phys. Chem., 90, 445. 1986

f. Lias, S.G.; Bartmess, J.E.; Liebman, J.F.; Holmes, J.L.; Levin, R.D.; Mallard, G.W.; J. Phys. Chem. Ref. Data, 17, Suppl. 1, 1988

g. Pedley, J.B.; Naylor, R.O.; Kirby, S.P.; Thermodynamic Data of Organic Compounds, Chapman and Hall, New York, 1987

h. Tschuikow-Roux, E. and Chen, Y.; J. Am. Chem. Soc., 111, 1511 1989.

i. Rogers, A.S.; Selected Values for Thermodynamic Properties of Chemical Compounds, Thermodynamic Research Center, Texas A&M Univ. 1982

j. Estimated by Group Additivity and NJIT bond energy.

APPENDIX B

DETAILED MECHANISM FOR CH_2Cl_2 AND CH_3Cl PYROLYSIS AND OXYDATION

$k = A \times T^n \times \exp(-Ea/RT)$

units for A: cm^3/mole-sec and sec^{-1}; Ea: Kcal/mole

ΔH_{rxn} taken as from stabilized adduct.

CH2S : singlet methylene, $^1CH_2$

DISSOC: apparent rate constant from DISSOC computer code
(QRRK unimolecular dissociation calculation, high pressure limit k listed above. DISSOC values used in kinetic code)

QRRK : apparent rate constant from CHEMACT computer code
high pressure limit k listed in Appendix C

Reaction	A	n	Ea	source
CH2Cl2 = CHCl + HCl	1.42E+14	0.0	105.	1
	1.82E+37	-7.43	85.7	DISSOC
CH2Cl2 = CH2Cl + Cl	1.02E+16	0.0	75.8	2,3
	1.60E+40	-7.84	83.6	DISSOC
CH2Cl2 + H = CH2Cl + HCl	7.00E+13	0.0	7.1	4
CH2Cl2 + Cl = CHCl2 + HCl	2.79E+13	0.0	2.94	4
CH2Cl2 + CH3 = CH4 + CHCl2	6.76E+10	0.0	7.2	4
CH2Cl2 + CH3 = CH3Cl + CH2Cl	1.40E+11	0.0	4.9	4
CH2Cl2 + O2 = CHCl2 + HO2	1.35E+13	0.0	51.8	20
CH2Cl2 + HO2 = CHCl2 + H2O2	6.67E+12	0.0	18.27	21
CH2Cl2 + OH = CHCl2 + H2O	2.83E+12	0.0	2.09	19
CH2Cl2 + O = CHCl2 + OH	6.00E+12	0.0	5.76	40
CH3Cl = CH3 + Cl	1.28E+15	0.0	83.0	15,30
	1.31E+37	-6.92	90.65	DISSOC
CH3Cl = CH2S + HCl				
	1.10E+28	-5.15	109.67	DISSOC
CH3Cl + H = CH3 + HCl	6.64E+13	0.0	7.62	4
CH3Cl + Cl = CH2Cl + HCl	3.16E+13	0.0	3.3	4
CH3Cl + O2 = CH2Cl + HO2	2.02E+13	0.0	54.2	22
CH3Cl + O = CH2Cl + OH	1.70E+13	0.0	7.3	4
CH3Cl + OH = CH2Cl + H2O	2.45E+12	0.0	2.7	4
CH3Cl + ClO = CH2Cl + HOCl	3.03E+11	0.0	10.7	38,19
CH3Cl + HO2 = CH2Cl + H2O2	1.00E+13	0.0	21.66	45
CH3Cl + CH3 = CH4 + CH2Cl	3.30E+11	0.0	9.4	4
CH2Cl + H2 = CH3Cl + H	3.90E+12	0.0	14.06	4,6
CH2Cl + O2 = CH2O + ClO	1.91E+14	-1.27	3.81	QRRK
CH2Cl + O2 = CH2ClOO	2.73E+33	-7.5	4.44	QRRK
CH2Cl + O = CH2ClO	1.29E+15	-1.98	1.1	QRRK
CH2Cl + O = CH2O + Cl	5.59E+13	-0.13	0.71	QRRK
CH2Cl + OH = CH2O + HCl	1.24E+22	-2.72	3.86	QRRK
CH2Cl + OH = CH2OH + Cl	2.00E+12	0.29	3.27	QRRK
CH2Cl + HO2 = CH2ClO + OH	1.00E+13	0.0	0.0	25,12
CH2Cl + ClO = CHClO + HCl	4.13E+19	-2.22	2.36	QRRK
CH2Cl + ClO = CH2ClO + Cl	4.15E+12	0.07	11.1	QRRK
CH2Cl + CH2O = CH3Cl + CHO	3.56E+11	0.0	6.2	24,4
CH2Cl + CH2Cl = C2H4Cl2	7.84E+45	-10.21	13.15	QRRK
CH2Cl + CH2Cl = CH2ClCH2 + Cl	9.34E+29	-4.94	14.07	QRRK
CH2Cl + CH2Cl = C2H3Cl + HCl	3.75E+35	-6.73	13.16	QRRK
CH2Cl + CHCl2 = C2H3Cl3	6.41E+33	-10.22	12.91	QRRK
CH2Cl + CHCl2 = CH2CCl2 + HCl	3.75E+36	-7.22	13.62	QRRK
CH2Cl + CHCl2 = CHClCHCl + HCl	1.22E+37	-7.20	13.64	QRRK
CH2Cl + CH3 = C2H5Cl	3.27E+40	-8.49	10.59	QRRK

Reaction	A	n	Ea	source
CH2Cl + CH3 = C2H4 + HCl	3.50E+29	-4.49	9.18	QRRK
CH2Cl + CH3 = C2H5 + Cl	9.27E+19	-2.07	10.13	QRRK
CH2Cl + H = CH3Cl	3.04E+25	-4.47	3.49	QRRK
CH2Cl + H = CH3 + Cl	5.12E+14	-0.22	0.31	QRRK
CH2Cl + H = CH2S + HCl	9.48E+04	1.91	2.6	QRRK
CHCl2 + CH3 = CH3CHCl2	2.28E+41	-8.68	11.62	QRRK
CHCl2 + CH3 = C2H3Cl + HCl	1.35E+30	-4.96	11.55	QRRK
CHCl2 + CH3 = CH3CHCl + Cl	2.74E+25	-3.45	12.81	QRRK
CHCl2 + CHCl2 = C2H2Cl4	9.08E+45	-10.56	13.17	QRRK
CHCl2 + CHCl2 = C2H2Cl3 + Cl	1.36E+30	-5.23	14.18	QRRK
CHCl2 + CHCl2 = C2HCl3 + HCl	6.72E+35	-7.11	13.21	QRRK
CHCl2 + H = CH2Cl2	4.81E+26	-4.82	3.81	QRRK
CHCl2 + H = CH2Cl + Cl	1.25E+14	-0.03	0.57	QRRK
CHCl2 + H2 = CH2Cl2 + H	4.30E+12	0.0	15.3	4,5
CCl3 + CH3 = C2H3Cl3	9.54E+46	-10.66	11.74	QRRK
CCl3 + CH3 = CH2CCl2 + HCl	1.62E+30	-5.33	8.64	QRRK
CCl3 + CH3 = CH3CCl2 + Cl	3.98E+22	-2.63	7.09	QRRK
CCl3 + CH2Cl = C2H2Cl4	4.01E+45	-10.15	10.67	QRRK
CCl3 + CH2Cl = C2HCl3 + HCl	4.74E+30	-5.08	8.81	QRRK
CCl3 + CH2Cl = C2H2Cl3 + Cl	5.90E+23	-2.84	8.96	QRRK
CCl3 + H2 = CHCl3 + H	5.01E+12	0.0	14.3	49
CCl3 + CH4 = CHCl3 + CH3	5.00E+12	0.0	14.9	49
CHCl + CHCl = CHClCHCl	4.00E+12	0.0	0.0	50
CHCl + O2 = CHClO + O	1.50E+13	0.0	2.86	50
CHCl + O = CHClO	1.00E+13	0.0	0.0	50
CHCl + O2 = CO + HOCl	1.20E+11	0.0	0.0	50
C2H3Cl + H = CH2ClCH2	5.01E+23	-4.21	8.47	QRRK
C2H3Cl + H = C2H4 + Cl	1.55E+13	-0.02	5.84	QRRK
C2H3Cl + H = C2H3 + HCl	1.20E+12	0.0	15.0	36
C2HCl3 + H = CH2ClCCl2	1.51E+23	-4.18	7.52	QRRK
C2HCl3 + H = C2H2Cl3	2.87E+22	-4.09	10.89	QRRK
C2HCl3 + H = CH2CCl2 + Cl	1.45E+13	-0.01	5.83	QRRK
C2HCl3 + H = CHClCHCl + Cl	7.37E+12	-0.01	9.22	QRRK
CH2CCl2 + H = C2H3Cl+ Cl	7.21E+12	0.0	7.51	QRRK
CHClCHCl + H = C2H3Cl + Cl	3.44E+13	0.03	5.89	QRRK
CHClCHCl = C2HCl + HCl	7.26E+13	0.0	69.09	50
CH2CCl2 = C2HCl + HCl	1.45E+14	0.0	69.22	50
C2HCl3 = C2Cl2 + HCl	7.26E+13	0.0	74.44	50
C2HCl + H = HCl + C2H	1.00E+13	0.0	17.03	50
C2HCl + H = C2H2 + Cl	2.00E+13	0.0	2.1	50
C2H4Cl2 = C2H3Cl + HCl	3.98E+13	0.0	58.0	30
	6.76E+19	-1.93	58.71	DISSOC

Reaction	A	n	Ea	source
CH3CHCl2 = C2H3Cl + HCl	2.80E+13	0.0	57.65	30
	2.94E+21	-2.37	59.46	DISSOC
CH3CHCl2 = CH3CHCl + Cl	6.65E+15	0.0	80.7	3,23
	3.17E+42	-8.10	92.67	DISSOC
C2H3Cl3 = CHClCHCl + HCl	1.39E+20	-2.03	60.45	DISSOC
C2H3Cl3 = CH2CCl2 + HCl	3.13E+19	-2.02	60.33	DISSOC
C2H2Cl4 = C2HCl3 + HCl	8.62E+21	-2.57	51.87	DISSOC
C2H5Cl = C2H4 + HCl	7.81E+19	-2.0	60.66	DISSOC
C2H5Cl = C2H5 + Cl	2.35E+43	-8.5	96.98	DISSOC
C2H5Cl + Cl = HCl + CH3CHCl	3.55E+13	0.0	15.0	4
C2H5Cl + Cl = HCl + CH2ClCH2	1.12E+13	0.0	15.0	4
C2H5Cl + H = HCl + C2H5	1.00E+14	0.0	7.9	4
C2H3Cl = C2H2 + HCl	3.16E13	0.0	45.27	30
	1.62E+28	-4.29	75.78	DISSOC
C2H3Cl = C2H3 + Cl	3.98E+15	0.0	87.0	26
	1.71E+38	-7.13	96.37	DISSOC
C2H6 = C2H5 + H	1.30E+16	0.0	100.7	7
	6.22E+47	-9.76	111.25	DISSOC
C2H6 = CH3 + CH3	8.00E+16	0.0	90.4	7
	5.34E+54	-11.12	112.21	DISSOC
C2H6 + H = C2H5 + H2	6.61E+13	0.0	3.6	4
C2H6 + Cl = C2H5 + HCl	4.37E+13	0.0	0.1	19
C2H6 + O = C2H5 + OH	2.51E+13	0.0	6.4	4
C2H6 + OH = C2H5 + H2O	8.85E+09	1.04	1.81	36
C2H5 = C2H4 + H	5.01E+13	0.0	40.9	7
	1.83E+39	-7.75	52.82	DISSOC
C2H5 + H = CH3 + CH3	1.35E+22	-2.17	7.0	QRRK
C2H5 + O = CH2O + CH3	1.00E+13	0.0	0.0	18
C2H5 + O2 = C2H4 + HO2	2.00E+12	0.0	4.99	11
C2H5 + HO2 = C2H4 + H2O2	3.01E+11	0.0	0.0	36
C2H4 + O2 = C2H3 + HO2	4.22E+13	0.0	57.62	36
C2H4 + CH3 = C2H3 + CH4	4.20E+11	0.0	11.11	11
C2H4 + OH = C2H3 + H2O	1.58E+04	2.75	4.173	36
C2H4 + H = C2H3 + H2	6.92E+14	0.0	14.5	8
C2H4 + Cl = C2H3 + HCl	2.39E+13	0.0	2.6	30
C2H4 = C2H2 + H2	2.95E+17	0.0	79.28	11
	8.52E+43	-8.32	121.24	DISSOC
C2H4 = C2H3 + H	2.00E+16	0.0	110.0	7
	8.53E+30	-5.87	118.24	DISSOC
C2H3 + H = C2H2 + H2	9.26E+13	0.0	0.0	36
C2H3 = C2H2 + H	3.16E+12	0.0	38.3	7
	6.24E+29	-5.29	46.5	DISSOC

Reaction	A	n	Ea	source
C2H3 + O2 = C2H2 + HO2	1.21E+11	0.0	0.0	36
C2H3 + O2 = CHO + CH2O	3.97E+12	0.0	-0.25	47
C2H2 + H2 = C2H3 + H	2.41E+12	0.0	65.0	36
C2H2 + HO2 = CH2CO + OH	6.03E+09	0.0	7.95	36
C2H2 + Cl = C2H + HCl	1.58E+14	0.0	16.9	30
C2H2 + O2 = C2H + HO2	1.21E+11	0.0	0.0	36
C2H2 + O = CH2 + CO	4.10E+08	1.5	1.69	11
C2H2 + O = HCCO + H	1.02E+07	2.0	1.9	13
C2H2 + OH = CH2CO+H	3.20E+11	0.0	0.2	13
C2H2 + OH = C2H + H2O	1.45E+04	2.68	12.04	36
C2H2 + H = C2H + H2	6.00E+13	0.0	23.66	11
C2H + O2 = CO + CH2	2.41E+12	0.0	0.0	36
C2H + H2 = C2H2 + H	1.15E+13	0.0	2.88	36
C2H + CH4 = C2H2 + CH3	1.81E+12	0.0	0.5	36
C2H + OH = CH2 + CO	1.81E+13	0.0	0.0	36
C2H + OH = C2H2 + O	1.81E+13	0.0	0.0	36
HCCO + H = CH2S + CO	3.00E+13	0.0	0.0	11
CH2CO + O = CH2 + CO2	1.74E+12	0.0	1.35	13
CH2CO + M = CH2 + CO + M	3.00E+15	0.0	75.98	13
CH2CO + H = HCCO + H2	5.00E+13	0.0	8.0	13
CH2CO + O = HCCO + OH	1.00E+13	0.0	8.0	13
CH2CO + OH = HCCO + H2O	7.50E+12	0.0	2.0	13
CH2CO + OH = CHO + CH2O	1.00E+13	0.0	0.0	11
CH2CO + H = CH3 + CO	7.00E+12	0.0	3.01	11
CH4 = CH3 + H	1.00E+16	0.0	105.0	7
	1.03E+33	-5.58	111.8	DISSOC
CH4 + H = CH3 + H2	1.55E+14	0.0	11.0	4
CH4 + Cl = CH3 + HCl	3.09E+13	0.0	3.6	46
CH4 + O2 = CH3 + HO2	4.04E+13	0.0	56.91	36
CH4 + O = CH3 + OH	1.02E+09	1.5	8.6	36
CH4 + OH = CH3 + H2O	1.93E+05	2.4	2.11	36
CH4 + HO2 = CH3 + H2O2	2.00E+13	0.0	18.0	9
CH4 + ClO = CH3 + HOCl	6.03E+11	0.0	15.0	37,19
CH3 + O2 = CH2O + OH	4.35E+13	-0.45	17.26	QRRK
CH3 + O2 = CH3O + O	2.86E+15	-0.315	30.86	QRRK
CH3 + O = CH2O + H	7.00E+13	0.0	0.0	10,11
CH3 + OH = CH3O + H	3.87E+12	-0.19	13.74	8
CH3 + HO2 = CH3O + OH	2.00E+13	0.0	0.0	12,36
CH3 + ClO = CH2O + HCl	3.47E+18	-1.80	2.07	QRRK
CH3 + ClO = CH3O + Cl	3.33E+11	0.46	0.03	QRRK
CH3O + M = CH2O + H + M	1.00E+14	0.0	25.1	36
CH3O + O2 = CH2O + HO2	6.62E+10	0.0	2.6	36

Reaction	A	n	Ea	source
CH3O + CO = CO2 + CH3	1.57E+13	0.0	11.8	36
CH3O + HO2 = CH2O + H2O2	3.01E+11	0.0	0.0	36
CH3O + CH3 = CH4 + CH2O	2.41E+13	0.0	0.0	36
CH3O + O = OH + CH2O	6.03E+12	0.0	0.0	36
CH3O + OH = H2O + CH2O	1.81E+13	0.0	0.0	36
CH3O + H = H2 + CH2O	1.99E+13	0.0	0.0	36
CH3O + Cl = HCl + CH2O	4.00E+14	0.0	0.0	36
CH3O + ClO = CH2O + HOCl	2.41E+13	0.0	0.0	31,36
CH2O + ClO = CHO + HOCl	5.50E+03	2.81	5.86	32,36
CH2O + CH3 = CH4 + CHO	1.00E+11	0.0	6.09	11
CH2O + H = CHO + H2	2.50E+13	0.0	3.99	10,11
CH2O + O = CHO + OH	3.50E+13	0.0	3.51	10,11
CH2O + OH = CHO + H2O	3.00E+13	0.0	1.19	10
CH2O + HO2 = CHO+ H2O2	1.00E+12	0.0	8.0	9,16
CH2O + Cl = CHO + HCl	5.00E+13	0.0	0.5	19
CH2O + O2 = CHO + HO2	2.05E+13	0.0	38.95	36
CH2O + M = CHO + H + M	5.00E+16	0.0	76.2	11
CH2OH + M = CH2O + H + M	1.00E+14	0.0	25.1	13
CH2OH + OH = H2O + CH2O	2.41E+13	0.0	0.0	13
CH2OH + CH3 = CH4 + CH2O	2.41E+12	0.0	0.0	13
CH2OH + O = OH + CH2O	4.22E+13	0.0	0.0	13
CH2OH + HO2 = H2O2 + CH2O	1.21E+13	0.0	0.0	13
CH2OH + Cl = HCl + CH2O	4.00E+14	0.0	0.0	36
CH2OH + H = H2 + CH2O	6.03E+12	0.0	0.0	13
CH2OH + O2 = HO2 + CH2O	5.00E+10	0.0	0.0	13
CHO + M = H + CO + M	2.50E+14	0.0	16.79	11
CHO + H = CO + H2	2.00E+14	0.0	0.0	10,11
CHO + O2 = CO + HO2	5.12E+13	0.0	1.69	36
CHO + O = CO + OH	3.01E+13	0.0	0.0	36
CHO + O = H + CO2	3.01E+13	0.0	0.0	36
CHO + OH = CO + H2O	3.01E+13	0.0	0.0	36
CH2 + O2 = CH2O + O	1.00E+14	0.0	3.7	8
CH2 + CH4 = CH3 + CH3	1.81E+05	0.0	0.0	36
CH2 + CH3Cl = CH3 + CH2Cl	9.10E+04	0.0	0.0	51
CH2 + H2 = CH3 + H	3.01E+09	0.0	0.0	36
CH2 + H2O = CH3 + OH	9.64E+07	0.0	0.0	36
CH2S + M = CH2 + M	1.00E+13	0.0	0.0	13
CH2S + O2 = CO + H2O	2.41E+11	0.0	0.0	13
CH2S + CH4 = C2H5 + H	9.43E+12	-0.13	6.62	QRRK
CH2S + CH4 = CH3 + CH3	3.45E+22	-2.48	7.46	QRRK
CH2S + CH4 = C2H6	5.78E+46	-10.31	12.83	QRRK
CH2S + CH3Cl = C2H5Cl	7.85E+31	-6.15	5.83	QRRK

Reaction	A	n	Ea	source
CH2S + CH3Cl = C2H4 + HCl	1.60E+18	-1.47	2.71	QRRK
CH2S + CH3Cl = C2H5 + Cl	3.09E+07	1.7	0.52	QRRK
CH2S + H2 = CH4	3.82E+25	-4.47	3.77	QRRK
CH2S + H2 = CH3 + H	1.27E+14	-0.08	0.13	QRRK
CO + OH = CO2 + H	4.40E+06	1.5	-0.741	13
CO + HO2 = CO2 + OH	5.80E+13	0.0	22.934	36
CO + O2 = CO2 + O	2.50E+12	0.0	47.8	13
CO + ClO = Cl + CO2	6.03E+11	0.0	17.4	19
CO + O + M = CO2 + M	6.17E+14	0.0	3.0	36
H + O2 = O + OH	1.69E+17	-0.9	17.39	36
H + O2 + M = HO2 + M	7.00E+17	-0.8	0.0	11
O + H2 = H + OH	1.08E+04	2.8	5.92	36
O + H2O = OH + OH	1.50E+10	1.14	17.24	10
H + H2O = H2 + OH	4.60E+08	1.6	18.56	10
H + OH + M = H2O + M	2.22E+22	-2.0	0.0	36
O2 + M = O + O + M	1.20E+14	0.0	107.55	13
H + O + M = OH + M	4.71E+18	-1.0	0.0	36
HO2 + M = H + O2 + M	1.21E+19	-1.18	48.61	36
H + HO2 = OH + OH	1.69E+14	0.0	0.87	36
H + HO2 = H2 + O2	6.62E+13	0.0	2.13	36
O + HO2 = OH + O2	2.00E+13	0.0	0.0	10,11
OH + HO2 = H2O + O2	2.00E+13	0.0	0.0	10
O + HCl = OH + Cl	5.24E+12	0.0	6.4	4
OH + HCl = Cl + H2O	2.45E+12	0.0	1.1	4
H + H + M = H2 + M	6.40E+17	-1.0	0.0	4
Cl + Cl + M = Cl2 + M	2.34E+14	0.0	-1.8	4
H + Cl + M = HCl + M	1.00E+17	0.0	0.0	17
H + HCl = Cl + H2	2.30E+13	0.0	3.5	4
H + Cl2 = HCl + Cl	8.51E+13	0.0	1.0	4
Cl + HO2 = HCl + O2	1.08E+13	0.0	-0.338	19
Cl + HO2 = ClO + OH	2.47E+13	0.0	0.89	19
Cl + H2O2 = HCl + HO2	6.62E+12	0.0	1.95	19
H2O2 + M = OH + OH + M	1.29E+33	-4.86	53.25	36
H2O2 + OH = HO2 + H2O	1.75E+12	0.0	0.32	36
H2O2 + O = HO2 + OH	9.63E+06	2.0	3.97	36
H2O2 + H = HO2 + H2	4.82E+13	0.0	7.95	36
H2O2 + H = H2O + OH	2.41E+13	0.0	3.97	36
H2O2 + O2 = HO2 + HO2	5.42E+13	0.0	39.74	36
CH2ClO = CH2O + Cl	4.73E+12	0.0	7.6	7,27
	4.53E+31	-6.41	22.56	DISSOC
CH2ClO = CHClO + H	3.27E+13	0.0	14.3	7,28
	1.83E+27	-5.13	21.17	DISSOC

Reaction	A	n	Ea	source
CHClO = CHO + Cl	1.99E+15	0.0	77.6	7,29
	8.86E+29	-5.15	92.92	DISSOC
CHClO = CO + HCl	1.10E+30	-5.19	92.96	DISSOC
CHClO + H = CHO + HCl	8.33E+13	0.0	7.4	19
CHClO + H = CH2O + Cl	6.99E+14	-0.58	6.36	QRRK
CHClO + OH = CClO + H2O	7.50E+12	0.0	1.2	33,11
CHClO + O = CClO + OH	8.80E+12	0.0	3.5	34,11
CHClO + Cl = CClO + HCl	2.40E+13	0.0	0.5	35,19
CHClO + O2 = CClO + HO2	4.50E+12	0.0	41.8	49
CHClO + ClO = CClO + HOCl	1.10E+13	0.0	0.5	49
CHClO + CH3 = CClO + CH4	2.50E+13	0.0	6.0	49
CHClO + CH3 = CH3Cl + CHO	1.50E+13	0.0	8.8	49
H2 + ClO = H + HOCl	6.03E+11	0.0	14.1	39,19
O + Cl2 = Cl + ClO	2.51E+12	0.0	2.72	48
H + Cl2 = HCl + Cl	8.59E+13	0.0	1.17	48
HOCl + OH = ClO + H2O	1.81E+12	0.0	0.99	19
HOCl + H = HCl + OH	9.55E+13	0.0	7.62	4,44
HOCl + Cl = Cl2 + OH	1.81E+12	0.0	0.26	19
HOCl + Cl = HCl + ClO	7.28E+12	0.0	0.1	4,41
HOCl + O = OH + ClO	6.03E+12	0.0	4.37	19
HOCl = Cl + OH	2.85E+15	0.0	54.2	42
	1.76E+20	-3.01	56.72	DISSOC
HOCl = H + ClO	1.76E+14	0.0	92.2	43
	8.12E+14	-2.09	93.69	DISSOC
CClO = CO + Cl	1.30E+14	0.0	8.0	49
CClO + OH = CO + HOCl	3.30E+12	0.0	0.0	49
CClO + O2 = CO2 + ClO	1.00E+13	0.0	0.0	49
CClO + Cl = CO + Cl2	4.00E+14	0.0	0.8	49
COCl2 + M = CClO + Cl + M	1.20E+16	0.0	75.5	49
COCl2 + OH = CClO + HOCl	1.00E+13	0.0	23.3	49
COCl2 + O = CClO + ClO	2.00E+13	0.0	17.0	49
COCl2 + H = CClO + HCl	5.00E+13	0.0	6.3	49
COCl2 + Cl = CClO + Cl2	3.20E+14	0.0	23.5	49
COCl2 + CH3 = CClO + CH3Cl	1.90E+13	0.0	12.9	49

Sources of Rate Constants

1. A = $10^{13.55}$x 4, Ea = ΔH_{rxn} + 7.5; (detail see text)

2. A factor based on thermodynamics and microreversibility.
A$_{-1}$ taken as that for $C_2H_5 + CH_3$ (A = 2.0 x 10^{13}
Ea = BE - RT. (this case Bond Energy is 77.8 Kcal)

3. Allara, D.L. and Shaw, R.J., J. Phys. Chem. Ref. Data, 9, 523,1980.

4. Kerr, J.A. and Moss, S.J., Handbook of Bimolecular and Thermo lecular Gas Reaction}, Vol. I & II, CRC Press Inc., 1981.

5. A factor taken as average that for $CH_2Cl + H_2$ and $CCl_3 + H_2$;
Ea from Evans--Polanyi plot.

6. A factor taken as 2 that for $CH_3 + H_2$ (A = 1.6 x 10^{12}) ;
Ea from Evans--Polanyi plot.

7. Dean, A.M., J. Phys. Chem., 89, 4600 1985.

8. Olson,D.B. and Gardiner,W.C. Jr., Combus. Flame, 32, 151, 1978

9. Cathonnet, M., Gaillard, F., Boettener, J.C., Cambray, P., Karmed, D., and Bellet, J.C., Twentieth Symposium (International) on Combustion, The Combustion Institute, pp 819--829, 1984.

10. Warnatz, J., Bockhorn, H., Moser, A., and Wenz, H.W., Nineteenth Symposium (International) on Combustion, The Combustion Institute, pp 167--179, 1982.

11. Warnatz, J.; Combustion Chemistry (W.C. Gardiner, Jr.,Ed.) Springer--Verlag, NY, 1984.

12. Hennessy, R.J., Robison, C., Smith, D.B., Twenty--first Symposium (International) on Combustion}/The Combustion Institute, pp. 761--772, 1986.

13. Miller, J.A., Mitchell, R.E., Smooke, M.D., and Kee, R.J., Nineteenth Symposium (International) on Combustion), The Combustion Institute, pp. 127--141, 1982.

14. Westbrook, C.K., and Dryer, F.A., Prog. Energy Combust. Sci., 10, 1 1984.

15. A factor taken as $10^{15.4}$ (Benson 1984)
Ea = ΔH_{rxn} - RT

16. Levy, J.M., Taylor, B.R., Longwell, J.P., and Sarofim, A.F., Nineteenth Symposium

(International) on Combustion, The Combustion Institute, pp. 167--179, 1982.

17. Ritter, E., Bozzelli, J.W., and Dean, A.M.'s paper accepted in J. Phys. Chem. 1988. Note -- This reference incorrectly lists Kerr and Moss as source of this rate constant. The rate constant was determined by evaluation of literature data and kinetics studies in these laboratories.

18. Cohen, N., Int. J. of Chem. Kinetics, Vol 18, 59-82, (1986).

19. Demore, W.B., Molina, M.J., Waston, R.T., Golden, D.M., Hampson, R.F., Kurylo, M.J., Howard, C.J., AR Ravishankara, and Sander, S.P., Chemical Kinetic and Photochemical Data for use in Stratospheric Modeling, Evaluation No. 8, JPL Publication 87-41, 1987

20. A factor taken as 1/3 that for $CH_4 + O_2$; Ea = ΔH_{rxn}.

21. A factor taken as 1/3 that for $CH_4 + HO_2$; Ea = $H_{rxn} + 8$.

22. A factor taken as 3/4 that for $CH_4 + O_2$; Ea = ΔH_{rxn}

23. A factor based on thermodynamics and microreversibility.
A_{-1} taken as that for $CH_3 + C_3H_7$ ($A = 2.0 \times 10^{13}$), EA = ΔH_{rxn}

24. A factor taken as 2 that for $CH_3 + CH_2O$
Ea = 6.2

25. A factor taken as 1/2 that for $CH_3 + HO_2$

26. Manion, J.A. and Louw, R., Recl. Trav. Chim. Pays-Bas 105, 442- 448, 1986.

27. A factor based on thermodynamics and microreversibility.
A_{-1} taken as that for $CH_3 + C_2H_4$ (log A = 11.5), EA = $\Delta H_{rxn} + 6$

28. A factor based on thermodynamics and microreversibility.
A_{-1} taken as that for $H + C_3H_6$ (log A = 12.9), EA = $\Delta H_{rxn} + 1$.

29. A factor based on thermodynamics and microreversibility.
A_{-1} taken as that for $CH_3 + C_2H_3$ ($A = 1.84 \times 10^{13}$), EA = ΔH_{rxn}

30. Benson, S.W. and Weissman, M., Int'l J. Chem. Kin. Vol. 16, 307, (1984).

31. Treated as CH3O + C2H5

32. Treated as CH2O + C2H5

33. A factor taken as 1/4 that for $CH_2O + OH$; Ea = 1.2

34. A factor taken as 1/4 that for $CH_2O + O$
Ea = 3.5
35. A factor taken as 1/4 that for $CH_2O + Cl$
Ea = 0.5

36. Tsang, W. and Hampson, R.F., J. Phys. Chem. Ref. Data 1986, 15, 1087.

37. A factor refer from Demore et.al. 1987 (source 19); $Ea = \Delta H_{rxn} + 4$

38. A factor taken as 1/2 that CH4 + ClO; $Ea = \Delta H_{rxn} + 4$

39. A factor refer from Demore et.al. 1987 (source 19); $Ea = \Delta H_{rxn} + 4$

40. Herron, J.T., J. Phys. Chem. Ref. Data 1988,17,967.

41. A factor taken as 1/6 that for C2H6 + Cl; Ea = 0.1

42. A factor based on thermodynamics and microreversibility.
A_{-1} taken as that for $CH_3 + CH_3$
$Ea = \Delta H_{rxn} - RT$

43. A factor based on thermodynamics and microreversibility.
A_{-1} taken as that for $H + C_2H_5$
$Ea = \Delta H_{rxn} - RT$

44. A factortaken as that for $CH_3Cl + H$; Ea = 7.62

45. A factor taken as 1/2 that for $CH_4 + HO_2$; $Ea = \Delta H_{rxn} + 8$.

46. Parmar, S.S. and Benson, S.W.; J. Phys. Chem., 92, 2652, 1988.

47. Slagle, I.R., Park, J.Y., Heaven, M.C., and Gutman, D.; J. Am. Chem. Soc., 106, 4356, 1984.

48. Baulch, D.L., Duxbury, J., Grant, S.J., Montague, D.C.; J. Phys. Chem. Ref. Data, 10, Suppl.1,1, 1981.

49. Won., YangSoo, PhD Thesis, NJIT, 1991

50. Wu, Y.P., PhD Thesis, NJIT, 1992

51. A factor taken as 1/2 that for $CH_4 + CH_2$

APPENDIX C

CHEMACT INPUT DATA

units for A : cm^3/mol-sec and sec^{-1}; Ea : Kcal/mole

ΔH_{rxn} taken as from stabilized adduct.

Activated complex Lennard-Jones parameters are estimated using critical property data tabulated in Reid, Prausnitz and Poling (The Properties and Gases and Liquids, 4th Ed.)

geometric mean frequencies are estimated using CPFIT computer code (Ritter, E.R., J. Chem. Inf. Comput. Sci. 31, 400-408,1991) and/or from "Table of Molecular Vibration Frequencies Consolidated Vol.I, Natl. Stand. Ref. Data Ser."; Shimanouchi, T., (U.S. Natl. Bur. Stand.) 1972, NSRDS--NBS 39.

Table C.1. $CH_2Cl + H$ QRRK calculation input parameters

$CH_2Cl + H <=====> [CH_3Cl]^{\#}$ ----> Products

	Reaction	A	Ea
k1	CH2Cl + H ---> CH3Cl	1.0E+14	0.0
k-1	CH3Cl ---> CH2Cl + H	8.9E+15	100.8
k2	CH3Cl ---> ^{1}CH2 + HCl	3.6E+13	101.7
k3	CH3Cl ---> CH3 + Cl	1.2E+15	81.6

k1 A_1 factor taken as that for 1-C_3H_7 + H,
(Allara,D.L. and Shaw, R.J., J. Phys. Chem. Ref. Data, 9,523, 1980)

k-1 thermodynamics and microreversibility <mr>

k2 Ea = H_{rxn} + 3.75 (evaluated literature for HCl eliminations)
A = (ekT/h) $\exp^{S/R}$ (Transition State Theory) S = 0.0

k3 A_3 factor based on thermodynamics and microreversibility.
A_{-3} taken as that for $C_2H_5 + CH_3$ (Allara & Shaw)
Ea = H_{rxn} - RT

<v> = 1575.0 cm^{-1}

Lennard-Jones parameters : σ = 4.18 Å, ε/k = 350.0 K

Table C.2. $CH_2Cl + CH_2Cl$ QRRK calculation input parameters

$CH_2Cl + CH_2Cl <=====> [CH_2ClCH_2Cl]^{\#}$ ----> Products

	Reaction	A	Ea
k1	CH2Cl + CH2Cl ---> CH2ClCH2Cl	4.0E+12	0.0
k-1	CH2ClCH2Cl ---> CH2Cl + CH2Cl	4.8E+17	89.2
k2	CH2ClCH2Cl ---> CH2ClCH2 + Cl	6.0E+15	80.7
k3	CH2ClCH2Cl ---> C2H3Cl + HCl	1.9E+13	55.4

k1. A_1 factor taken as that for 1-C_3H_7 + 1-C_3H_7
(Allara,D.L. and Shaw, R.J., J. Phys. Chem. Ref. Data, 9,523, 1980)

k-1 thermodynamics and microreversibility <mr>.

k2. A_2 factor based on thermodynamics and microreversibility.
A_{-2} taken as that for $C_3H_7 + CH_3$ (Allara & Shaw)
Ea = H_{rxn} - RT

k3 Ea = H_{rxn} + 38 (evaluated HCl eliminate rate data)
A = (ekT/h) $\exp^{S/R}$ (Transition State Theory) x Degeneracy
S = -4.0

<v> = 797.2 cm^{-1}

Lennard-Jones parameters : σ = 5.12 Å, ε/k = 471.2 K

Table C.3. CH_2Cl + OH QRRK calculation input parameters

$CH_2Cl + OH <=====> [CH_2ClOH]^{\#} ----> Products$

	Reaction	A	Ea
k1	CH2Cl + OH ---> CH2ClOH	1.6E+13	0.0
k-1	CH2ClOH ---> CH2Cl + OH	2.4E+16	91.0
k2	CH2ClOH ---> CH2OH + Cl	5.5E+15	81.2
k3	CH2ClOH ---> CH2O + HCl	7.6E+13	40.6

k1 A_1 factor taken as that for $CH_2Cl + CH_3$
(Allara,D.L. and Shaw, R.J., J. Phys. Chem. Ref. Data, 9,523, 1980)
k-1 thermodynamics and microreversibility.
k2 A_3 factor based on thermodynamics and microreversibility.
A_{-3} taken as that for $C_2H_5 + CH_3$ (Allara & Shaw)
Ea = H_{rxn} - RT
k3 Ea = H_{rxn} + 38 (evaluated HCl eliminate rate data)
A = (ekT/h) $exp^{S/R}$ (Transition State Theory) x Degeneracy
S = -4.0

<v> = 1200.0 cm^{-1}
Lennard-Jones parameters : σ = 4.61 Å, ε/k = 535.0 K

Table C.4. CH_2Cl + ClO QRRK calculation input parameters

$CH_2Cl + ClO <=====> [CH_2ClOCl]^{\#} ----> Products$

	Reaction	A	Ea
k1	CH2Cl + ClO ---> CH2ClOCl	6.5E+12	0.0
k-1	CH2ClOCl ---> CH2Cl + ClO	2.3E+16	86.3
k2	CH2ClOCl ---> CH2ClO + Cl	3.0E+15	64.0
k3	CH2ClOCl ---> CHClO + HCl	9.6E+12	34.0

k1 A_1 factor taken as 1/2 that for $CH_3 + ClO$ (Table 9, k1)
k-1 thermodynamics and microreversibility.
k2 A = (ekT/h) $exp^{S/R}$
(Benson,S.W., "Thermochemical Kinetics", John Wiley & Son, 2nd ed. N.Y., 1976.
CH3I ---> CH3 + I) S = 9.0, Ea = H_{rxn} - RT
k3 Ea = Ring Strain + abstraction + H_{rxn}
A = (ekT/h) $exp^{S/R}$ (Transition State Theory) x Degeneracy
S = -4.0

<v> = 797.2 cm^{-1}
Lennard-Jones parameters : σ = 5.12 Å, ε/k = 471.2 K

Table C.5. $CH_2Cl + O$ QRRK calculation input parameters

$CH_2Cl + O \Longleftrightarrow [CH_2ClO]^{\#} \longrightarrow$ Products

	Reaction	A	Ea
k1	CH2Cl + O ---> CH2ClO	2.0E+13	0.5
k-1	CH2ClO ---> CH2Cl + O	1.2E+16	84.5
k2	CH2ClO ---> CH2O + Cl	3.0E+13	7.0
k3	CH2ClO ---> CHO + HCl	7.3E+13	34.0

k1. A_1 factor taken as 1/3 that for $CH_3 + O$
(Washido & Bayes, J. Chem. Phys. 73, 1665, 1980)
k_{-1} thermodynamics and microreversibility.
k2. A factor taken as that CCCC. ---> C2H5 + C=C
(Dean, A.M., J. Phys. Chem. 1985)
Ea = H_{rxn} + 7.0
k3 Ea = Ring Strain + abstraction + H_{rxn}
A = (ekT/h) $\exp^{S/R}$ (Transition State Theory) x Degeneracy
S = 0.0

<v> = 1247.0 cm^{-1}
Lennard-Jones parameters : σ = 4.61 Å, ε/k = 535.0 K

Table C.6. $CH_2Cl + O_2$ QRRK calculation input parameters

$CH_2Cl + O_2 \Longleftrightarrow [CH_2ClOO.]^{\#} \Longleftrightarrow [C.H_2OOCl]^{\#} \longrightarrow CH_2O + ClO$

	Reaction	A	Ea
k1	CH2Cl + O2 ---> CH2ClOO.	4.0E+12	0.0
k-1	CH2ClOO. ---> CH2Cl + O2	3.5E+15	25.4
k2	CH2ClOO. ---> C.H2OOCl	4.8E+12	26.0
k-2	C.H2OOCl ---> CH2ClOO.	3.0E+11	19.0
k3	C.H2OOCl ---> CH2O + ClO	5.0E+13	1.00

k1 A_1 factor taken as that for 1-$C_3H_7 + O_2$
(Mark et.al. Chem. Phys. Lett. vol. 132, p417, 1986)
k-1 thermodynamics and microreversibility <mr>.
k2 A = (ekT/h) $\exp^{S/R}$ (Transition State Theory) S = -4.0, Estimate a barrier of 26 Kcal/mol (19 Kcal for ring strain and 7 Kcal for ROO. abstraction of Cl)
k-2 <mr>
k3 A_3 factor based on <mr>; A_{-3} taken as 1/2 that for $CH_2O + OH$
(Dean, A.M. and Westmoreland, P.R. Int'l. J. of Chem. Kinetics, Vol. 19, 207-228, 1987) Ea = 1.0
<v> = 1116.0 cm^{-1}
Lennard-Jones parameters : σ = 4.90 Å, ε/k = 356.0 K

Table C.7. $CH_2Cl + CH_3$ QRRK calculation input parameters

$CH_2Cl + CH_3 <=====> [CH_2ClCH_3]^{\#}$ ---->Products

	Reaction	A	Ea
k1	CH2Cl + CH3 ---> CH2ClCH3	2.00E+13	0.0
k-1	CH2ClCH3 ---> CH2Cl + CH3	1.63E+17	90.6
k2	CH2ClCH3 ---> C2H4 +HCl	3.24E+13	56.6
k3	CH2ClCH3 ---> C2H5 + Cl	2.17E+15	84.1

k1 A_1 factor taken as that for $C_3H_7 + CH_3$ (A =2.0 E+13)(Allara,D.L. and Shaw, R.J., J. Phys. Chem. Ref. Data, 9,523, 1980) (Bond energy ref: Weissman,M and Benson,S.W., J. Phys. Chem., 87, 243, 1983)

k-1 thermodynamics and microreversibility. Ea = 0.0,

k2 Benson,S.W., "Thermochemical Kinetics", John Wiley & Son, 2nd ed. N.Y., 1976

k3 A_3 based on <mr>, A_{-3} taken as that $CH_3CH_2 + CH_3$ (A = 2.0 E+13)
Ea = ΔHr - RT

<v> = 1265.3 cm^{-1}

Lennard-Jones parameters : σ = 4.90 Å, ε/k = 300.0 K

Table C.8. $CH_2Cl + CHCl_2$ QRRK calculation input parameters

$CH_2Cl + CHCl_2 <=====> [CH_2ClCHCl_2]^{\#}$ ---->Products

	Reaction	A	Ea
k1	CH2Cl + CHCl2 ---> CH2ClCHCl2	3.97E+12	0.0
k-1	CH2ClCHCl2 ---> CH2Cl + CHCl2	5.28E+17	90.1
k2	CH2ClCHCl2 ---> CH2CCl2 +HCl	4.80E+12	52.2
k3	CH2ClCHCl2 ---> CHClCHCl + HCl	1.92E+13	52.6

k1 A_1 factor as 1/2 that for $C_4H_9 + 2\text{-}C_3H_7$ (A = 7.94 E+12) (Allara,D.L. and Shaw) (Bond energy ref: Weissman,M and Benson,S.W., J Phys. Chem., 87, 243, 1983)

k-1 thermodynamics and microreversibility. Ea = 0.0,

k2 Ea = H_{rxn} + 38.5 (evaluated HCl eliminate rate data)
A = (ekT/h) $exp^{S/R}$ (Transition State Theory) x Degeneracy
S = -4.0

k3 $A_3 = 10^{13.72} * 10(-4/4.6) * 4$
Ea = ΔH + 38.5

<v> = 678.7 cm^{-1}

Lennard-Jones parameters : σ = 5.72 Å, ε/k = 498.9 K

Table C.9. CH_3 + ClO QRRK calculation input parameters

$CH_3 + ClO \Longleftrightarrow [CH_3OCl]^{\#} \longrightarrow$ products

	Reaction	A	Ea
k1	CH3 + ClO ---> CH3OCl	1.3E+13	0.0
k-1	CH3OCl ---> CH3 + ClO	3.7E+15	90.3
k2	CH3OCl ---> CH3O + Cl	3.0E+15	63.8
k3	CH3OCl ---> CH2O + HCl	1.4E+13	34.0

k1 A_1 factor taken as 1/2 that for CH_3 + OH
(Dean et al. Int'l J. Chem. Kin., 19, 207,1987.)
k-1 thermodynamics and microreversibility.
k2 $A = (ekT/h)\ exp^{S/R}$
(ref: Benson CH3I ---> CH3 + I) S = 9.0
Ea = H_{rxn} - RT
k3 Ea = Ring Strain + abstraction + H_{rxn}
$A = (ekT/h)\ exp^{S/R}$ (Transition State Theory) x Degeneracy
S = -4.0

<v> = 1111.0 cm^{-1}
Lennard-Jones parameters : σ = 5.12 Å, ε/k = 537.0 K

Table C.10. CH_3 + $CHCl_2$ QRRK calculation input parameters

$CH_3 + CHCl_2 \Longleftrightarrow [CH_3CHCl_2]^{\#} \longrightarrow$ Products

	Reaction	A	Ea
k1	CH3 + CHCl2 ---> CH3CHCl2	1.5E+12	0.0
k-1	CH3CHCl2 ---> CH3 + CHCl2	2.0E+17	91.9
k2	CH3CHCl2 ---> CH3CHCl + Cl	3.9E+15	76.8
k3	CH3CHCl2 ---> C2H3Cl + HCl	4.0E+13	55.4

k1 A_1 factor taken as that for CH_3 + 2-C_4H_9
(Allara,D.L. and Shaw, R.J., J. Phys. Chem. Ref. Data, 9,523, 1980)
k-1 thermodynamics and microreversibility.
k2 A_2 factor based on <mr>, A_{-2} taken as that for C_3H_7 + CH_3 (Allara & Shaw)
Ea = H_{rxn} - RT
k3 Ea = H_{rxn} + 38 (evaluated HCl eliminate rate data)
$A = (ekT/h)\ exp^{S/R}$ (Transition State Theory) x Degeneracy
S = -4.0

<v> = 797.2 cm^{-1}
Lennard-Jones parameters : σ = 5.12 Å, ε/k = 471.2 K

Table C.11. $CHCl_2$ + $CHCl_2$ QRRK calculation input parameters

$CHCl_2 + CHCl_2 <=====> [CHCl_2CHCl_2]^{\#} ----> Products$

	Reaction	A	Ea
k1	CHCl2 + CHCl2 ---> CHCl2CHCl2	1.2E+12	0.0
k-1	CHCl2CHCl2 ---> CHCl2 + CHCl2	5.9E+17	88.6
k2	CHCl2CHCl2 ---> CHCl2CHCl + Cl	6.7E+15	74.6
k3	CHCl2CHCl2 ---> C2HCl3 + HCl	1.9E+13	51.1

k1 A_1 factor taken as 1/4 that for 1-C_4H_9 + 1-C_4H_9
(Allara,D.L. and Shaw, R.J., J. Phys. Chem. Ref. Data, 9,523, 1980)

k-1 thermodynamics and microreversibility.

k2 A_2 factor based on <mr>, A_{-2} taken as that for C_4H_9 + CH_3 (Allara & Shaw)
Ea = H_{rxn} - RT

k3 Ea = H_{rxn} + 38 (evaluated HCl eliminate rate data)
A = (ekT/h) $exp^{S/R}$ (Transition State Theory) x Degeneracy
S = -4.0

<v> = 578.0 cm^{-1}
Lennard-Jones parameters : σ = 5.91 Å, ε/k = 525.9 K

Table C.12. CH_2CHCl + H QRRK calculation paramters

$CH_2CHCl + H <=====> [CH_2CH_2Cl]^{\#} ----> Products$

	Reaction	A	Ea
k1	C2H3Cl + H ---> CH2CH2Cl	1.33E+13	5.8
k-1	CH2CH2Cl ---> C2H3Cl + H	1.27E+13	45.1
k2	CH2CH2Cl ---> C2H4 + Cl	3.13E+13	20.7
k3	CH2CH2Cl ---> C2H3 + HCl	9.60E+12	62.3

k1 A_1 factor taken as 1/3 that for CH_2CH_2 + H (A=4.0 E+13,Ea=2.6)(Allara and Shaw)
Ea taken as average of C_2H_4 + H and C_2Cl_4 + H
(Tsang, W. and Walker, J.A., poceeding 23rd Symposium on Combustion Int'l Combustion Inst. p139, 1991; C_2Cl_4 + H, Ea=9.0)

k-1 thermodynamics and microreversibility.

k2 A_2 from <mr>, A_{-2} taken as that for CH_2CH_2 + Cl (A = 1.6 E+13, Ea = 0.0)
(Kerr,J.A. and Moss,S.J. ,"Handbook of Bimolecular and Termolecular Gas Reaction Vol. I & II", CRC Press Inc.,1981)

k3 Ea = H_{rxn} + 38 (evaluated HCl eliminate rate data)
A = (ekT/h) $exp^{S/R}$ (Transition State Theory) x Degeneracy
S = -4.0

<v> = 1265.3 cm^{-1}
Lennard-Jones parameters : σ = 4.9 Å, ε/k = 300.0 K

Table C.13. CH_2CCl_2 + H QRRK calculation paramters

$CH_2CCl_2 + H <=====> [CH_2CHCl_2]^{\#}$ ----> Products

	Reaction	A	Ea
k1	CH2CCl2 + H ---> CH2CHCl2	7.00E+12	7.5
k-1	CH2CHCl2 ---> CH2CCl2 + H	8.08E+12	43.8
k2	CH2CHCl2 ---> C2H3Cl + Cl	4.62E+14	22.4
k3	CH2CHCl2 ---> CHClCH + HCl	2.40E+13	57.7

k1 A_1 factor taken as 1/2 that for C_2Cl_4 + H (A=1.4 E+13)
(Tsang, W. and Walker, J.A., Proceeding 23rd Symposium on Combustion Int'l Combustion Inst. p139, 1991)

k-1 thermodynamics and microreversibility.

k2 A_2 based upon <mr>, for $CH_2CHCl + Cl = CH_2CHCl_2$
with A_{-2} = 2.0 E+13 and Ea_{-2} = 1.5
(Kerr,J.A. and Moss,S.J. ,"Handbook of Bimolecular and Termolecular Gas Reaction Vol. I & II", CRC Press Inc., 1981)

k3 Ea = H_{rxn} + 38 (evaluated HCl eliminate rate data)
A = (ekT/h) $\exp^{S/R}$ (Transition State Theory) x Degeneracy
S = -4.0

<v> = 736.0 cm^{-1}
Lennard-Jones parameters : σ = 5.1 Å, ε/k = 435.9 K

Table C.14. CHClCHCl + H QRRK calculation parameters

$CHClCHCl + H <=====> [CH_2ClCHCl]^{\#}$ ----> Products

	Reaction	A	Ea
k1	CHClCHCl + H ---> CH2ClCHCl	2.60E+13	5.8
k-1	CH2ClCHCl ---> CHClCHCl + H	1.41E+13	47.2
k2	CH2ClCHCl ---> C2H3Cl + Cl	1.72E+14	27.3
k3	CH2ClCHCl ---> CH2CCl. + HCl	2.40E+13	57.7

k1 A_1 factor taken as 2 that for C_2H_3Cl + H (A=1.3 E+13)
(Tsang, W. and Walker, J.A., Proceeding 23rd Symposium on Combustion Int'l Combustion Inst. p139, 1991)

k-1 thermodynamics and microreversibility.

k2 A_2 based upon <mr>, for $CH_2CHCl + Cl = CH_2CHCl_2$
with A_{-2} = 2.0 E+13 and Ea_{-2} = 1.5 (Kerr,J.A. and Moss,S.J. 1981)

k3 Ea = H_{rxn} + 38 (evaluated HCl eliminate rate data)
A = (ekT/h) $\exp^{S/R}$ (Transition State Theory) x Degeneracy
S = -4.0

<v> = 736.0 cm^{-1}
Lennard-Jones parameters : σ = 5.1 Å, ε/k = 435.9 K

Table C.15. $CHClCCl_2$ + H QRRK calculation parameters

$CHClCCl_2 + H \Longleftrightarrow [CH_2ClCCl_2]^{\#} \longrightarrow$ Products

	Reaction	A	Ea
k1	CHClCCl2 + H ---> CH2ClCCl2	1.33E+13	5.8
k-1	CH2ClCCl2 ---> CHClCCl2 + H	1.18E+13	49.5
k2	CH2ClCCl2 ---> CH2CCl2 + Cl	7.30E+13	22.5
k3	CH2ClCCl2 ---> C2HCl2 + HCl	9.60E+12	64.5

k1 A_1 factor taken as that for C_2H_3Cl + H (A=1.33 E+13)
(Tsang, W. and Walker, J.A., Proceeding 23rd Symposium on Combustion Int'l Combustion Inst. p139, 1991;

k-1 thermodynamics and microreversibility.

k2 A_2 based upon <mr>, for $C_2Cl_4 + Cl = C_2Cl_5$
with A_{-2} = 1.26 E+13 and Ea_{-2} = 0.0 (Kerr,J.A. and Moss,S.J. 1981)

k3 Ea = H_{rxn} + 38 (evaluated HCl eliminate rate data)
A = (ekT/h) $exp^{S/R}$ (Transition State Theory) x Degeneracy
S = -4.0

<v> = 666.62 cm^{-1}
Lennard-Jones parameters : σ = 5.6 Å, ε/k = 510.0 K

Table C.16. $^1CH_2 + H_2$ QRRK calculation parameters

$^1CH_2 + H_2 \Longleftrightarrow [CH_4]^{\#} \longrightarrow$ Products

	Reaction	A	Ea
k1	^{1}CH2 + H2 ---> CH4	7.0E+13	0.0
k-1	CH4 ---> ^{1}CH2 + H2	5.9E+15	119.34
k2	CH4 ---> CH3 + H	1.0E+16	105.0

k1 Miller, J.A. and Bowman, C.T., Prog. Energy. Combust. Sci., p 1 , 1989.

k-1 thermodynamics and microreversibility.

k2 Dean, A. M., J. Phys. Chem., 89, 4600, 1985

<v> = 1957.0 cm^{-1}
Lennard-Jones parameters : σ = 3.76 Å, ε/k = 148.6 K

Table C.17. $^1CH_2 + CH_4$ QRRK calculation input data

$^1CH_2 + CH_4 <====> [CH_3CH_3]^{\#}$ ----> Products

	Reaction	A	Ea
k1	^{1}CH2 + CH4 ---> C2H6	4.00E+13	0.0
k-1	C2H6 ---> ^{1}CH2 + CH4	1.46E+16	103.78
k2	C2H6 ---> CH3 + CH3	8.00E+16	90.4
k3	C2H6 ---> C2H5 + H	1.30E+16	100.7

k1 Miller, J.A. and Bowman, C.T., Prog. Energy. Combust. Sci., p 1 , 1989.
k-1 thermodynamics and microreversibility.
k2 Dean, A. M., J. Phys. Chem., 89, 4600, 1985
k3 Dean, A. M., J. Phys. Chem., 89, 4600, 1985

<v> = 1509.0 cm^{-1}
Lennard-Jones parameters : σ = 4.342 Å, ε/k = 246.8 K

Table C.18. $^1CH_2 + CH_3Cl$ QRRK calculation input parameters

$^1CH_2 + CH_3Cl <====> [CH_2ClCH_3]^{\#}$ ----> Products

	Reaction	A	Ea
k1	^{1}CH2 + CH3Cl---> C2H5Cl	2.00E+13	0.0
k-1	C2H5Cl ---> ^{1}CH2 + CH3Cl	8.71E+15	108.68
k2	C2H5Cl ---> C2H4 + HCl	3.24E+13	56.6
k3	C2H6 ---> C2H5 + Cl	2.17E+15	84.1

k1 A_1 factor taken as that for $^1CH_2 + CH_4$ (A =4.0 E+13)
k-1 thermodynamics and microreversibility. Ea = 0.0,
k2 Benson,S.W., "Thermochemical Kinetics", John Wiley & Son, 2nd ed. N.Y., 1976
k3 A_3 based on thermodynamics and microreversibility.
A_{-3} taken as that $CH_3CH_2 + CH_3$ (A = 2.0 E+13)
Ea = ΔHr - RT

<v> = 1265.3 cm^{-1}
Lennard-Jones parameters : σ = 4.898 Å, ε/k = 300.0 K

APPENDIX D

EXPERIMENT AND MODELING RESULTS FIGURES

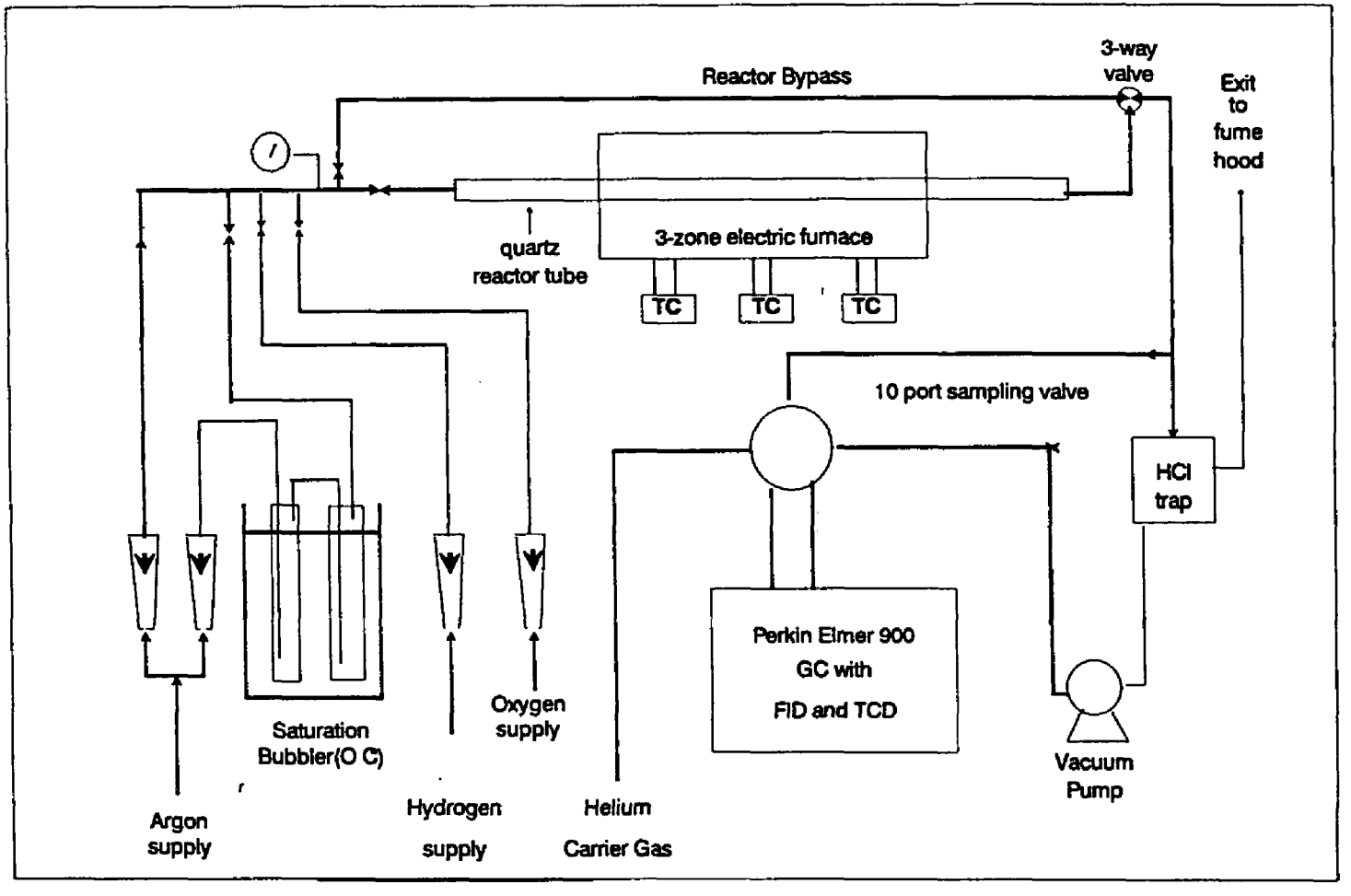

Fig 2.1 Experimental Apparatus

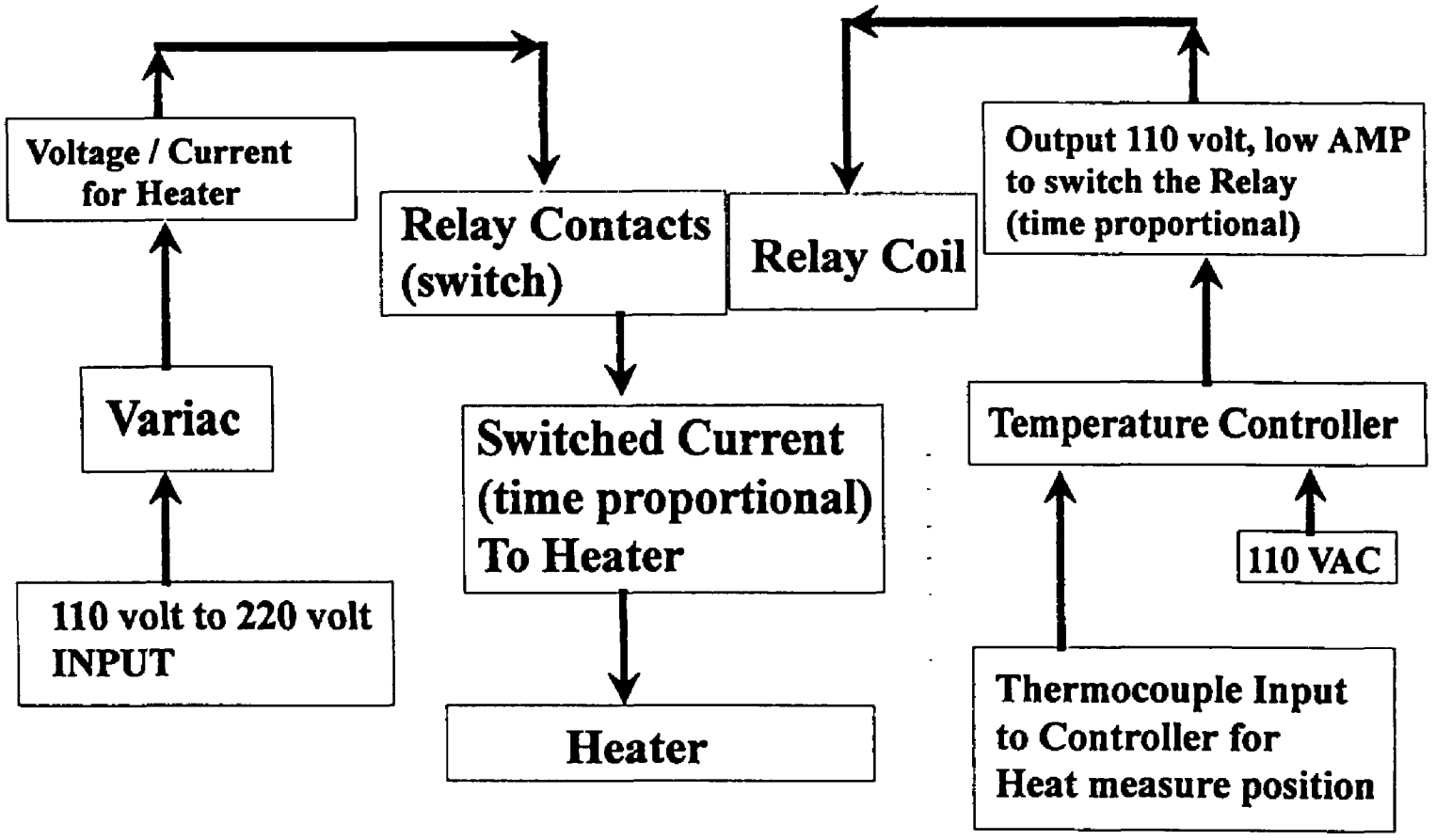

Fig 2.2 Schematic of Voltage and Thermocouple Input to Temperature Controller

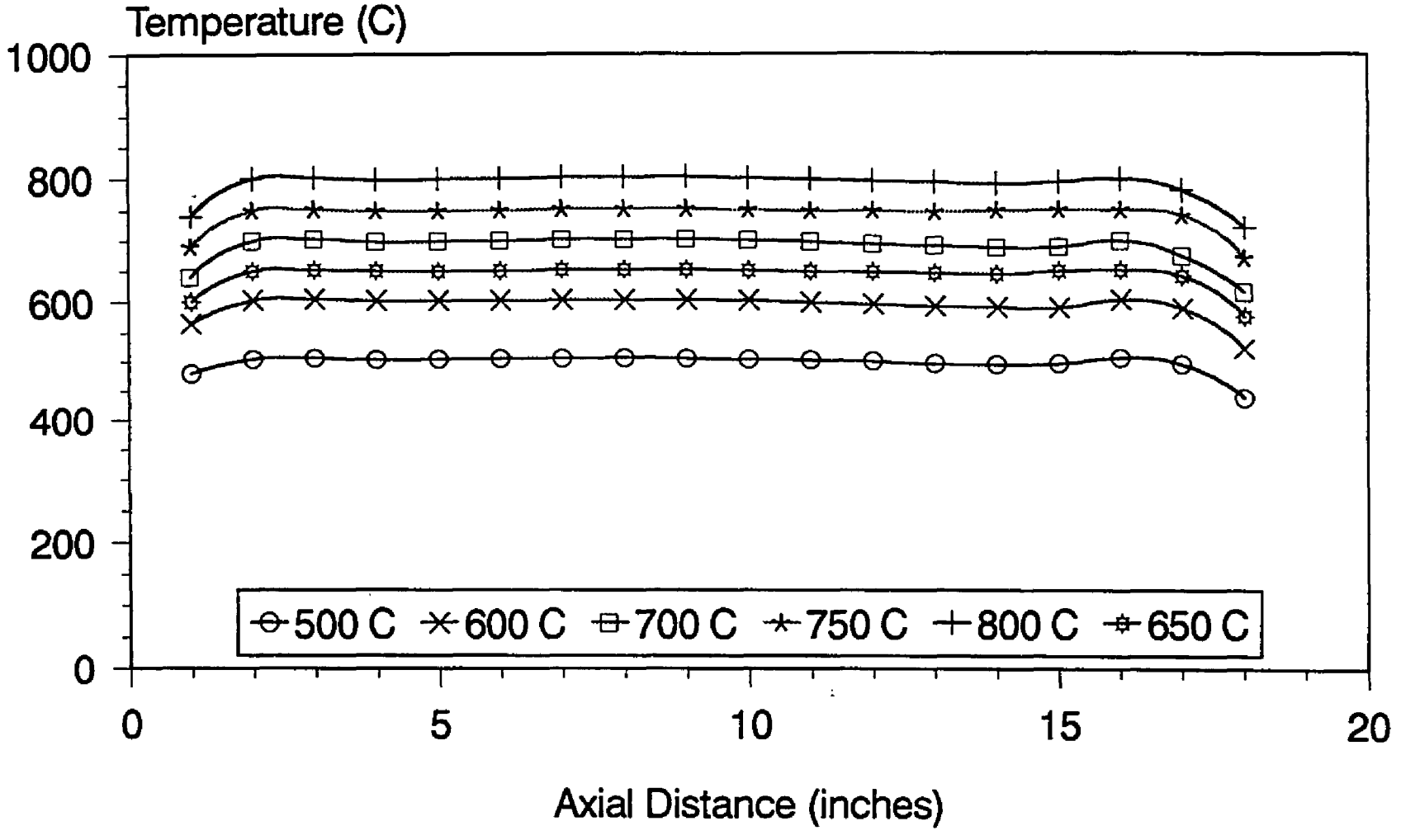

Fig 2.3 Temperature Profile

Column: 1.5m x 1/8" OD, 1% AT-1000 on Graphpac GB

Detector: FID, 250 C

Temperature: 35 C, 2 min, 15 C/min. to 200 C

Carrier Gas: He, 25 ml/min.

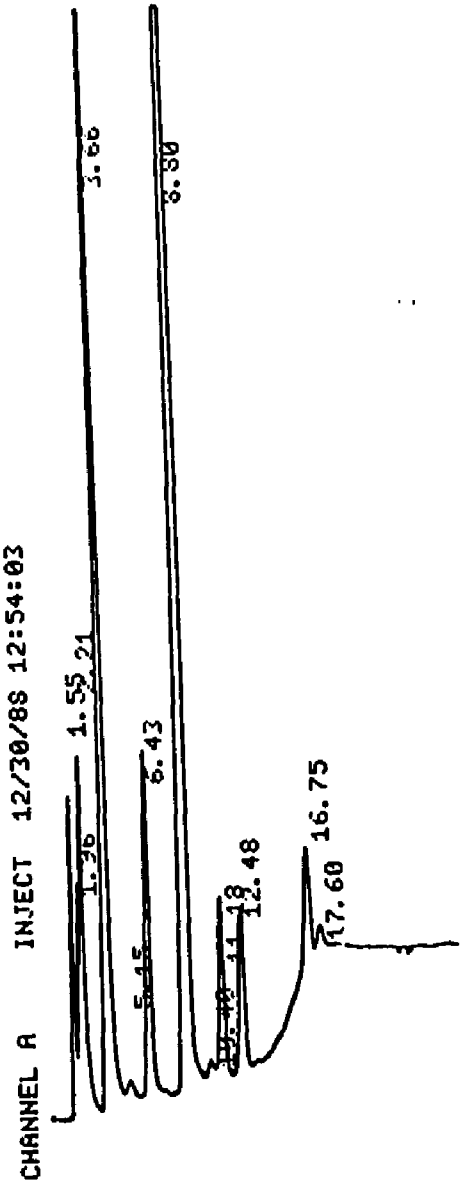

Figure 2.4 Sample Chromatogram of $CH_2Cl_2/O_2/H_2$ Decomposition

Column: 1.8m x 1/8" OD, GCA-013 SPHEROCARB 100/200

Detector: TCD, 100 C, 175 mA

Temperature: 35 C, 2 min, 15 C/min. to 200 C

Carrier Gas: He, 30 ml/min.

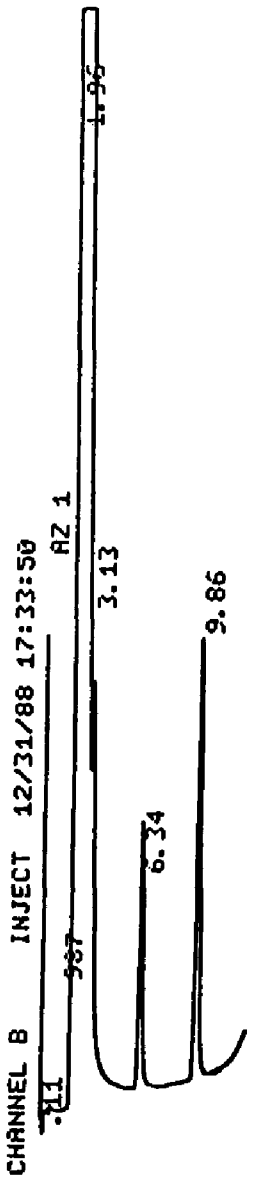

Figure 2.5 Sample Chromatogram of $CH_2Cl_2/O_2/H_2$ Decomposition

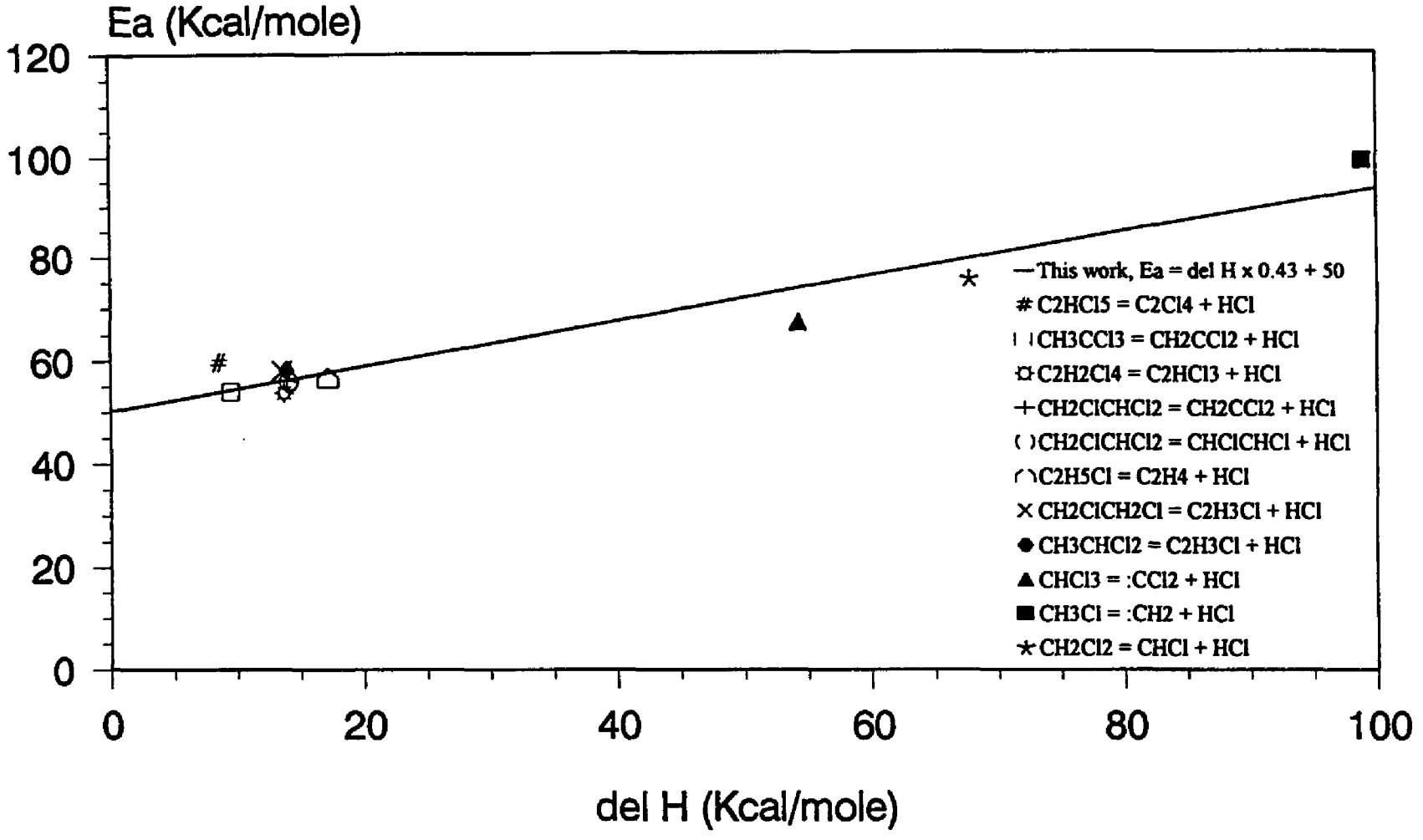

Fig. 4.1 Energy Barrier for HCl elimination

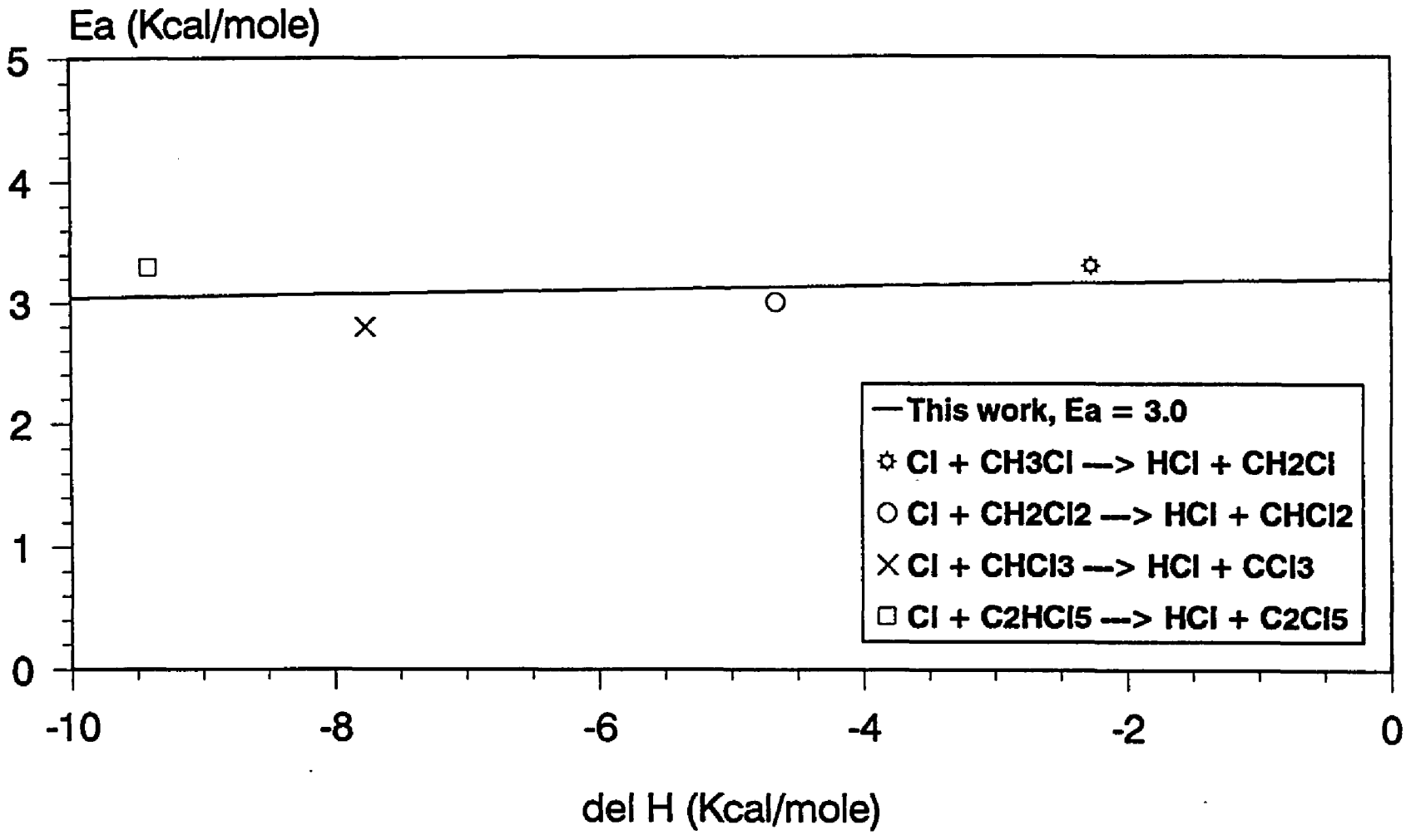

Fig 4.2 Evans-Polanyi Plot, Cl + CHC ---> HCl + R'.

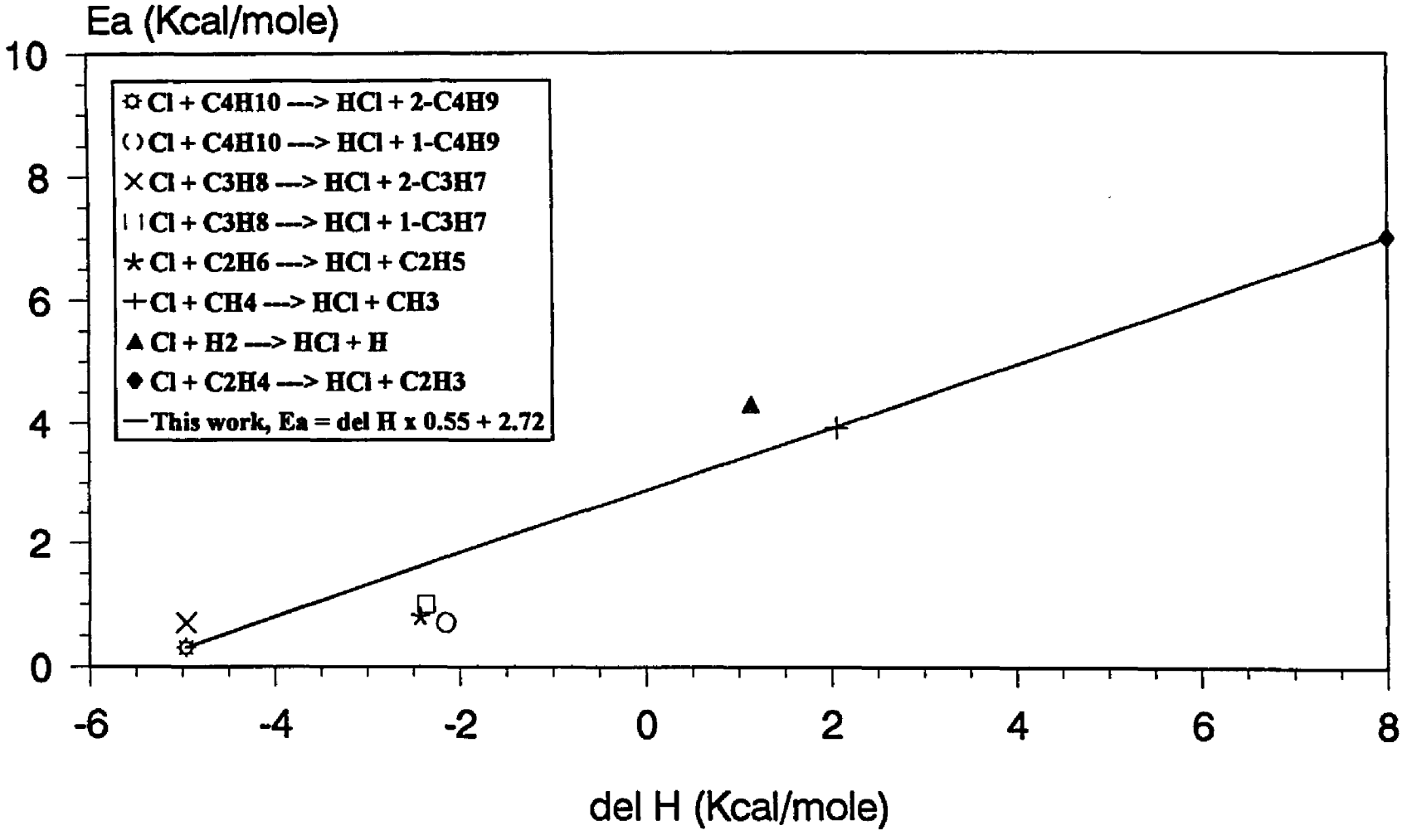

Fig. 4.3 Evans-Polanyi Plot, Cl + RH —> HCl + R.

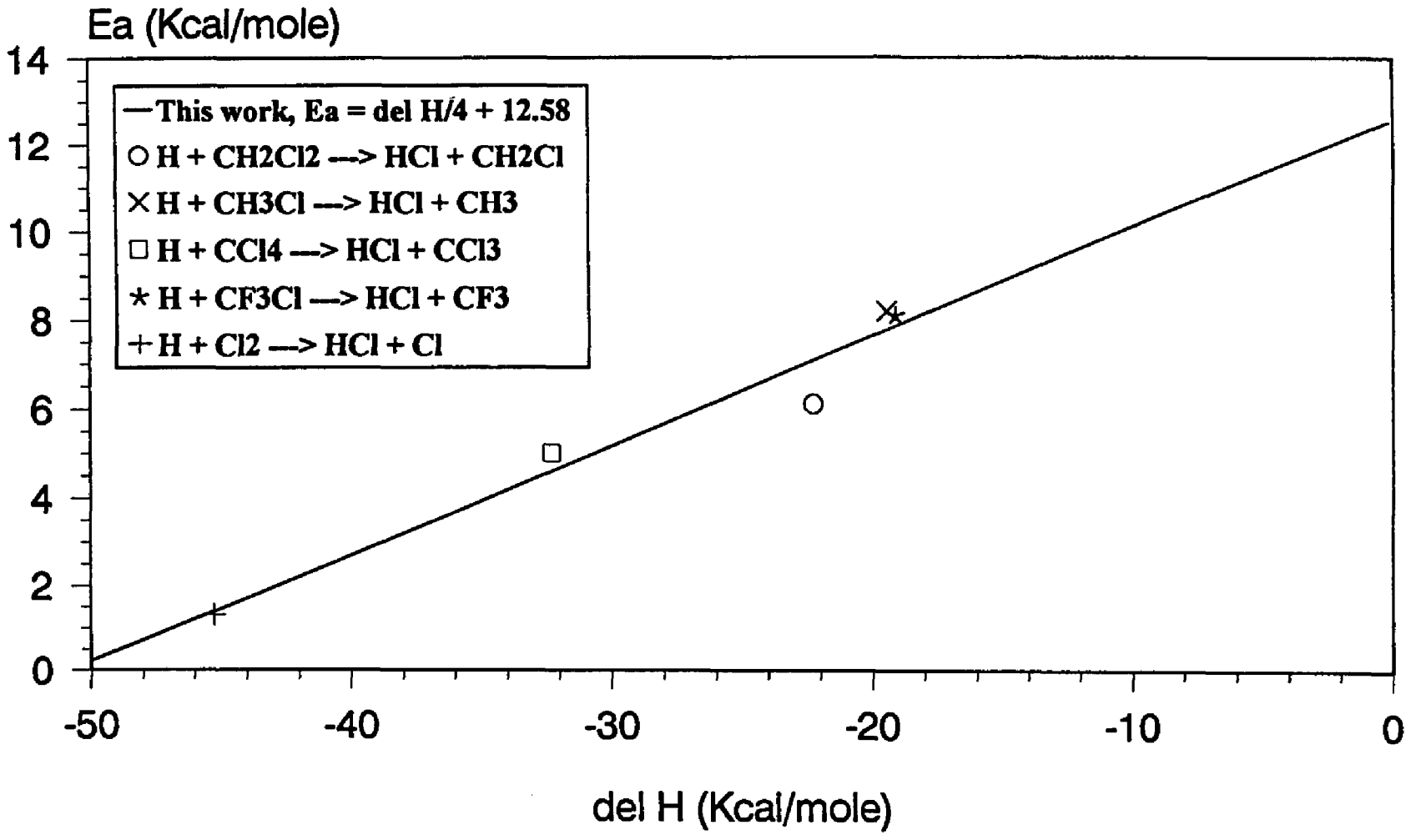

Fig. 4.4 Evans-Polanyi Plot, H + RCl —> HCl + R.

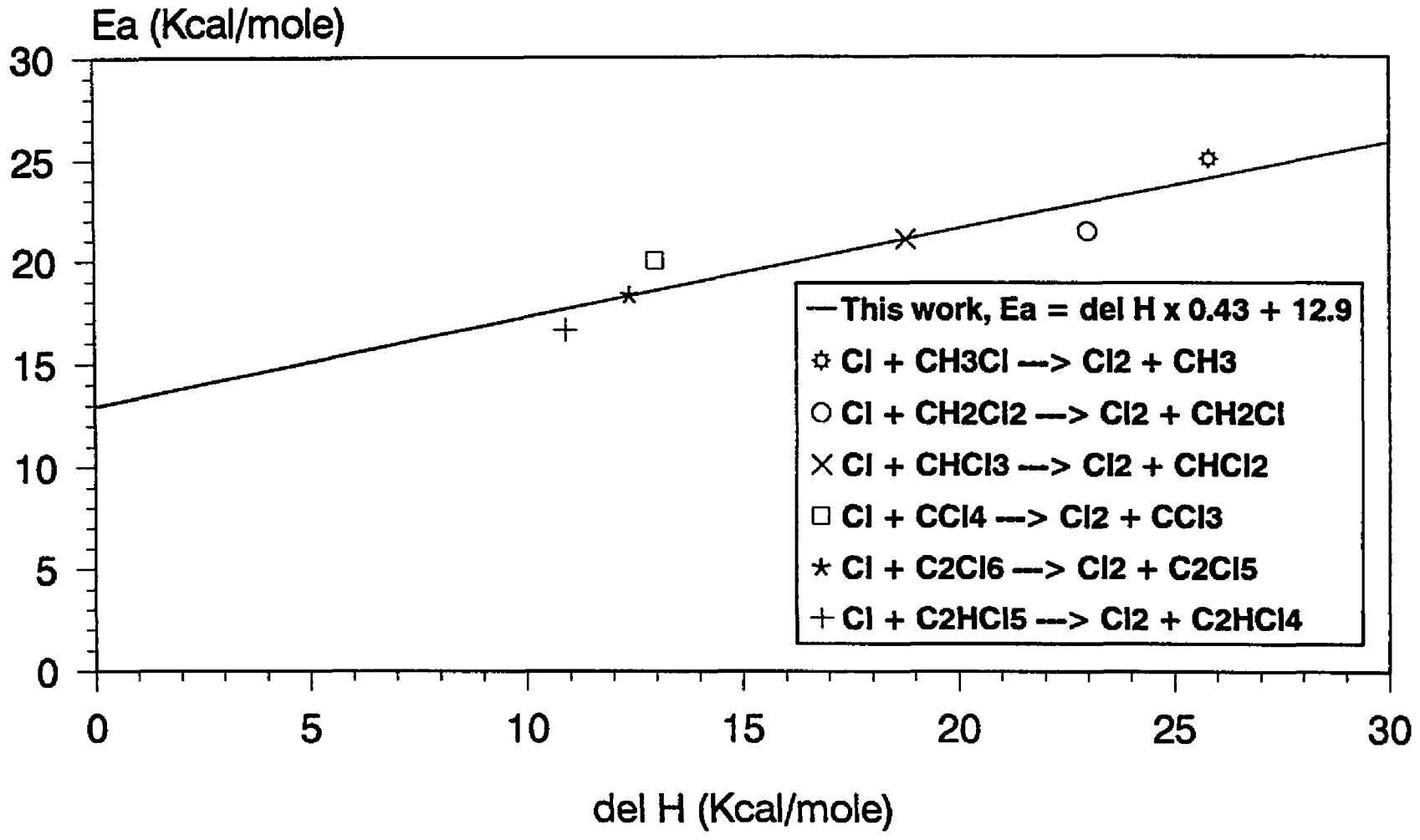

Fig. 4.5 Evans-Polanyi Plot, Cl + RCl ---> Cl2 + R.

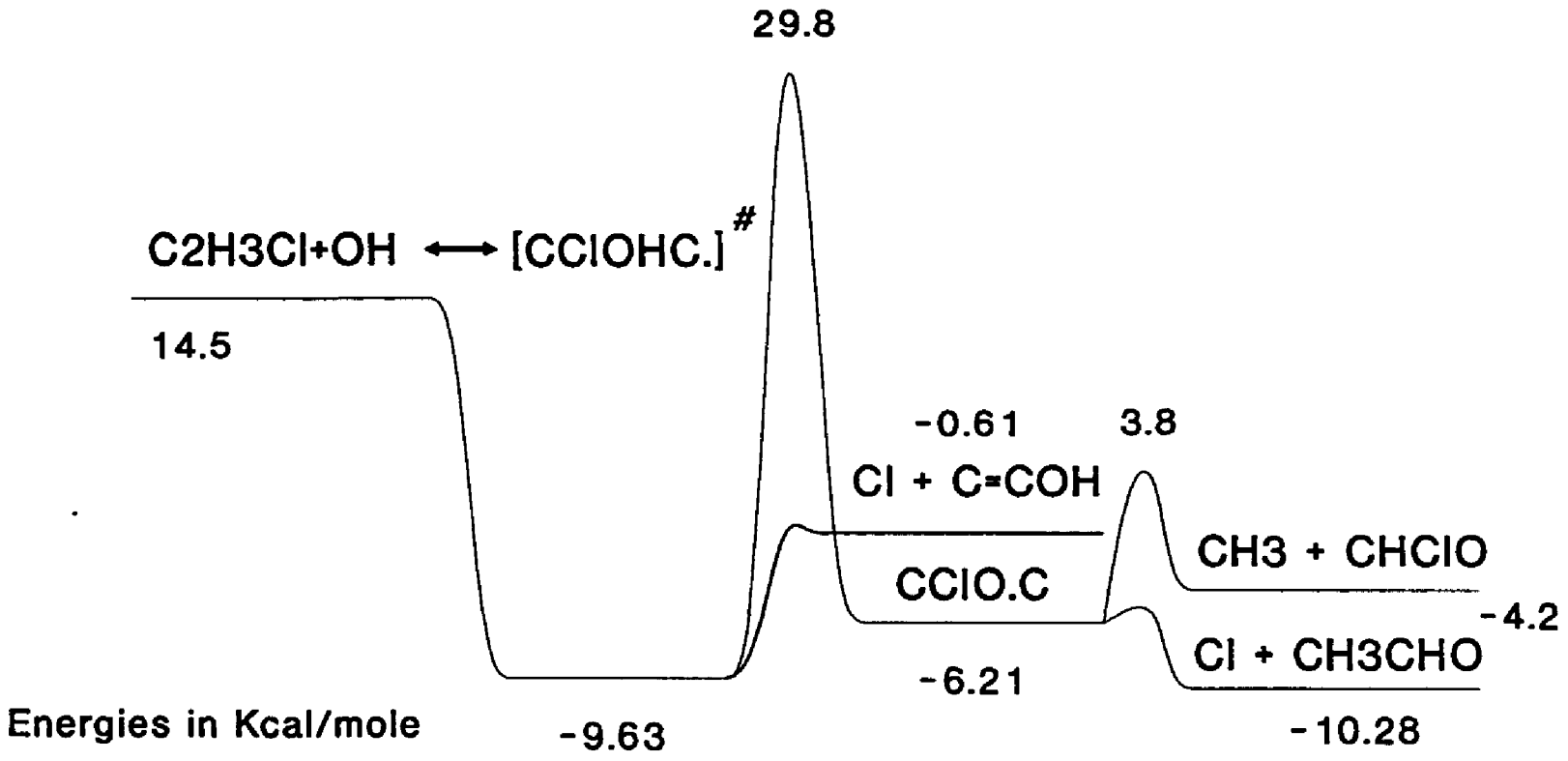

Fig 5.1 Energy level for C2H3Cl+OH alpha addition

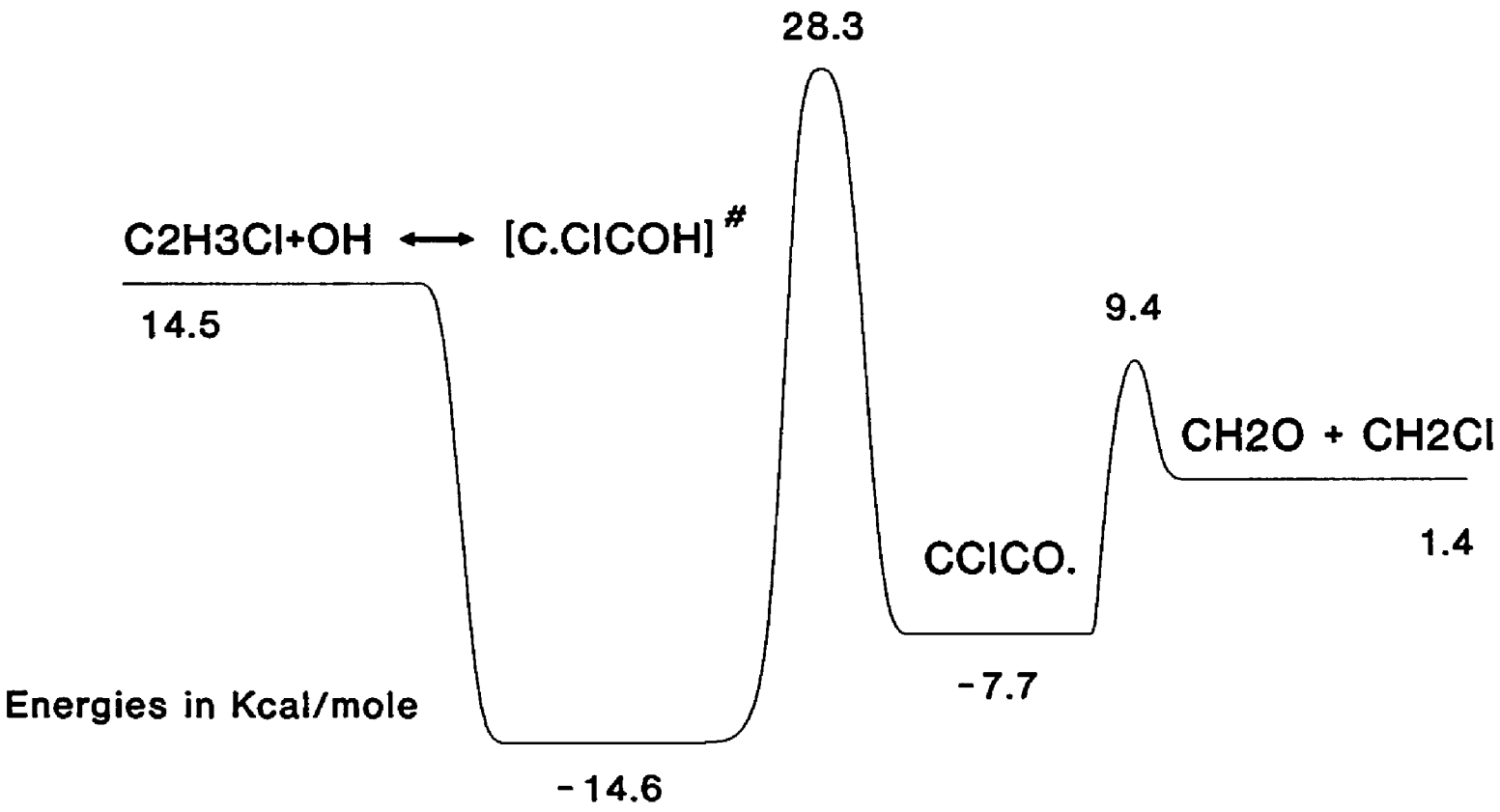

Fig 5.2 Potential energy diagram for C2H3Cl+OH beta addition

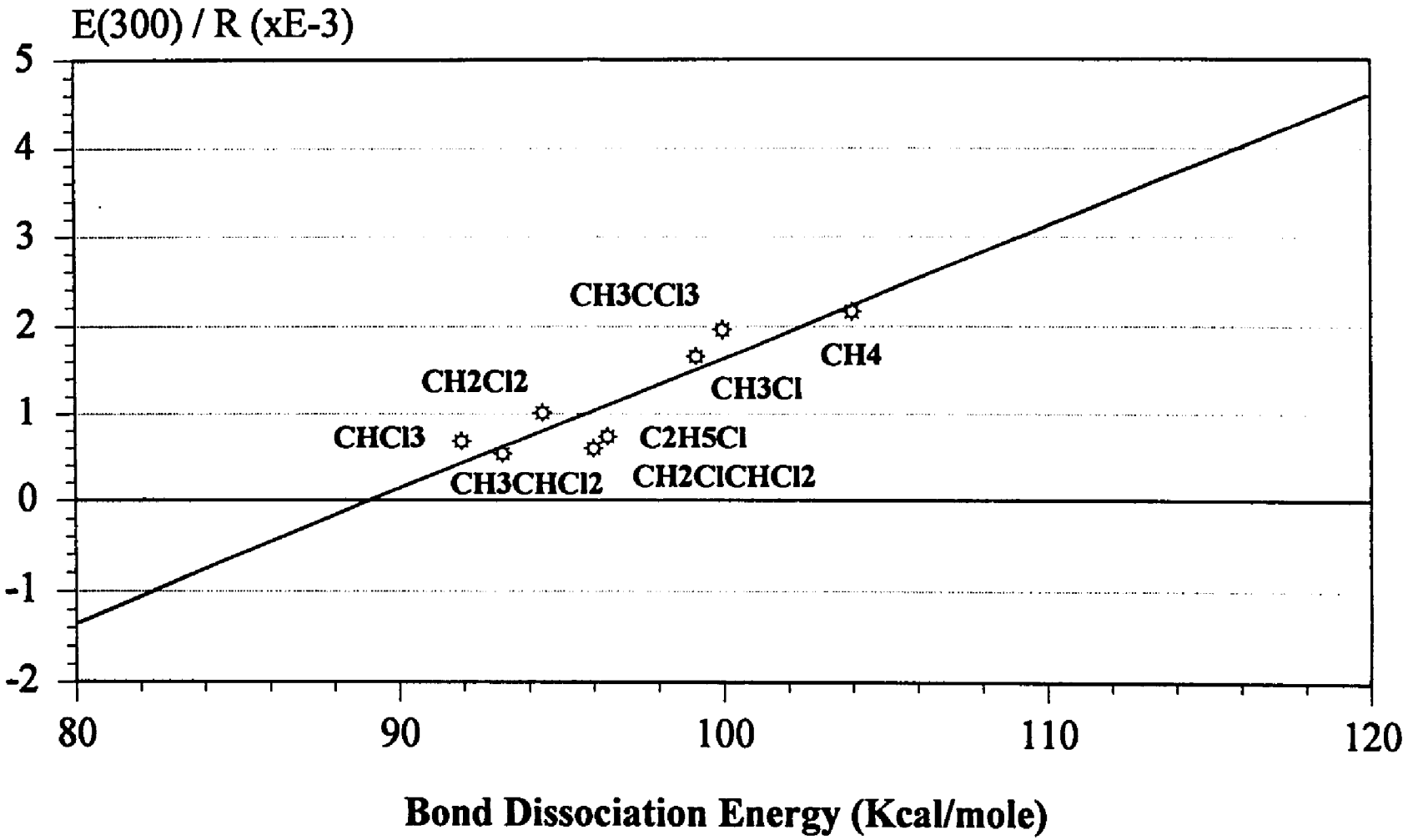

Fig. 5.3 MOdified Evans-Polanyi plot of OH abstraction of H atom from CHC

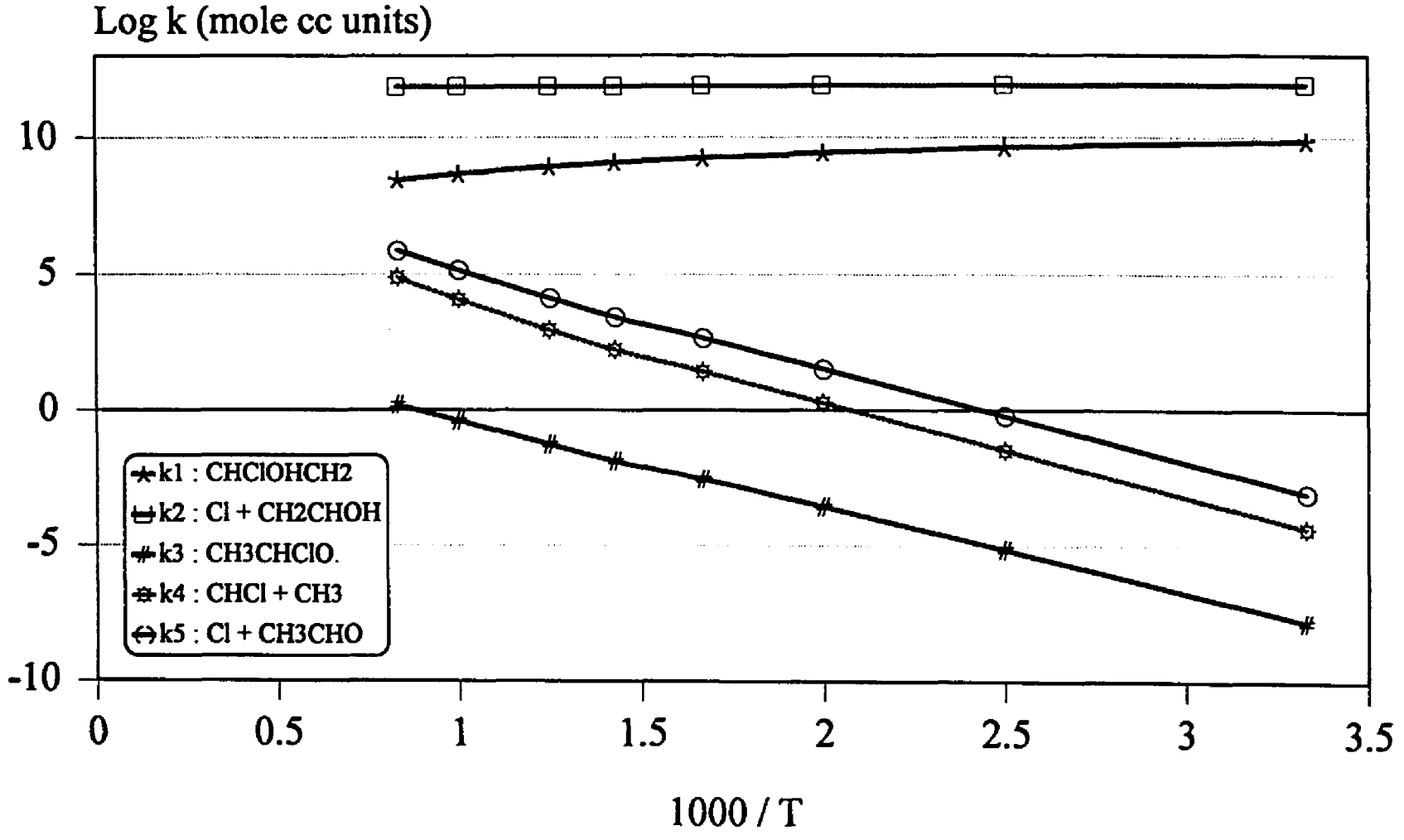

Fig. 5.4 Plot of the rate constants for alpha addition reaction versus 1000/T at 760 torr

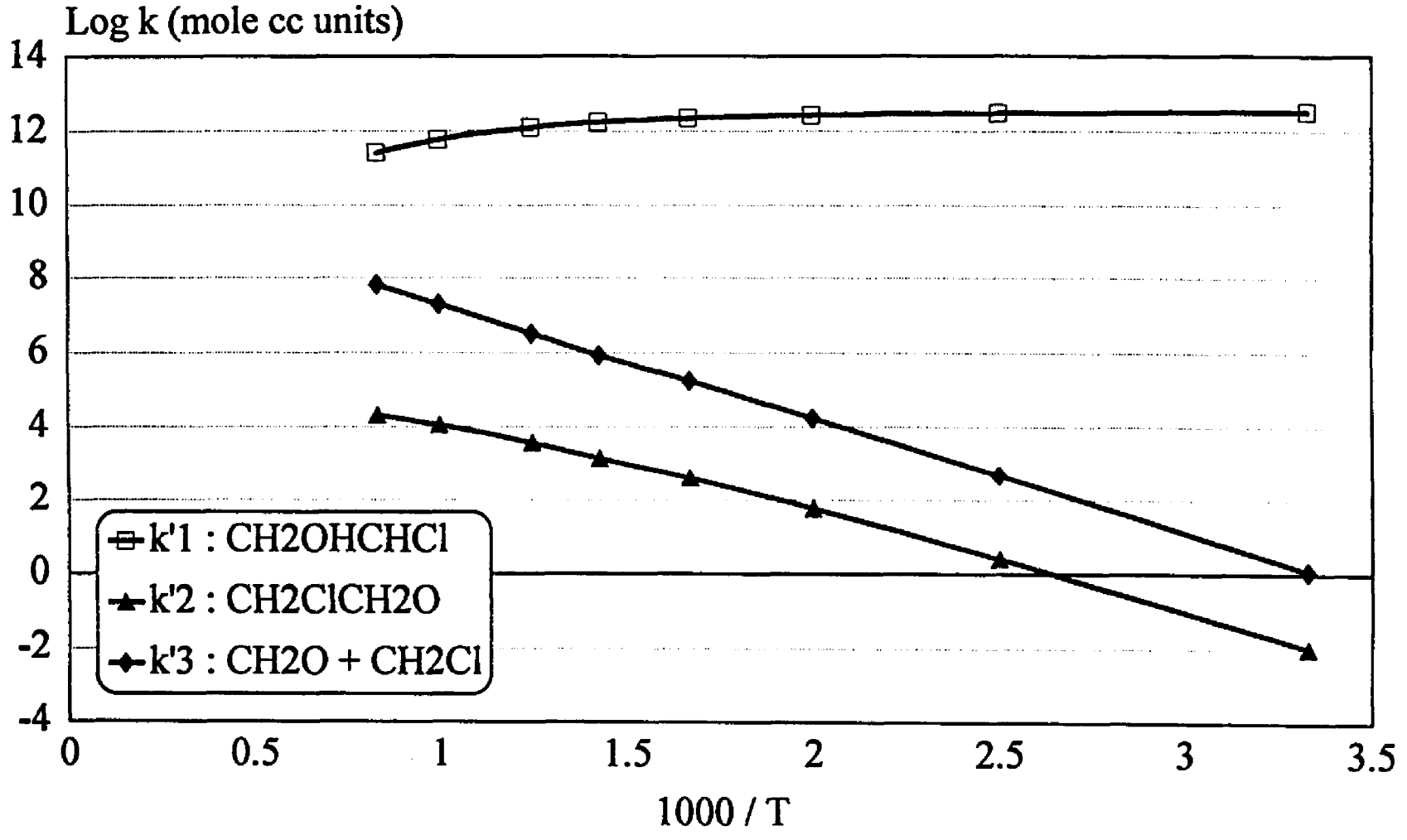

Fig. 5.5 Plot of the rate constants for beta addition reaction versus 1000/T at 760 torr

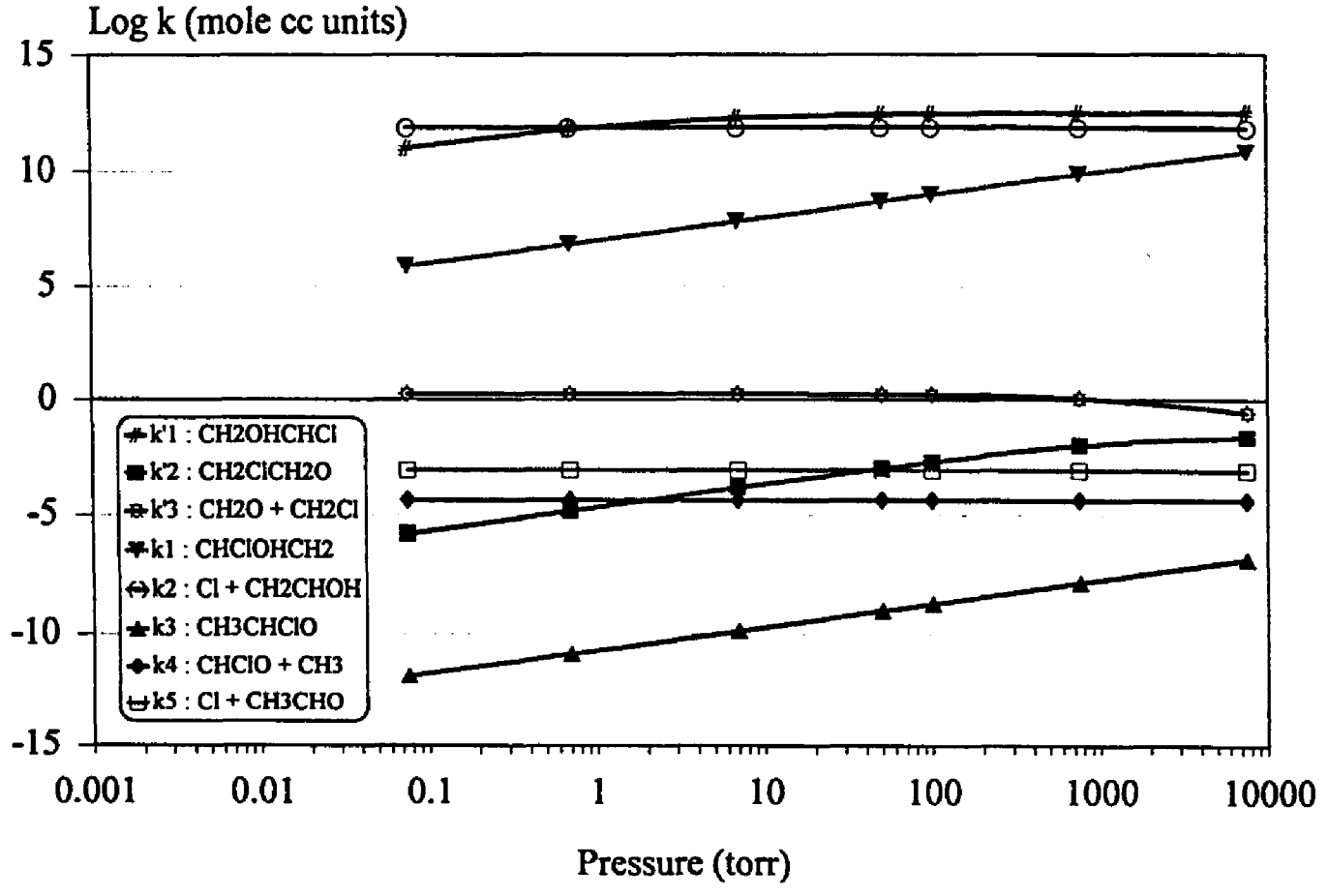

Fig 5.6 Major Reaction Products from The Reaction of Vinyl Chloride + OH Plotted versus Pressure at 300 K

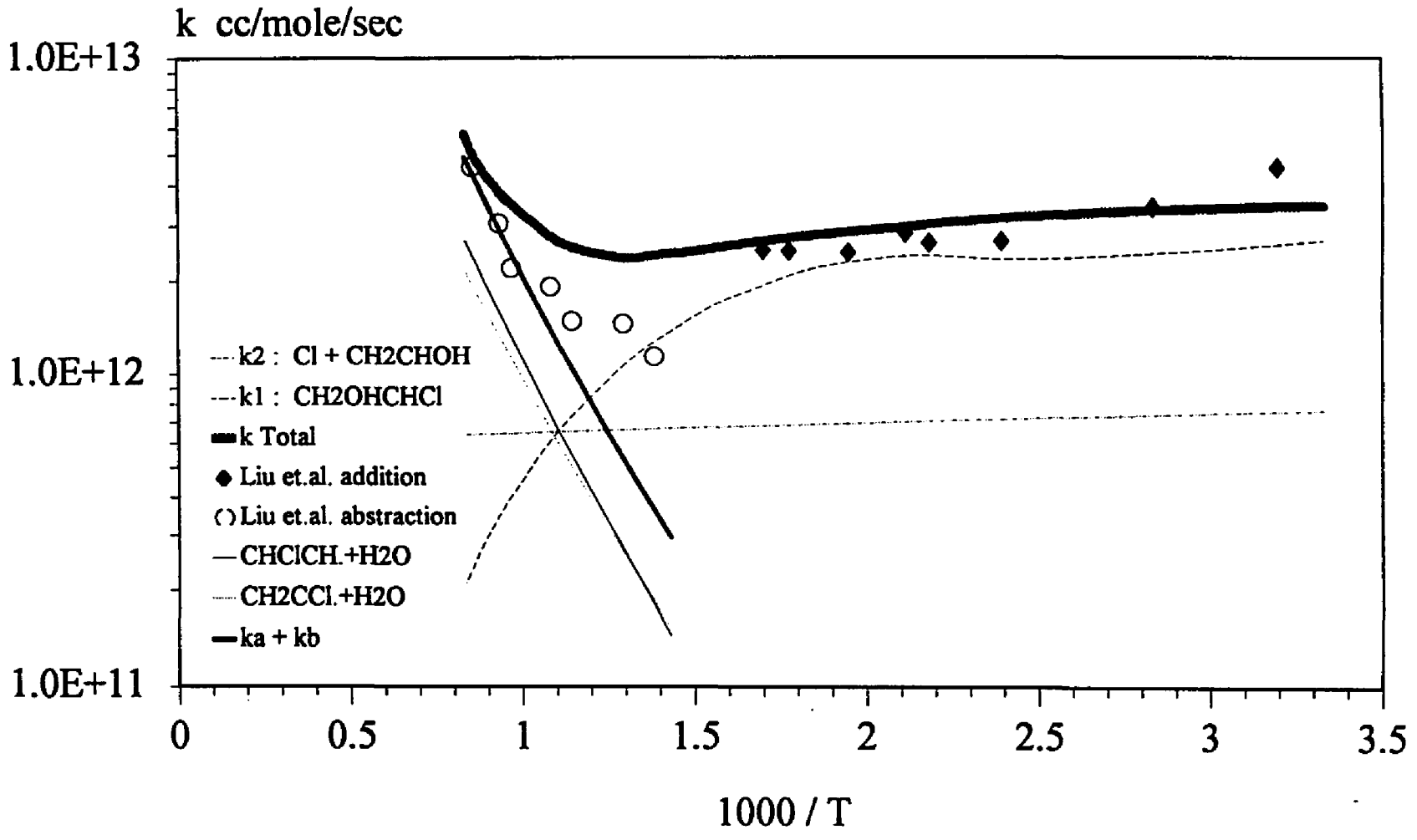

Fig. 5.7 Comparison of calculated results for C2H3Cl + OH to experimental data at 760 torr versus 1000/T

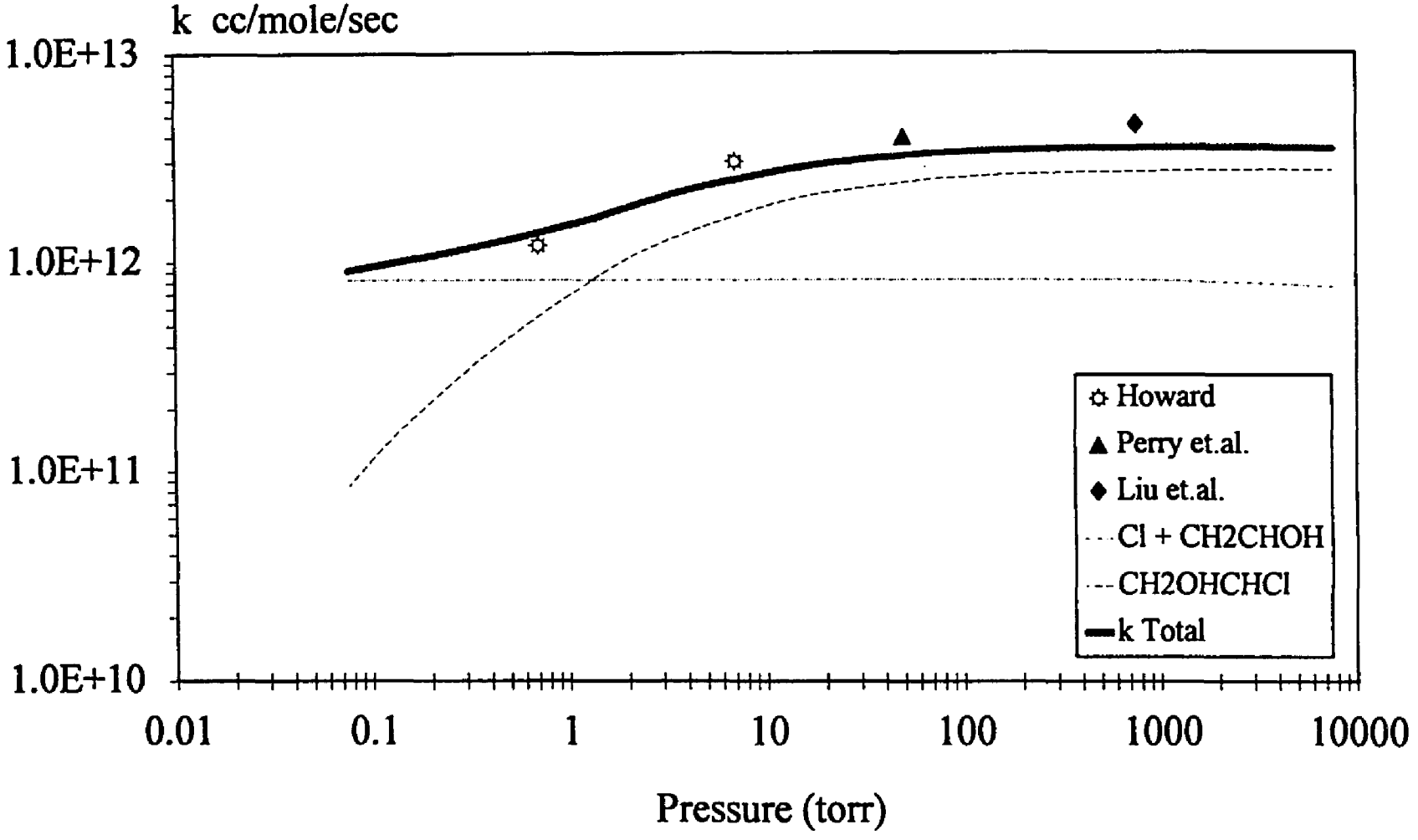

Fig. 5.8 Comparison of calculated results for C2H3Cl to experiments at room temperature versus pressure

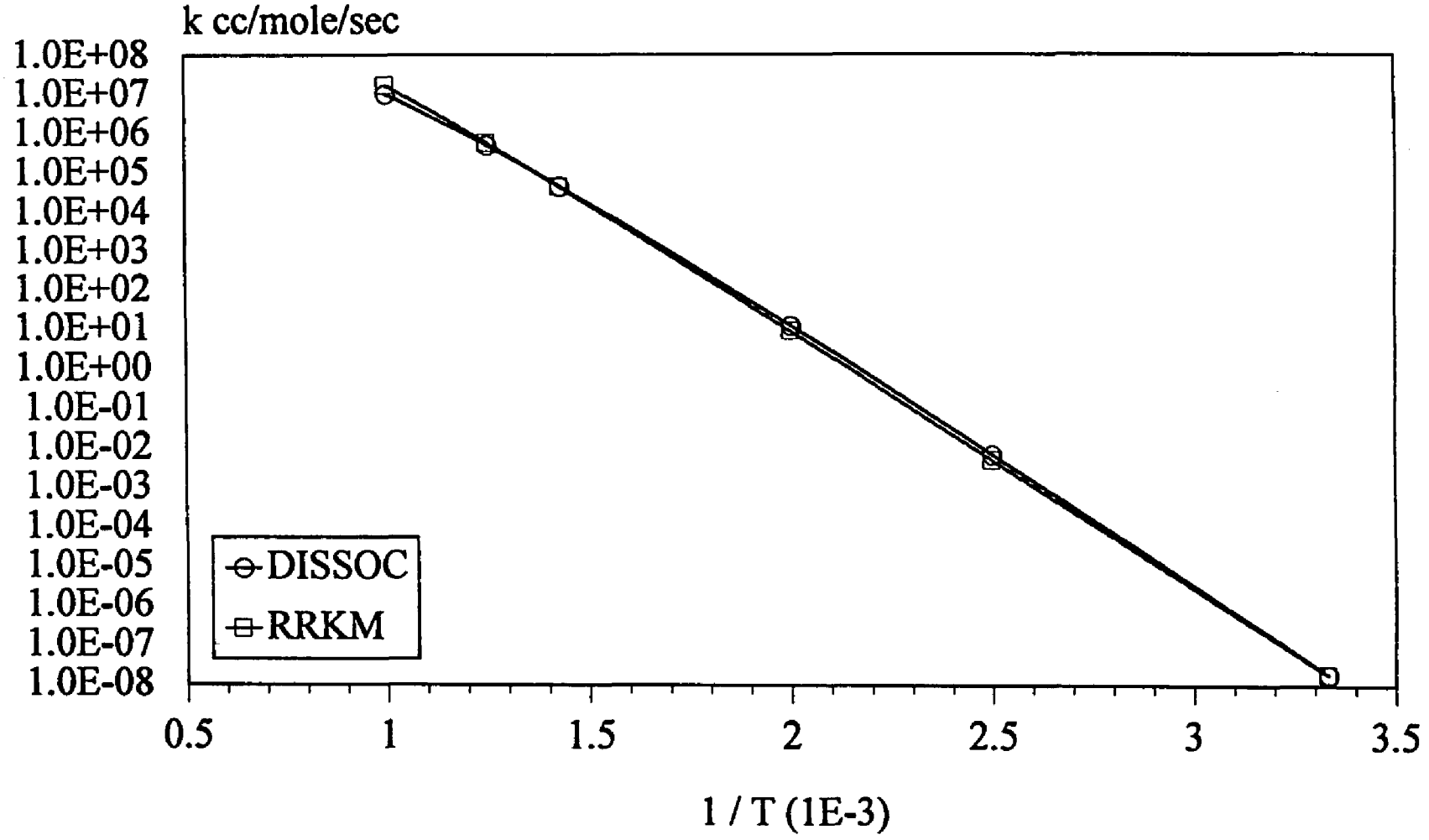

Fig. 5.9 Comparison of calculated results for CH2OHC.HCl —> C2H3Cl + OH dissociation reaction at 760 torr versus 1/T

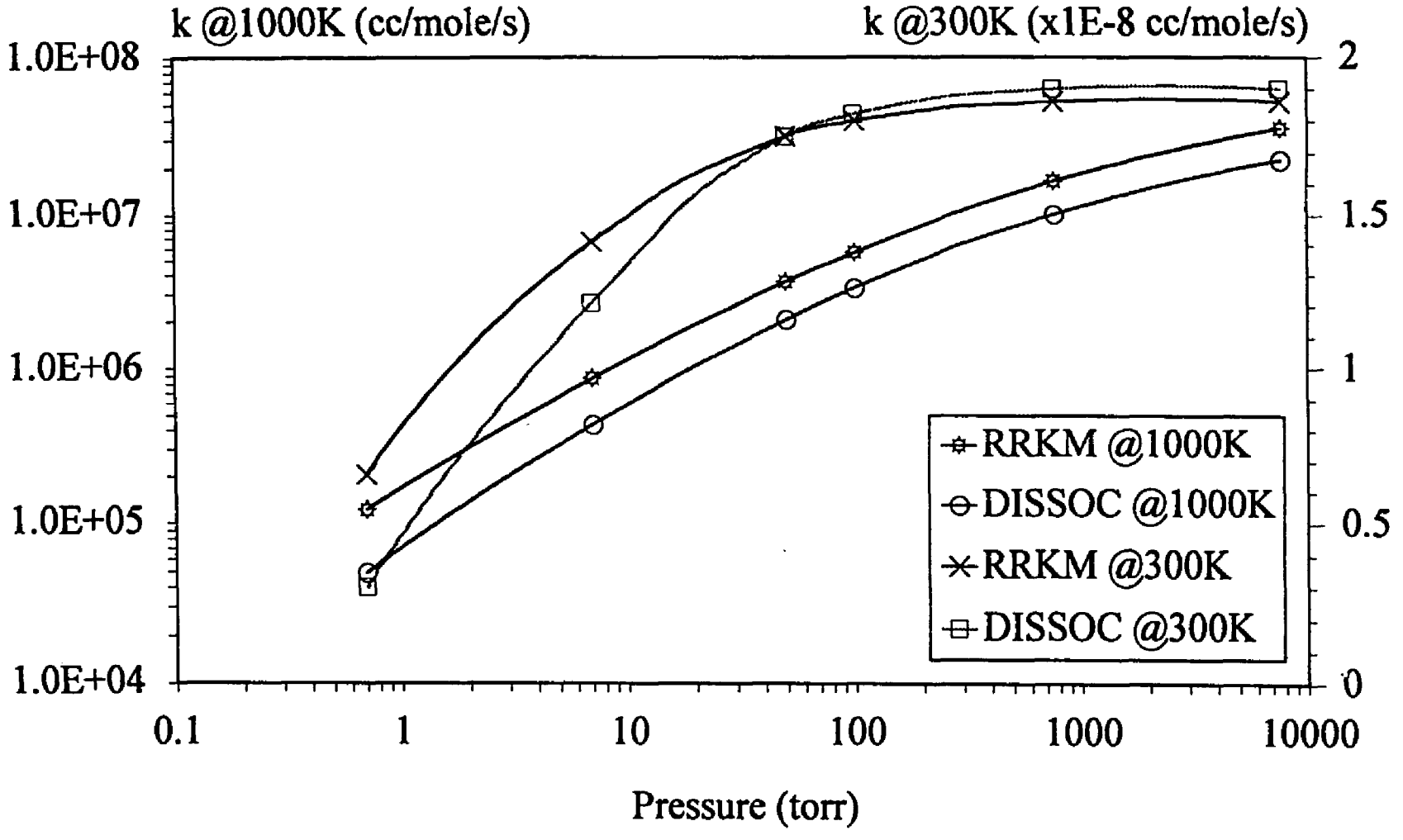

Fig. 5.10 Comparison of calculated results for CH2OHC.HCl —> C2H3Cl + OH dissociation reaction versus pressure

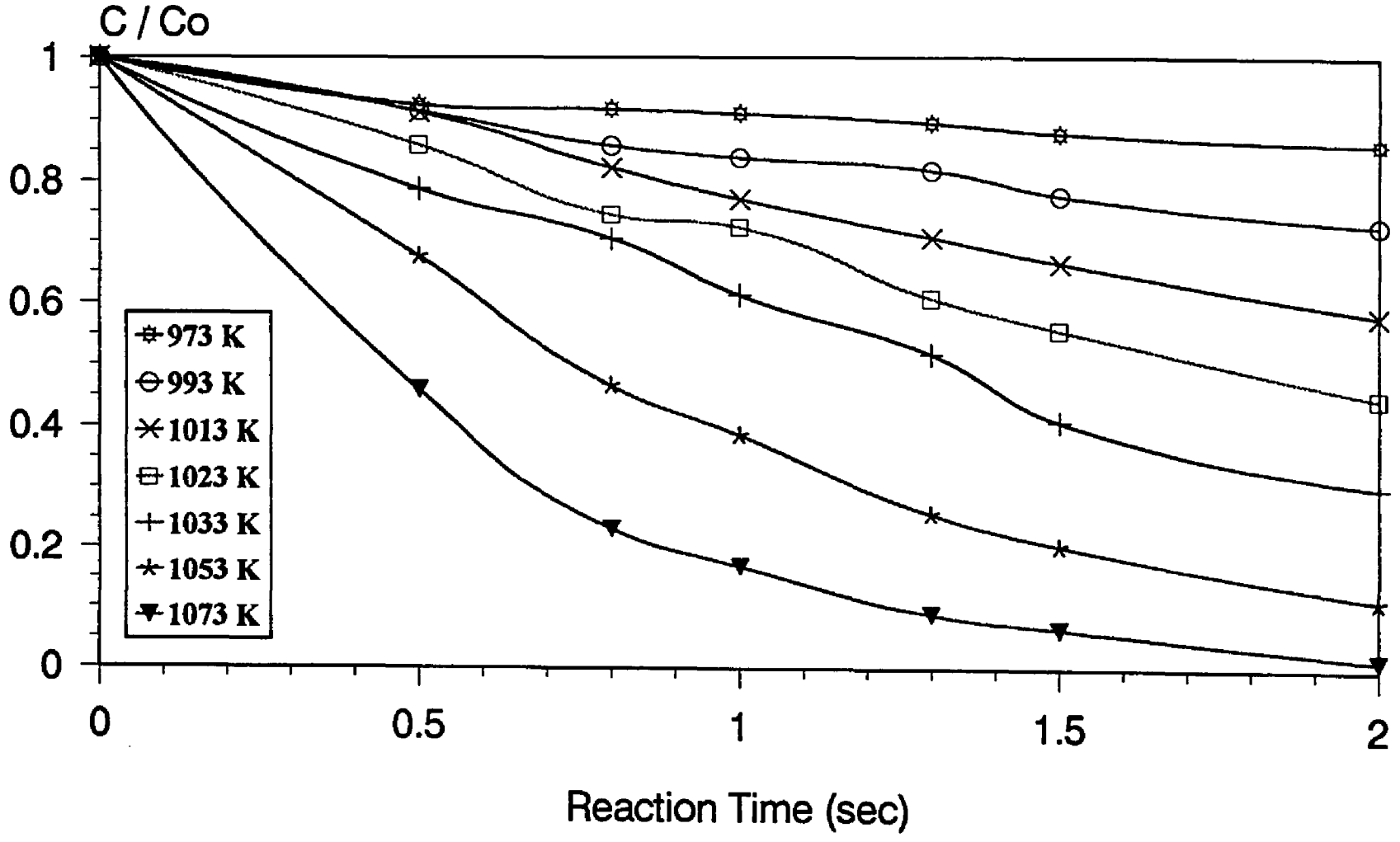

Fig 6.1 CH2Cl2 conversion versus time at different temperature. Reactant ratios: O2:H2:CH2Cl2:Ar=1:1:1:97

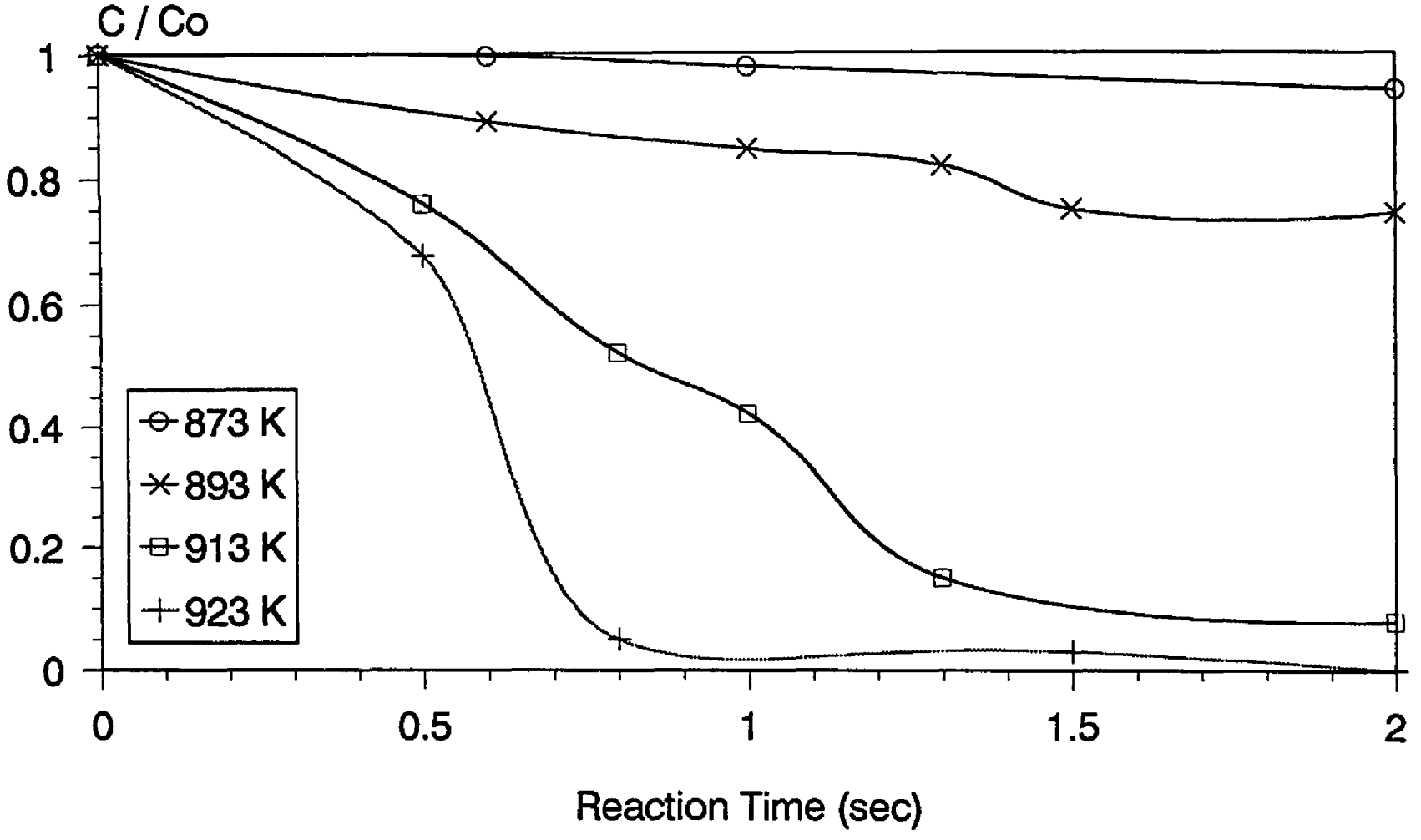

Fig 6.2 CH2Cl2 conversion versus time at different temperatures. Reactant ratios: O2:H2:CH2Cl2=98:1:1

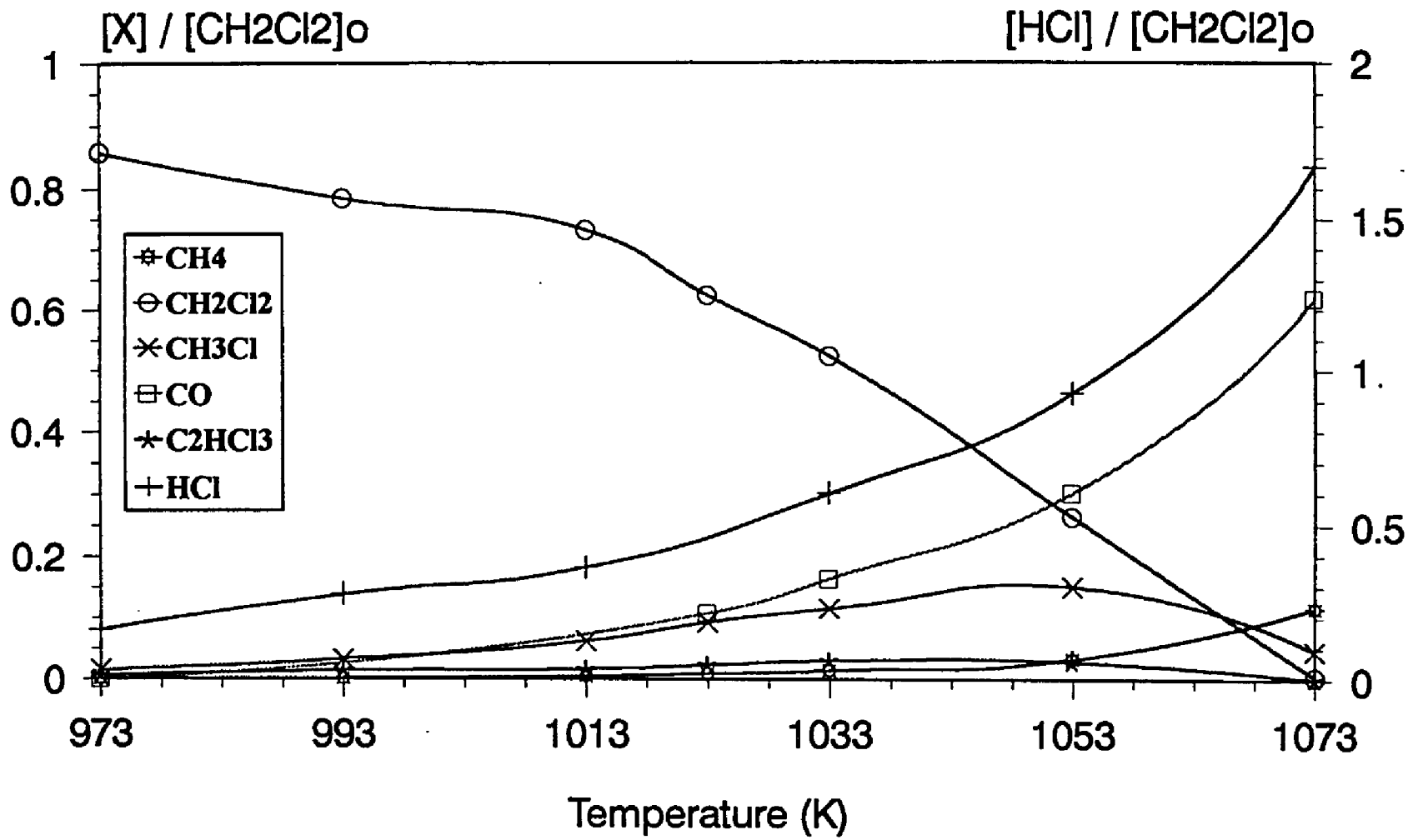

Fig 6.3 Major product distribution for CH2Cl2 decomposition. 1 sec. residence time, Reactant ratios: O2:H2:CH2Cl2:Ar=2:2:1:95

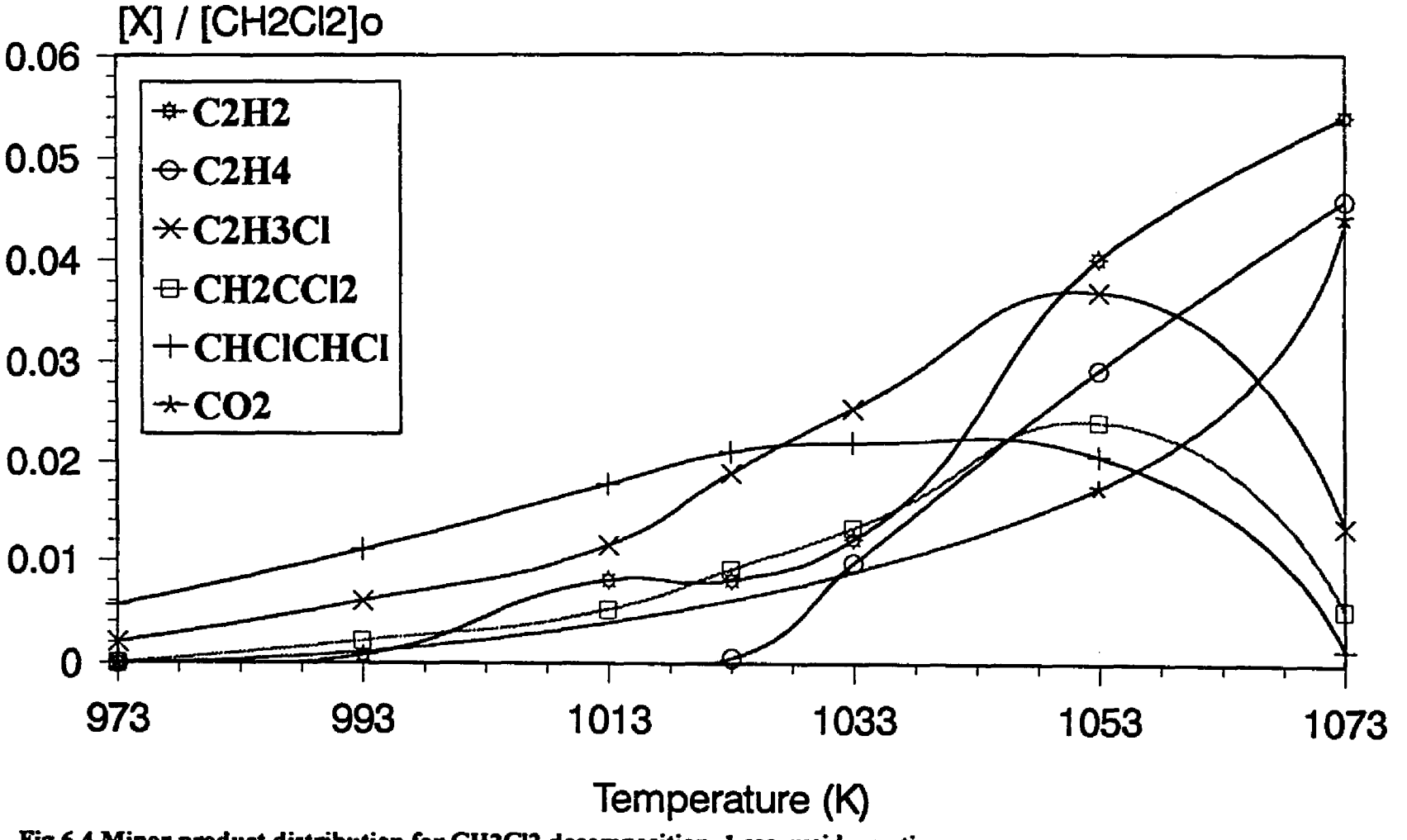

Fig 6.4 Minor product distribution for CH2Cl2 decomposition. 1 sec. residence time, Reactant ratios: O2:H2:CH2Cl2:Ar=2:2:1:95

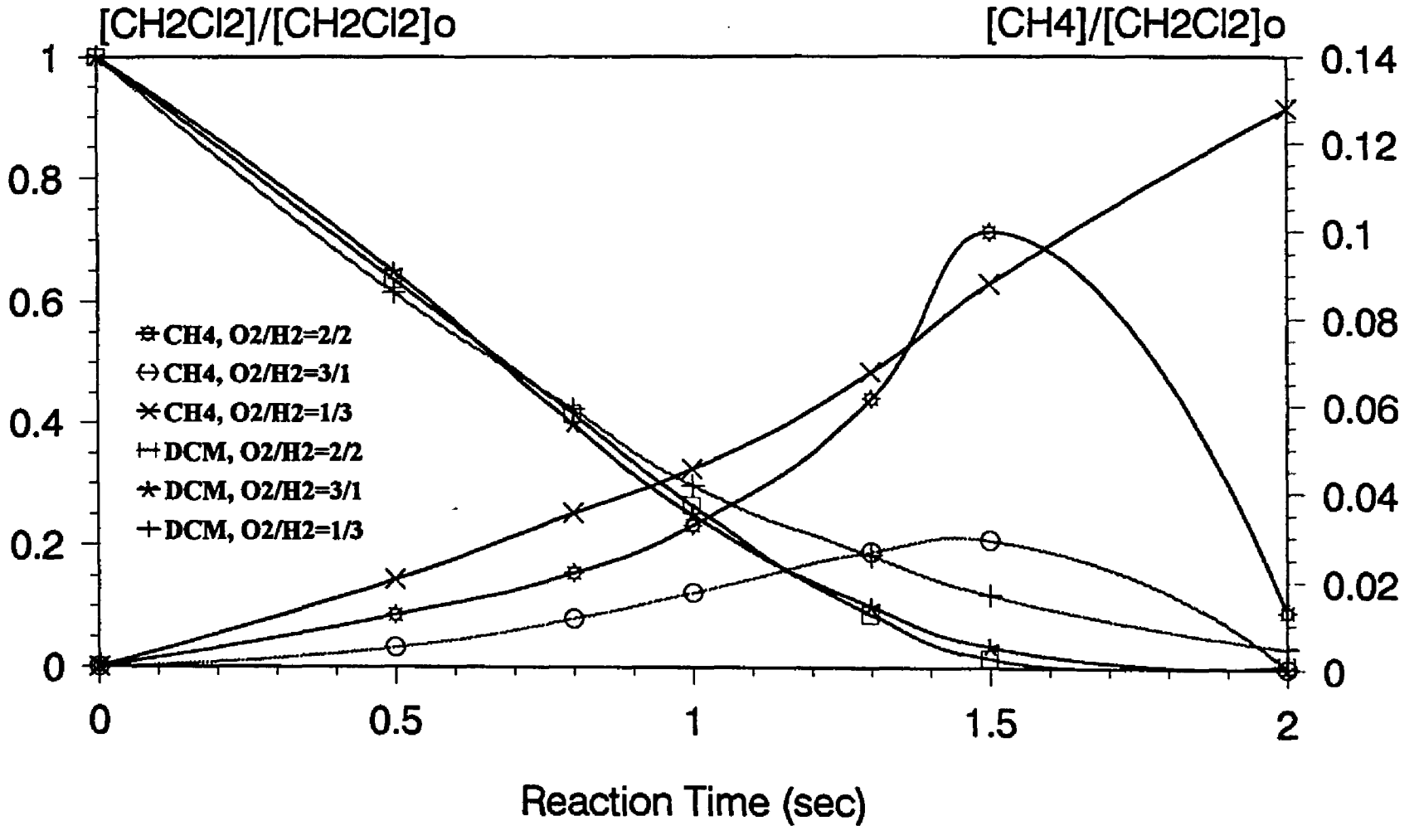

Fig 6.5 Comparison of CH2Cl2 conversion and products at 1053K, 1% CH2Cl2 with different O2/H2 feed ratios

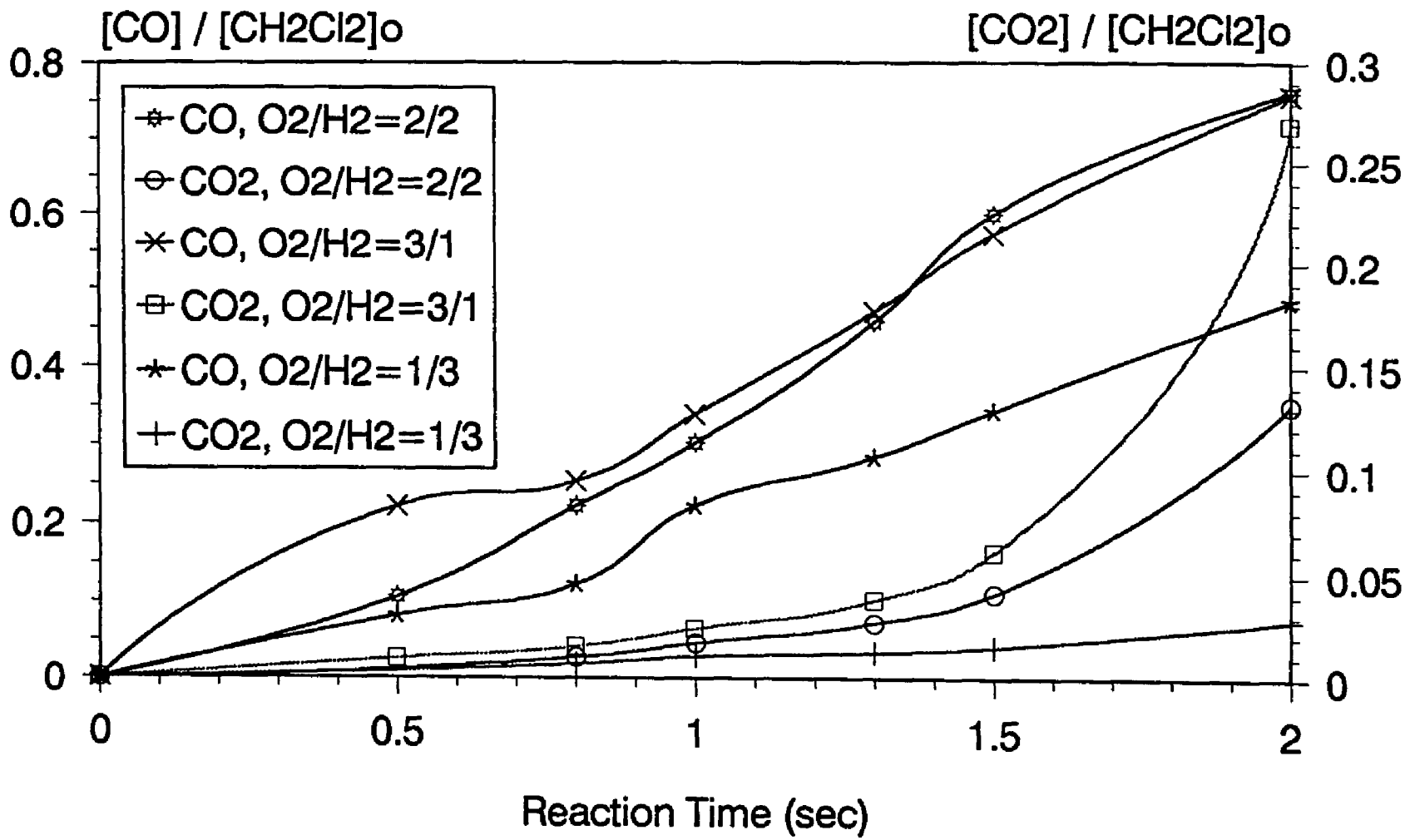

Fig 6.6 Comparison of CO and CO2 production at 1053K, 1% CH2Cl2 with different O2/H2 feed ratios.

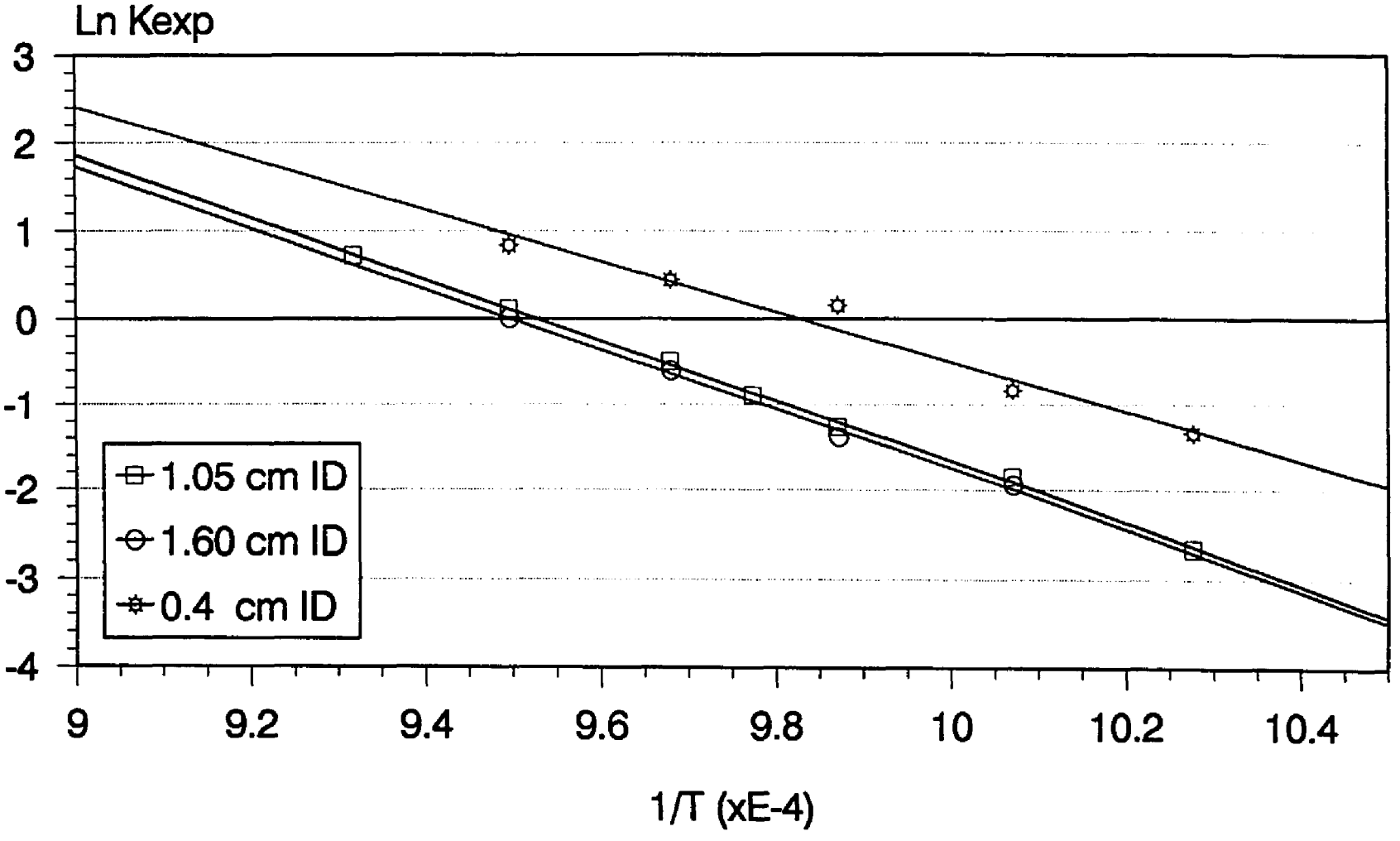

Fig 6.7 Arrhenius behavior of global Kexp for CH2Cl2/O2/H2

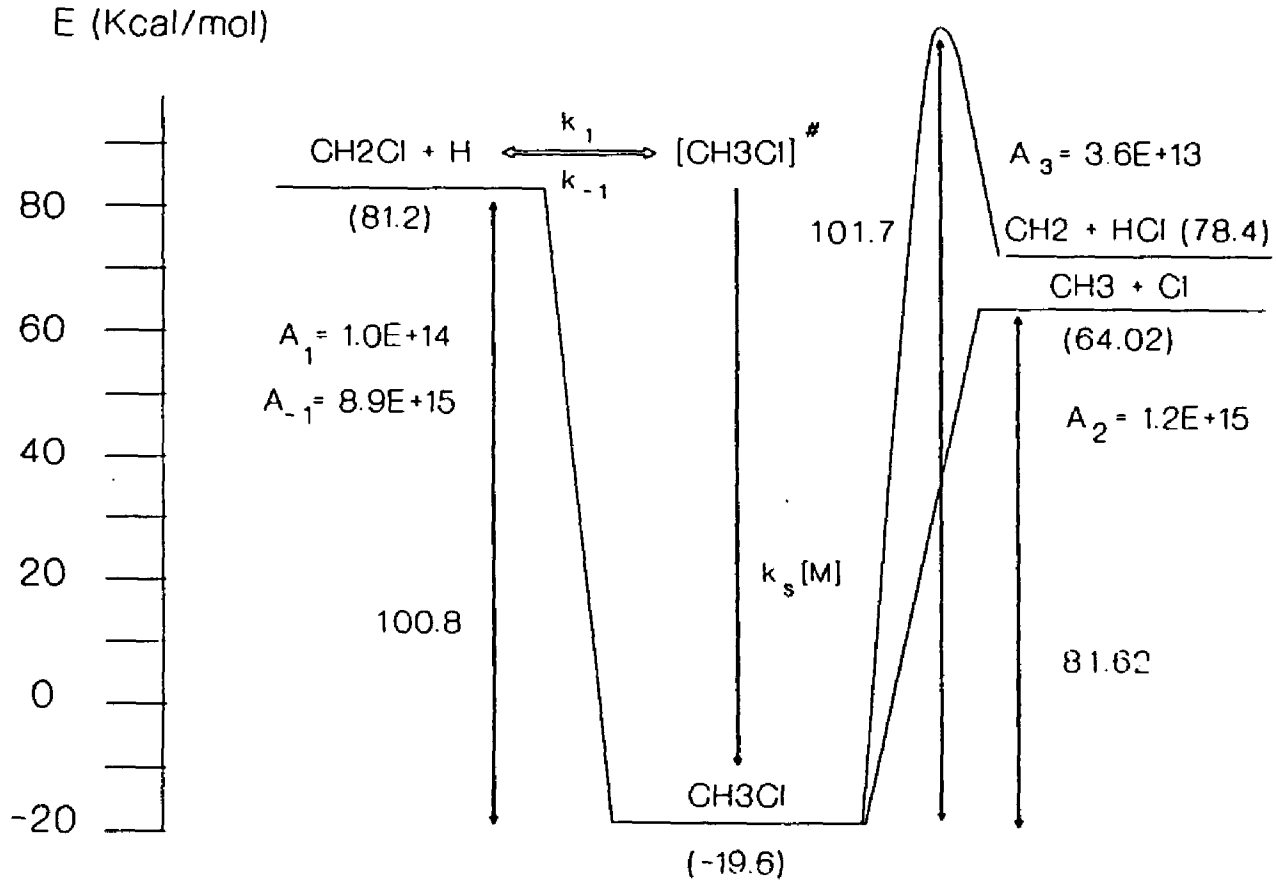

Fig 6.8 Energy Level for $CH_2Cl + H$ Reaction

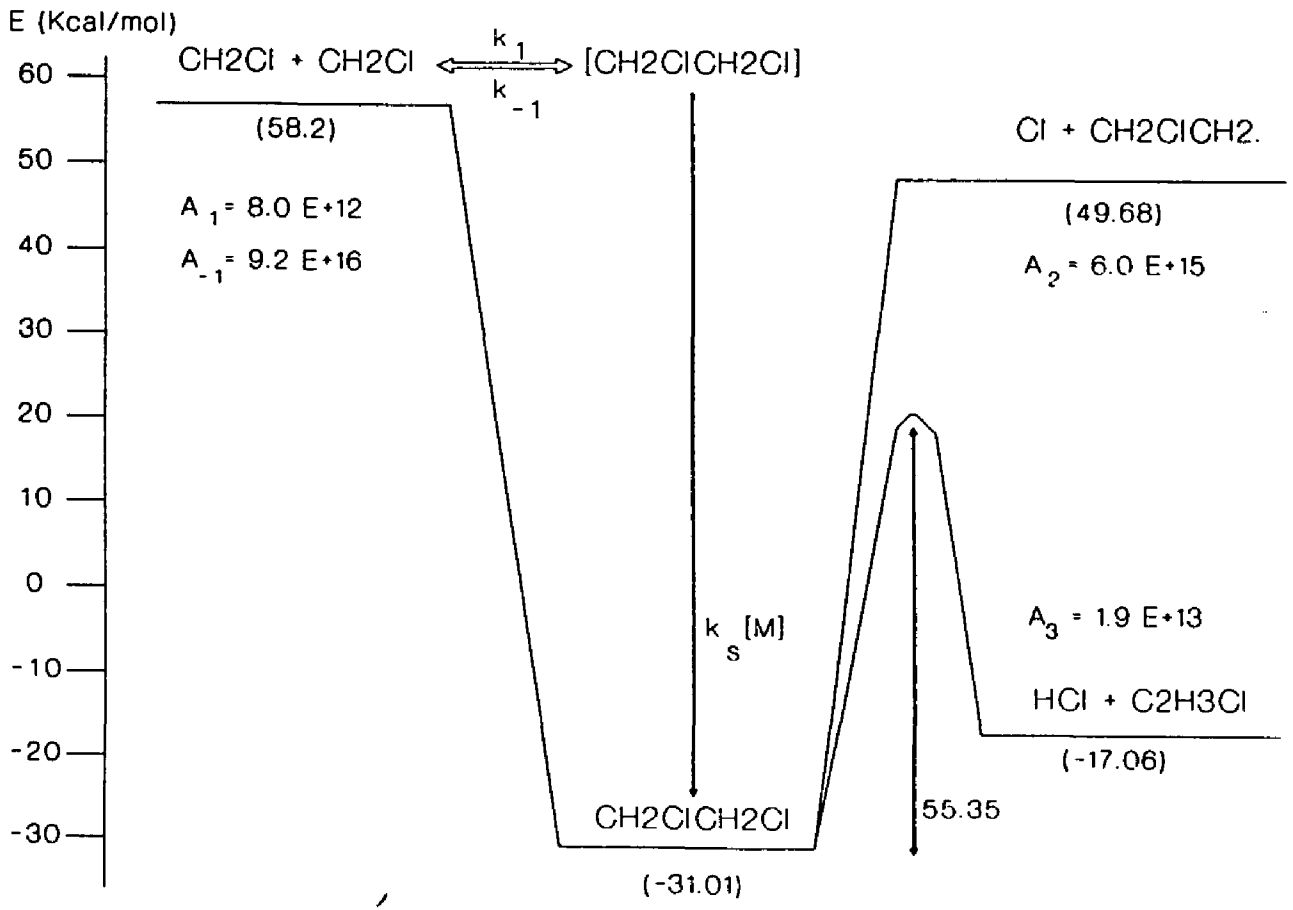

Fig 6.9 Energy Level for $CH_2Cl + CH_2Cl$ Reaction

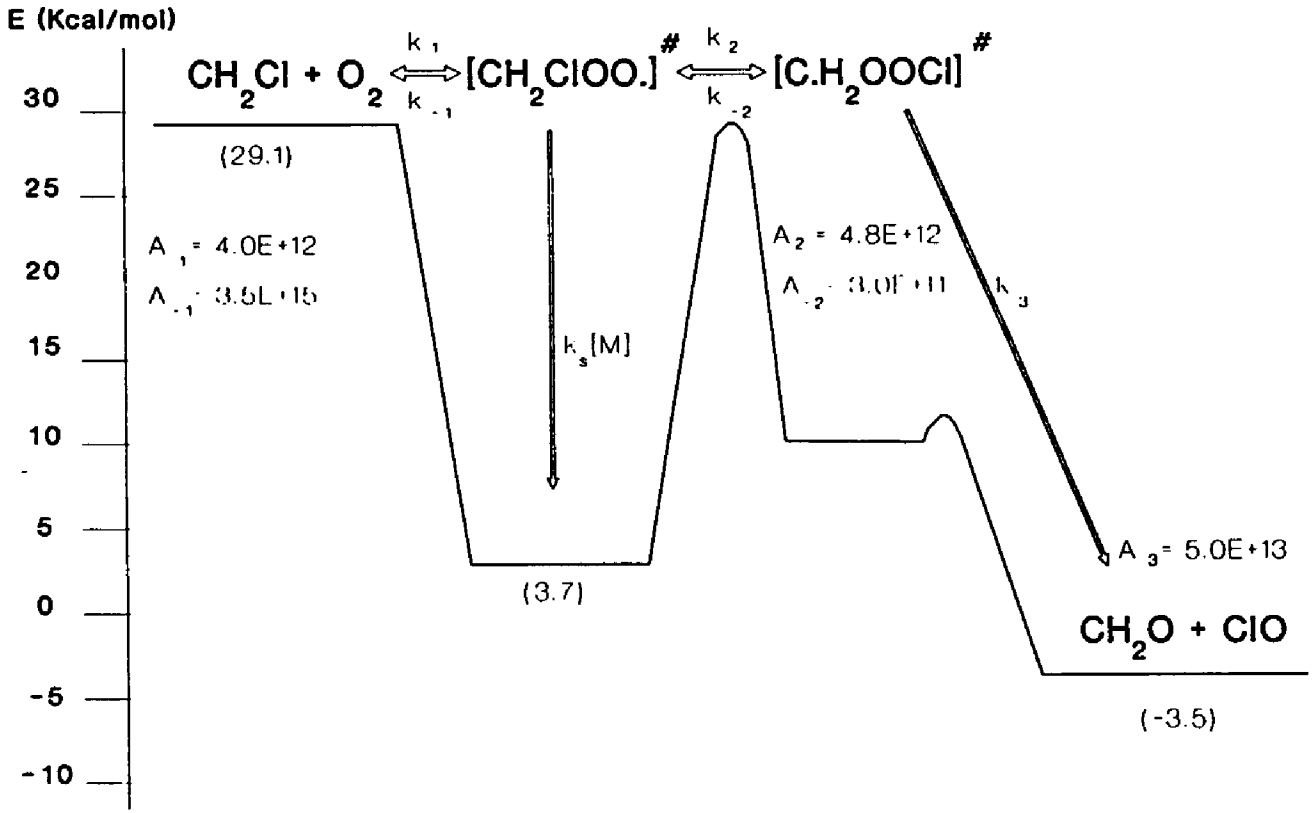

Fig 6.10 Energy Level for $CH_2Cl + O_2$ Reaction

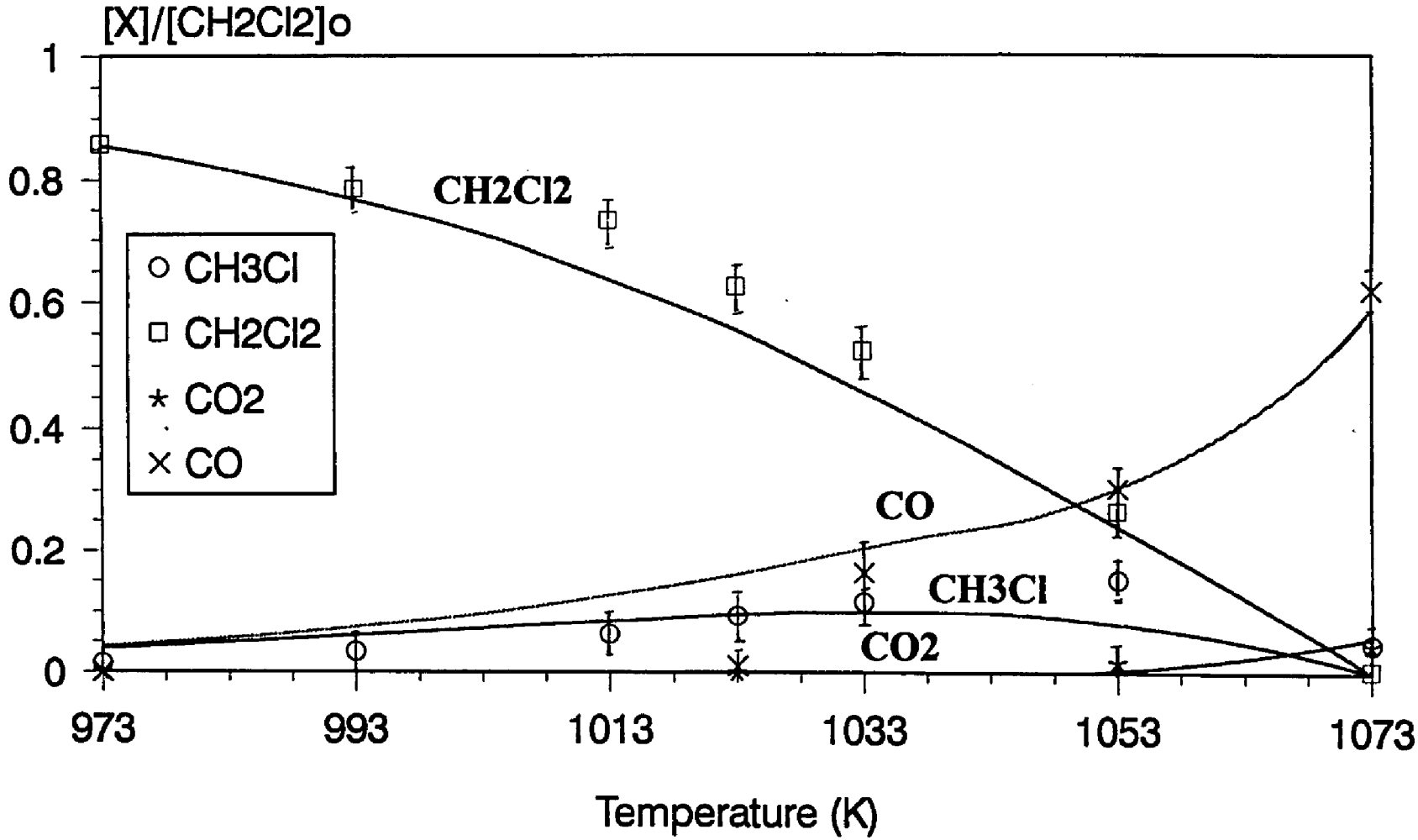

Fig 6.11 Comparison of calculated and experimental product distribution versus tempeature. 1 sec. residence time, Reactant ratios: O2:H2:CH2Cl2:Ar=2:2:1:95

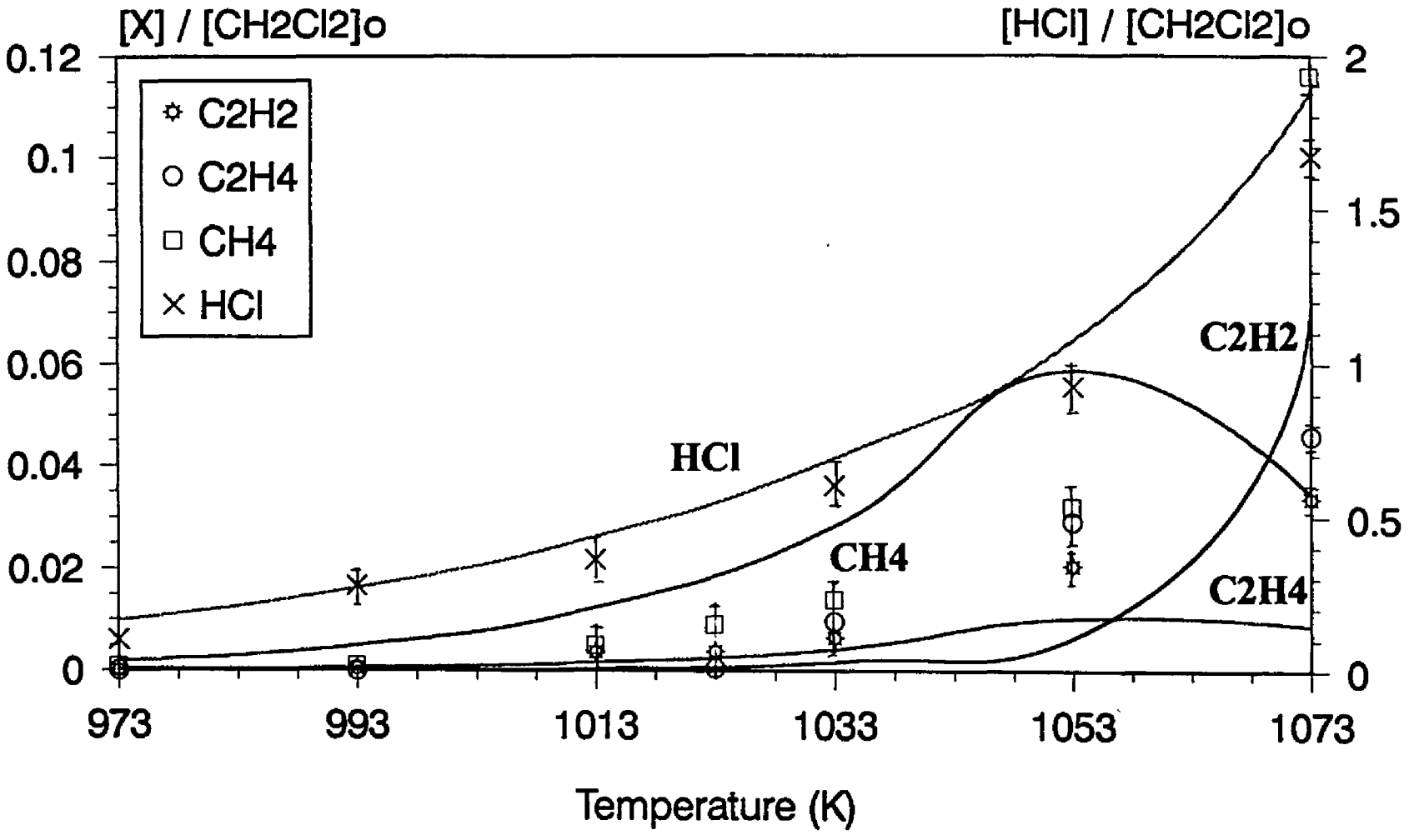

Fig 6.12 Comparison of calculated and experimental product distribution versus tempeature. 1 sec. residence time, Reactant ratios: O2:H2:CH2Cl2:Ar=2:2:1:95

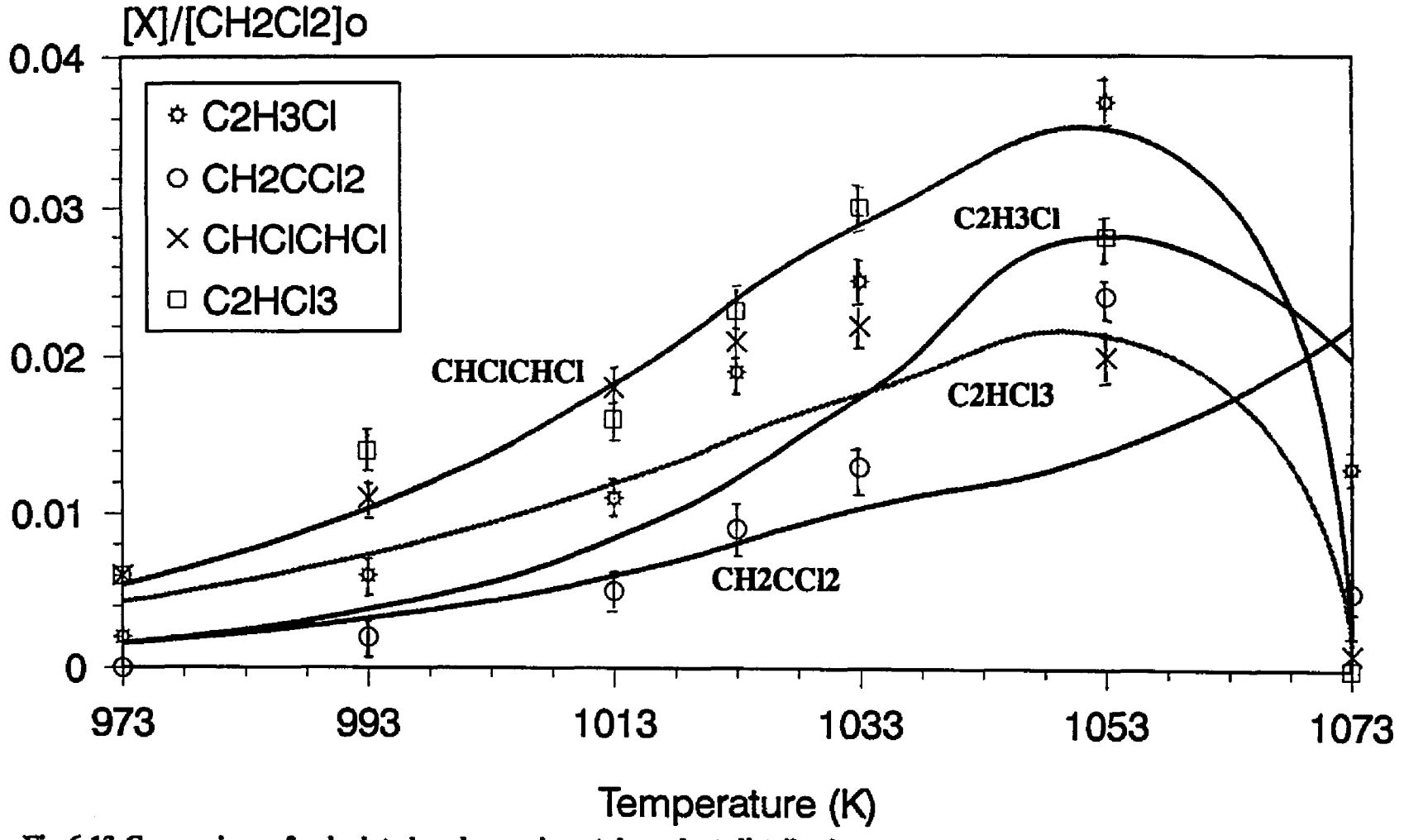

Fig 6.13 Comparison of calculated and experimental product distribution versus tempeature. 1 sec. residence time, Reactant ratios: O2:H2:CH2Cl2:Ar=2:2:1:95

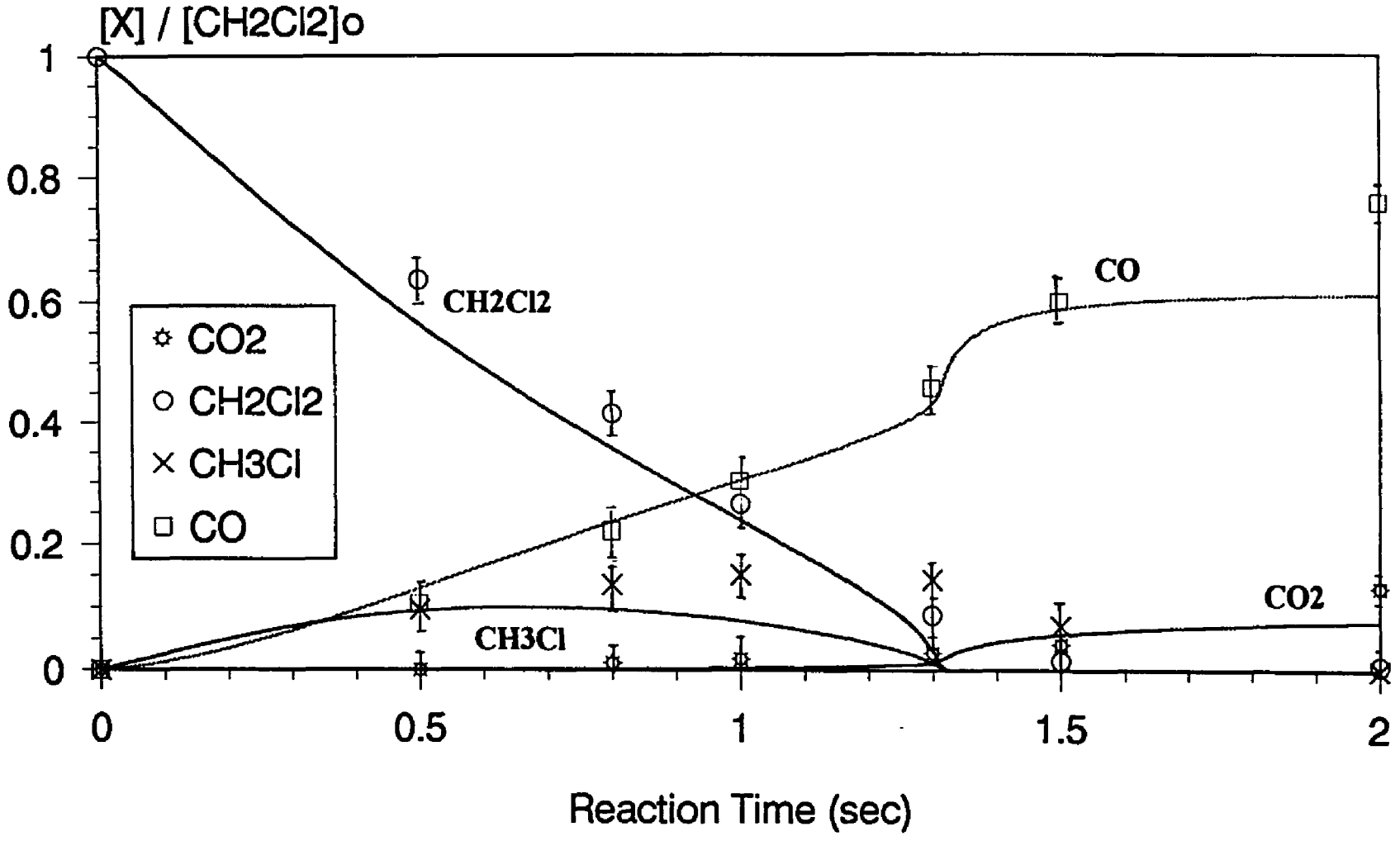

Fig 6.14 Comparison of calculated and experimental product distribution versus residence time at 1053K, Reactant ratios: O2:H2:CH2Cl2:Ar=2:2:1:95

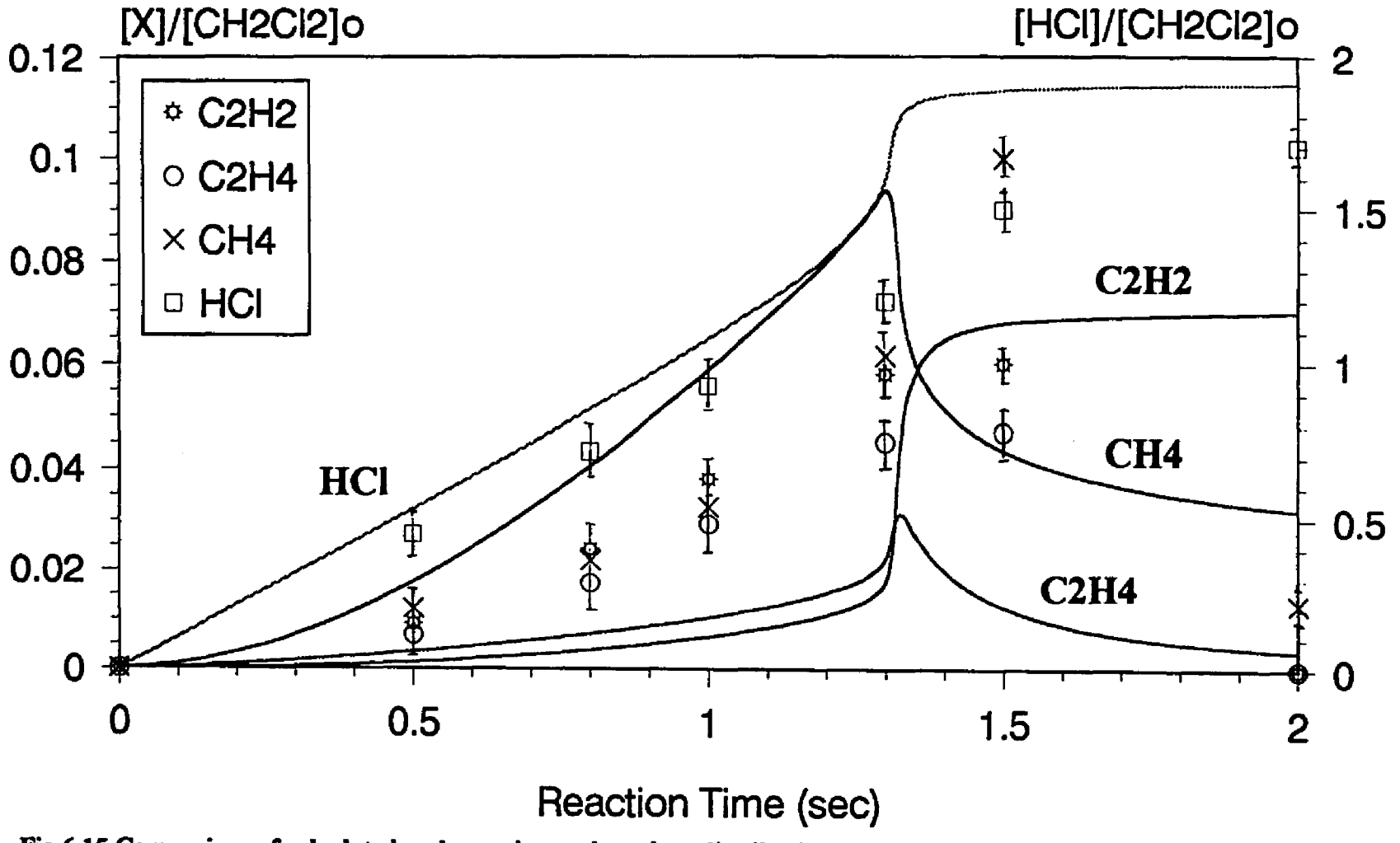

Fig 6.15 Comparison of calculated and experimental product distribution versus residence time at 1053K, Reactant ratios: O2:H2:CH2Cl2:Ar=2:2:1:95

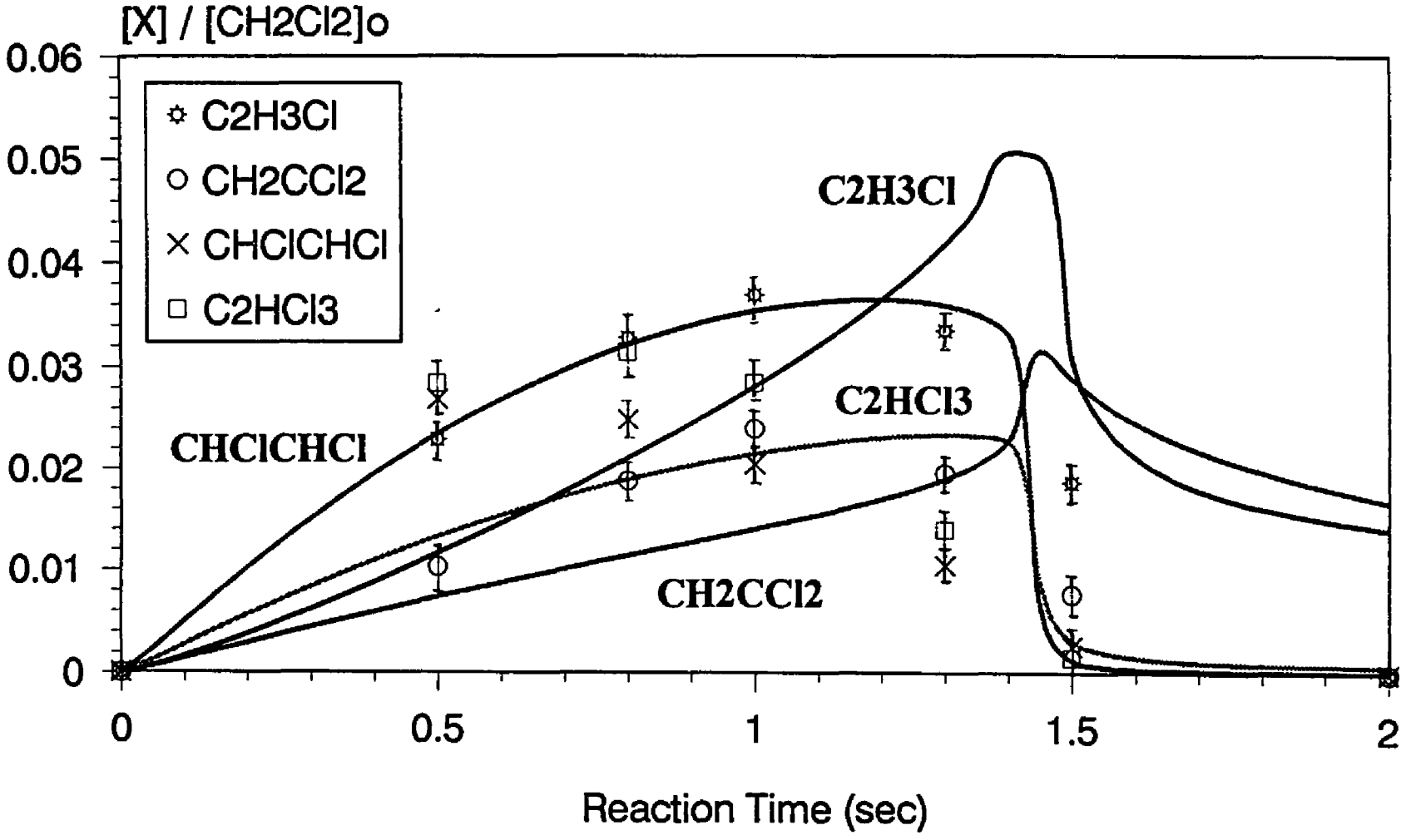

Fig 6.16 Comparison of calculated and experimental product distribution versus residence time at 1053K, Reactant ratios: O2:H2:CH2Cl2:Ar=2:2:1:95

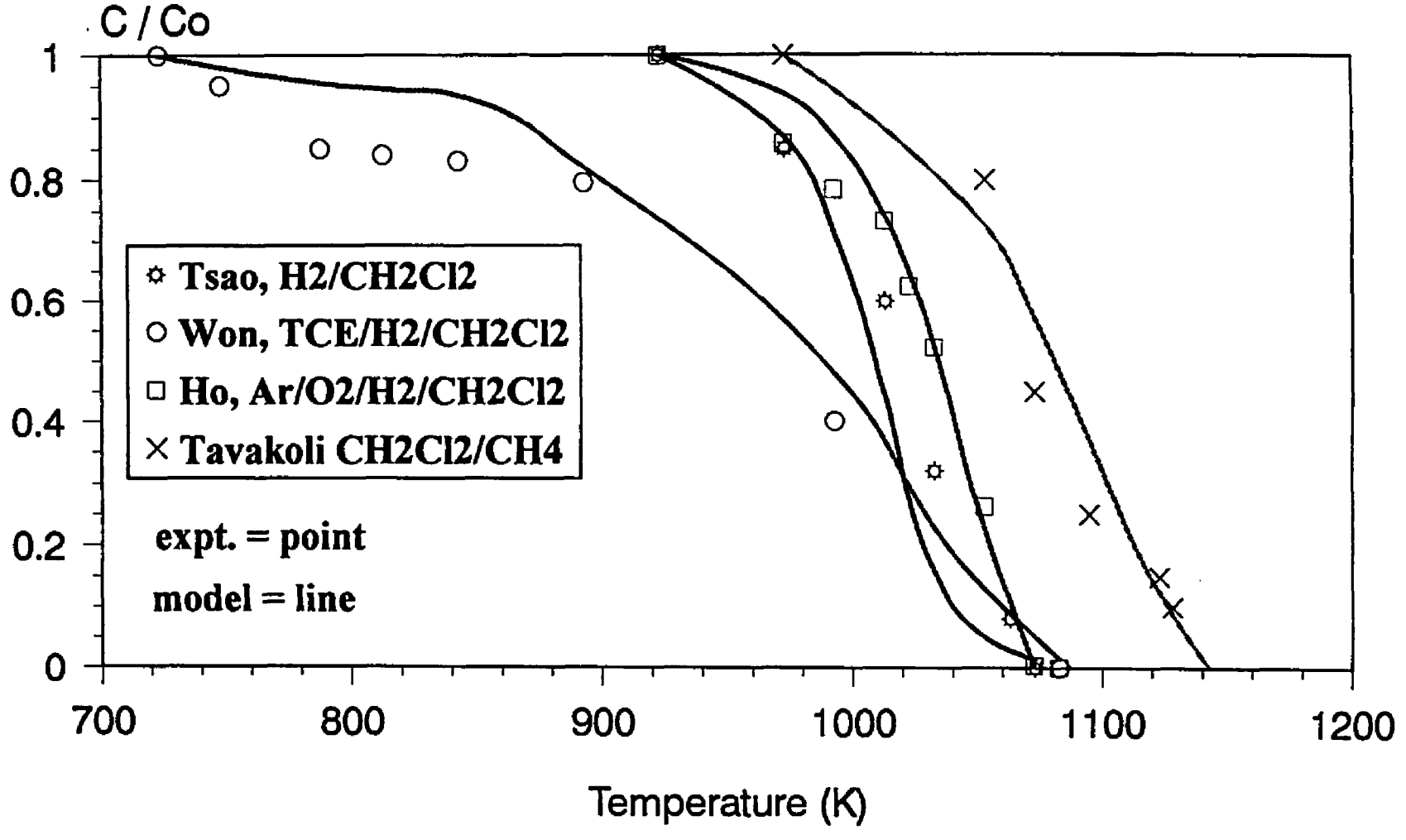

Fig 6.17 Comparison of experimental data and model predictions with data of other studies.

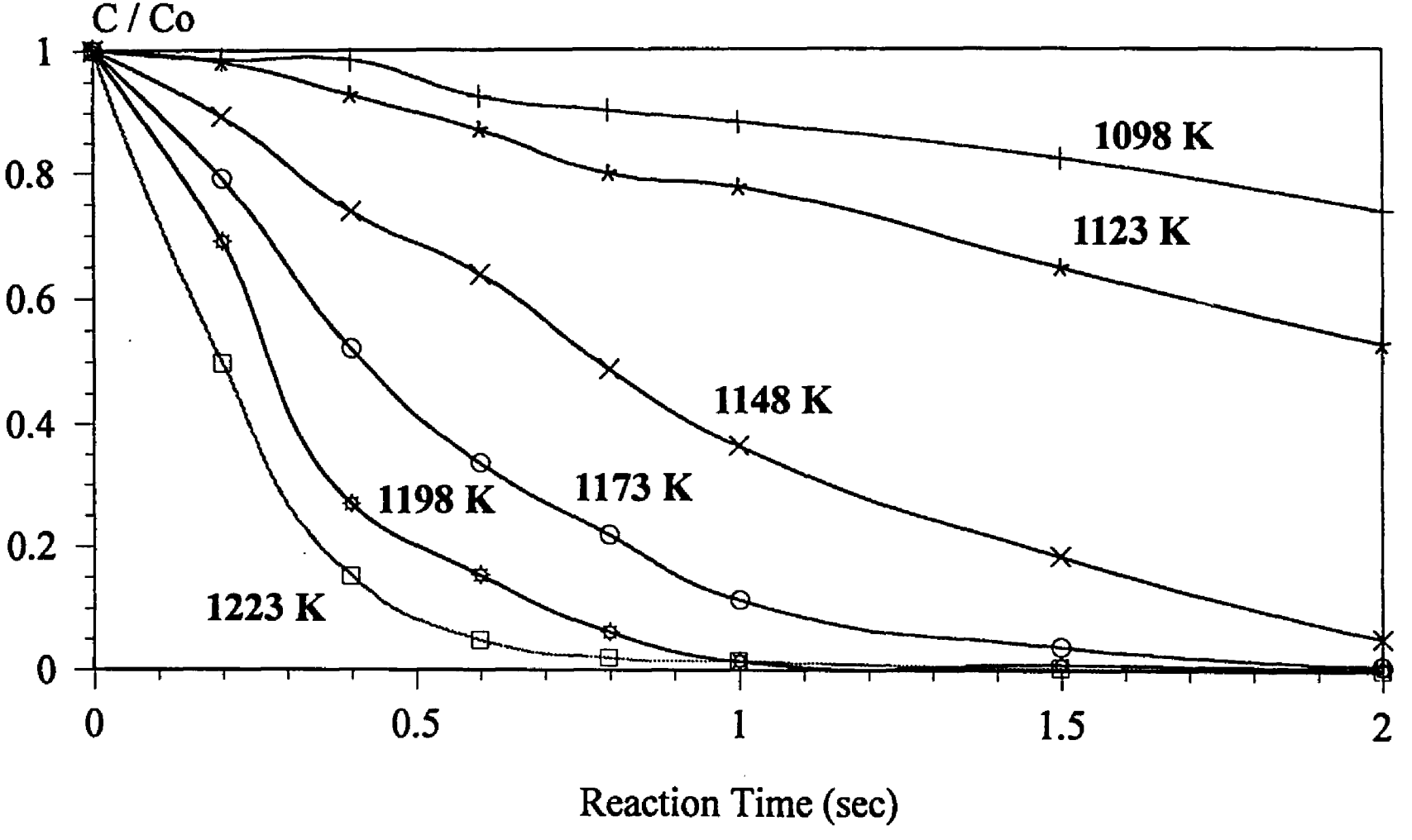

Fig 7.1 Conversion versus time at different temperature, Reactant ratios: O2:H2:CH3Cl:Ar=1:1:2:96

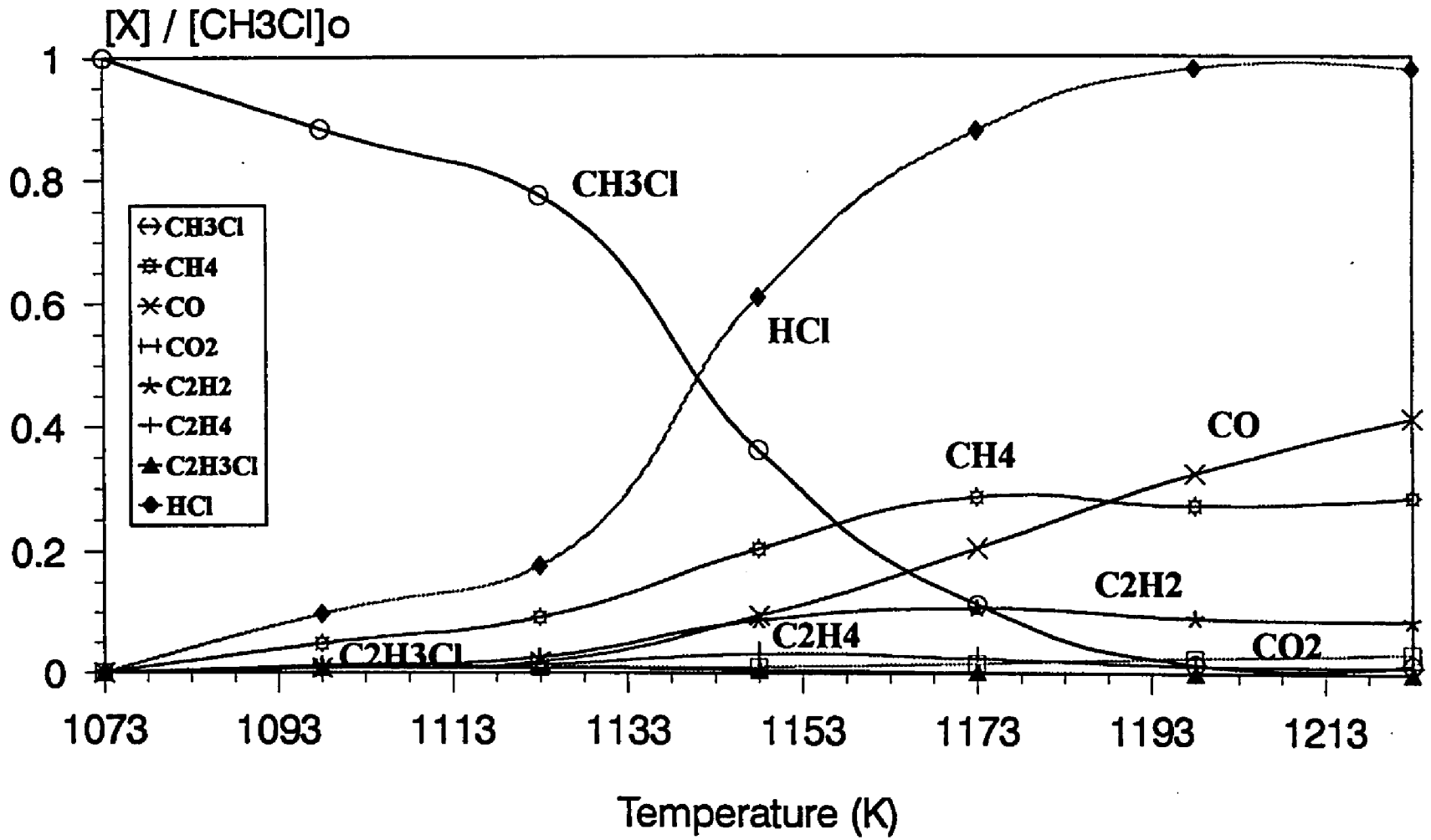

Fig 7.2 Product distribution for CH3Cl decomposition versus temperature at 1 sec residence time.
Reactant ratios: O2:H2:CH3Cl:Ar=1:1:2:96

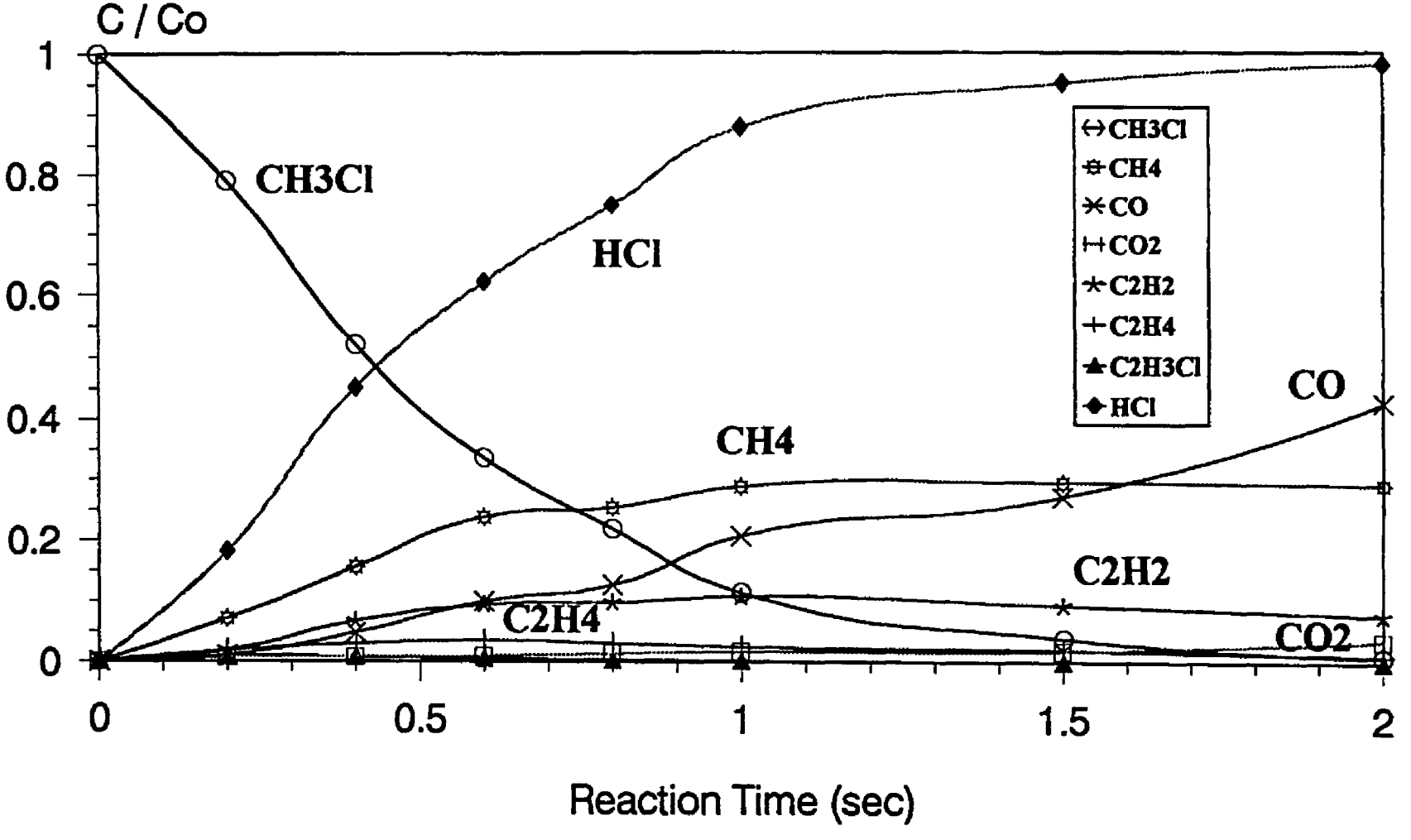

Fig 7.3 Product distribution for CH3Cl decomposition versus residence time at 1148K.
Reactant ratios: O2:H2:CH3Cl:Ar=1:1:2:96

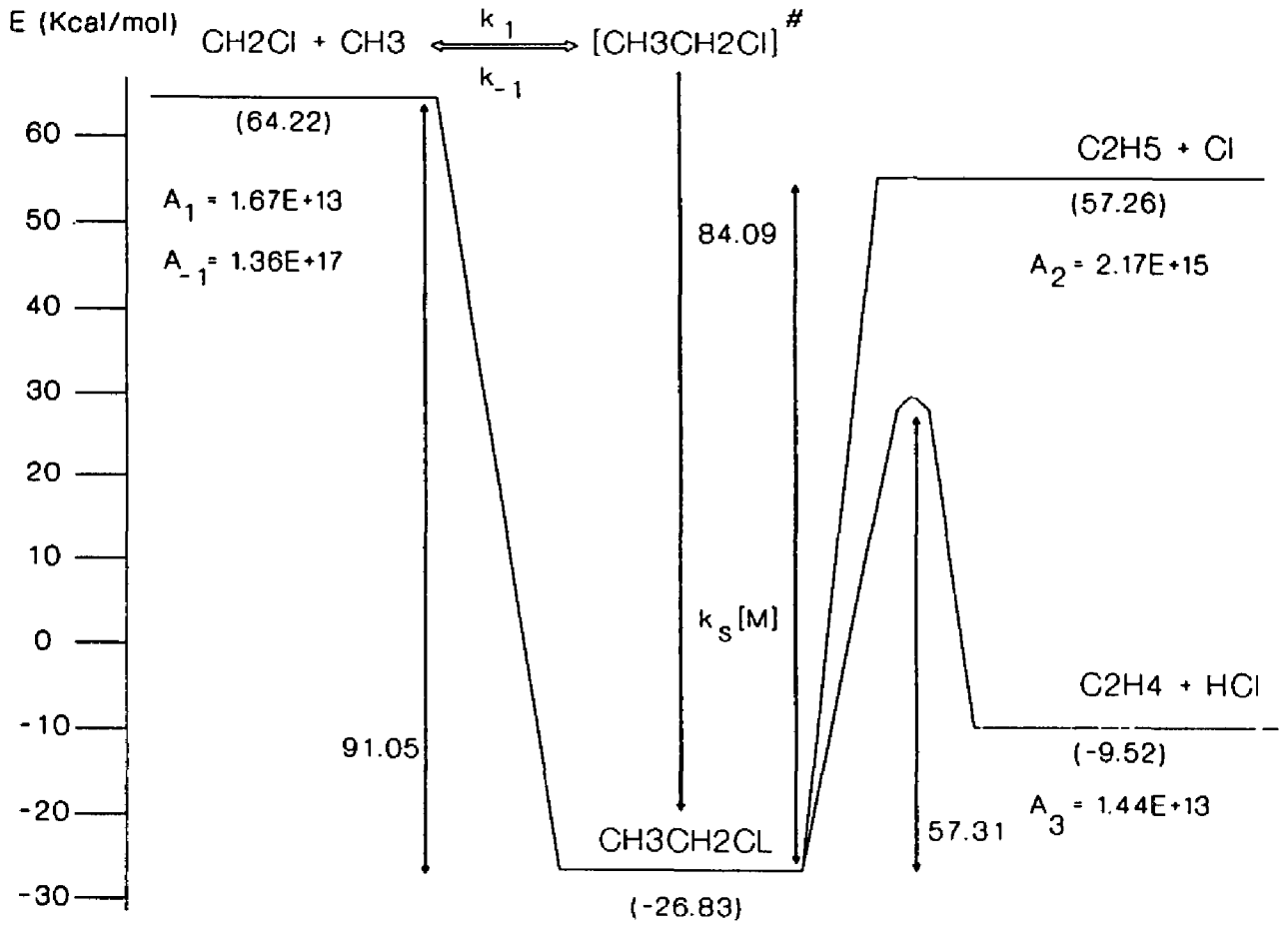

Fig 7.4 Energy Level for $CH_2Cl + CH_3$ Reaction

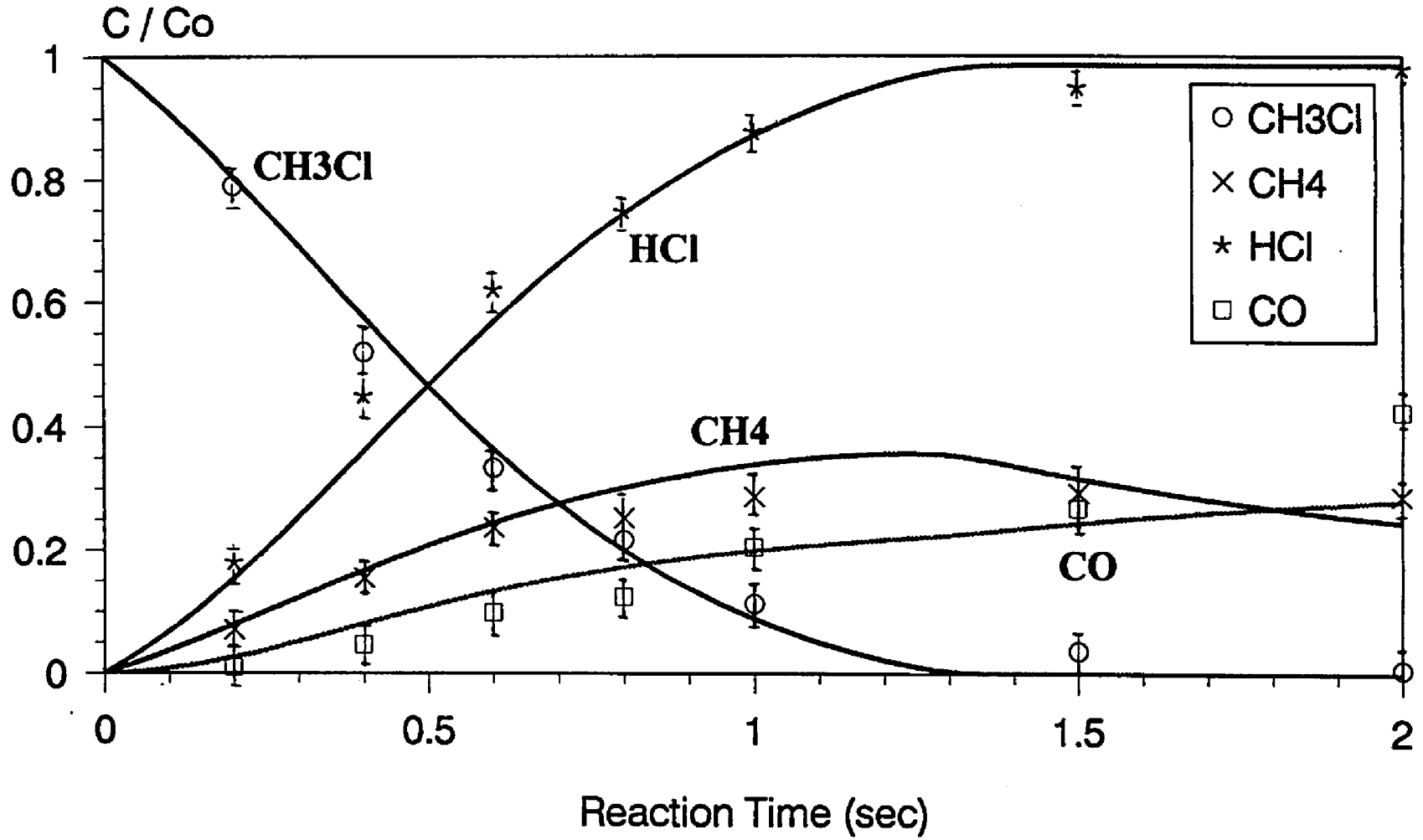

Fig 7.5 Comparison of calculated and experimental product distribution versus residence time at 1173K. Reactant ratios: O2:H2:CH3Cl:Ar=1:1:2:96

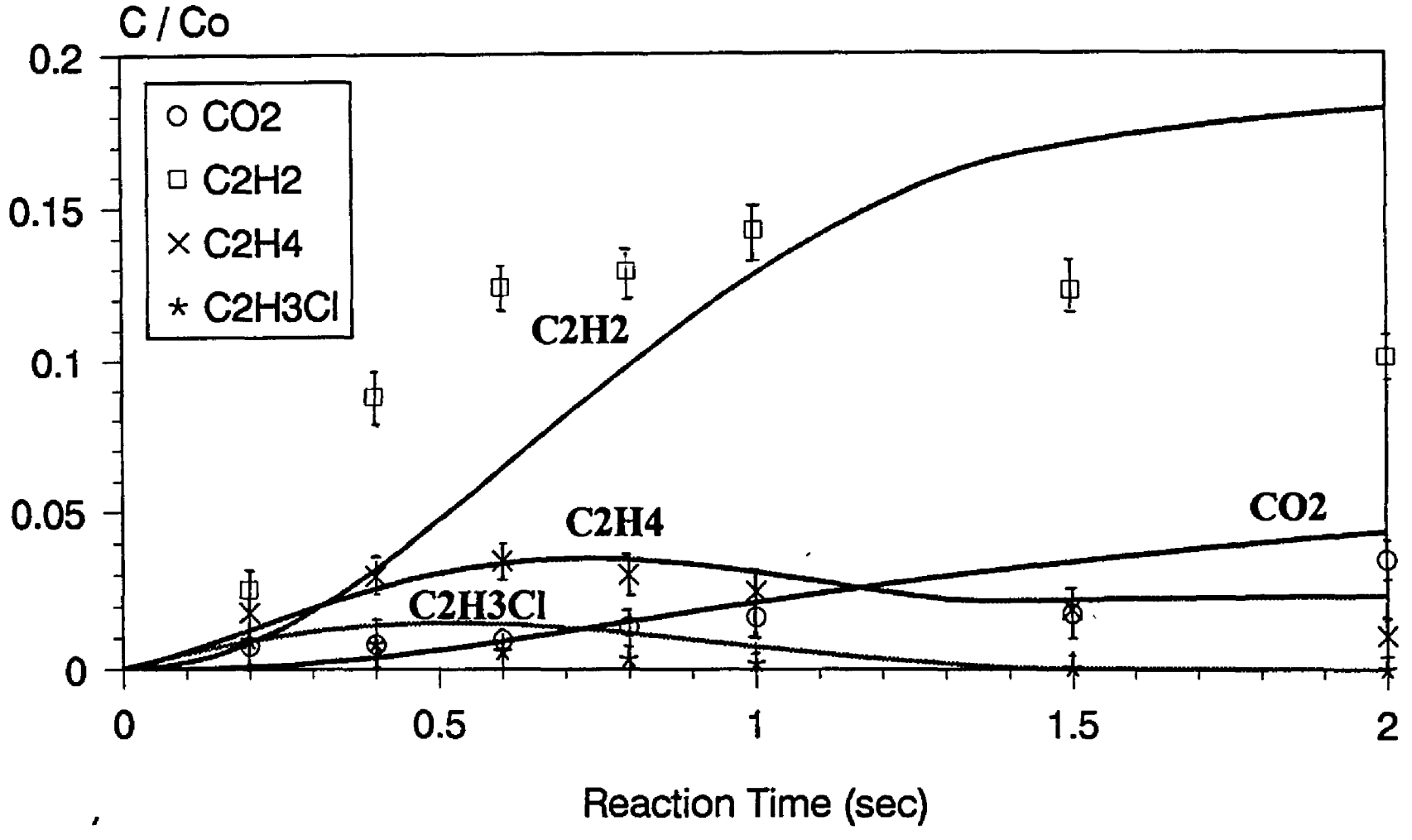

Fig 7.6 Comparison of calculated and experimental product distribution versus residence time at 1173K. Reactant ratios: O2:H2:CH3Cl:Ar=1:1:2:96

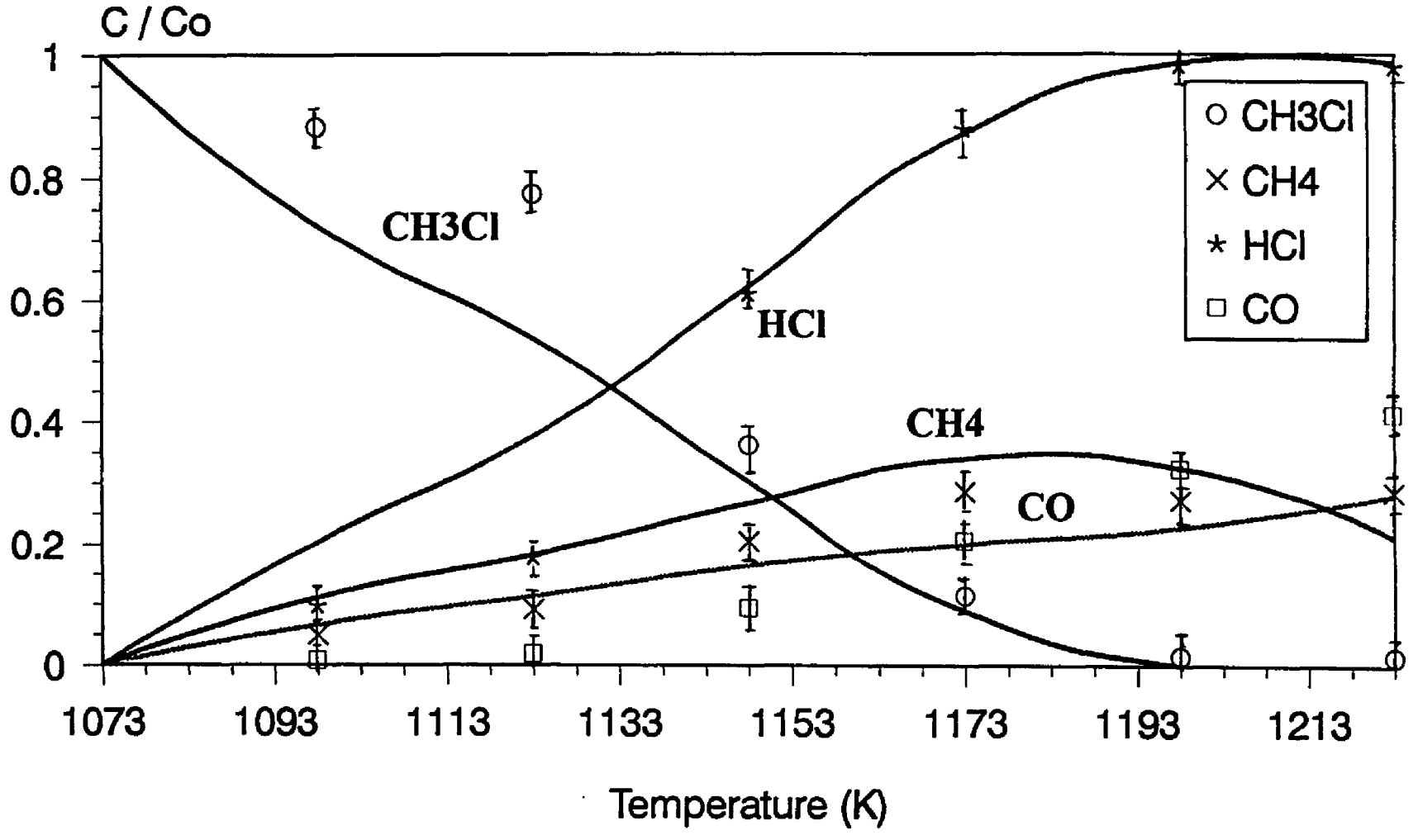

Fig 7.7 Comparison of calculated and experimental product distribution versus temperature at 1 sec. residence time. Reactant ratios: O2:H2:CH3Cl:Ar=1:1:2:96

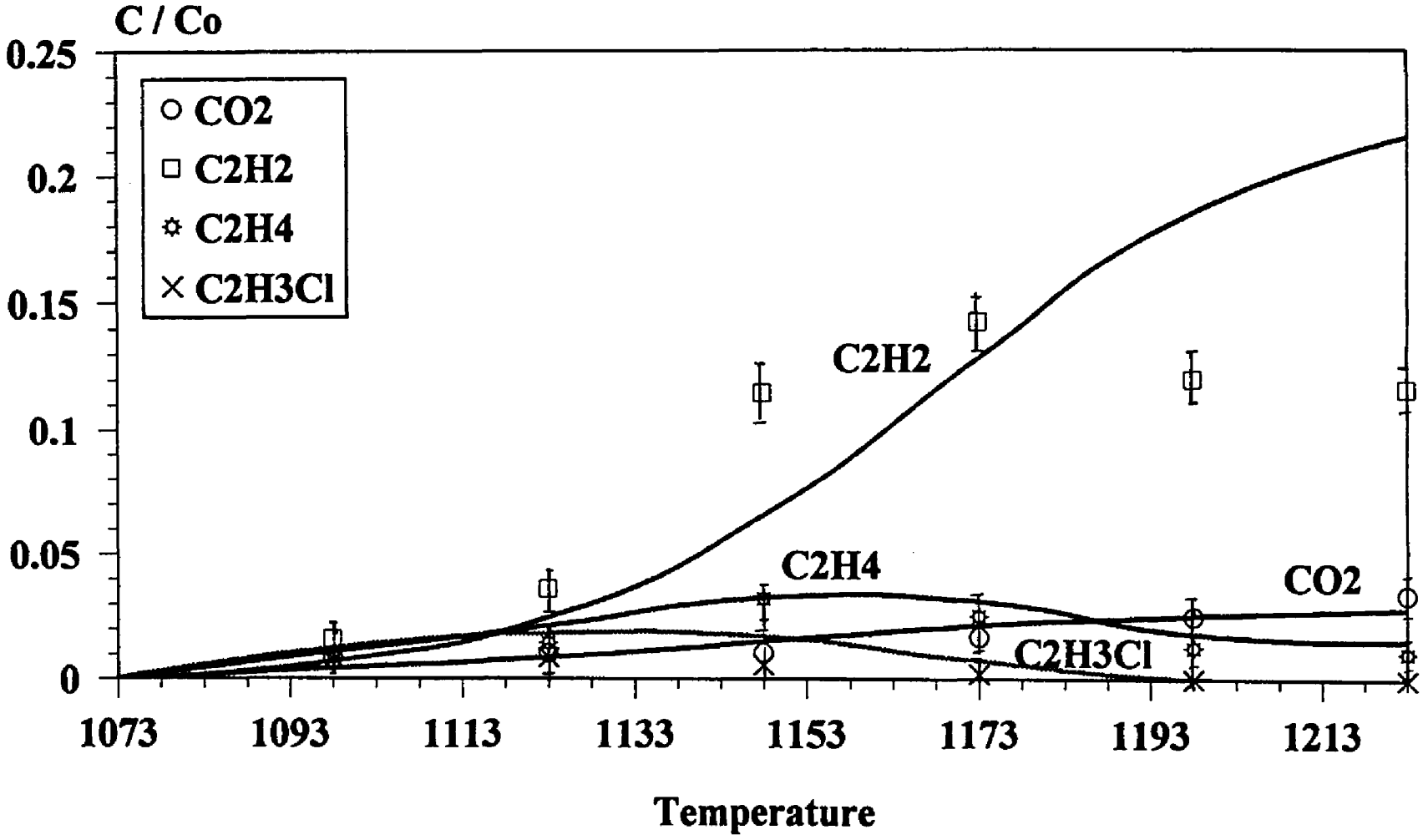

Fig 7.8 Comparison of calculated and experimental product distribution versus temperature at 1 sec. residence time. Reactant ratios: O2:H2:CH3Cl:Ar=1:1:2:96

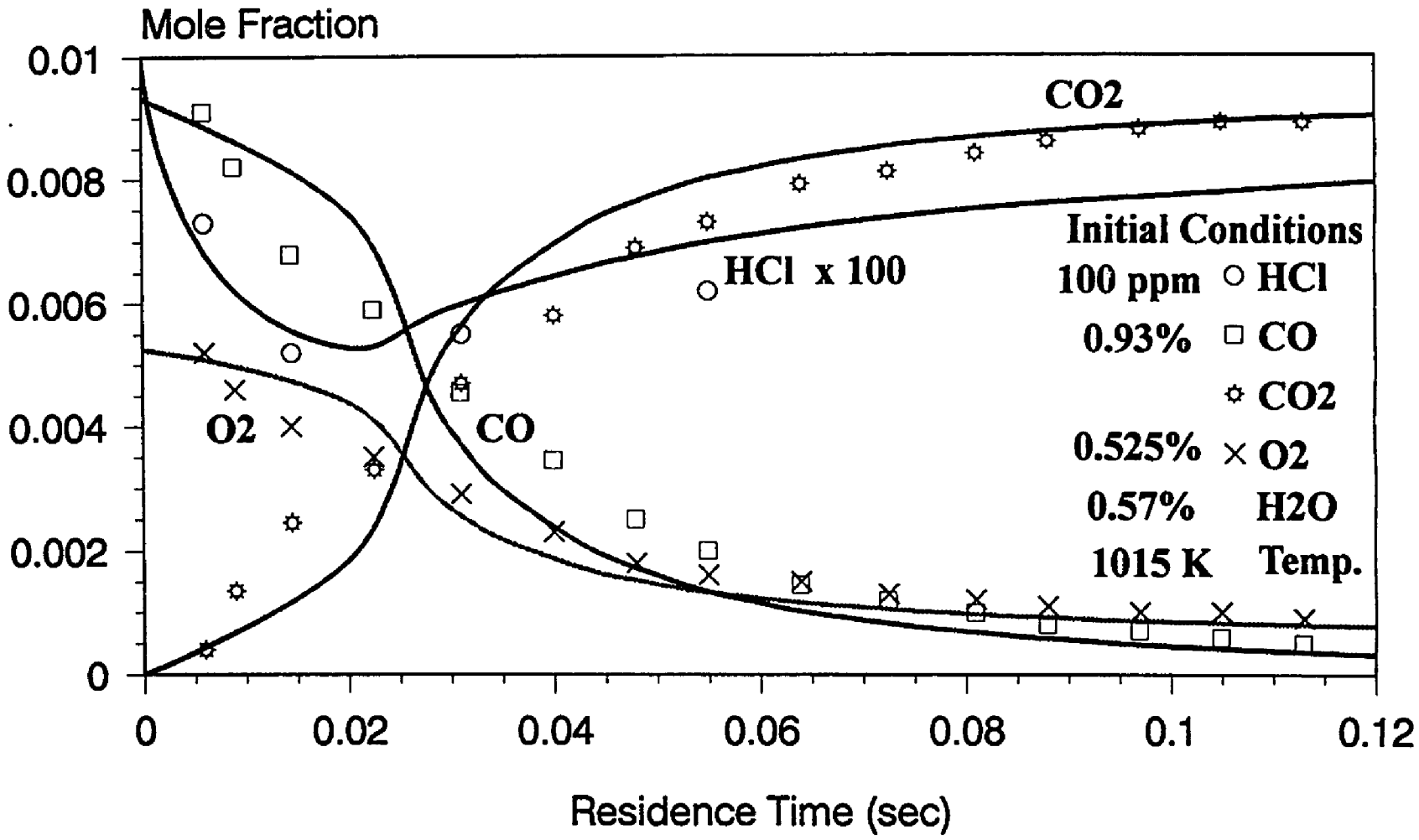

Fig 7.9 Comparison of our model with Princeton experimental data using temperature profile of princeton flow reactor.

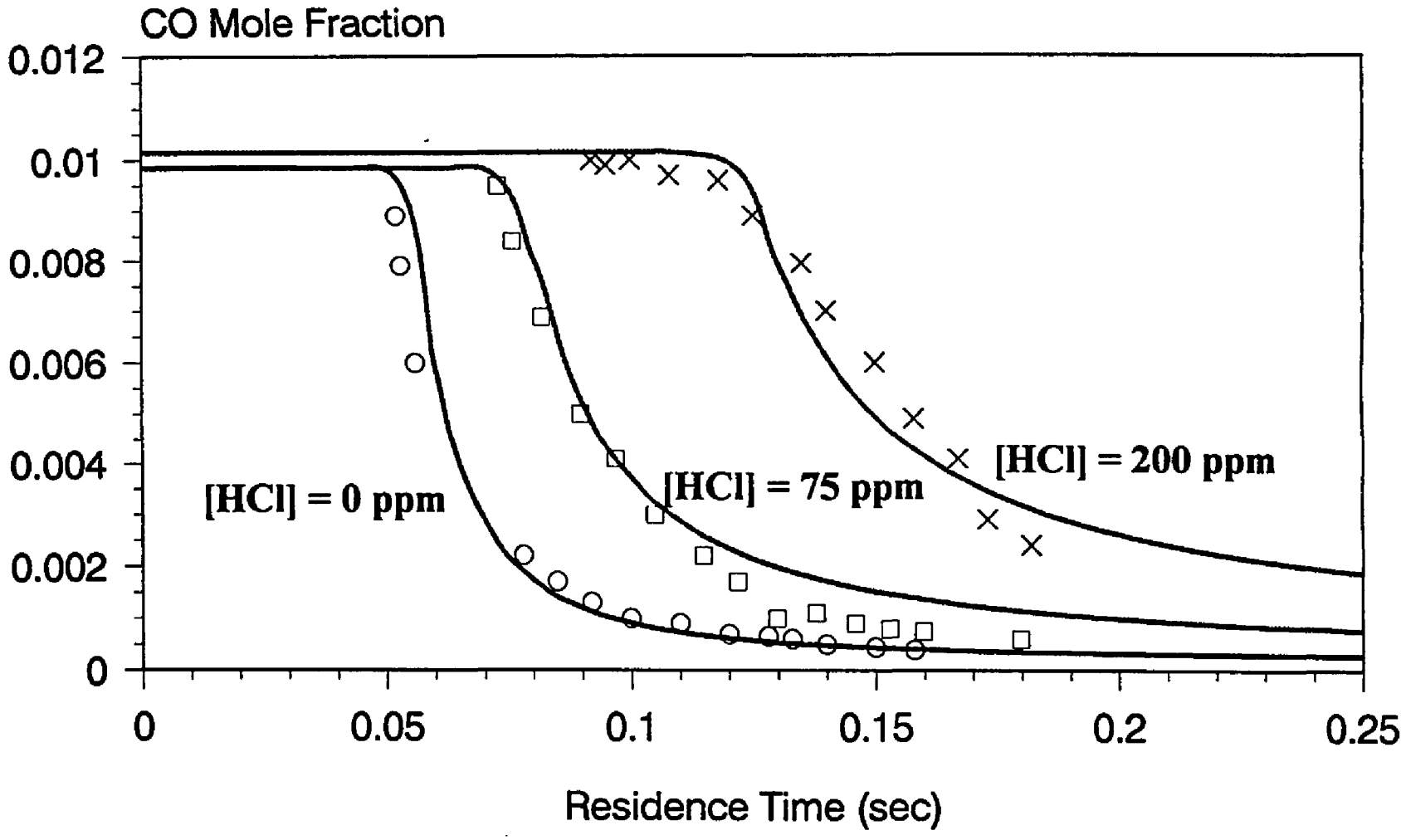

Fig 7.10 Comparison of model and experimental data for CO oxidation with different HCl concentration added.

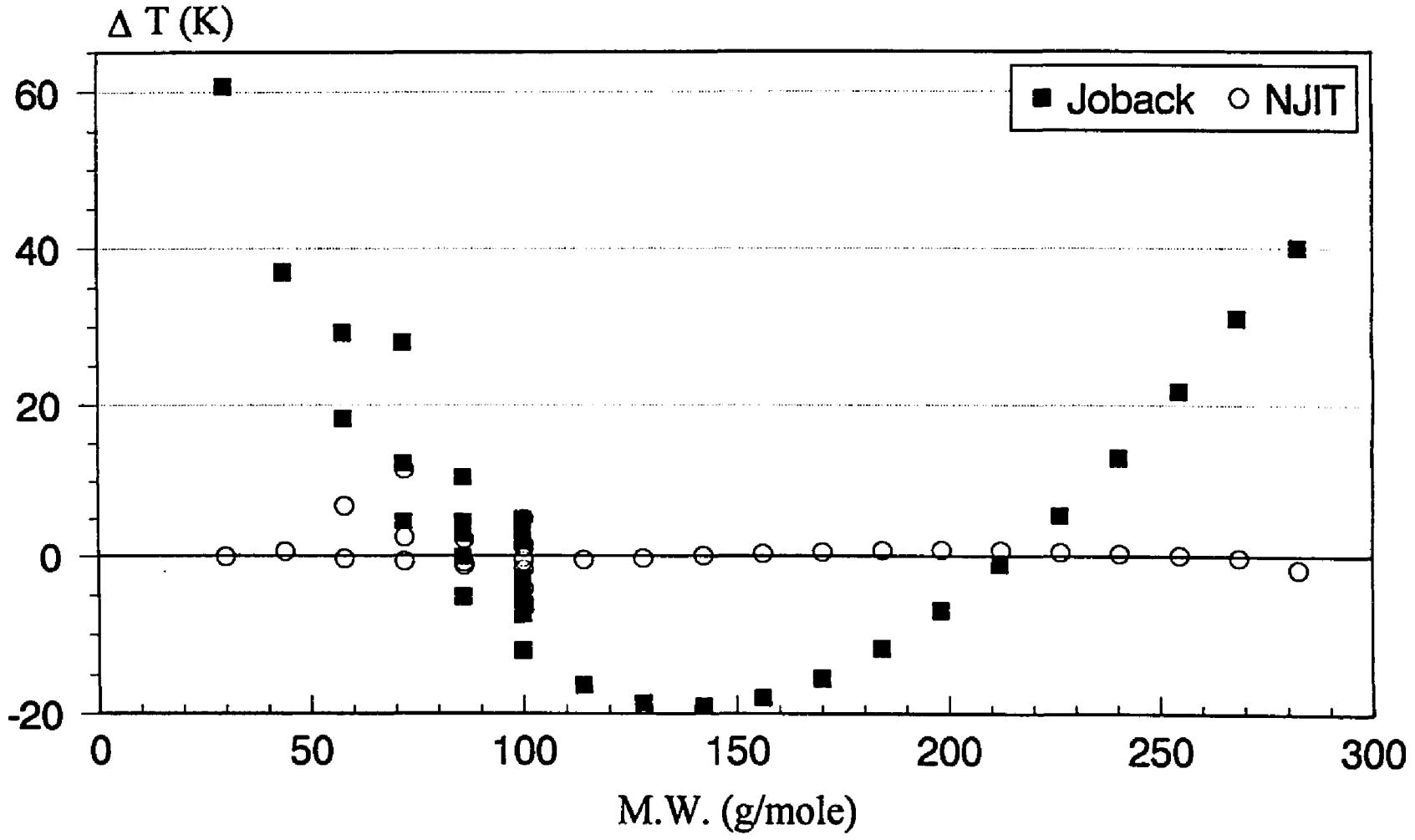

Fig 8.1 Plot of Residuals on Tb of Alkanes

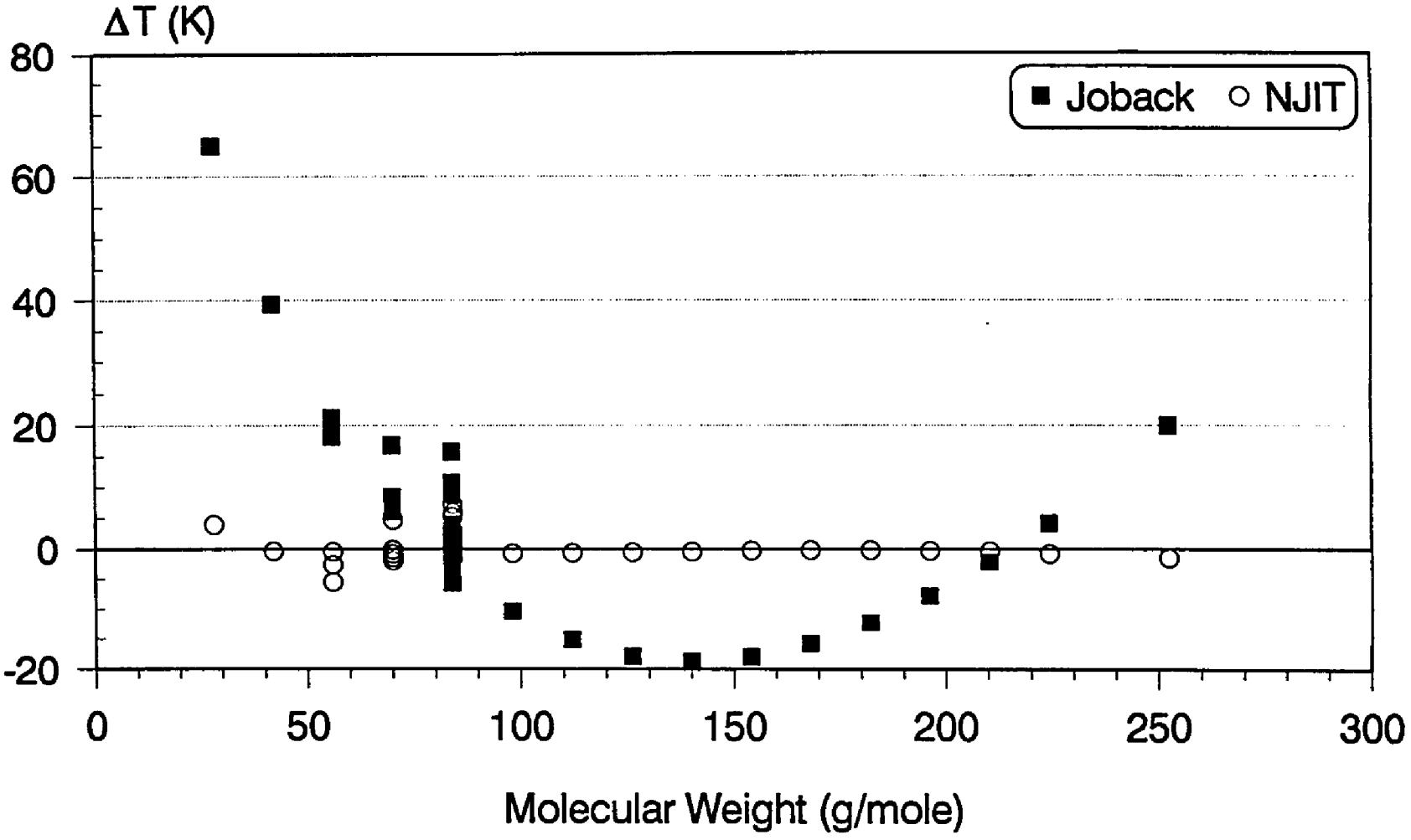

Fig 8.2 Plot od Residuals on Tb of Alkenes

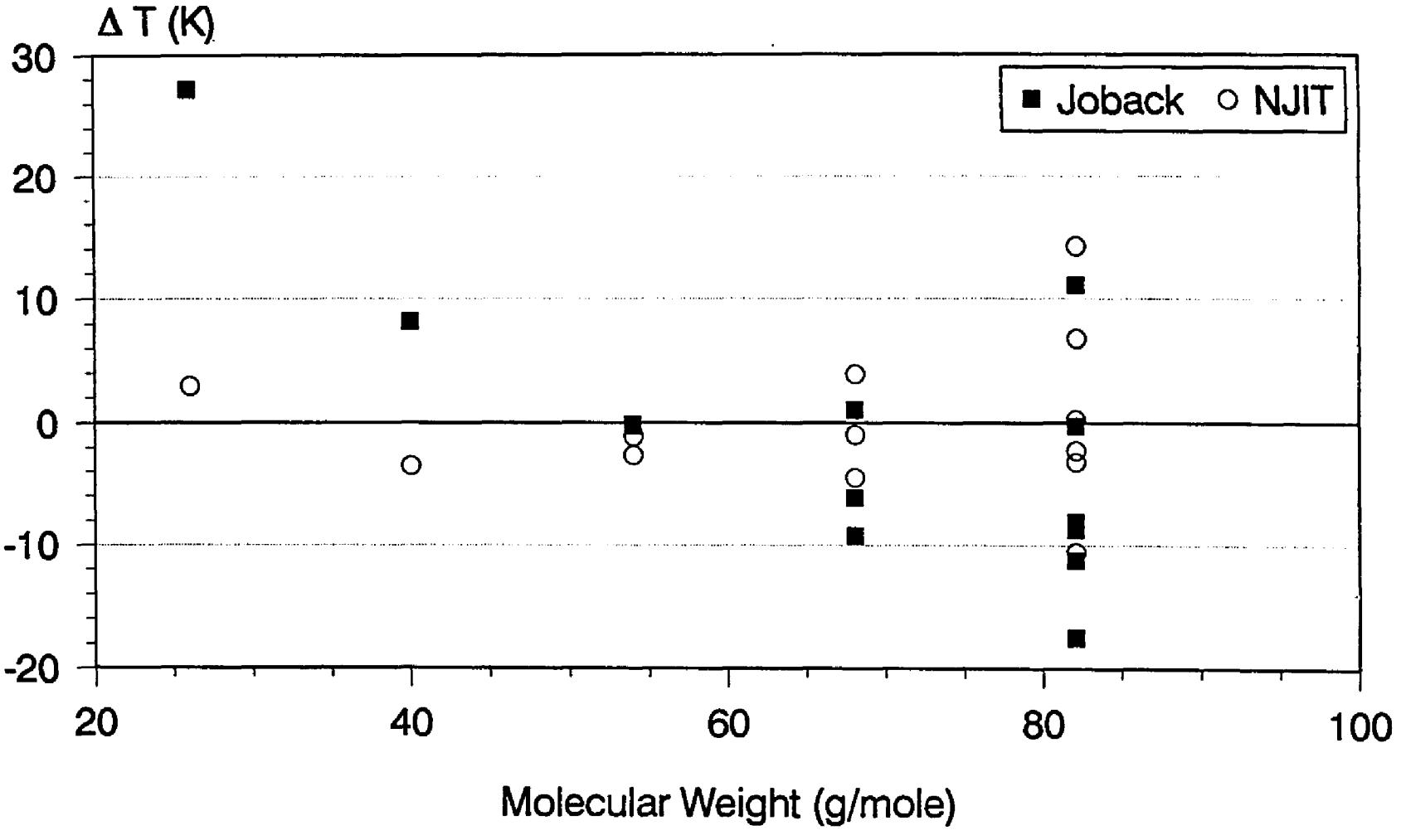

Fig 8.3 Plot of Residuals on Tb of Alkynes

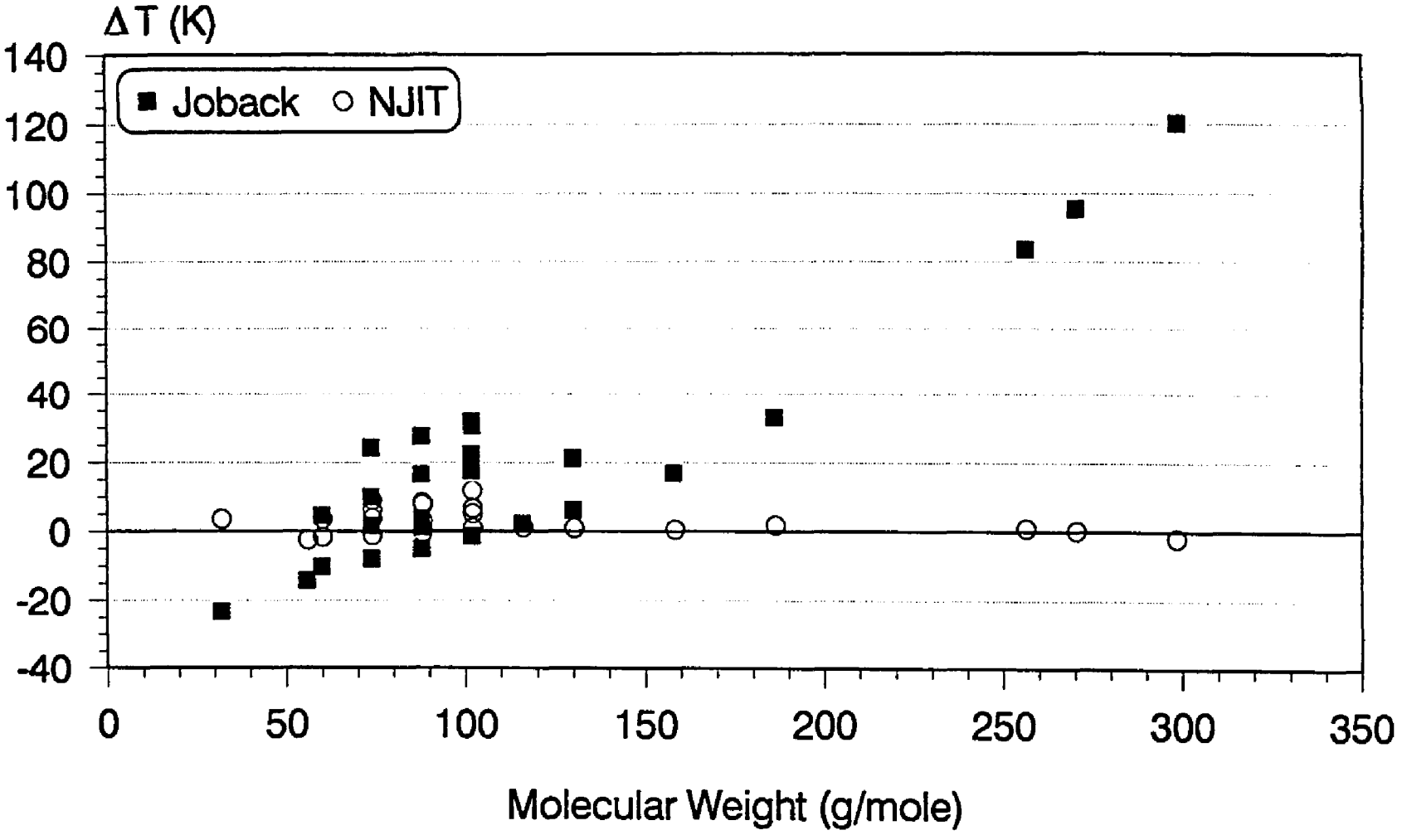

Fig 8.4 Plot of Residuals on Tb of Alcohols

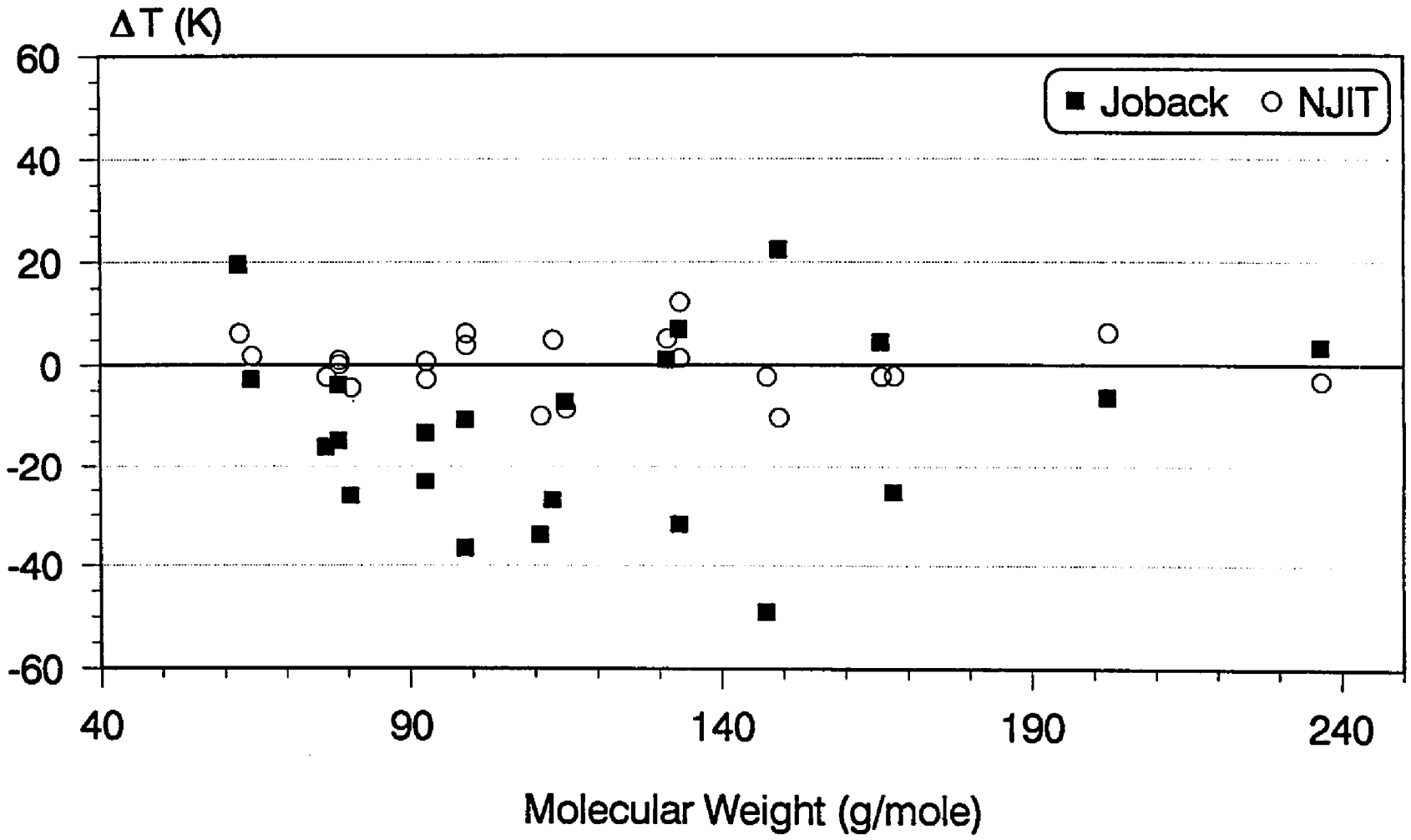

Fig 8.5 Plot of Residuals on Tb of Chlorocarbons

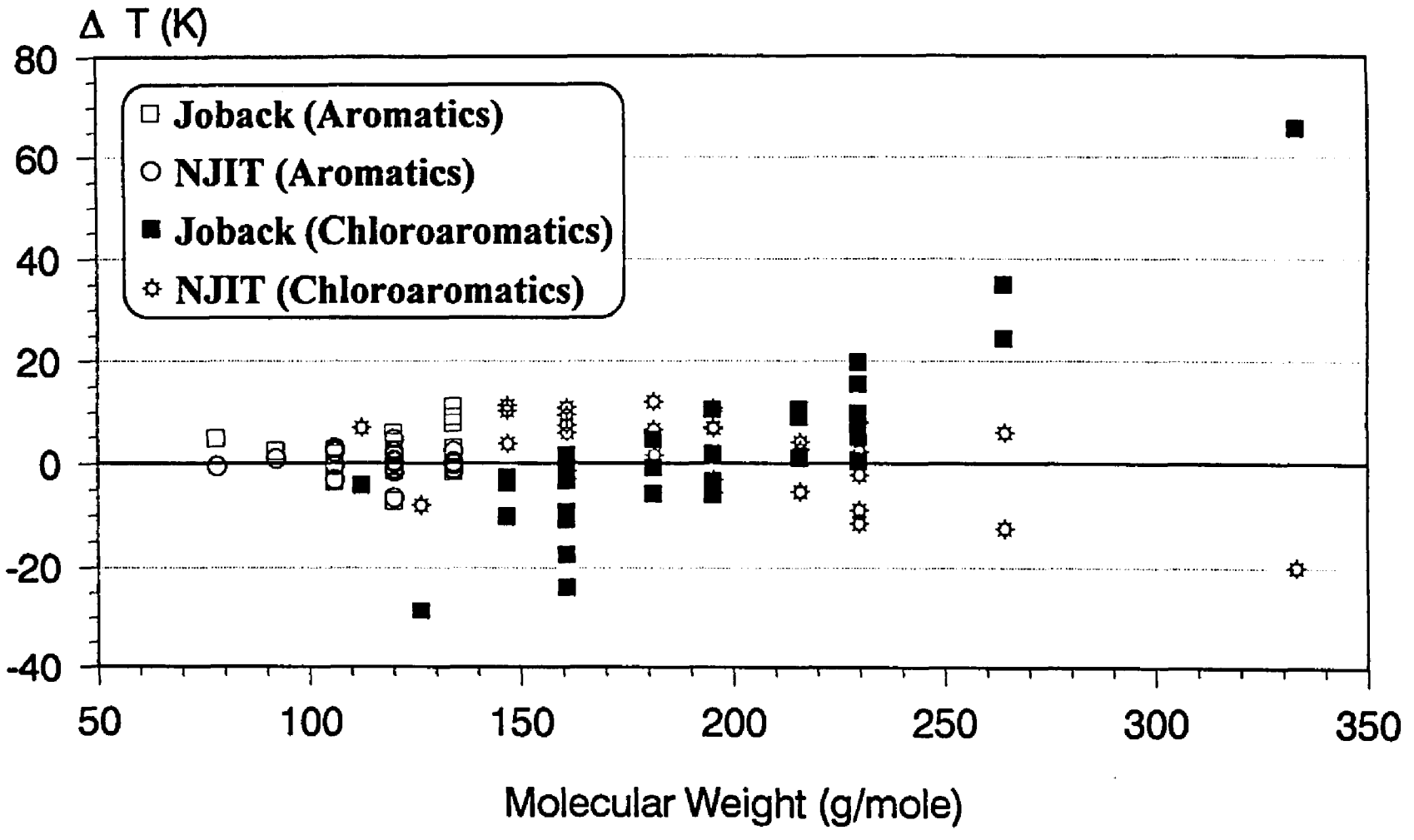

Fig 8.6 Plot of residuals on Tb of Aromatics

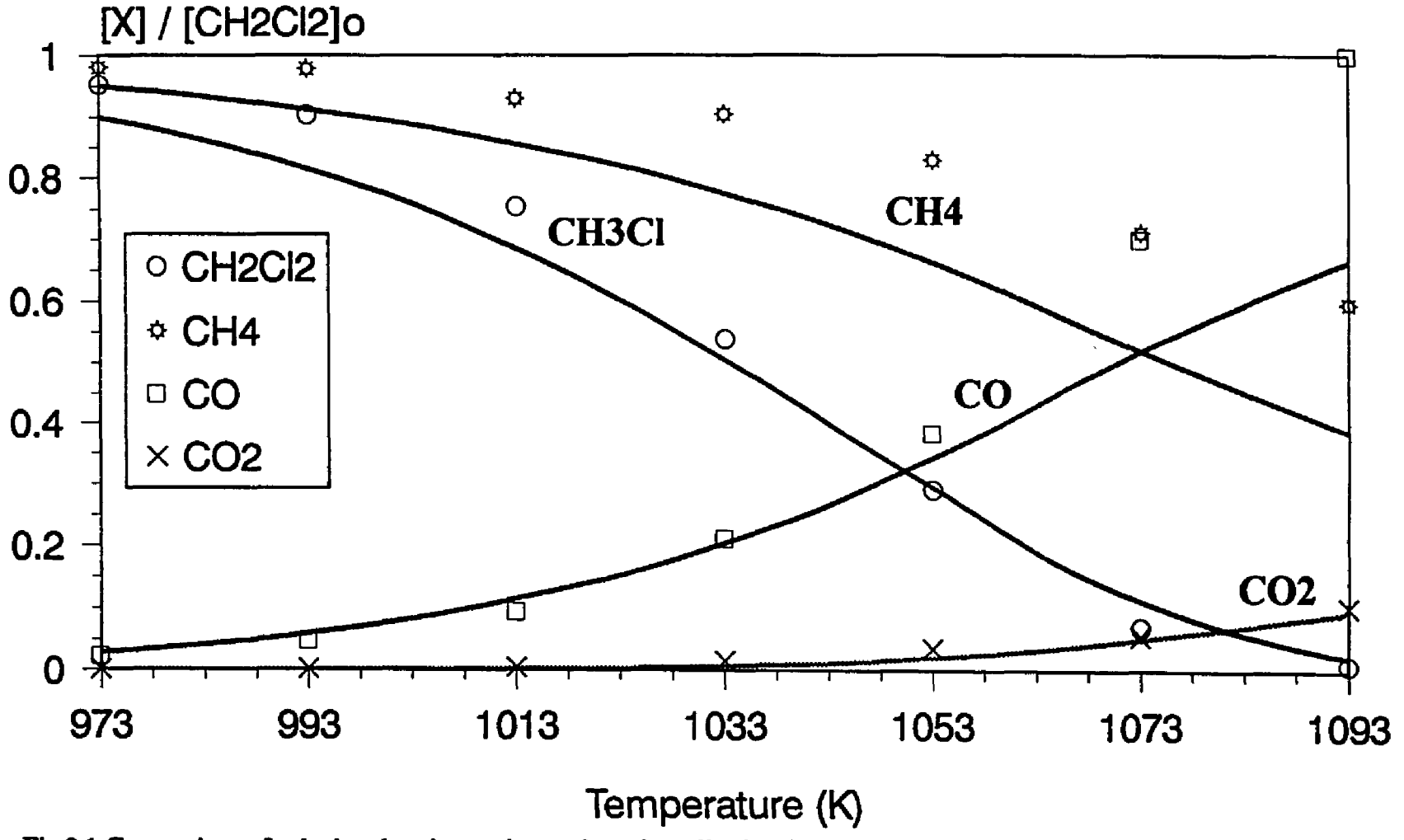

Fig 9.1 Comparison of calculated and experimental product distribution versus temperature at 1 sec. residence time. Reactant ratios: O2:CH4:CH2Cl2:Ar=4:1:1:94

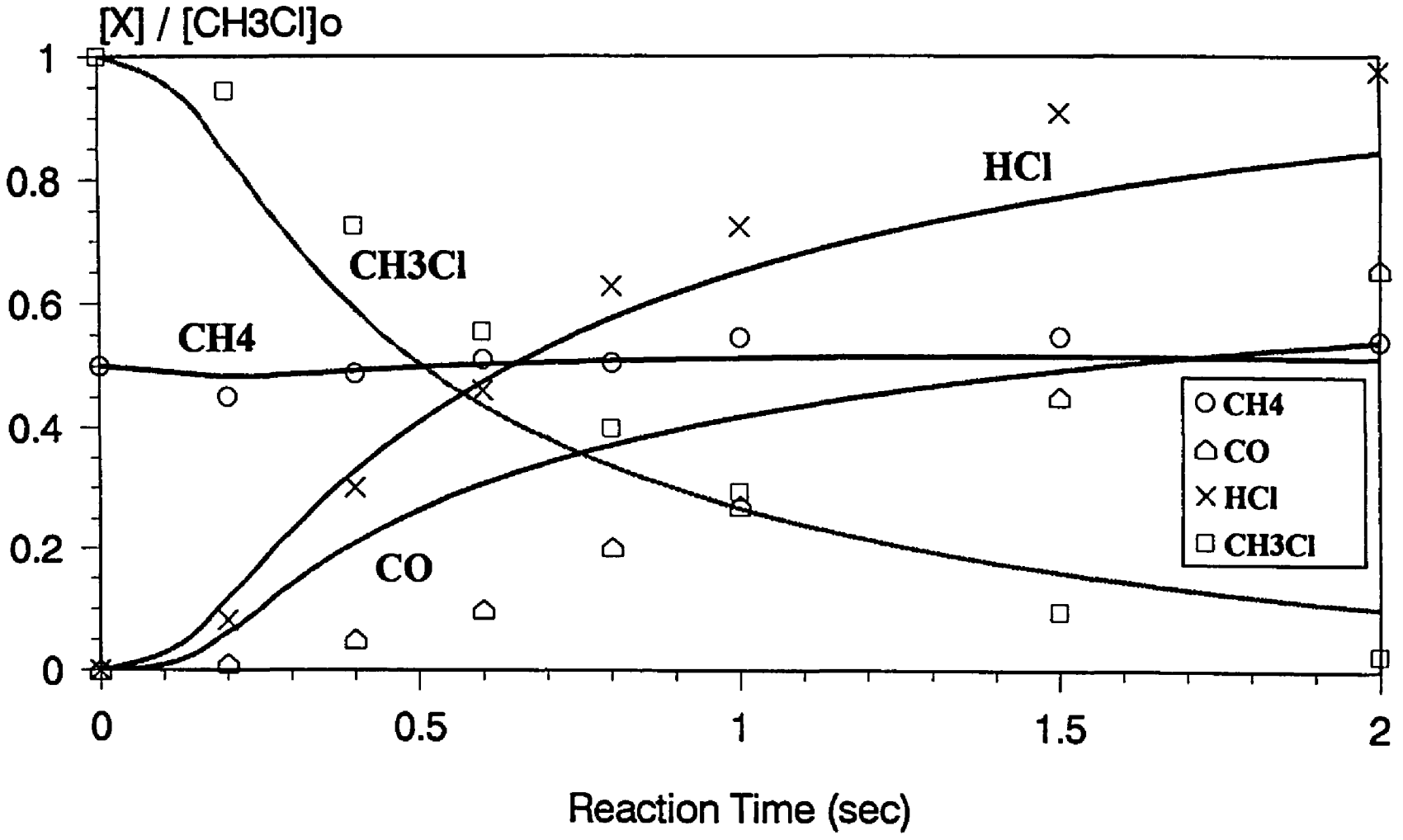

Fig 9.2 Comparison of calculated and experimental product distribution versus residence time at 1173K.
Reactant ratios: O2:CH4:CH3Cl:Ar=2:1:2:95

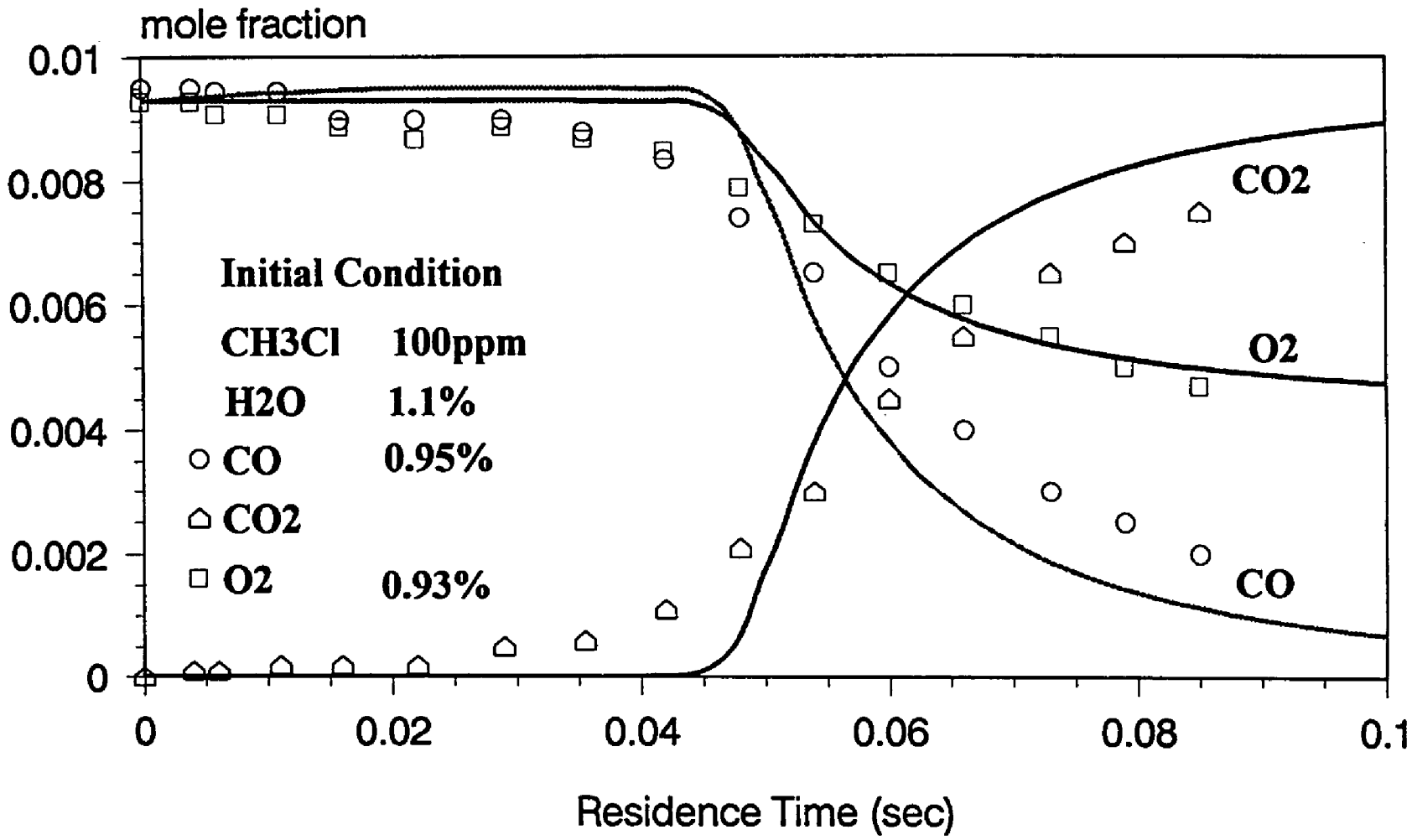

Fig 9.3 Comparison of our model with Roesler et al. experimental data.

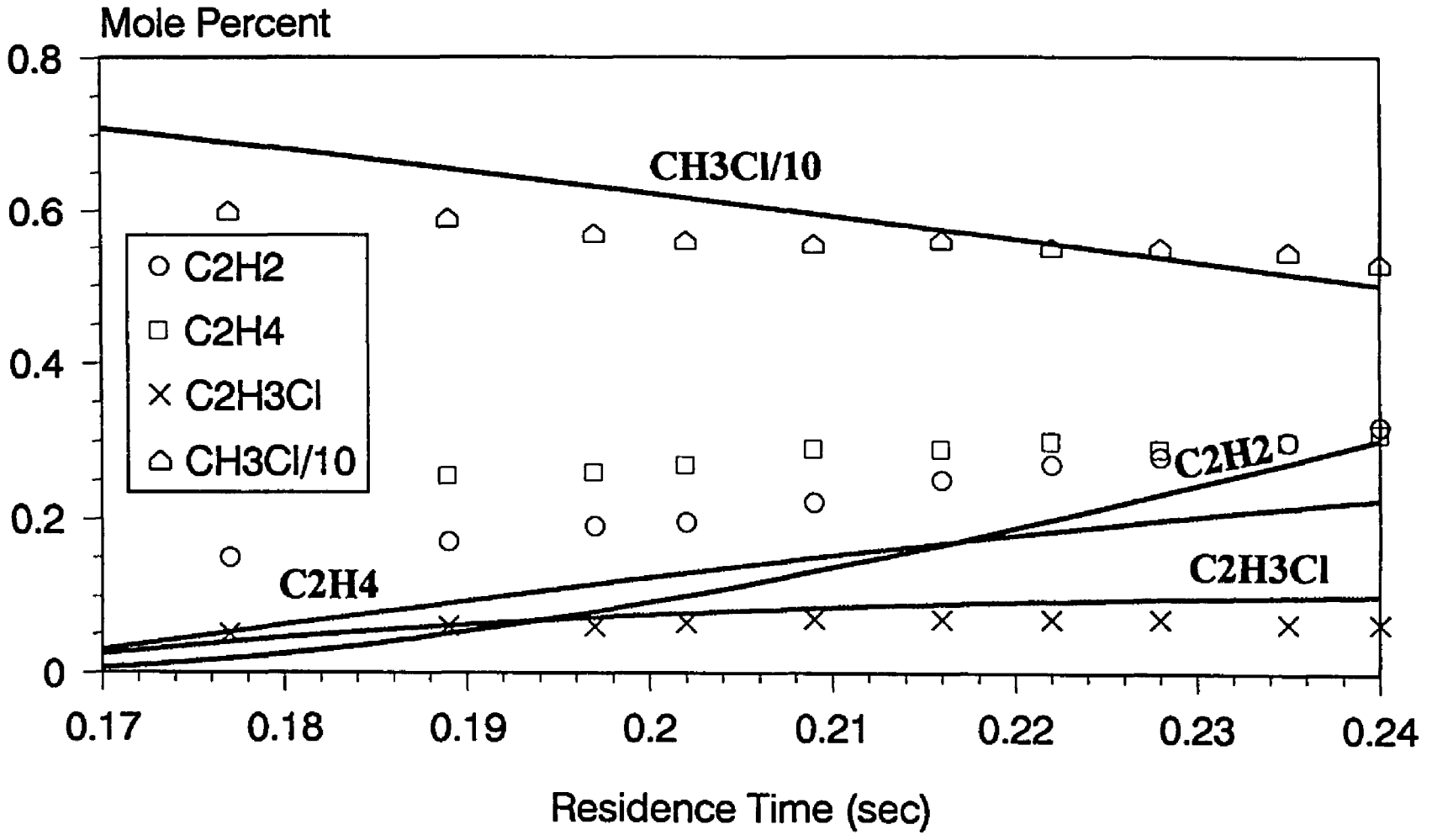

Fig 9.4 Comparison of calculated and experimental product distribution versus residence time at 1253K. Reactant ratios: O2:CH3Cl:Ar=2.05:7.32:90.6

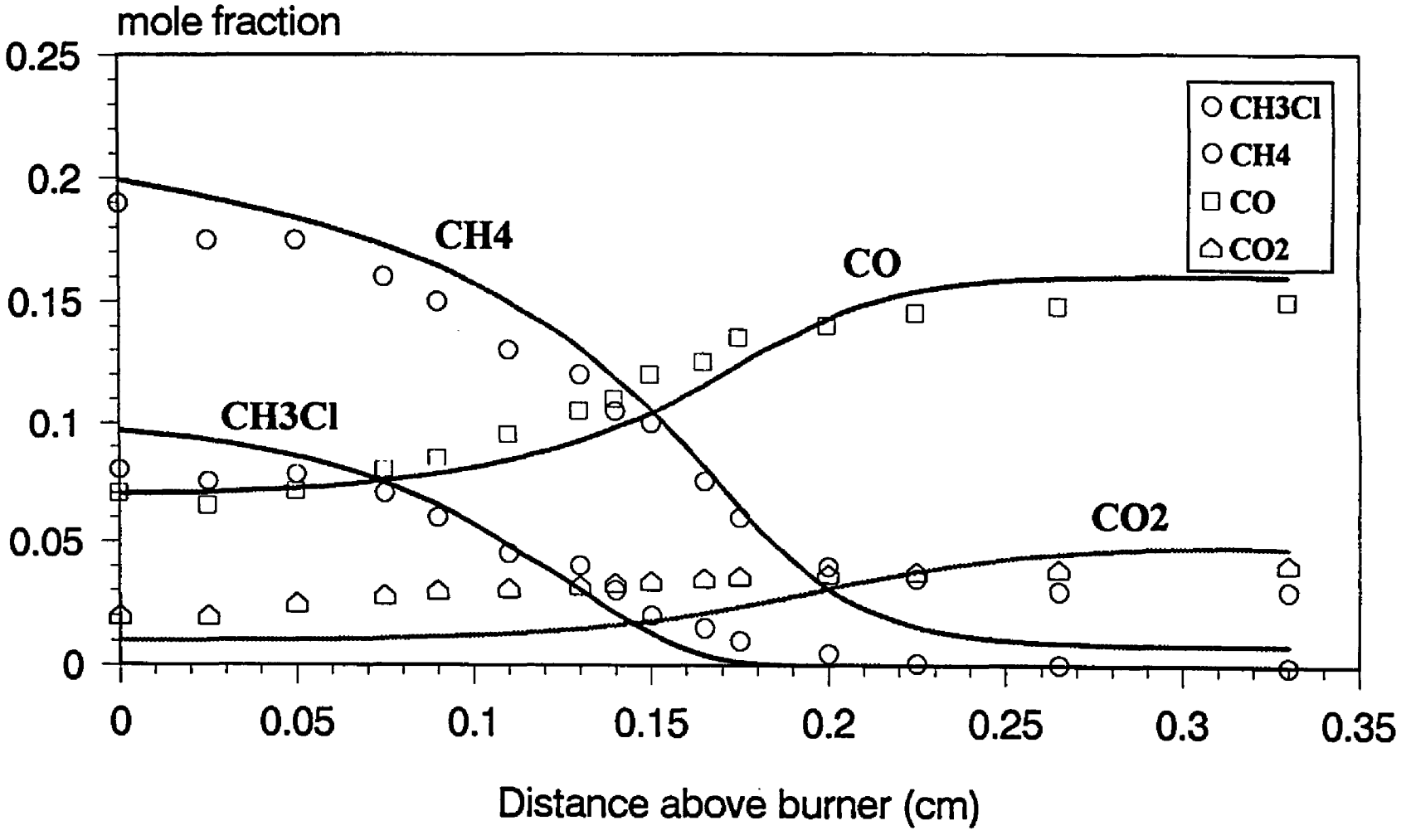

Fig 9.5 Comparison of our model with Karra et al. flame data

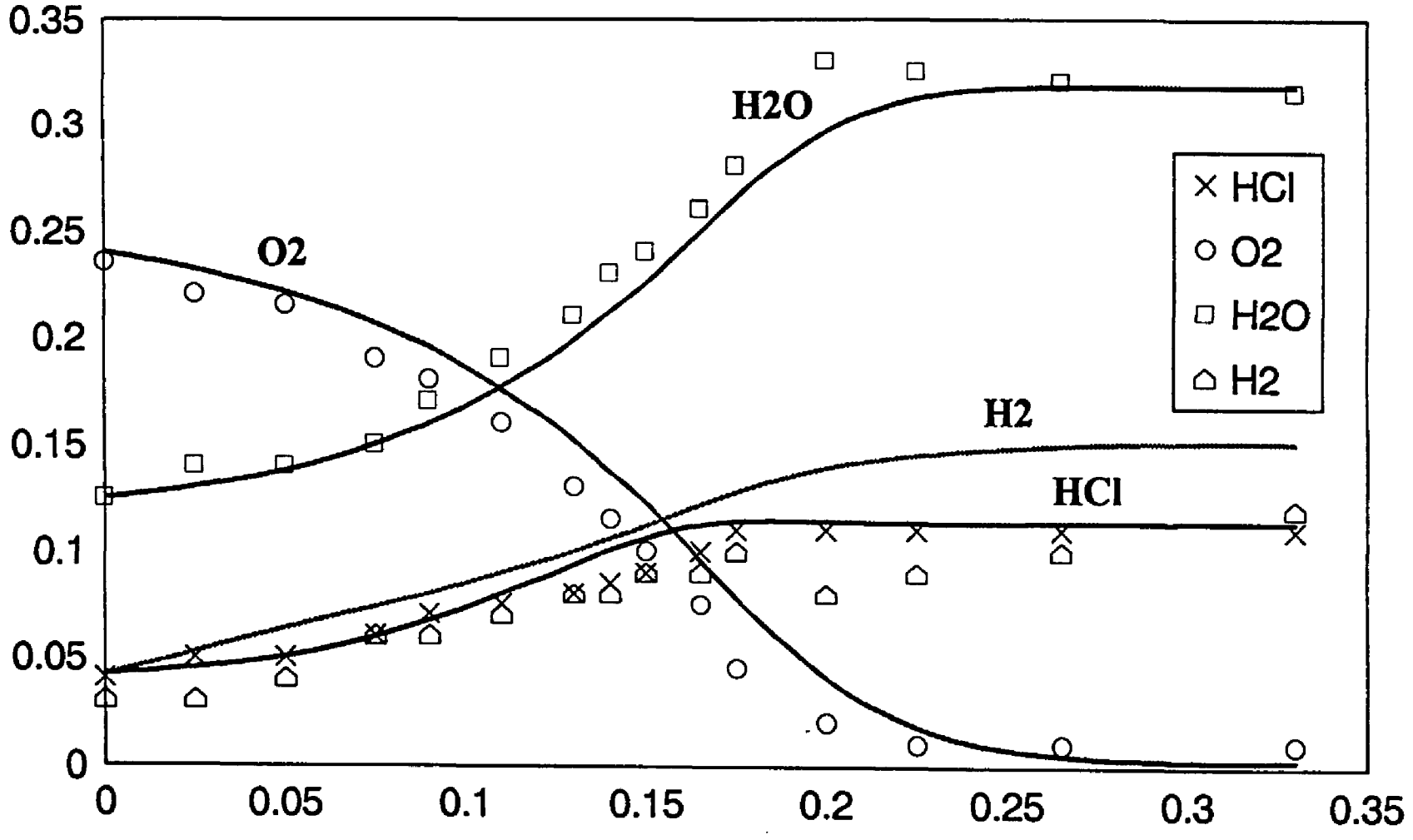

Fig 9.6 Comparison of our model with Karra et al. flame data

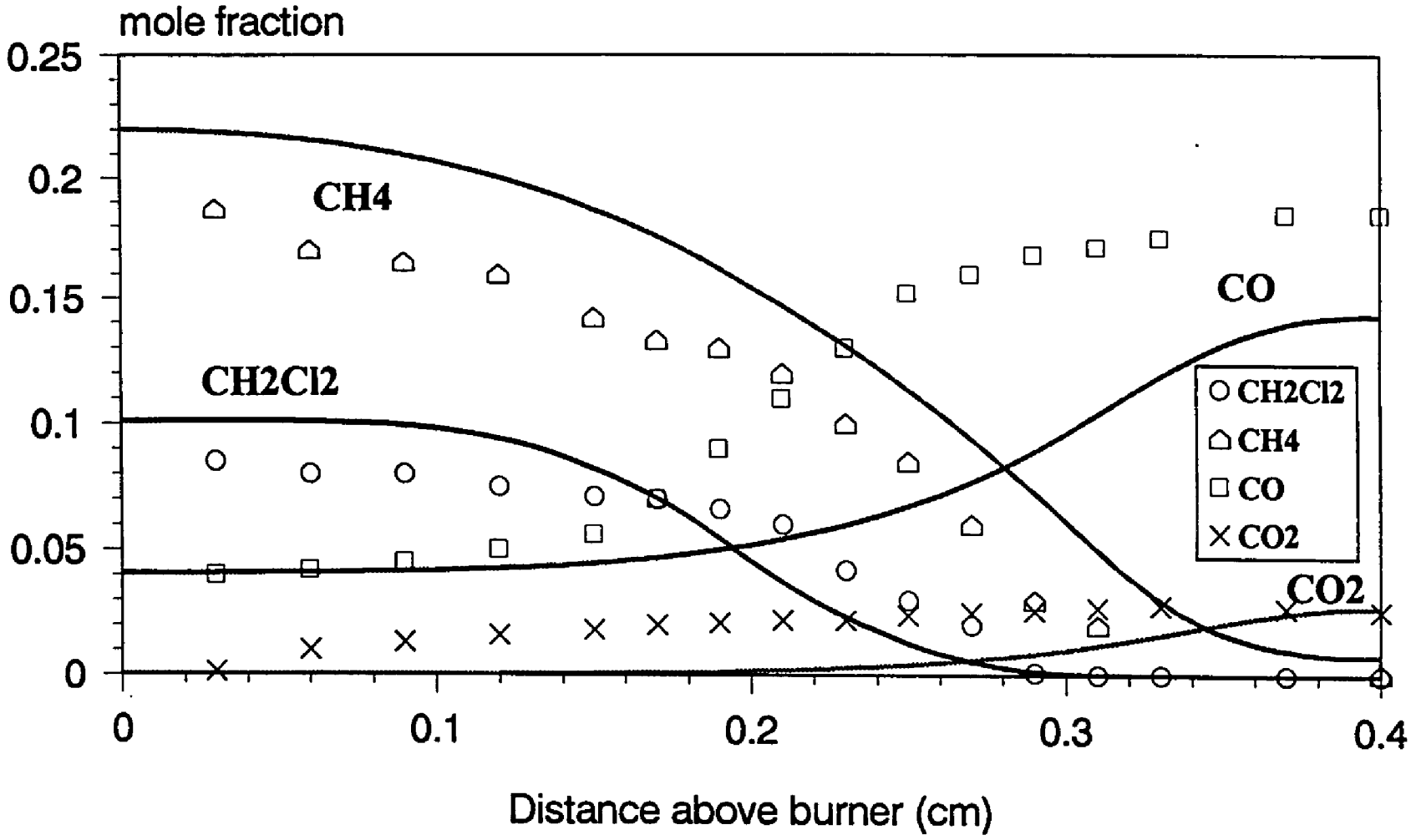

Fig 9.7 Comparison of our model with Qun et al. flame data

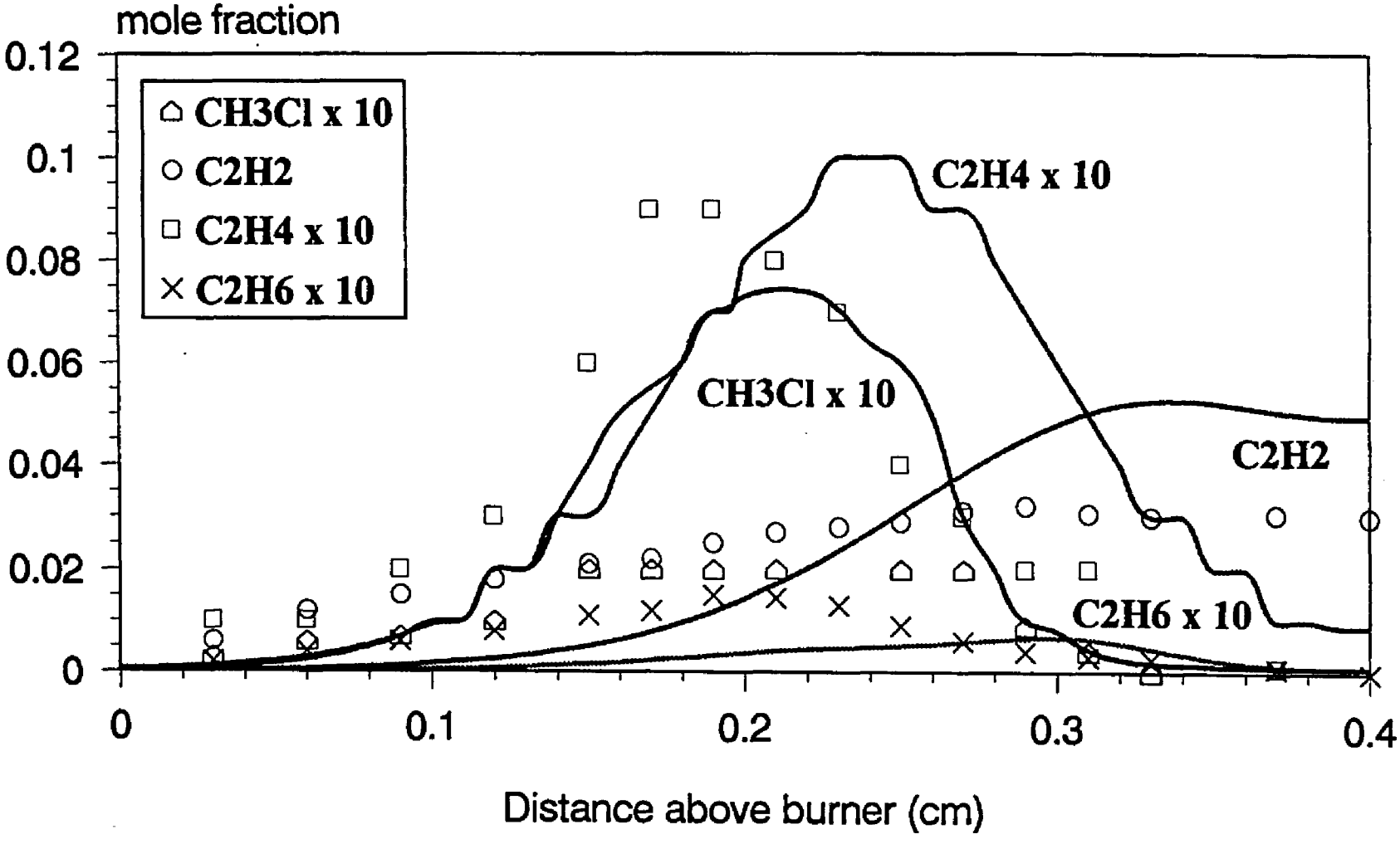

Fig 9.8 Comparison of our model with Qun et al. flame data

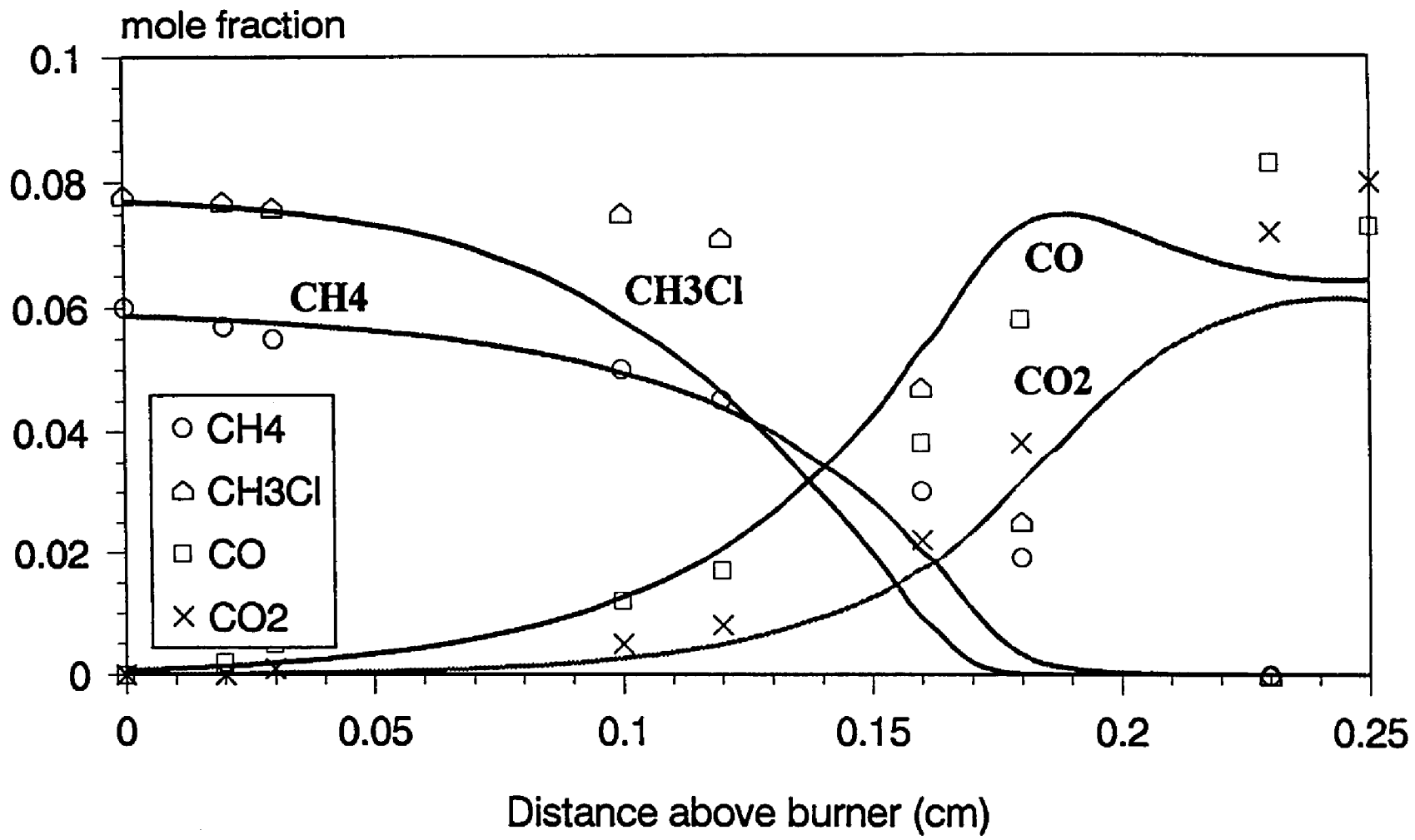

Fig 9.9 Comparison of our model with Miller et al. flame data

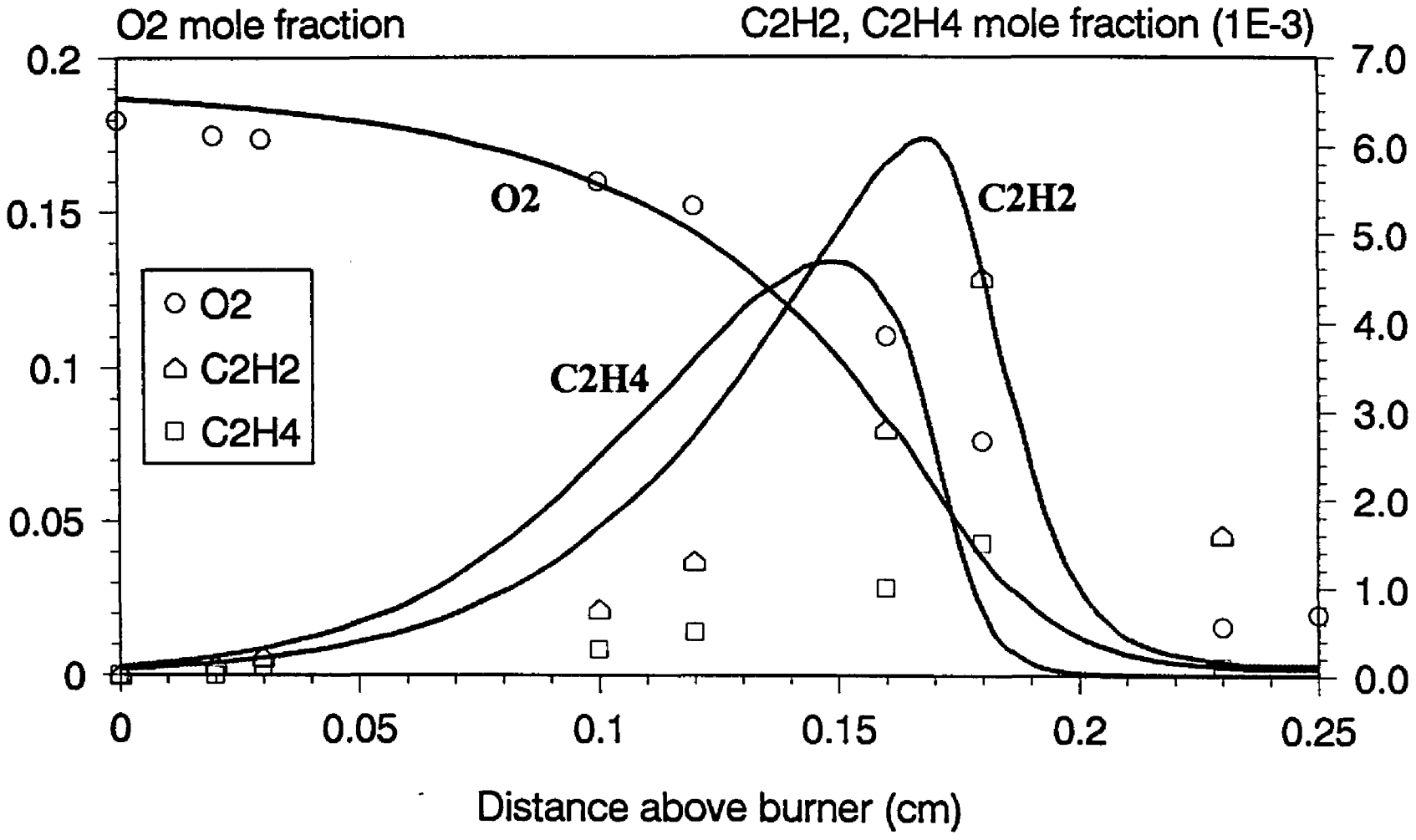

Fig 9.10 Comparison of our model with Miller et al. flame data

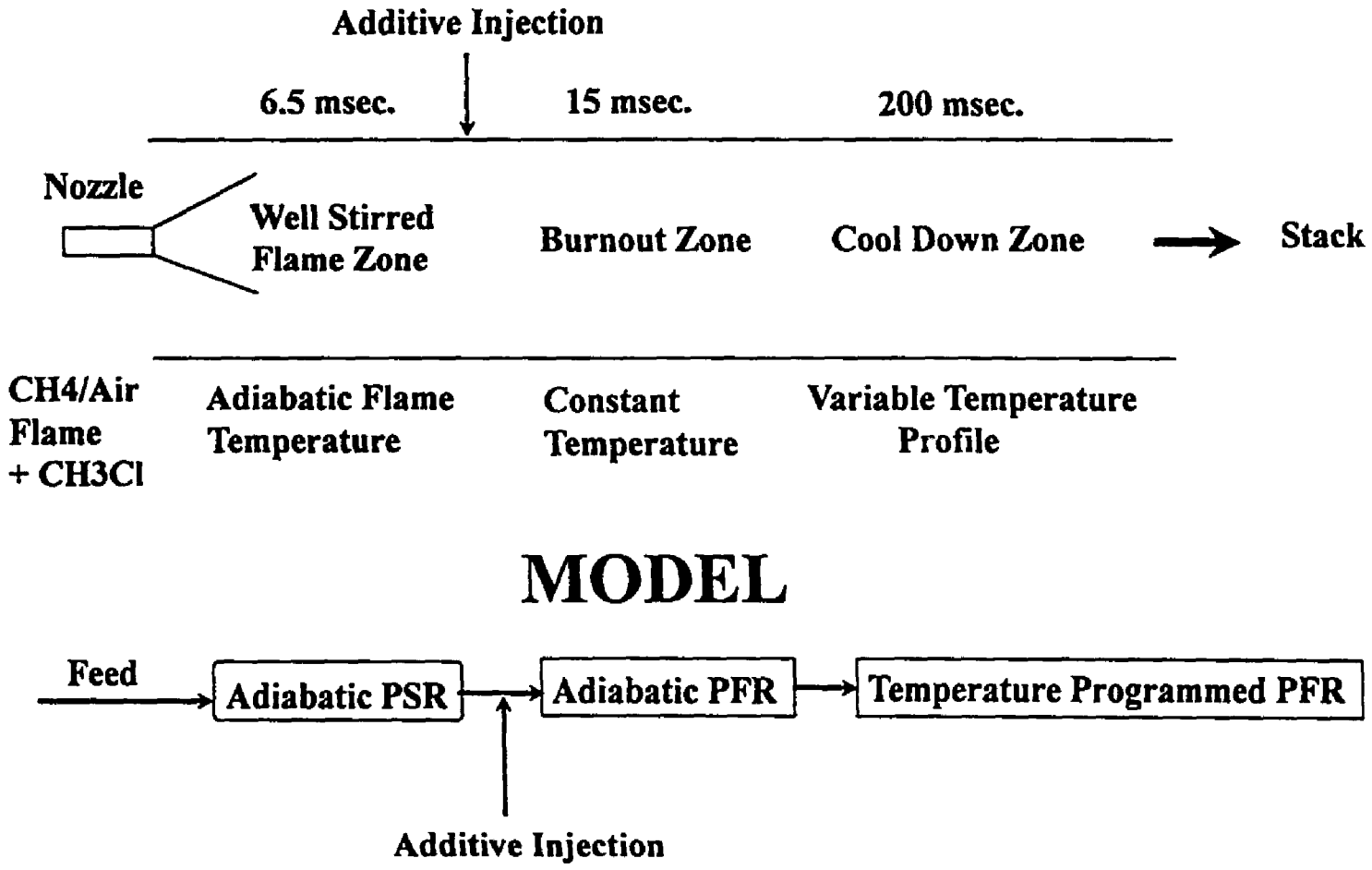

Fig 10.1 Turbulent Flow Incinerator Simulation

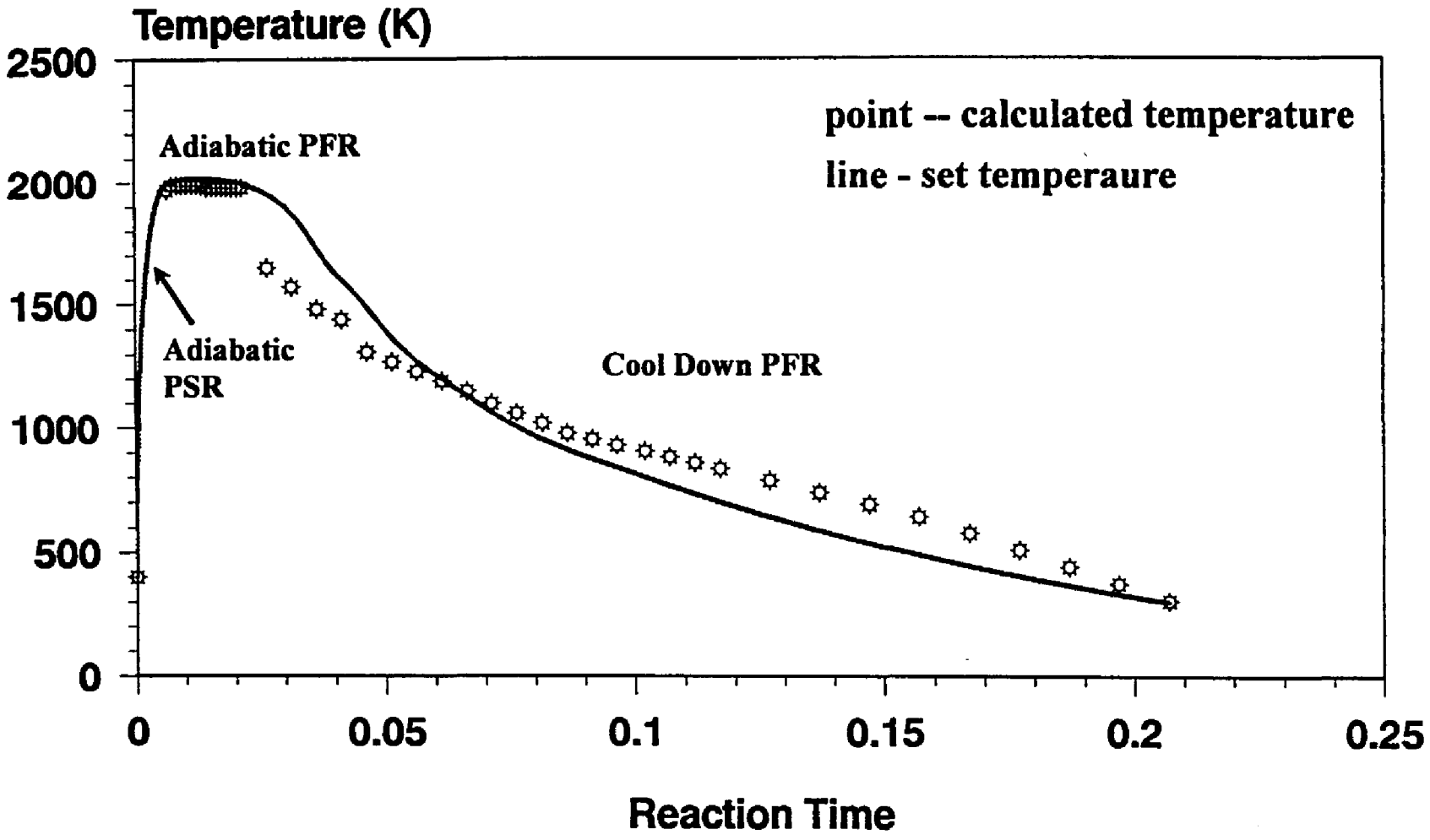

Fig 10.2 Incinerator simulation temperature profile

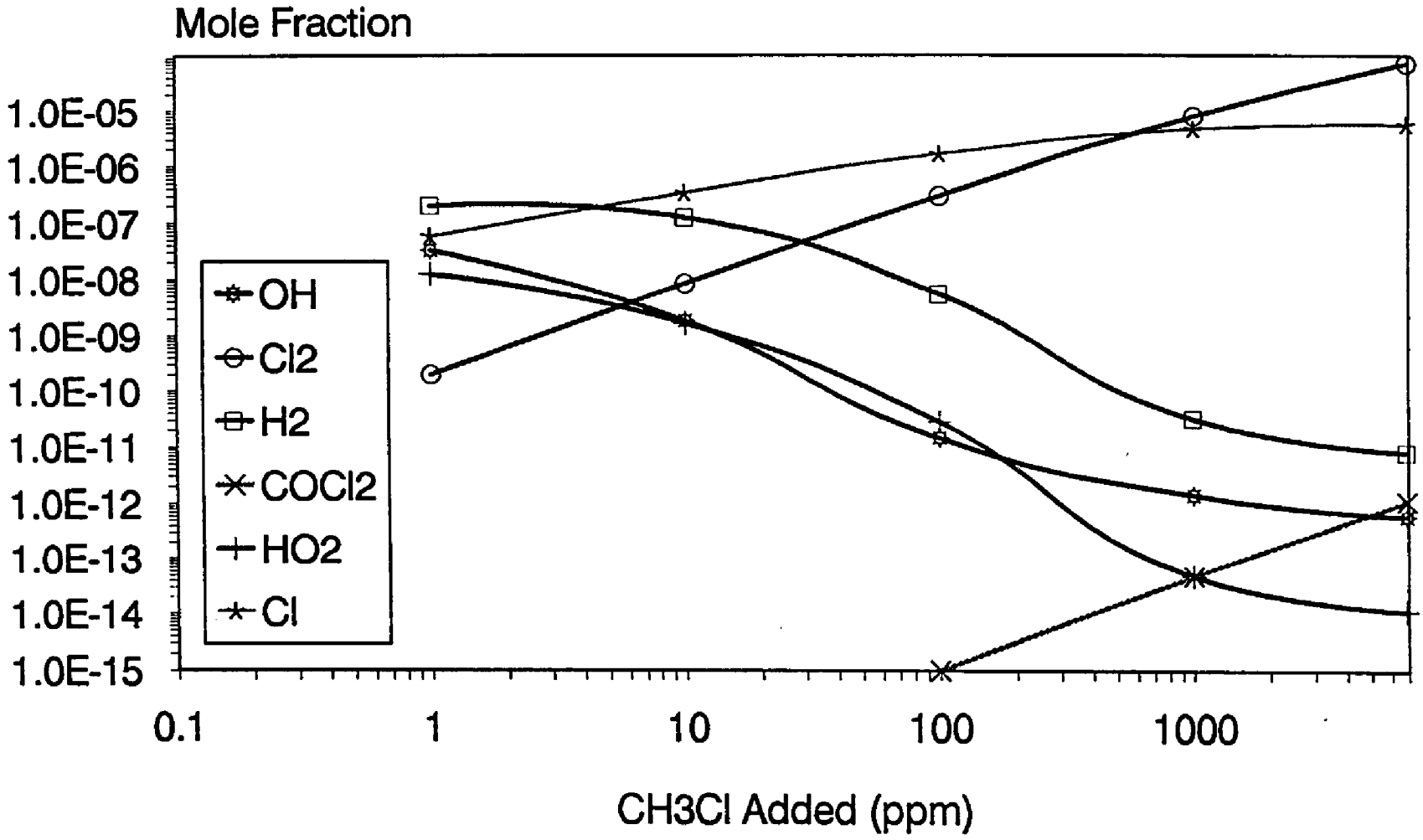

Fig 10.3 Effect of CH3Cl added in CH4/Air under fuel lean condition (equivalence ratio 0.8); calculated in burnout zone

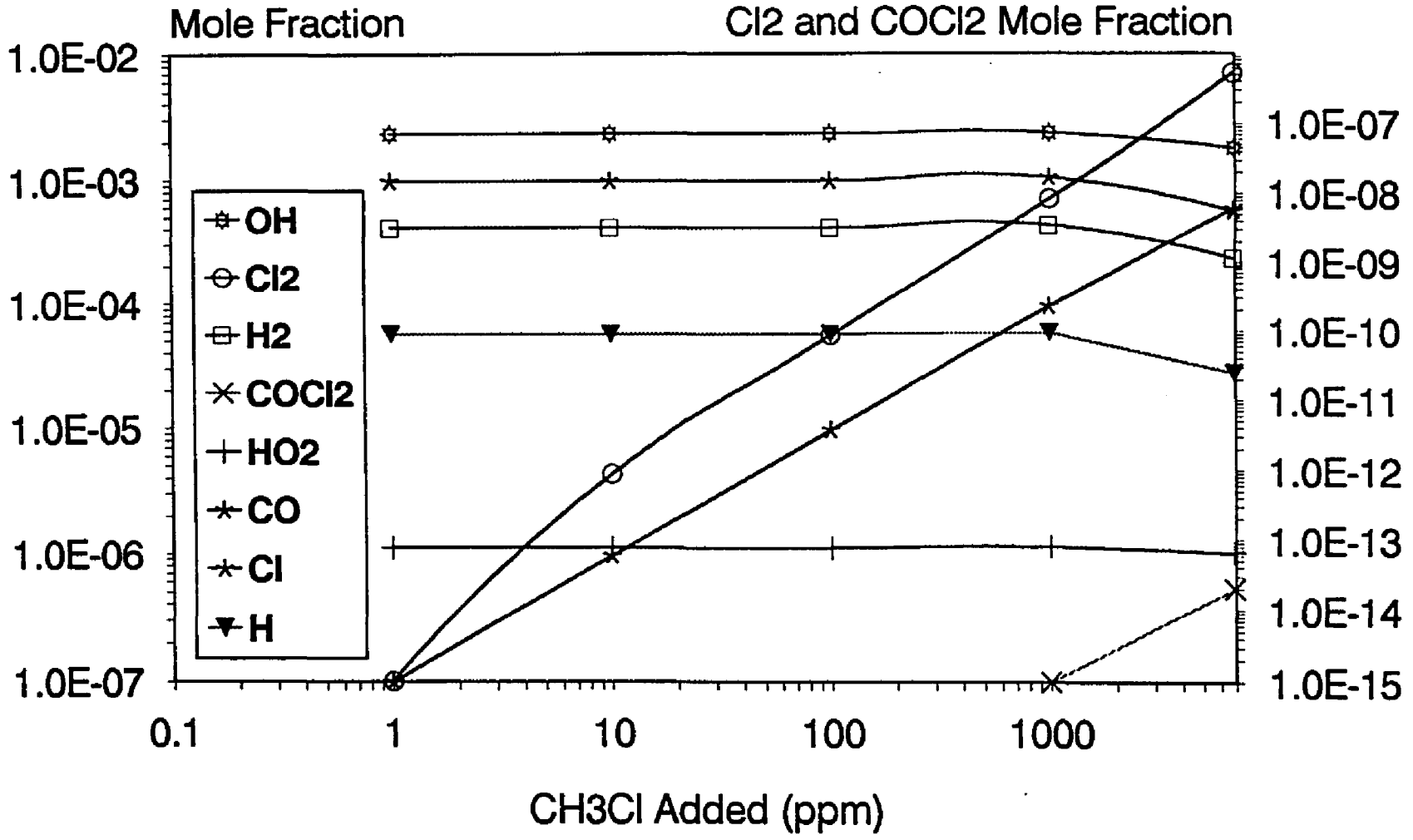

Fig 10.4 Effect of CH3Cl added in CH4/Air under fuel lean condition (equivalence ratio 0.8); calculated at exit 320K.

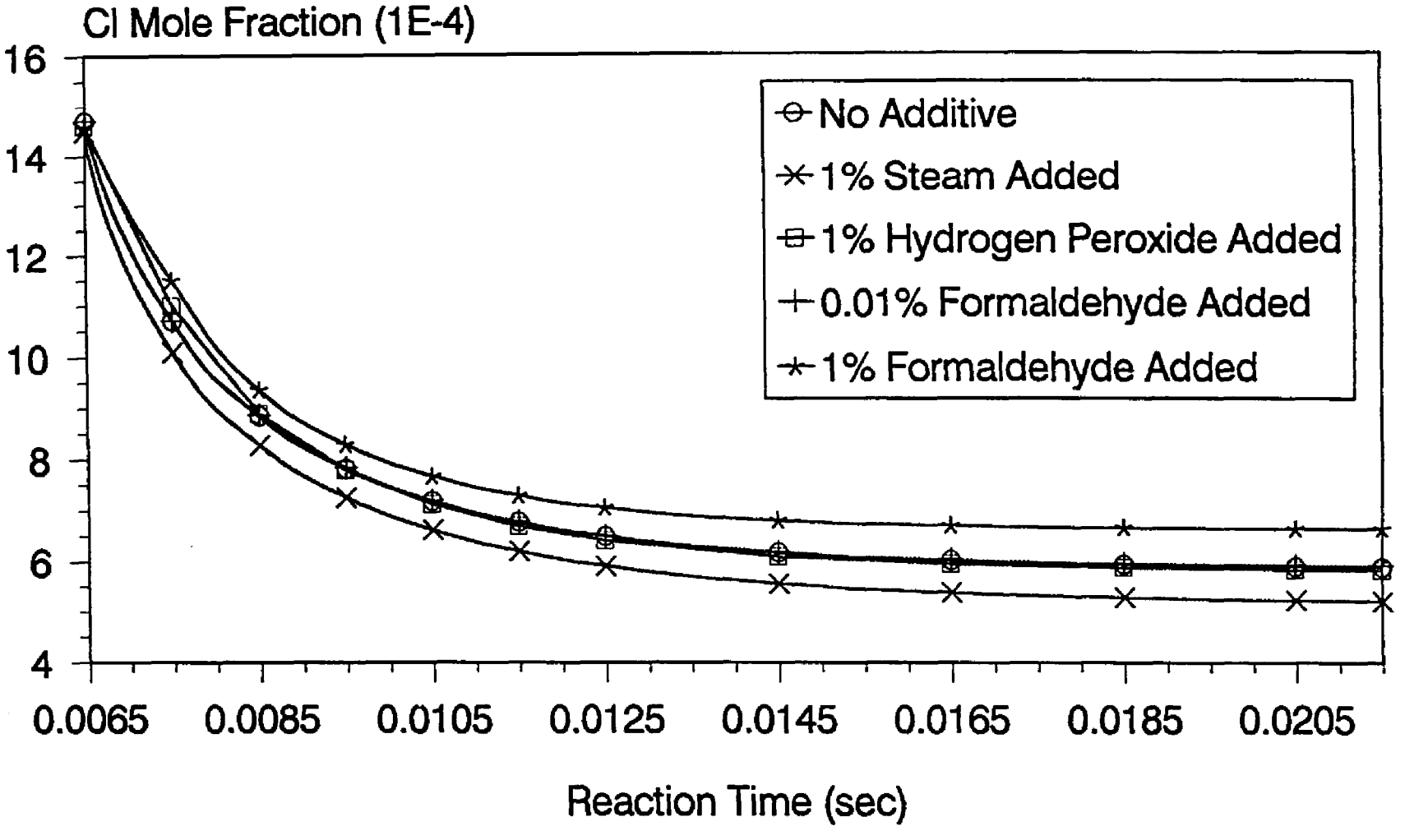

Fig 10.5 Cl atom mole fraction versus reaction time in the high temperature burnout zone

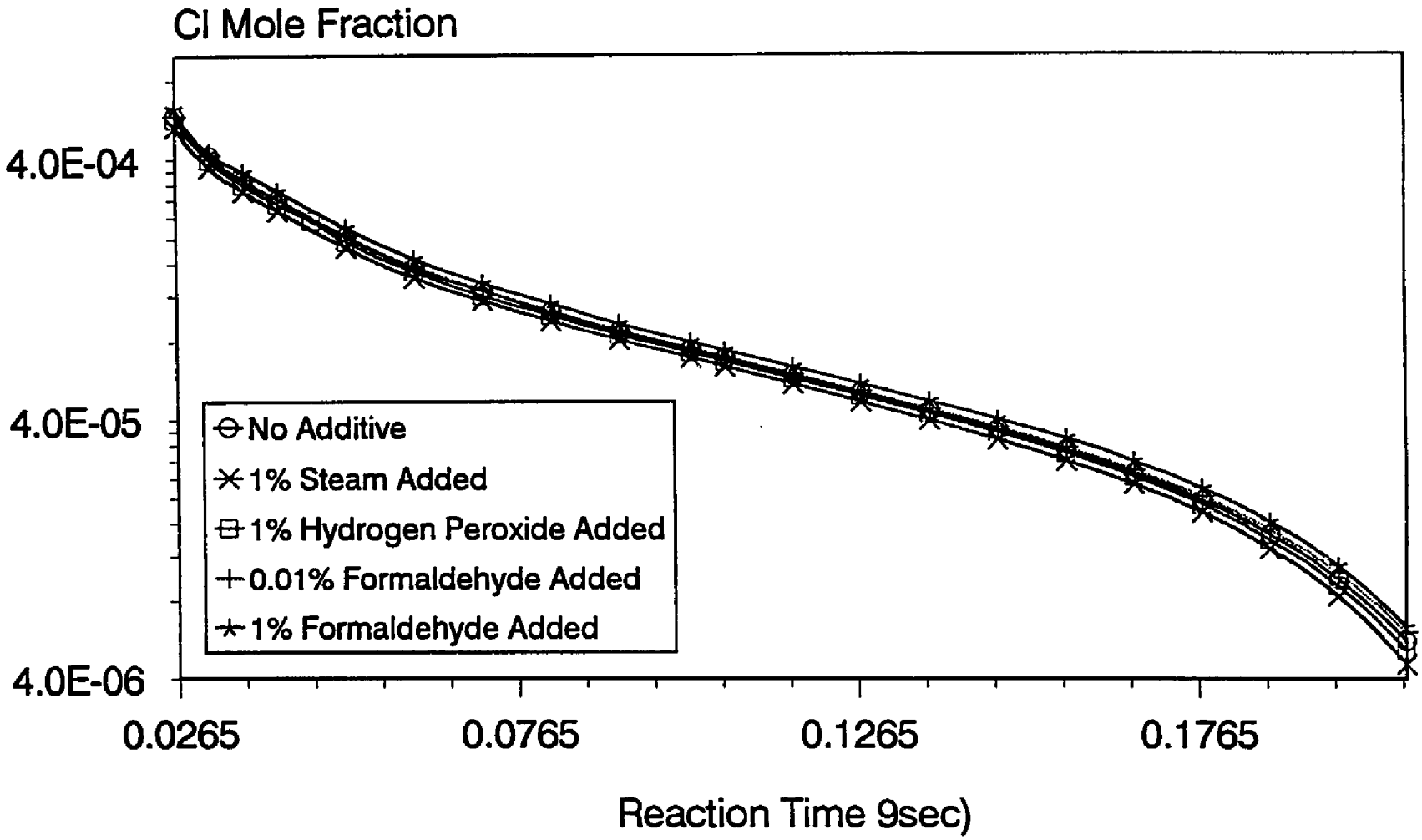

Fig 10.6 Cl atom mole fraction versus reaction time in the low temperature cool down zone

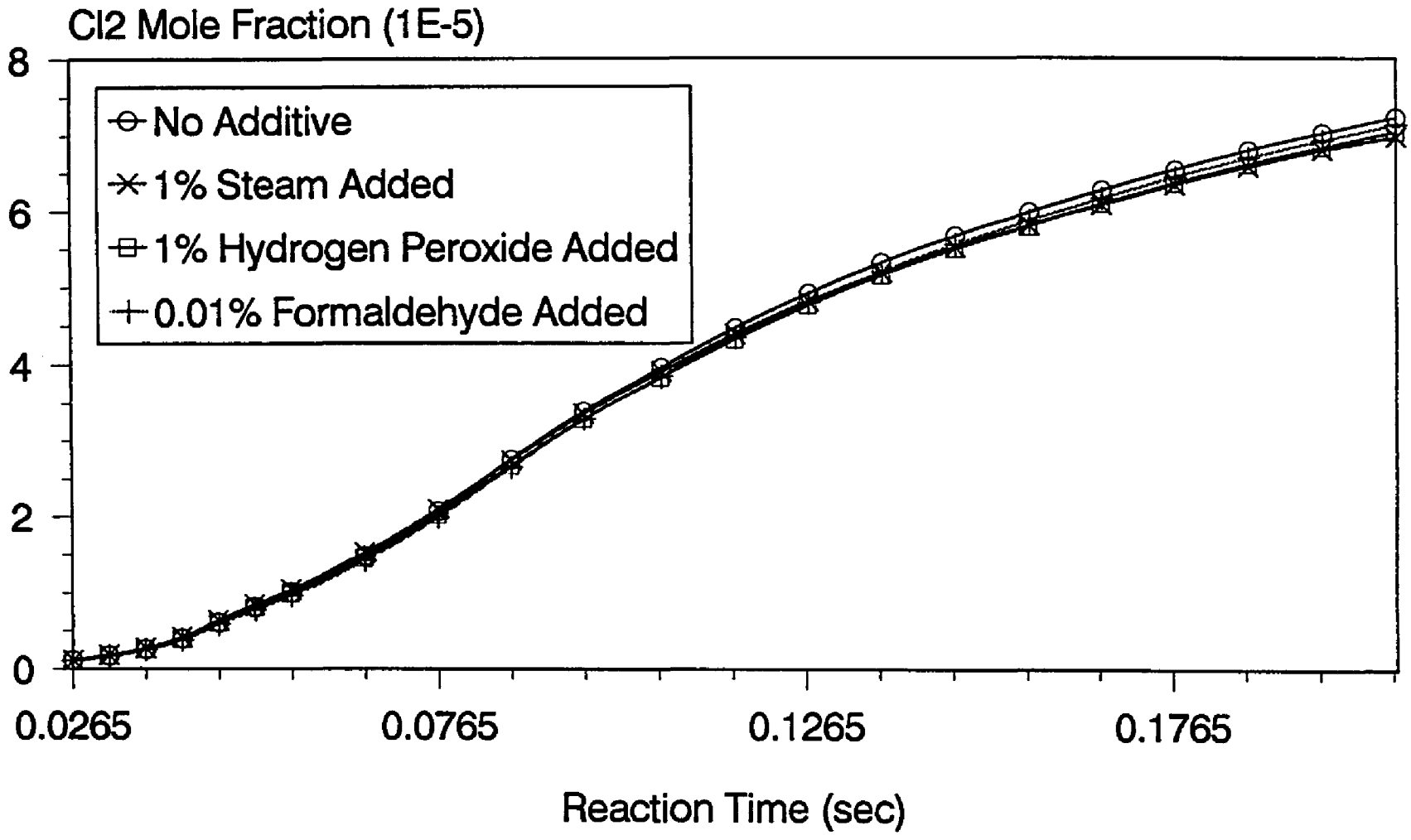

Fig 10.7 Cl2 mole fraction versus reaction time in the low temperature cool down zone

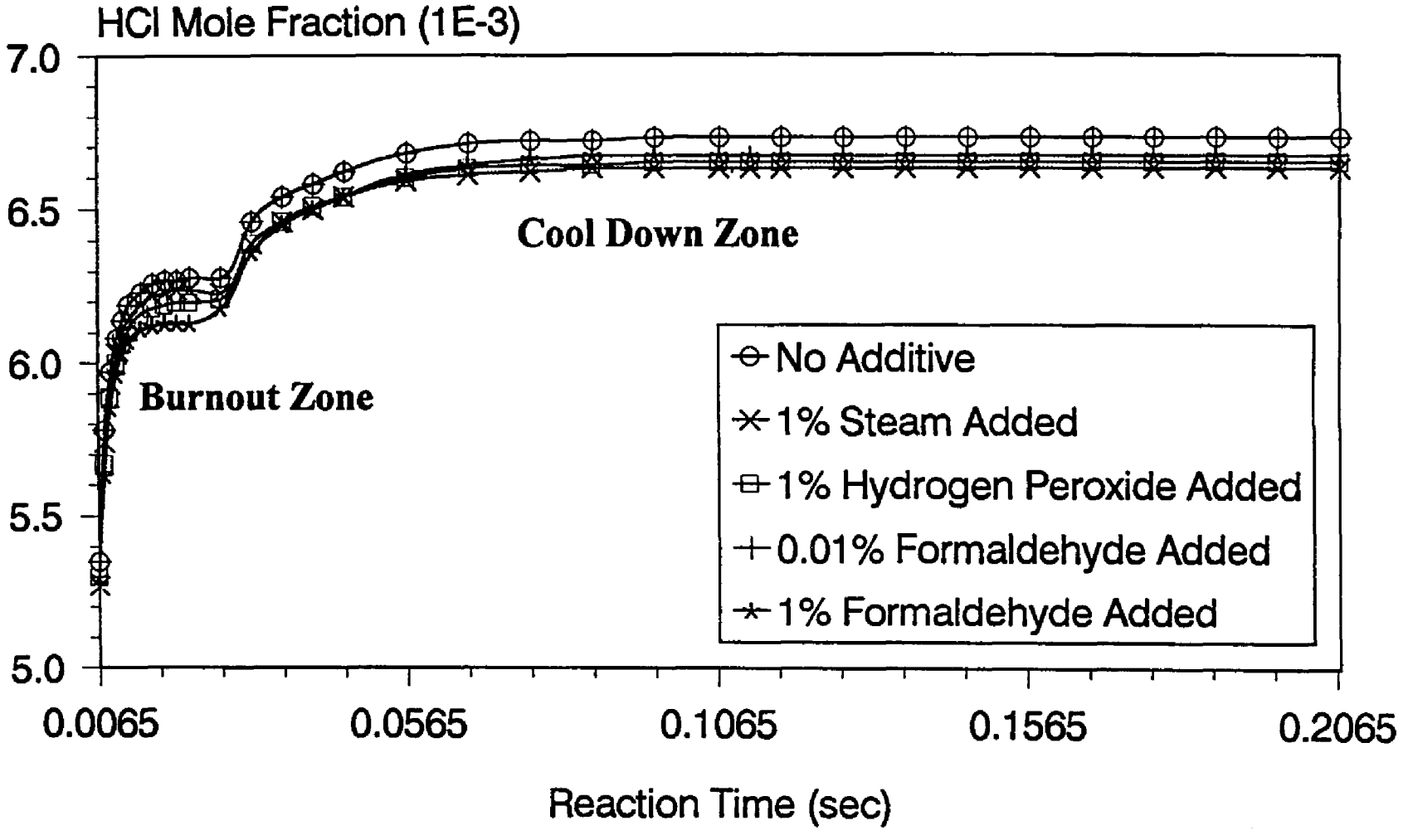

Fig 10.8 HCl mole fraction versus reaction time throughout the reactor

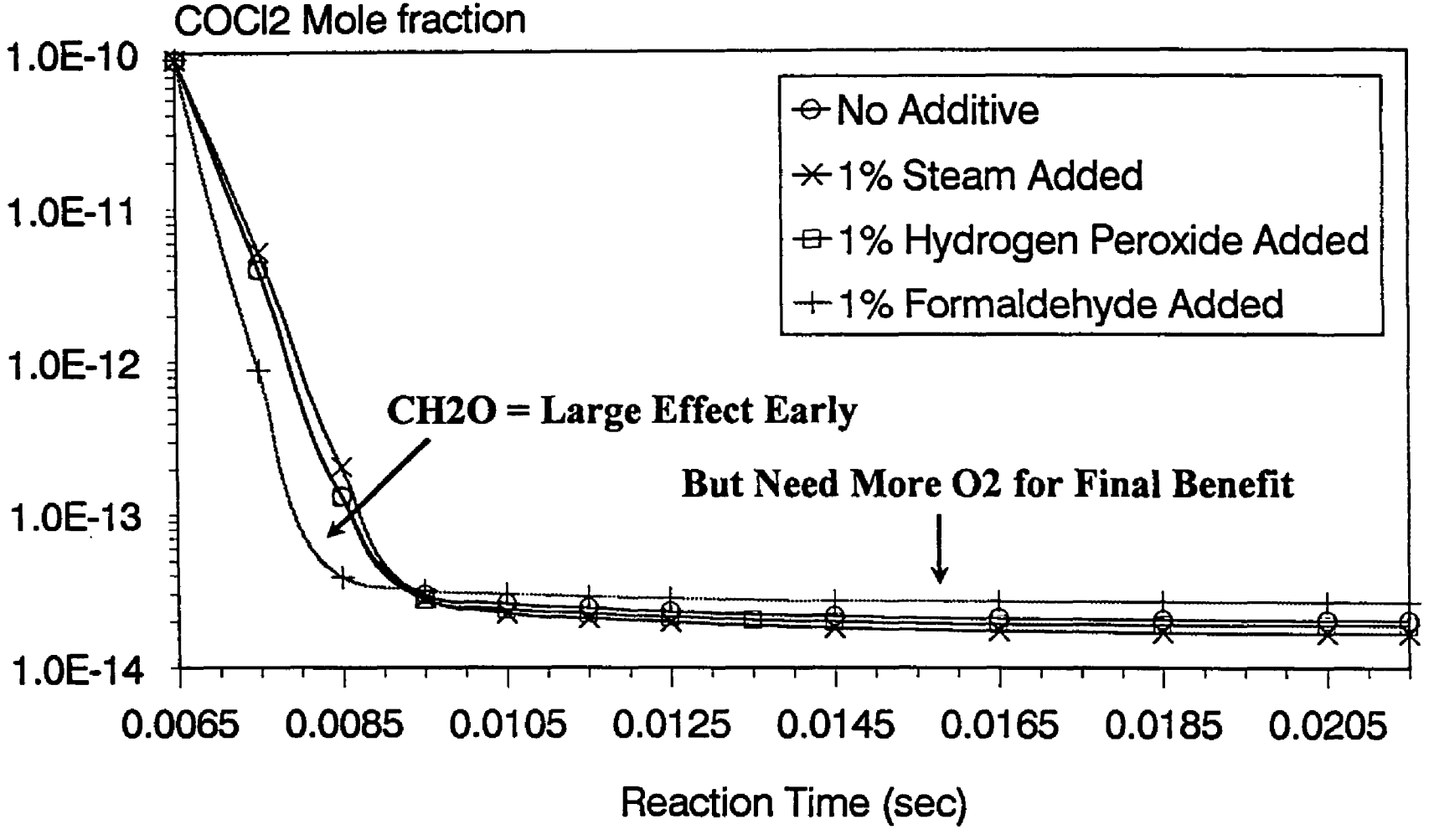

Fig 10.9 COCl2 mole fraction versus reaction time in the high temperature burnout zone

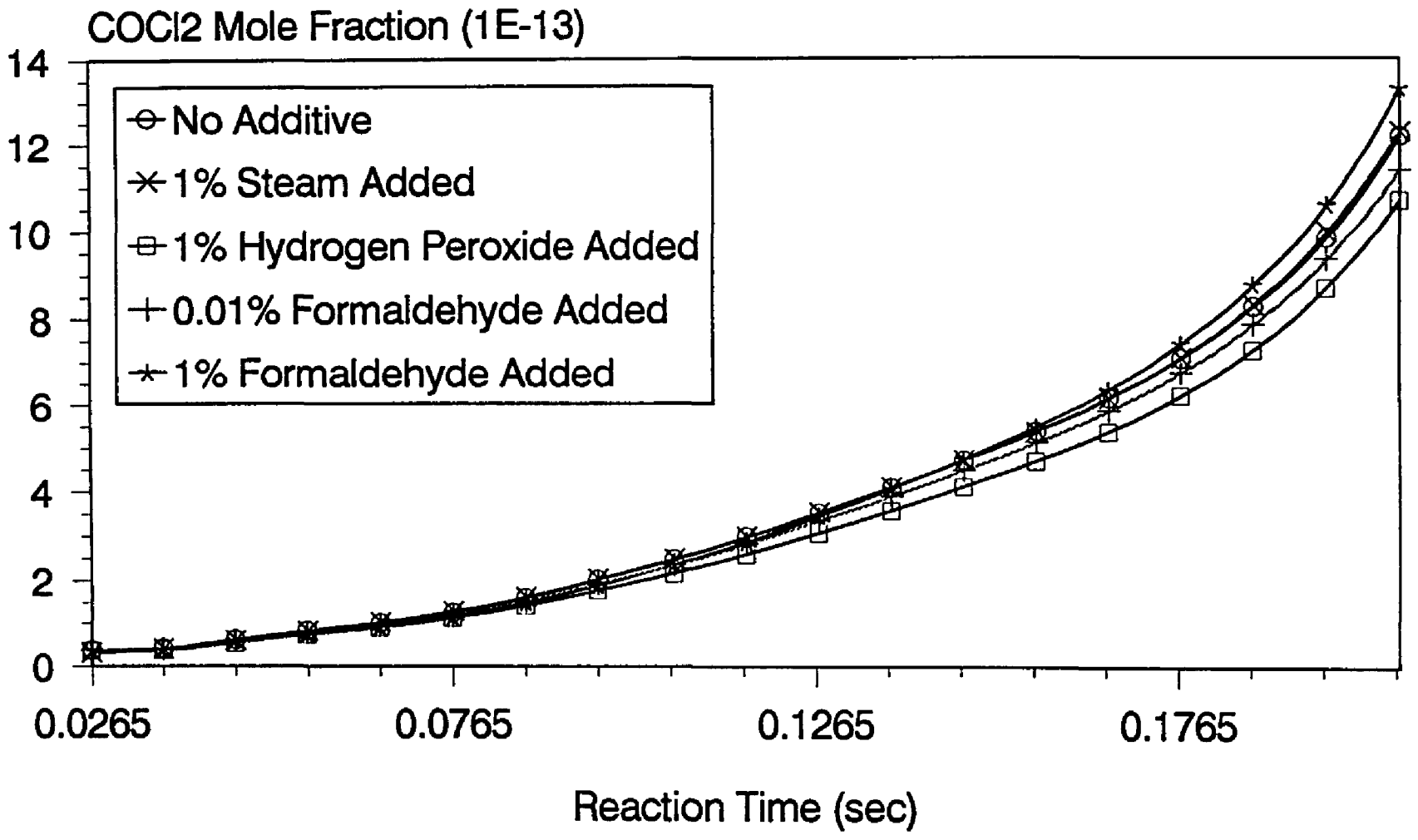

Fig 10.10 COCl2 mole fraction versus reaction time in the low temperature cool down zone

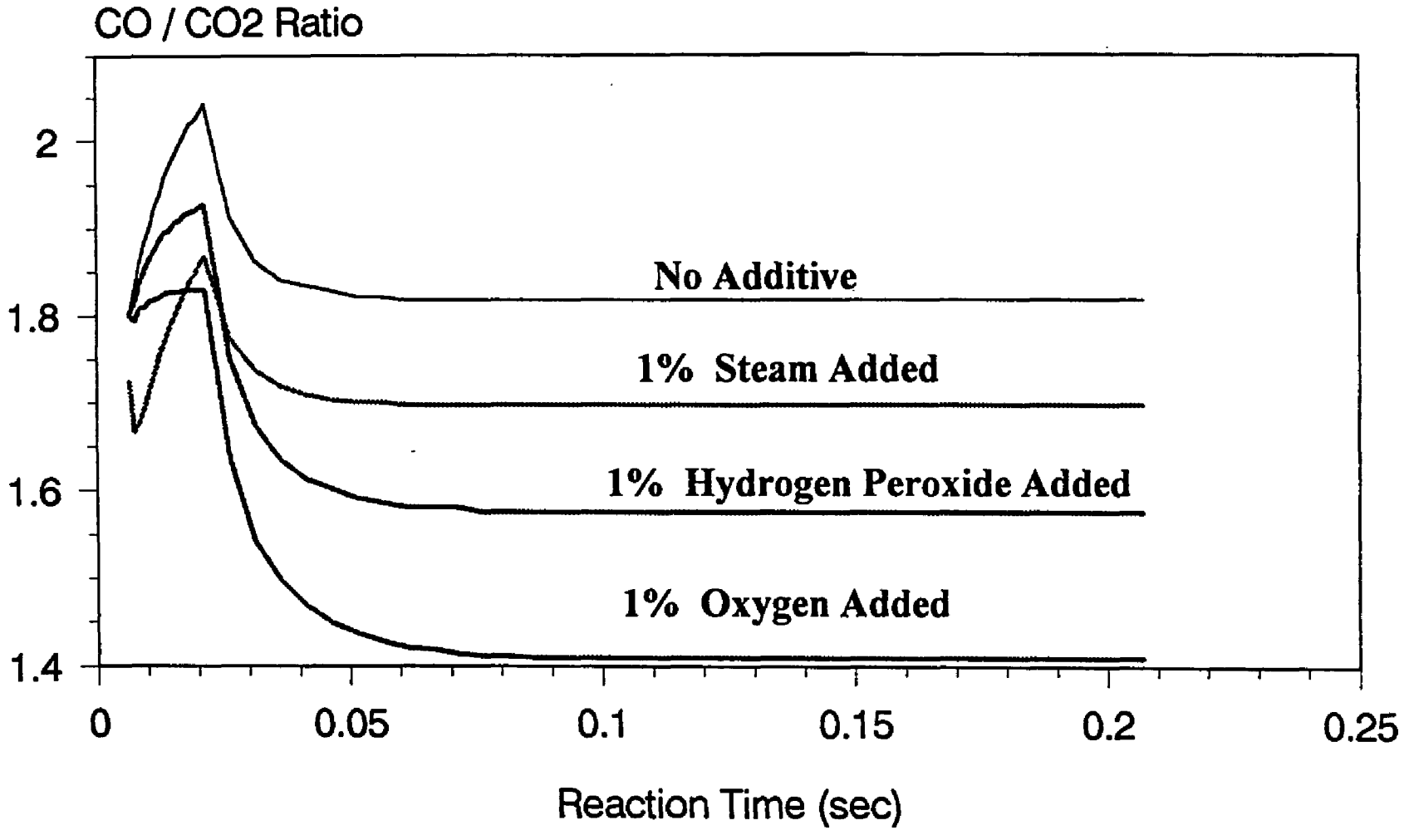

Fig 10.11 CO/CO2 ratio versus reaction time under fuel rich condition (equivalence ratio 1.5)

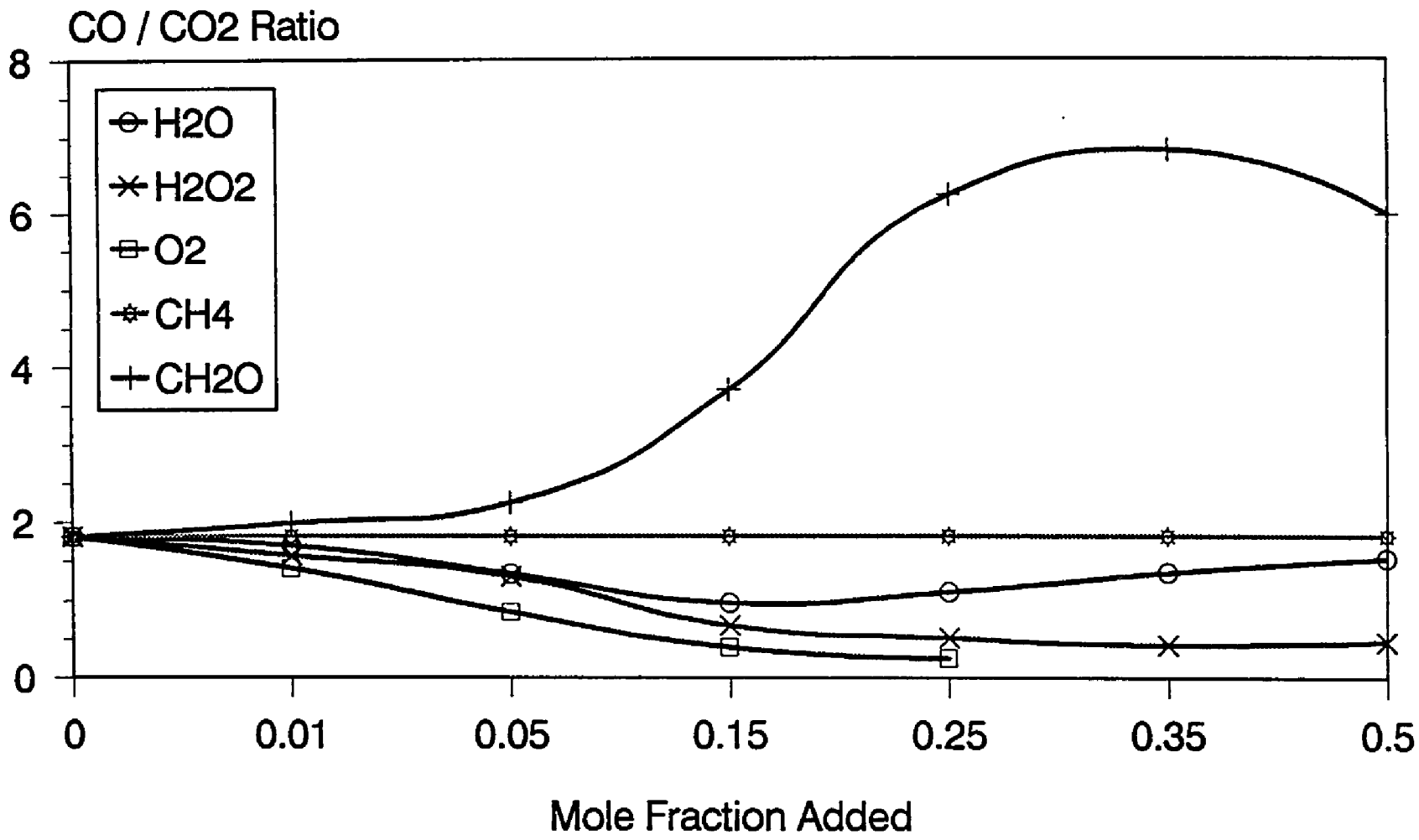

Fig 10.12 CO/CO2 ratio calculated at exit 320K under fuel rich condition (equivalence ratio 1.5)

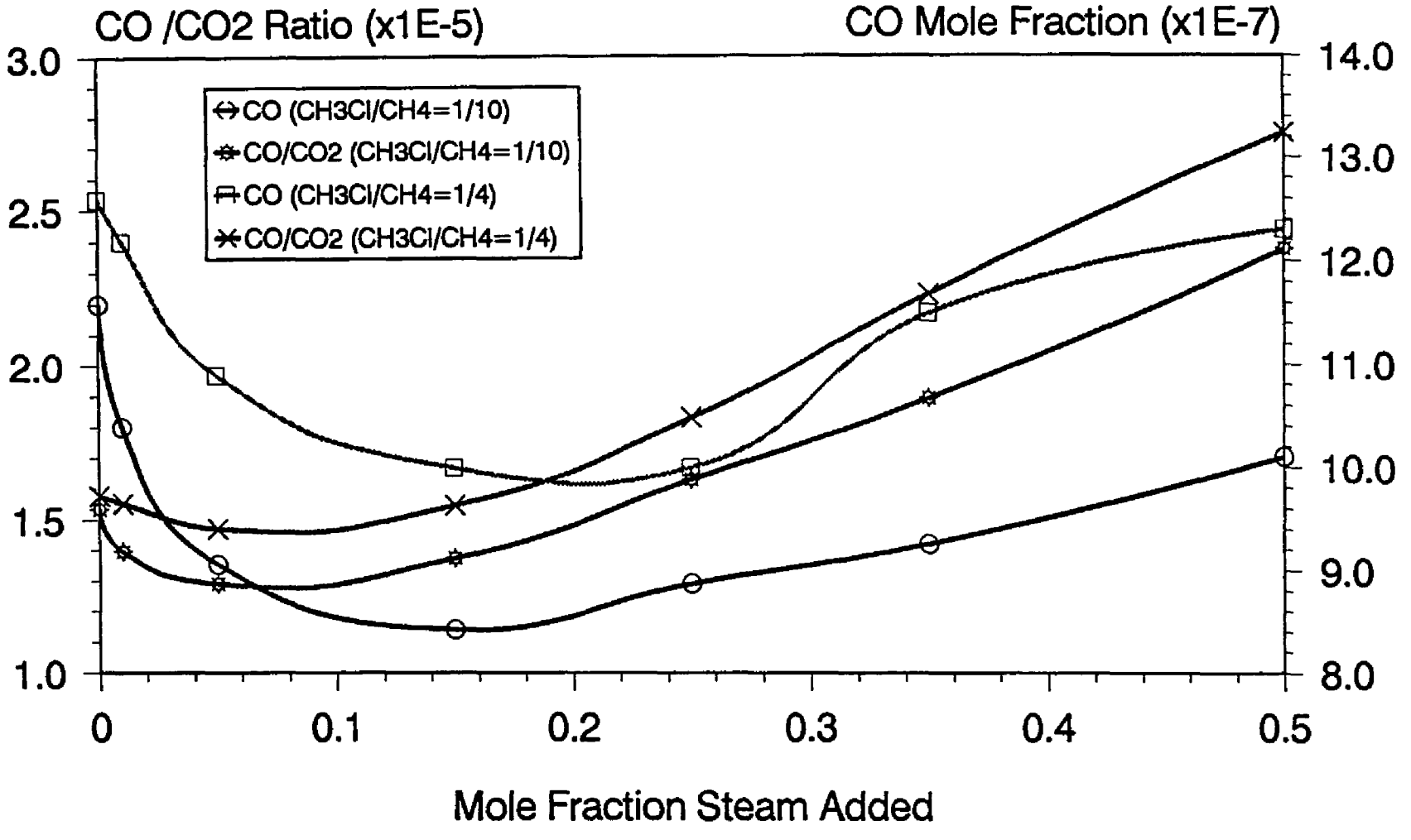

Fig 10.13 CO/CO2 ratio versus addition of steam under fuel lean condition (equivalence ratio 0.8)

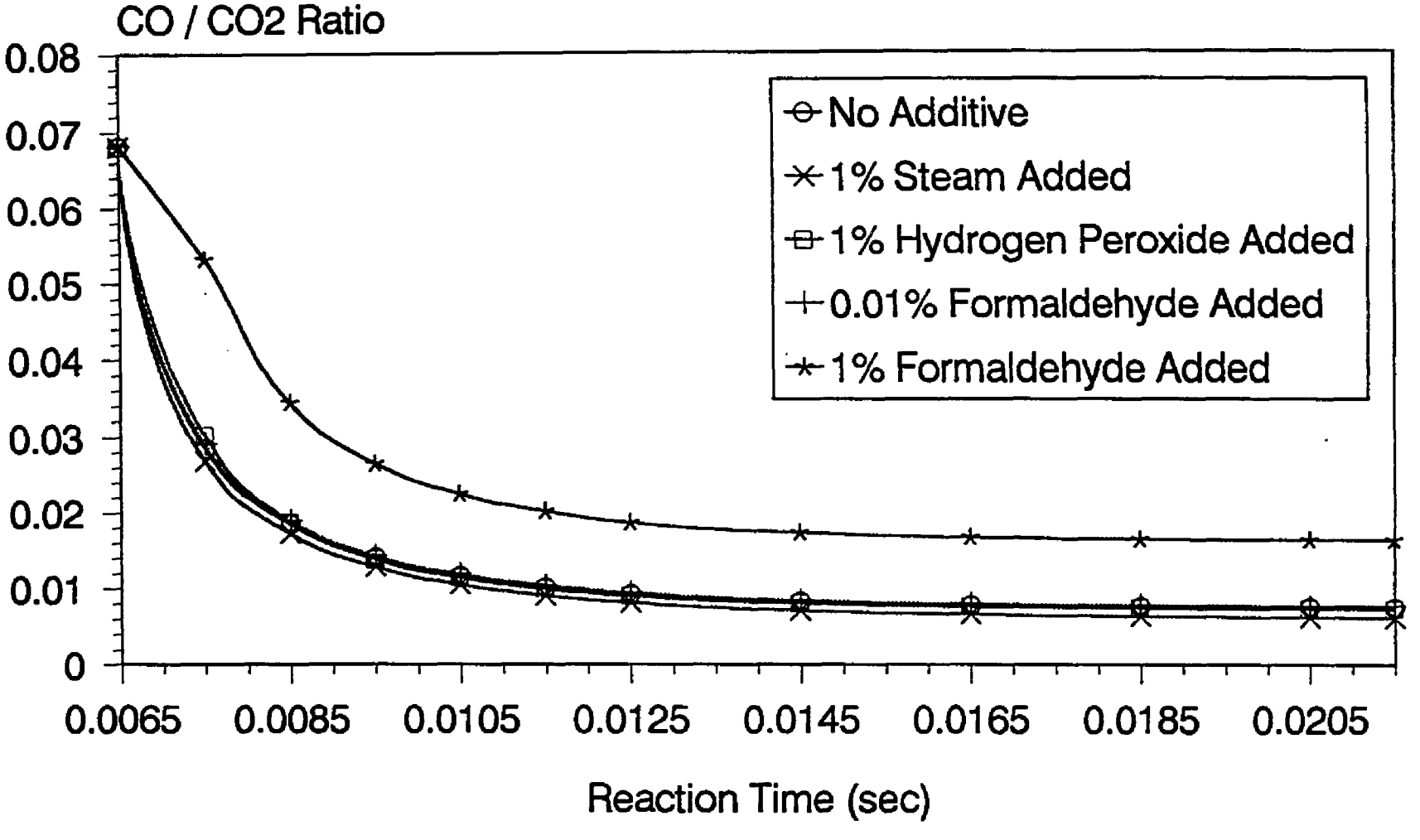

Fig 10.14 CO/CO2 ratio versus reaction time in the high temperature burnout zone

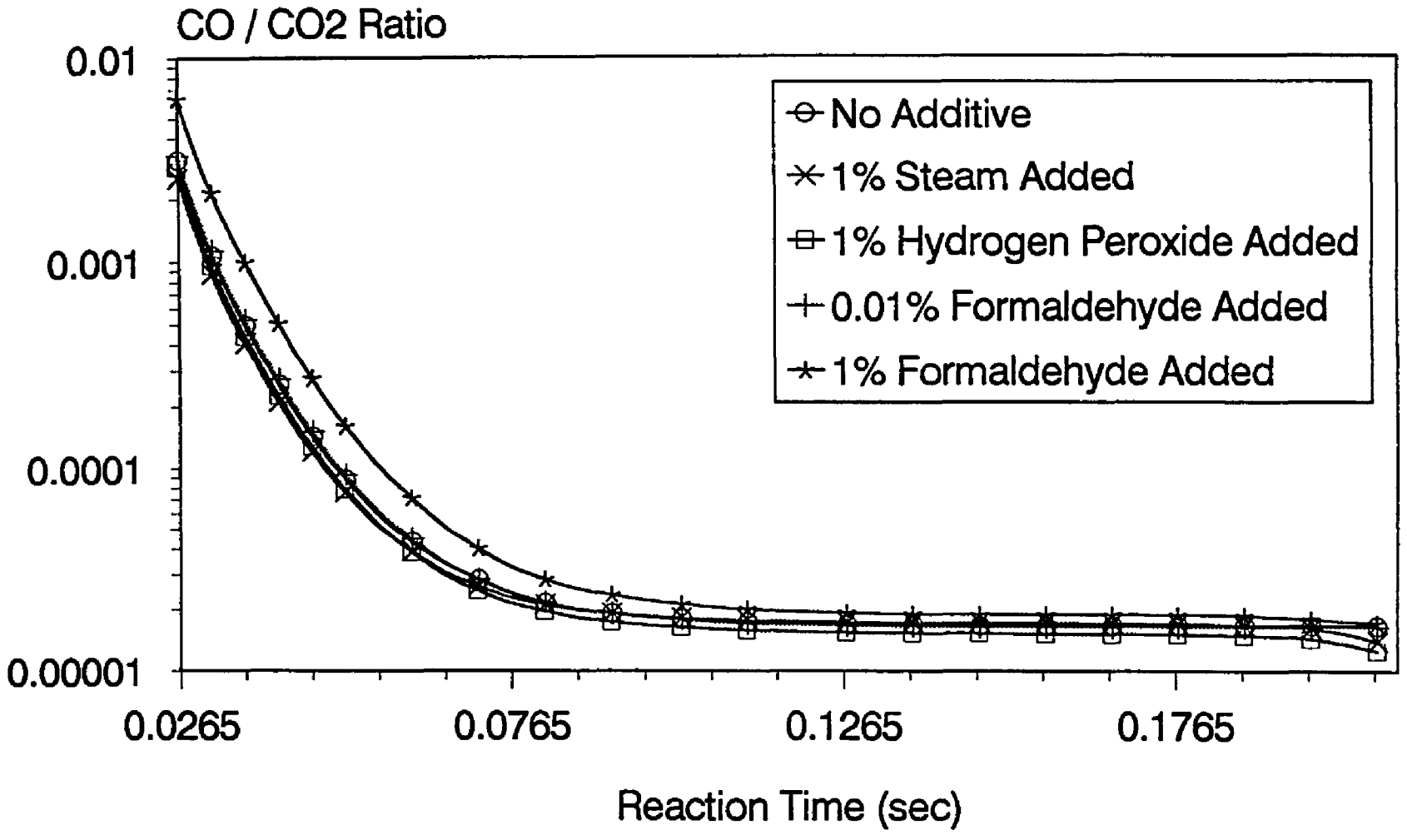

Fig 10.15 CO/CO2 ratio versus reaction time in the low temperature cool down zone

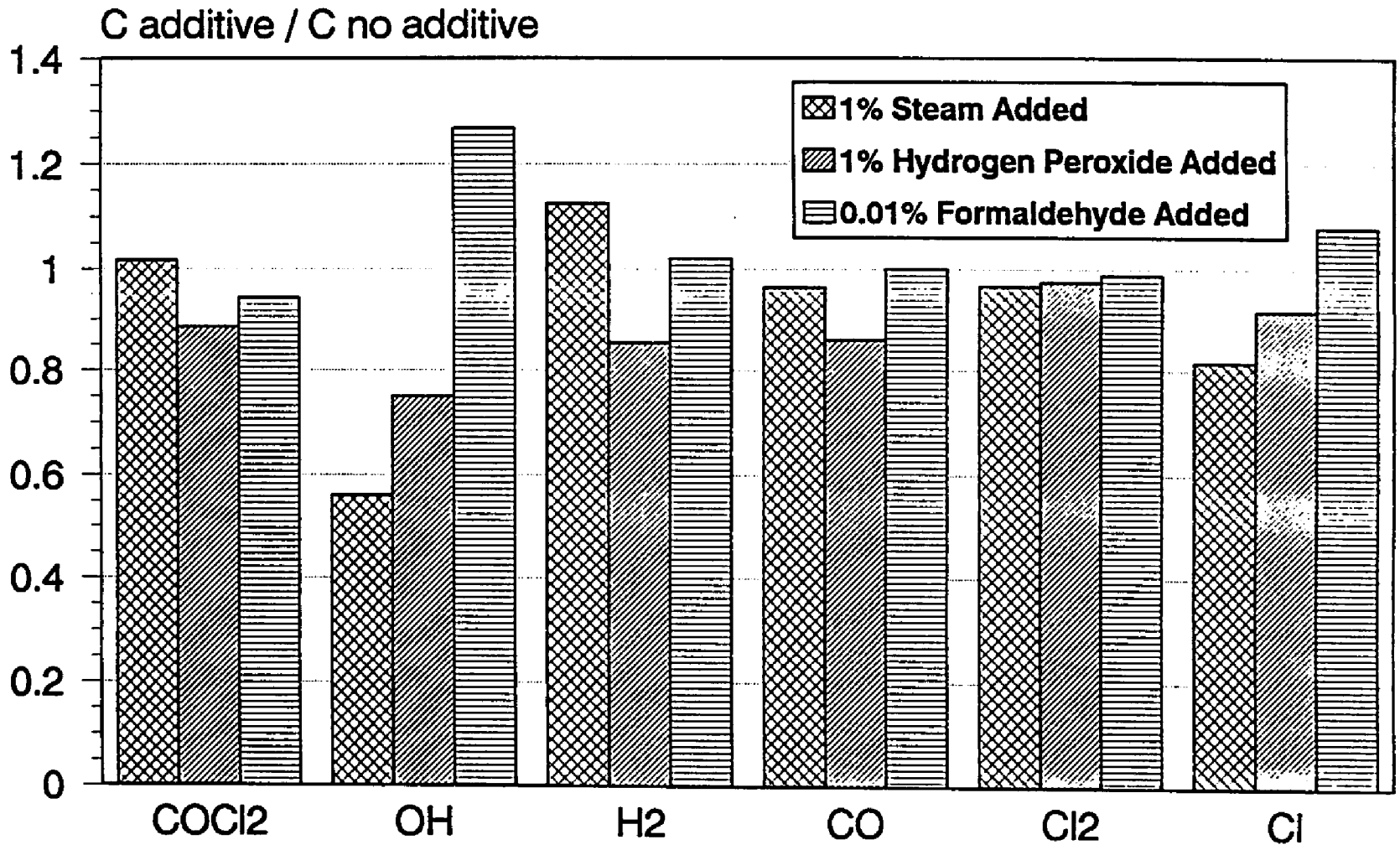

Fig 10.16 Fraction change in products versus additive.

REFERENCES

1. Cherimisimoff, P.N.; Pollution Engineering, p42 - 49, Feb. 1987.

2. Westbrook, C.K.; 19th Symposium (International) on Combustion, p 126, The Combustion Inst., 1982.

3. Karma, D. and Senkan, S.M., Combust. Sci. Tech.; 54, 333, 1987.

4. Chang, W.D., Karra, S.D., and Senkan, S.M., Combust. Sci. Tech., 49, 107, 1986.

5. Benson S.W. and Weissman, M., Int'l J. Chem. Kin., Vol.16, 307, 1984.

6. Dean, A.M., J. Phys. Chem.; 89, 4600, 1985.

7. Dean, A.M. and Bozzelli, J.W., Comb. Sci. & Tech., 80, 63, 1991.

8. Tsao, H. M.Sc. thesis, New Jersey Inst. Tech. 1987.

9. Huang, S.H.; M. Sc. Thesis, New Jersey Inst. Tech. 1987.

10. Won, Y.S. and Bozzelli, J.W., American Society of Mechanical Engineering HTD-Vol. 104, p 131 1988.

11. Shilov, A. E., et al., J. Fiz. Kim., vol. 33, 6, 1959.

12. Holbrook, K. A.; Trans. Faraday Soc., 57, 2151, 1961.

13. Frost, W., et al., Can. J. Chem., 43, 3052, 1965.

14. Kondo, O., et al., Bull. Chem. Soc. Jpn., 53, 2133, 1980.

15. LeMoan, G., C. R. Aczd. Sci., Paris, 258, 1535, 1964.

16. Karra, S.B., Gutman, D., and Senkan, S.M.; Combust. Sci. Tech. vol. 60, 45, 1988.

17. Miller, D.L., Senser, D.W., Cundy, V.A., and Matula, R.A.; Hazardous Waste, vol. 1, no. 1, p 1, 1984.

18. Roesler, J.F., Yetter, R.A., and Dryer, F.L.; Combst. Sci. Tech., vol. 85, p 1, 1992.

19. Koshland, C.P., Lee, S., and Lucas, D.; Combust. Flame, vol. 92, 106, 1993.

20. Hung, S.L. and Pfefferle L.D.; Comb. Sci. & Tech., vol. 87, p91, 1993.

21. Skoog, D.A.; Principles of Instrumental Analysis, Saunders College Publishing, New York,1985.

22. Benson, S.W., Thermochemical Kinetics, John Wiley, New York, 1976.

23. Ritter, E.R. and Bozzelli, J.W., Int. J. Chem. Kinetics, 23, 767, 1991.

24. Ritter, E.R., J. Chem. Info. Sci. 31, 400, 1991.

25. Allara, D.L. and Shaw, R.J.; J. Phys. Chem. Ref. Data, 9, 523, 1980.

26. Baulch, D.L., Duxbury, J., Grant,S.J., and Montague, D.C.; J. Phys. Chem. Ref. Data, Supplement 1, 10, 1981.

27. Atkinson, R.A. et al.; J. Phys. Chem. Ref. Data, 18, 881, 1989.

28. National Institute Standard and Technology Kinetics Data base, NIST Gaithersburg, MD 1989.

29. Bozzelli lectue handout

30. Zabel, F.; Int. J. Chem. Kinetic; 9, 655, 1977.

31. Kerr, J.A. and Moss, S.J.: Handbook of Bimolecular and Termolecular Gas Reaction Vol. I & II, CRC Press Inc., 1981.

32. Barat, R.B. and Bozzelli, J.W.; J. Phys. Chem., 96, 2494, 1992.

33. Howard, C.J., J. Chem. Phys. 65, 4771, 1976.

34. Perry, R.A., Atkinson, R., and Pitts, J.N., J. Chem. Phys. 67, 458, 1977.

35. Liu, A., Mulac, W.A., and Jonah, C.D., J. Phys. Chem. 93, 4092, 1989.

36. Bozzelli, J.W., Magee, K., Karim, H.MD., Dean, A.M., and Chang, A.Y.; paper submitted to J. Phys. Chem. August 1993.

37. Chen, Y. and Tschuikow-Roux, E., J. Phys. Chem. 96, 7266, 1992.

38. Lay, L.T., Ritter, E.R., and Bozzelli,J.W., Chemical and Physical Processes in Combustion, 1993, in press.

39. Benson, S.W.; Can. J. Chem., 61, 881, 1983.

40. Reid, R.C., Prausnitz, J.M., and Polling, B.E., Properties of Gases and Liquids, 4th Ed., McGraw Hill, New York, 1989.

41. Ben Amotz, D. and Herschbach, D.R., J. Phys. Chem. 94, 3393, 1990.

42. Cohen, N., Int. J. Chem. Kinetics, 14, 1339, 1982; 15, 503, 1983.

43. Cohen, N. and Westberg, K.R.; Int. J. Chem. Kinetics, 18, 99, 1986.

44. Cohen, N. and Benson, S.W.; J. Phys. Chem. 91, 162, 1987.

45. Cohen, N.; Int. J. Chem. Kinetics, 21, 909, 1989.

46. Lewis, G.N., Randall, M.; Pitzer, K.S., and Brewer, L.; Thermodynamics, 2nd Ed.; McGraw-Hill, New York, 1961.

47. Gilbert, R.G. and Smith, S.C.; Theory of Unimolecular and Recombination Reactions; Blackwell Scientific Publications, 1990.

48. Troe, J.; J. Phys. Chem., 83, 114, 1979.

49. Chuang, S.C. and Bozzelli, J.W., Environ. Sci. Tech., 20, 568, 1986.

50. Chang, S.H. and Bozzelli, J.W. AICHE J., 33, 1207, 1987.

51. Y. S. Won and J. W. Bozzelli, Combustion Science and technology, 85, 347, 1992.

52. Abbatt and Anderson, J. Phys. Chem., 95, 2382, 1991.

53. J. F. Blake, S. G. Wierschke, and W. L. Jorgensen; J. America Chemical Society, 111, 1919, 1989.

54. E. Arunan, S.J. Wategaonkar and D.W. Setser, J. Phys. Chem. 95, 1539, 1991.

55. Lias, S.G.; Bartmess, J.E.; Liebman, J.F.; Holmes,J.L.; Levin, R.D.; Mallard, G.M. J. Am. Chem. Soc. 107, 6089, 1985.

56. Ibid, J. Phys. Chem. Ref. Data, 17, Suppl. 1, 1988.

57. NIST Structures and Properties Database Number 25; Gaithersburg, MD 20899.

58. Paulino, J. A., Squires, R. R, J. Am. Chem. Soc., 113, 5573, 1991.

59. CHEMKIN computer code SAND87-8007.UC-4 supplied by Sandia National Labs, Livermore, CA. R.J. Kee and J.A. Miller.

60. Ritter, E., Bozzelli, J.W., and Dean, A.M. J. Phys. Chem., 94, 2493, 1990.

61. Karra, S.B. and Senkan, S.M., I&EC RESEARCH, 27, 447, 1988.

62. Tavakoli, J. and Bozzelli, J.W., paper presented at the Central States Technology Meeting, The Combust. Inst. Argonne, IL May 1987.

63. Unpublished studies on reactions of chloroform in methane/oxygen and 1,1,1 trichloroethane in methane/oxygen atmosphere. This laboratory, where initial decay of the hydrocarbon is observed with chlorocarbon present is observed to be faster than when the chlorocarbon is not present.
(M.S. Thesis Yo-pin Wu 1989)

64. SENS is modification by NJIT of an early version of the SENKIN computer code SAND87-8248.UC-4 supplied by Sandia National Labs, Livermore, CA. R.J. Kee and A.E. Lutz.

65. Barat, R.B., Sarafim, A.F., Longwell, J.P., and Bozzelli, J.W. ; Comb. Sci. Tech.; vol. 74, p. 361, 1990

66. Roessler, J.F., Yetter, R.A., and Dryer, F.L; Comb. Sci. Tech.; vol 82, p.87, 1992.

67. Miller, J.A. and Bowman, C.T.; Energy and Combustion Science, 1, 1989.

68. Westmoreland P.R., Howard, J.B., Longwell, J.P., and Dean, A.M.; AICHE Journal, 32, 12, 1971, 1986.

69. FLAME computer code SAND87-8240.UC-4 supplied by Sandia National Labs, Livermore, CA. Kee, R.J., Grcar, J.F., Smooke, M.D., and Miller, J.A. 20.

70. Myers, R.Thomas, J. Phys. Chem. Vol.83, No.2, 1979.

71. More, R. and Capparelli, A.L., J. Phys. Chem. 84, 1870-1871, 1980.

72. Hansen, P.J. and Jurs, P.C., Anal. Chem., 59, 2322-2327, 1987.

73. Lai, W.Y., Chen, D.H., and Maddox, R.N., Ind. Eng. Chem. Res., 26, 1072, 1987.

74. Reid, R.C., Prausnitz, J.M., and Sherwood, T.K., The Properties of Gases and Liquids, 3th ed. McGraw-Hill, New York, 1977.

75. Reid, R.C., Prausnitz, J.M., and Poling, B.E., The Properties of Gases and Liquids, 4th ed. McGraw-Hill, New York, 1988.

76. CRC Handbook of Chemistry and Physics, 71th ed.; Weast, R.C. Ed.; The Chemical Rubber Co.; Cleveland, OH, 1991.

77. McClellan, A.L., Tables of Experimental Dipole Moments, Freeman, San Francisco, 1963.

78. Minikin, V.L., Osipov, O.A., and Zhdanov, Y.A.; Dipole Moments in Organic Chemistry, trans. from the Russian by B.J. Hazard, Plenum, New York, 1970.

79. MOPAC computer code 6th Ed, supplied by Frank J. Seiler Research Laboratory, United State Air Force Academy; Stewart, J.J.; 1990.

80. Mason, E.A. and Monchick, S.C. ; Theory of Transport Properties of Gases, 9th Intern. Symp. Combust., Academic, New York, 1963.

81. Chung, T.H., Lee, L.L., and Starling, K.E.; Ind. Eng. Chem. Fundam., 23, 8, 1984.

82. TRANSCALC computer code; poster section in Twenty-fourth International Symposium on Combustion, Sydney, Australia, July 5-10 1992.

83. Ho, W., Yu, Q.R., and Bozzelli, J.W.; Comb. Sci. Tech., 85, 23, 1992.

84. Ho, W. Barat, R.B., and Bozzelli, J.W.; Combustion and Flame, 88, 265, 1992.

85. Chiang H.M. and Bozzelli J.W.; Proceeding of Central and Eastern States Joint Technical Meeting, The Combustion Institute, New Orleans, LA, March 15-17, 1993

86. Roesler, J.F., Yetter, R.A., and Dryer, F.L.; poster section, Third International Congress on Toxic Combustion By-Products, MIT, Cambridge, MA, June 14-16, 1993.

87. Karra, S.B. and Senkan, S.M., Ind. Eng. Chem. Res., 27, 1163, 1988.

88. Qun, M. and Senkan, S.M., Hazardous Waste & Hazardous Materials, Vol. 7, No. 1, 1990.

89. Tsang, W.; Combustion Science and Technology, vol. 74, 99, 1990.

90. Tsang, W.; Waste Management, vol. 10, 217, 1990.

91. Lyon, R.; Twenty-Third Symposium (International) on Combustion, The Combustion Institute, 903, 1990.

92. Cooper, C.D. and Clausen, C.A.; Journal of Hazardous Materials, 24, 288, 1990.

93. Cooper, C.D. and Clausen, C.A.; Journal of Hazardous Materials, 27, 273, 1991.

94. Cobos, C.J., Baulch,D.L., Cox,R.A., Esser,C., Frank,P., Just,Th., Kerr,J.A., Troe,J., Pilling,M.J., Walker,R.W., and Warnatz,J.; J. Phys. Chem. Ref. Data 1992

95. Ritter, E.R. and Barat, R.B.; Third International Congress on Toxic Combustion By-Products, poster section, MIT, Cambridge, MA,1993.

96. Ho, W. and Bozzelli, J.W.; Twenty-Fourth Symposium (International) on Combustion, The Combustion Institute, p943, 1992.

97. Miller, G., Cundy, V.A. and Lester T.; paper Submitted to Combst Sci. Tech, April 1993.

98. Puri, I.K., M.H. Yang, and Lee, K.Y.; Comb. Flame, vol. 92, p. 419, 1993.

99. Puri, I.K. and Lee, K.Y.; Comb. Flame, vol. 92, p. 440, 1993.

100. Hammins, A.; paper presented at NIST Fluorocarbon Flame Inhibition Workshop, New Orleans La, Mar 15, 1993.

101. Brouwer, J., Longwell, J.P., Sarofim, A.F., Barat, R.B., and Bozzelli, J.W. ; Comb. Sci. and Tech. vol. 85, p. 87, 1992.

102. Barat, R.B. et al.; poster section, Twenty-Fourth Symposium (International) on Combustion, The Combustion Institute, 1992. (paper submitted to Comb. and Flame 1993)